AN INVESTIGATION INTO THE MECHANISM OF ACTION OF EMODEPSIDE AND OTHER NOVEL ANTHELMINTIC COMPOUNDS

By

Kathryn Bull

A thesis presented for the degree of

DOCTOR OF PHILOSOPHY

of the

UNIVERSITY OF SOUTHAMPTON

in the

FACULTY OF MEDICINE, HEALTH AND LIFE SCIENCES
DIVISION OF CELL SCIENCES

March 2008

UNIVERSITY OF SOUTHAMPTON

ABSTRACT

FACULTY OF MEDICINE, HEALTH AND LIFE SCIENCES
DIVISION OF CELL SCIENCES

Doctor of Philosophy

AN INVESTIGATION INTO THE MECHANISM OF ACTION OF EMODEPSIDE AND OTHER NOVEL ANTHELMINTIC COMPOUNDS

Kathryn Bull

Anthelmintic drugs are used as a control measure for parasitic nematode infections. However, heavy reliance on these compounds has led to the development of parasite resistance and a consequent need to develop new anthelmintics that function via novel biological pathways. In this project, seven potential anthelmintics were examined for activity in the free-living nematode *C. elegans*. Of the seven compounds, those belonging to the cyclooctadepsipeptide group were shown to inhibit *C. elegans* pharyngeal pumping. The most potent of the compounds tested was emodepside, which has previously been shown to act as a potent broad-spectrum anthelmintic. The major aim of this project was to define and characterise the mechanism of action of emodepside using the free-living nematode *C. elegans*.

Emodepside potently inhibited the locomotion and pharyngeal pumping of adult and larval stage 4 (L4) *C. elegans*. The L4 pharynx demonstrated reduced emodepside sensitivity in the presence, but not absence, of the intact cuticle, suggesting that the L4 cuticle reduces drug access. Continuous exposure of *C. elegans* to emodepside from egg to adult resulted in a slowing of worm development, possibly due to the paralysis of locomotion and pharyngeal pumping, which are important for food location and ingestion. Emodepside inhibited *C. elegans* egg laying behaviour, but not egg production or egg hatching. These results suggest that emodepside functions at the neuromuscular junction of the pharyngeal, vulval and body wall muscles to produce paralysis of pharyngeal pumping, egg laying and locomotion.

Analysis of specific *C. elegans* gene mutants for their sensitivity to the inhibition of pharyngeal 5-HT response by emodepside strongly suggested that the anthelmintic functions primarily via the Ca^{2+}-activated K^+ channel SLO-1, with minor contributory roles performed by the G protein-coupled receptor LAT-1, and the G proteins $G\alpha_q$ and $G\alpha_o$. The *C. elegans slo-1 (js379)* null demonstrated a high level of resistance to emodepside, which was abolished upon rescue of *slo-1* expression in neurons. Rescue of *slo-1* expression in the pharyngeal muscles did not restore emodepside sensitivity, suggesting that neuronal SLO-1 is activated by emodepside to achieve paralysis of pharyngeal pumping. A gain-of-function mutant for SLO-1 that increases the Ca^{2+} sensitivity of the channel was found to be hypersensitive to emodepside, suggesting that emodepside manipulates the Ca^{2+} sensitivity of SLO-1 to facilitate its activity.

To establish how emodepside is affecting SLO-1, the role of this channel in the pharynx was investigated. The *slo-1 (js379)* null possessed a longer mean pump duration and a disrupted pattern of pumping. Rescue of neuronal SLO-1 restored the wild type phenotype, suggesting that neuronal SLO-1 contributes to the control of pharyngeal pumping via the regulation of neurotransmitter release. Therefore, it is possible that emodepside may function by increasing the Ca^{2+} sensitivity of neuronal SLO-1 at the pharyngeal neuromuscular junction, resulting in an inhibition of neurotransmitter release and muscle paralysis. However, whole cell patch clamp recordings from pharyngeal muscle cells showed that emodepside inhibits SLO-1 currents rather than activating them. It is possible that the different intracellular environments afforded by pharyngeal neurons and muscle may result in the SLO-1 channel being modified differently in these two locations. This could produce a neuronal channel that is stimulated by emodepside and a muscle channel inhibited by the drug.

Interestingly, the *lat-1 (ok1465)* mutant was resistant to the effect of emodepside on pharyngeal pumping but not locomotion, suggesting that components of the molecular pathways involved in emodepside activity at the pharyngeal and body wall muscle neuromuscular junctions may be subtly different.

The cyclooctadepsipeptides verticilide, PF1022-222 and PF1022-888 were also shown to inhibit *C. elegans* pharyngeal pumping. The *slo-1 (js379)* and *lat-1 (ok1465)* null mutants demonstrated reduced sensitivity to all three compounds, suggesting that SLO-1 and LAT-1 are involved in the mechanism of action of these compounds as well as emodepside. SLO-1 and LAT-1 are not known to be involved in the mechanism of action of any other currently available anthelmintic, highlighting the novel functioning of the compounds tested in this project, and their potential as anthelmintics that could break resistance.

Acknowledgements

Firstly, I would like to thank my Mum and Dad, without whose support none of this would have been possible.

A very special thank you to Dr Alan Cook, Dr David Marsden, Marcus Guest and Dr Neline Kriek for their excellent technical help and advice. Thank you to my supervisors Professor Robert Walker and Professor Lindy Holden-Dye, and to Professor Achim Harder at Bayer AG.

I am grateful to Bayer AG (Germany), for their financial support.

Publications

Holden-Dye, L., O'Connor, V., Hopper, N. A., Walker, R. J., Harder, A., **Bull, K.**, Guest, M. (2007) SLO, SLO, quick, quick, slow: calcium-activated potassium channels as regulators of *Caenorhabditis elegans* behaviour and targets for anthelmintics. *Invertebrate Neuroscience*, 7, 199-208.

Guest, M., **Bull, K.**, Walker, R. J., Amliwala, K., O'Connor, V., Harder, A., Holden-Dye, L., Hopper, N. A. (2007) The calcium-activated potassium channel, SLO-1, is required for the action of the novel cyclo-octadepsipeptide anthelmintic, emodepside, in *Caenorhabditis elegans*. *International Journal for Parasitology*, 37, 1577-88.

Mitchell, P. H., **Bull, K.**, Glautier, S., Hopper, N. A., Holden-Dye, L., O'Connor, V. (2007) The concentration-dependent effects of ethanol on *Caenorhabditis elegans* behaviour. *The Pharmacogenomics Journal*, 7, 411-7.

Bull, K., Cook, A., Hopper, N. A., Harder, A., Holden-Dye, L., Walker, R. J. (2006) Effects of the novel anthelmintic emodepside on the locomotion, egg-laying behaviour and development of *Caenorhabditis elegans*. *International Journal for Parasitology*, 6, 627-36.

Franks, C. J., Holden-Dye, L., **Bull, K.**, Luedtke, S., Walker, R. J. (2006) Anatomy, physiology and pharmacology of *Caenorhabditis elegans* pharynx: a model to define gene function in a simple neural system. *Invertebrate Neuroscience*, 3, 105-22.

Amliwala, K., **Bull, K.**, Willson, J., Harder, A., Holden-Dye, L., Walker, R. J. (2004) Emodepside, a cyclo-octadepsipeptide anthelmintic with a novel mode of action. *Drugs of the Future*, 29, 1015-1024.

Bull, K., Willson, J., Holden-Dye, L., Walker, R. (2006) The potent inhibitory action of the anthelmintic emodepside in the *C. elegans* pharynx requires the latrophilin-like receptor LAT-1 but not LAT-2. *European Worm Meeting Abstract 52*. Available at www.imbb.forth.gr/ewm2006

Bull, K., Harder, A., Holden-Dye, L., Walker, R. (2004) Further investigations to characterize the physiological effects of the novel anthelmintic emodepside on *C. elegans*. *UK C. elegans Meeting Abstract*. Available at www.ucl.ac.uk/~ucbtday/UK_worms.html

Bull, K., Harder, A., Holden-Dye, L., Walker, R. (2004) Further investigations to characterize the physiological effects of the novel anthelmintic emodepside on *C. elegans*. *European Worm Meeting Abstract 22*. Available at www.wormbase.org ID: WBPaper00024728.

CONTENTS

Figures

Tables

ABBREVIATIONS

5-HT	5-Hydroxy-Tryptamine
ACh	Acetylcholine
ADH	Alcohol dehydrogenase
cDNA	Complementary deoxyribonucleic acid
DAG	Diacylglycerol
DMSO	Dimethyl sulfoxide
DNA	Deoxyribonucleic acid
dsRNA	Double stranded ribonucleic acid
EPG	Electropharyngeogram
GABA	γ-amino butyric acid
GluCl	Glutamate-gated chloride channel
IBTX	Iberiotoxin
IP_3	Inositol triphosphate
IPTG	Isopropyl-β-D-Thiogalactopyranoside
nAChR	Nicotinic acetylcholine receptor
NAD	Nicotinamide adenine dinucleotide
NGM	Nematode growth medium
PF1022A	cyclo(D-lactyl-L-N-methylleucly-D-3-phenyllactyl-L-N-methylleucyl-D-lactyl-L-N-methylleucyl-D-3-phenyllactyl-L-N-methylleucyl)
PIP_2	Phosphatidylinositol-4,5-bisphosphate
PLCβ	Phospholipase-Cβ
RNA	Ribonucleic acid
RNAi	Ribonucleic acid interference
SNARE	Soluble *N*-ethylmaleimide-sensitive factor attachment protein receptor
SNAP-25	Soluble *N*-ethylmaleimide-sensitive factor attachment protein of 25 kDa
SNP	Single nucleotide polymorphisms
VAMP	Vesicle-associated membrane protein

CHAPTER 1
INTRODUCTION

1.1 The nematodes

Pseudocoelomate nematode worms (roundworms) are found within the phylum Nematoda. Nematodes may exist as either free-living or parasitic organisms, the former being found in a wide variety of habitats including the soil, freshwater and marine environments. Within the ecosystem, free-living nematodes play a crucial role in the cycling of chemicals and organic nutrients by acting as detritivores or decomposers, by consuming fungi, bacteria and other microflora and microfauna

Parasitic nematodes are capable of infecting a huge number of animal or plant species, often causing diseases which pose a serious threat to the survival of humans, animals and crops in both the tropical and temperate climates (Geary et al., 1999a). In the agricultural and livestock industry, parasitic infection of crop plants or livestock often causes severe losses in productivity and represents an economically limiting factor for industries such as cereal farming as well as sheep and cattle farming. As animal parasites, nematodes can infect almost all the animal phyla, including humans. It has been estimated that one-third of the global human population is infected with one or more species of parasitic helminth, and consequently, nematode diseases are now recognised as one of the most serious causes of human morbidity and early mortality (Bundy & de Silva, 1998).

The important human parasitic diseases can be epidemiologically divided into three subsets: those caused by intestinal parasites and transmitted by their eggs or larvae, such as *Strongyloides stercoralis*, and *Ascaris lumbricoides*; diseases caused by vector-transmitted filarial nematode species, including *Loa loa* and *Onchocerca volvulus*; and diseases caused by parasites in either larval or adult form and not involving insect transmission. The parasites in the final group do not have a simple direct life cycle or infective free-living eggs and larvae. Members of this subset include the *Toxocara* species, which are found only as larvae within humans, and *Trichinella spiralis*, which lives as an adult within the human intestine (reviewed in Whitfield, 1993). Table 1.1 illustrates the major parasitic nematode species causing important diseases in humans, and summarizes their geographical distribution.

Type of Parasitic Nematode	Name of Species	Geographical Distribution
Intestinal Parasites	*Strongyloides stercoralis*	Worldwide in tropical zone
	Ancylostoma duodenale	Worldwide in tropics and subtropics plus mediterranean fringes
	Necator americanus	Worldwide in tropics and subtropics including south east states of USA
	Enterobius vermicularis	Cosmopolitan
	Ascaris lumbricoides	Cosmopolitan
	Trichuris trichiura	Cosmopolitan
Filarial Parasites	*Wychereia bancrofti*	Asia, Africa, S. America, Pacific Islands
	Brugia malayi	South East Asia
	Onchocerca volvulus	Yemen, Africa, Southern and Central America
	Loa loa	Western and Central Africa
	Dipetalonema perstans	Africa and South America
	Dipetalonema streptocerca	Western and Central Africa
	Mansonella ozzardi	South America, Caribbean
Other Nematodes	*Toxocara* spp. (only larvae in humans)	Cosmopolitan
	Dracunculus medinensis	Africa, Middle East, Pakistan, India
	Trichinella spiralis (adults intestinal)	Cosmopolitan

Table 1.1 Important nematode species causing human disease
Adapted from Whitfield. P. J. (1993).

In view of the serious problems that parasitic nematode infections cause for humans, animals and plants, considerable effort has been expended to control these diseases. A variety of different control programmes have been employed and are still being used, including vector control, biological control, vaccination, and environmental manipulation detrimental to the parasite. Anti-parasitic drugs called anthelmintics form another important and highly successful control measure. Numerous investigations have revealed that these drugs may act at several biochemical sites in the parasite, or may act more specifically, often targeting certain nematode receptors or ion channels present at the neuromuscular junction to therapeutically benefit the host organism.

The continual heavy reliance on anthelmintic drugs is believed to be the major driving factor behind the development of resistance in many strains of parasitic nematode. The problem of anthelmintic resistance has now reached critical proportions in the agricultural industry of many regions, including Latin America, Southern USA, Australia, New Zealand and large areas of Africa (Waller, 1997). This has triggered increased investment in the search for new anthelmintics that operate via novel biological pathways, enabling them to overcome the resistance problem.

The cyclic depsipeptide group is a class of compounds containing members which exhibit strong potential as new anthelmintics (Geary et al, 1999a). Emodepside, a semi-synthetic derivative of the cyclic depsipeptide PF1022A, is a promising new anthelmintic drug that demonstrates high efficacy against a broad range of parasitic nematodes in a number of different host species (Conder et al., 1995; Harder et al., 2003; Samson-Himmelstjerna et al., 2000; Sasaki et al., 1992; Zahner et al., 2001a, 2001b). Most importantly, emodepside has been shown to act against parasitic nematode strains which are resistant to currently used anthelmintics, suggesting that the anthelmintic utilizes a novel mechanism of action that could be capable of breaking the resistance problem (Harder et al., 2003).

In this study, the free-living nematode *Caenorhabditis elegans* was employed to investigate the mechanism of action for emodepside and other novel anthelmintic compounds. Previous research has strongly indicated that emodepside targets specific receptors and second messenger signaling pathways at the *C. elegans* neuromuscular junction (Saeger et al., 2001; Harder et al., 2003; Willson et al., 2003, 2004). Therefore, by investigating how emodepside disrupts normal functioning at the neuromuscular junction (NMJ) a greater understanding of neuromuscular signaling and its control at a molecular level can be attained.

1.2 *C. elegans*

C. elegans is a free-living, non-parasitic member of the rhabditid nematode family, and is typically found within the soil environment of temperate climates, where it feeds primarily on bacteria. There are two sexes: the self-fertilising hermaphrodite (shown in figure 1.1) and the male. The hermaphrodite worm is approximately 1mm long at adulthood, with the males being typically slightly smaller.

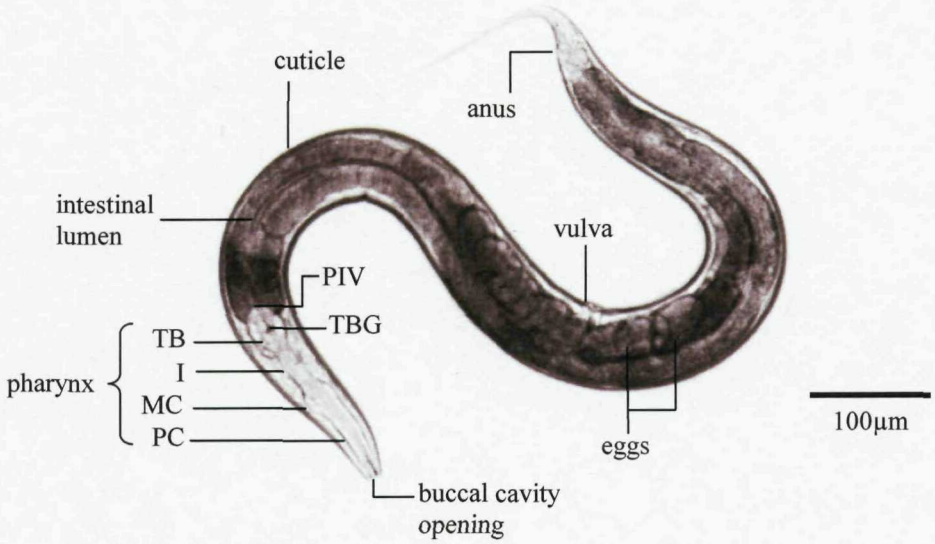

Figure 1.1 A gravid adult wild type (Bristol N2 strain) *C. elegans*
The opening to the buccal cavity is the mouth of the worm and is also termed the stomodaeum. The pharynx is the feeding organ of the worm and consists of the: procorpus (PC), metacorpus (MC), isthmus (I) and terminal bulb (TB). Within the terminal bulb is the grinder (TBG) which breaks down ingested bacteria before it enters the intestine. Separating the pharynx from the intestine is the pharyngeo-instestinal valve (PIV), which prevents bacteria re-entering the pharynx from the gut. The vulva is the muscular opening through which the eggs are expelled. The anus, from which waste is expelled, is also known as the proctodaeum. More detail on nematode anatomy is given in chapter 1, section 1.3, page 16.

1.2.1 The *C. elegans* life cycle

The life cycle of *C. elegans* is relatively short and is temperature-dependent. Development of the worm from the egg to the sexually mature, egg-laying adult occurs in approximately 5.5 days at 15°C, 3.5 days at 20°C, and 2.5 days at 25°C. The worms hatch from their eggs as juveniles, which then develop through four larval stages. The transition between each larval stage is characterised by a moult, during which new cuticle is synthesized. After the fourth moult, the mature adult is produced and remains fertile for approximately four days. During this time, the hermaphrodite worms will

undergo self-fertilization, or will mate with male *C. elegans* if present. After this period of adult fertility, the hermaphrodites will live for an additional ten to fifteen days, during which time each unmated worm will produce 300 to 350 progeny, and each mated hermaphrodite can produce over 1000 progeny. Importantly, if adverse environmental conditions, such as lack of food, are experienced by *C. elegans* early in its developmental life cycle, the worm is capable of entering cryptobiosis at the second or third larval moult. This leads to the production of the dauer larva, which is a third larval stage worm that does not feed and can survive for up to three months without undergoing any further development. If food supplies later become available once more, the dauer larvae will resume development to the fourth larval stage, and will then continue through its life cycle as normal (Burglin et al., 1998). Figure 1.2 illustrates the life cycle of *C. elegans*, including the alternative developmental pathway that leads to dauer formation.

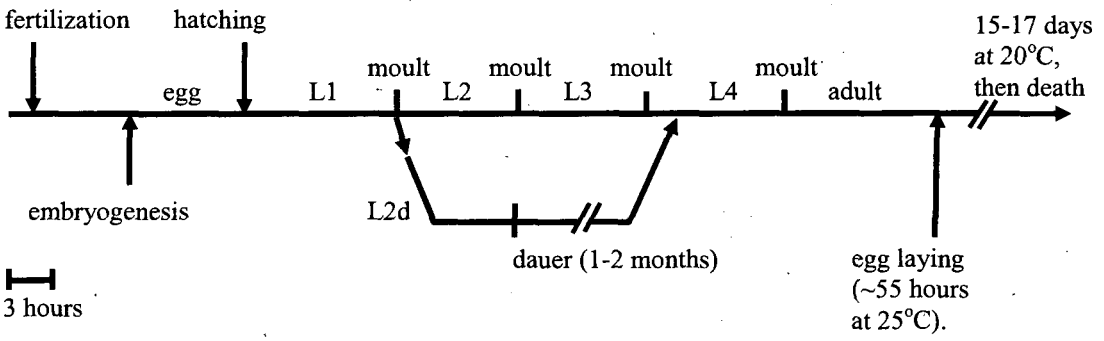

Figure 1.2 The life-cycle of *C. elegans*.
Adapted from Burglin et al. (1998).
The time line is approximately to scale, except where indicated by breaks. The four larval stages (L1-L4), the adult stage (pre- and post egg laying), and the dauer stage are shown. If food is limited in early development, *C. elegans* take an alternative developmental pathway (L2d), and at the L2/L3 moult they become dauer larvae, which do not develop further and can survive without feeding for 1-2 months.

1.2.2 *C. elegans* as a model organism

The development and spread of anthelmintic resistance has eroded the utility of the major commercially available anthelmintics, and is constantly reducing the options for treatment of helminth infection. The discovery and development of novel anthelmintics is essential to preserve the economic and health advantages gained through chemotherapy. However, the costs of drug development continue to escalate dramatically, and therefore, the methodology used to discover new drugs becomes a primary concern. Random screening of infected animals has enabled the development of

all currently used anthelmintics, but the expensive nature of such screening techniques necessitated a new approach to drug discovery.

The anatomic and genetic simplicity of *C. elegans* has promoted the intensive use of this nematode as a model animal system, with the aim of obtaining insights into the development, neurobiology and genetics of 'higher' multicellular organisms (Burglin et al., 1998; Kamath & Ahringer, 2003). *C. elegans* is an excellent model organism for these purposes because it demonstrates a level of complexity sufficient to exhibit many biological properties found in higher multicellular organisms, as well as being simple enough to describe in complete terms (Hashmi et al., 2001; Wood, 1988). Importantly, *C. elegans* displays not only morphological similarities to other nematodes but also shares processes, pathways and characteristics found in parasitic nematodes, such as dauer formation, moulting, and reproduction (Hashmi et al., 2001). The widespread use of *C. elegans* as a model system stems partly from its application in genetically based studies on drug resistance in the worm, studies which have facilitated the clarification of anthelmintic mechanisms of action. For example, genetic studies done in *C. elegans* have provided evidence that benzimidazoles act by interfering with the dynamics of tubulin polymerization (Driscoll et al., 1989). Research utilizing cDNAs cloned from *C. elegans* has shown that the macrocyclic lactones operate by opening glutamate-gated chloride channels, and that mutations to subunits of these channels can confer high-level resistance to specific members of this anthelmintic class (Cully et al., 1996; Sangster & Gill, 1999).

As an experimental model system, *C. elegans* offers many advantages: it has a rapid life-cycle, it is easy and inexpensive to maintain and propagate on agar plates with a lawn of *E. coli*, it is easy to transfer worms or their eggs from plate to plate, and they can be frozen and stored long-term (Burglin et al., 1998). In comparison, parasitic organisms, particularly those of humans, are difficult to grow and maintain, making genetic and transgenic analysis much more difficult and expensive (Blaxter, 1998). An additional advantage of *C. elegans* as a model system is that the worm remains transparent throughout its development, allowing the use of differential interference contrast (Nomarski) microscopy. Cell division during worm development is largely invariant, which has enabled the complete cell lineage to be defined in the worm. This information, when combined with the current detailed anatomical knowledge of *C. elegans*, has enabled the fate of each cell to be precisely described during development

(Burglin et al., 1998). Importantly, the *C. elegans* research community has developed numerous powerful laboratory techniques to enable incredibly detailed understanding of the biology of this free-living nematode worm. Such techniques include methods for creating and rescuing mutant phenotypes, RNA interference, genetic crosses and transformations, as well as *in situ* hybridization and immunolocalization (Fraser et al., 2000; Fire et al., 1998; Hashmi et al., 2001). In 1998, *C. elegans* became the first multicellular eukaryote to have its genome completely sequenced, revealing vital information on the molecular, physiological, and developmental mechanisms employed by this nematode, further promoting its use as a model system (Burglin et al., 1998; Hashmi et al., 2001; Kamath & Ahringer, 2003).

Despite the numerous advantages of *C. elegans* as a model for parasitic nematodes there are major disadvantages. It is to be expected that adaptive evolution will have resulted in parasitic nematodes possessing many biological and physiological features specific to their parasitic life strategies and therefore not found in free-living *C. elegans*. Modern phylogenetic analysis using small subunit ribosomal RNA has grouped *C. elegans* in Clade V of the phylum nematoda with the parasitic strongylid nematodes including *H. contortus*, *N. brasiliensis* and the *Necator* human hookworms (see figure 1.3; Blaxter, 1998).

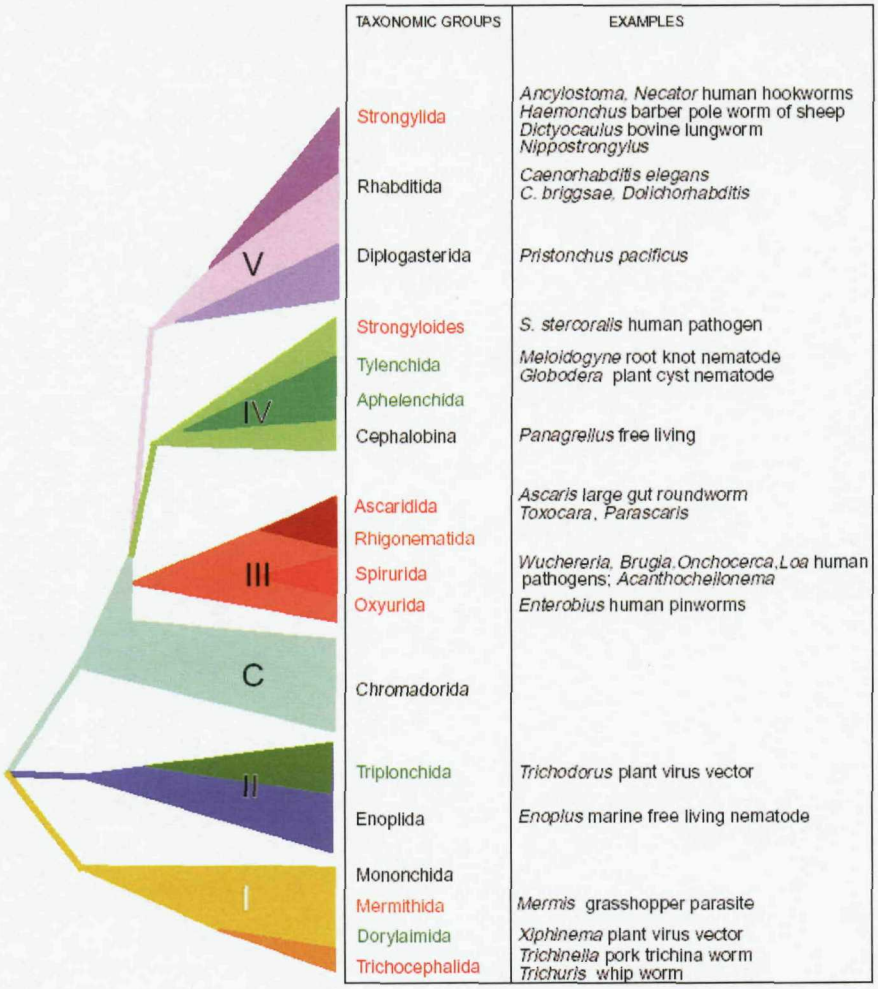

Figure 1.3 A schematic of the phylum nematoda (adapted from Blaxter, 1998).
C. elegans is a rhabitid nematode, grouped with the diplogasterids and animal-parasitic strongylids in clade V. Clade IV groups together the free-living cephalobes, plant-parasitic tylenchids, fungal-feeding aphelenchids, and animal-parasitic strongyloids. Clade III contains several closely related major human parasites, including *Ascaris*. Clade III, IV and V are traditionally called the secernentea, which arose from the microbivorous aquatic nematodes of clade C called the chromadorida. Clade II includes the plant-parasitic triplonchida and free-living enoplida. Clade I groups the insect-parasitic mermithida, plant-parasitic dorylaimida, animal-parasitic trichocephalida and free-living mononchida.

It might be assumed that *C. elegans* would possess greater genetic similarity to parasitic nematodes more closely related phylogenetically, such as the species in Clade V. Analysis of the approximately 250,000 expressed sequence tag (EST) sequences currently available from all nematodes showed that 50–70% of sequences from Clade V species have significant similarity to *C. elegans* predicted proteins. However, even the more distantly related parasitic *Trichuris* species of Clade I have been shown to possess similarity to *C. elegans* in around 45% of their genes (Parkinson et al., 2004). Therefore, *C. elegans* does show significant genetic similarity to many parasitic species in the phylum nematoda, but there exist many genetic differences (over 50% of *Trichuris* species genes are different to *C. elegans*), and these genes may be key factors

in determining the applicability of *C. elegans* as a model for specific nematode species. It must also be considered that a gene in *C. elegans* may possess a homolog gene in a parasitic nematode, but the protein product may perform different roles in the different species, even when genetically rescued in the alternative parasitic/free-living environment. For example, RNAi and genetic mutant analysis has revealed that the cathepsin L protease gene of *C. elegans*, essential for the degradation of yolk protein during embryonic development, is highly conserved in a number of parasitic nematodes (Britton & Murray, 2004). Whilst knockout of this gene in *C. elegans*, either by RNAi or genetic mutation, leads to almost total embryonic lethality, this phenotype was shown to be rescued with the putative homologue from *H. contortus* but not *B. malayi*. As *B. malayi* is a filarial parasite whose development is not dependent on egg yolk as a nutrient source, these results are explainable, and suggest that *C. elegans* is a better model for *H. contortus* cathepsin L protease function than for the *B. malayi* protease (Britton & Murray, 2006, 2002; Hashmi et al., 2002).

Behm et al. (2005) strongly recommend a coordinated RNAi- and genomics-based strategy for identifying and validating antifilarial drug targets. For this strategy, Behm proposes an initial phase combining three techniques for target identification: (1) RNAi- and mutagenesis-based screens of *C. elegans* to identify potential targets, followed by homolog screening in *B. malayi* and *O. volvulus* for mutants with severe defects in viability; (2) bioinformatics studies of filarial genome sequences to identify additional candidate targets that are not present in *C. elegans* but are conserved in yeast and *Drosophila*; (3) integration of data from parasite biochemistry investigations that have identified new targets experimentally. Following this initial stage, Behm et al. (2005) propose that a Target Selection Team would consider all candidates and prioritise them for functional assessment by RNAi in *B. malayi* according to specific criteria shown in table 1.2. Candidate targets that elicit suitable RNAi phenotypes in *B. malayi* would be used to identify potential anthelmintics. However, Behm et al. (2005) acknowledge that RNAi techniques for *B. malayi* are, at present, highly labour intensive and expensive, therefore, this technique would need to be improved considerably before the proposed strategy for drug target identification could be implemented. Another problem with the proposed strategy is revealed by initial sequence comparison of the *C. elegans* and *B. malayi* genomes which indicates that although there is chromosomal linkage of genes, there is little local synteny, making identification of orthologous genes more difficult (Britton & Murray, 2006).

Criteria for selecting suitable antifilarial drug targets	
Selectivity and validation	(i) Either: ▪ Target is absent from mammals, or ▪ Target has molecular properties that distinguish it from related mammalian proteins, and/or ▪ Evidence exists that the target can be selectively chemically inhibited or agonized relative to other members of the same protein family (ii) Evidence (RNAi, knockouts, inhibitors, etc.) that the target is essential for growth, survival or fertility
'Druggability'	Priority is given to: ▪ Molecules with a small-molecule ligand-binding pocket (e.g. channels, receptors, transporters and enzymes) ▪ Molecules that have precedents (i.e. existing drugs or ligands)
Structure	▪ Amino acid sequence of the target is known ▪ Desirable, but not essential: crystal or NMR structure of related proteins is known or obtainable, preferably with bound cofactors, inhibitors or agonists/antagonists
'Assayability'	(i) Important features: ▪ Expression precedent available ▪ Existing biochemistry/enzymology ▪ Single subunit is desirable ▪ Specific readout that can be predicted, especially optical, that is compatible with high-throughput screening ▪ Active site chemistry available (ii) Other desirable features include: ▪ Focused chemical library already available for the class of molecule ▪ Cell-based assays ▪ Assays with functional endpoints ▪ Assays with fewer steps (e.g. washes)
Potential for development of resistance	▪ Absence of isoforms of the target with varying susceptibility within a species ▪ Absence of biochemical 'bypass' reactions to circumvent function of the target

Table 1.2 Antifilarial Drug Target Selection Criteria proposed by Behm et al. (2005) for prioritizing potential drug targets identified by a combination of RNAi-based and genomics-based screening of model organisms such as *C. elegans* and parasites such as *B. malayi*, as well as bioinformatics studies and biochemical research in parasites.

In conclusion, the *C. elegans* model has contributed enormously to current understanding of nematode biology and has proved vital in the understanding of anthelmintic mechanisms of action. However, aspects of parasitic nematode biology which facilitate their host-dependent lifestyle can not be precisely modelled by the free-living *C. elegans*. Therefore, a greater understanding of the biology of nematode parasitism is crucial, and must be combined with current knowledge of *C. elegans* to produce a more accurate and detailed comprehension of parasite physiology.

1.2.3 RNA interference (RNAi) in *C. elegans* and parasitic nematodes

Genetic interference mediated by double-stranded RNA (RNAi) has been a valuable tool in the analysis of gene function in *C. elegans* (Fire, 1999; Simmer et al., 2002; Timmons et al., 2001). A variety of species, including *C. elegans*, exhibit the defence response in which exogenous double stranded RNA (dsRNA) acts as a trigger to produce premature loss of endogenous RNAs which possess sequence identity to the dsRNA (Timmons et al., 2001).

RNAi delivery to *C. elegans* can be achieved by several methods: microinjection of dsRNA; feeding on bacteria expressing dsRNA; soaking in dsRNA; and transformation with hairpin constructs that produce dsRNA (Fire et al., 1998; Timmons & Fire, 1998; Simmer et al., 2003; Wang & Barr, 2005). It is the ability of the RNAi to 'spread' to cells located some distance from the initial site of dsRNA entry that enables delivery methods such as injection to produce robust interference throughout the injected animal, including the germ cells (Timmons et al., 2001). *C. elegans* genes involved in the uptake of dsRNA (during the soaking method for example) and the spreading of RNAi throughout the worm (following dsRNA injection for example) have been identified, including *sid-1*. *C. elegans sid-1* encodes a transmembrane protein expressed strongly in cells that directly contact the worm environment, and *sid-1* mutants appear defective in the uptake of externally supplied dsRNA and the spread of RNAi within the worm (Feinberg & Hunter, 2003; Tijsterman et al., 2004; Winston et al., 2007, 2002). *Drosophila* cells transformed with an expression construct containing *C. elegans sid-1* results in dsRNA uptake by the cells, suggesting that *C. elegans* SID-1 can function in other species (Feinberg & Hunter, 2003).

Biochemical experiments in *Drosophila* have enabled the identification of many of the proteins and protein complexes that have an important role in the RNAi reaction (Hammond et al., 2001, 2000; Nykanen et al., 2001). It has been proposed that the exogenous dsRNA is first cleaved into short RNA fragments of approximately 23 base pairs by the enzyme RNAse III (DICER) (Bernstein et al., 2001). *In vitro* and *in vivo* studies in *Drosophila* and *C. elegans* have shown that this activity is crucial for the RNAi process. *In vivo* experiments in *C. elegans* have also indicated that a complex of the RDE-4 protein, DICER, and an RNA helicase called DRH-1 are required for short interfering RNA (siRNA) production during RNAi (Parrish & Fire, 2001; Tabara et al.,

2002). The siRNA is incorporated into a protein complex named RISC (RNA-inducing silencing complex), and then binds in a complementary fashion to the mRNA (Hammond et al., 2000). The RISC complex induces a break in the target mRNA in the region covered by the siRNA molecule, leading to the degradation of the mRNA transcribed from the target gene (Elbashir et al., 2001).

A bacterial library has been constructed corresponding to approximately 86% of the estimated 19,000 predicted genes in *C. elegans*. This library enables RNAi by feeding to be a high-throughput functional genetic tool, and has already proved successful in the screening for genes involved in embryonic development, aging, and genome stability (Kamath & Ahringer, 2003).

RNAi by feeding involves PCR amplification of a DNA fragment of the gene of interest, followed by cloning of this fragment into a vector containing the T7 promoter sites flanking each side of the multiple cloning site (MCS), which enables production of dsRNA from the vector by T7 polymerase. Plasmid vectors containing the DNA fragment are transformed into the bacterial strain HT115(DE3), an RNase III-deficient strain of *E. coli* in which the T7 RNA polymerase is only expressed in the presence of IPTG (isopropyl-β-D-thiogalactopyranoside). The RNase III deficiency of HT115(DE3) is believed to lead to the production of more stable dsRNA within the bacteria, thereby improving the efficacy of RNAi by feeding (Kamath & Ahringer, 2003).

A number of *C. elegans* strains have been identified that enhance the efficiency of RNAi. These strains typically contain a mutation in a gene encoding a protein that negatively regulates the RNAi process, for example, loss-of-function mutations in the *rrf-3* gene produce worms with significantly increased sensitivity to RNAi by feeding. The *rrf-3* gene encodes a putative RNA-directed RNA polymerase (RdRP) which appears to negatively regulate RNAi (Sijen et al., 2001; Simmer et al., 2002). Another *C. elegans* strain used for RNAi experiments is the *eri-1* mutant. The *eri-1* gene encodes a protein that degrades siRNAs, and therefore, loss-of-function mutations in *eri-1* have been shown to produce *C. elegans* with improved sensitivity to RNAi (Kennedy et al., 2004; Timmons, 2004).

The successful use of RNAi in *C. elegans* as a tool for analysing gene function combined with the conservation of the RNAi mechanism in a wide range of organisms,

including protozoa, insects and mammals, has suggested that RNAi could be applied to parasitic nematodes to discover the genes involved in anthelmintic activity and resistance (Misquitta & Paterson, 1999; Ngo et al., 1998; Wianny & Zernick-Goertz, 2000). However, the application of RNAi to parasitic nematodes has produced extremely variable levels of success. In animal parasitic nematodes, the RNAi technique has been attempted for 28 genes, with significant reduction in mRNA achieved for 13 of these. In *H. contortus*, of the eleven genes for which RNAi has been attempted against, two genes have been successfully targeted, and in *O. ostertagi* three of the eight genes targeted with RNAi have shown mRNA reduction (Geldhof et al., 2006; Visser et al., 2006). Limited success of RNAi in *N. brasiliensis*, *B. malayi*, *O. volvulus*, *A. suum* and *T. colubriformis* has also been reported (e.g. Islam et al., 2005; Issa et al., 2005; Lustigman et al., 2004). Importantly, only RNAi by external application of dsRNA or siRNA has been attempted in these experiments, therefore requiring the uptake and spreading of the RNAi throughout the parasite to achieve success. Significantly, *Drosophila* and *Caenorhabditis* species other than *C. elegans*, such as *C. briggsae*, have been shown to be susceptible to RNAi when dsRNA is supplied internally but not externally (Baird & Chamberlin, 2006; Winston et al., 2007; Zappe et al., 2006). This suggests that in these species, the core cellular machinery for RNAi is present and functional, but the molecular components required for RNAi uptake and/or spread have non- or reduced-function. Supporting this, transformation of *C. briggsae* with an expression construct for *C. elegans* SID-2, which has been shown to be important in the uptake of dsRNA, has resulted in susceptibility to RNAi when dsRNA as applied externally (Feinberg & Hunter, 2003; Winston et al., 2007). It is possible that the successful use of RNAi on parasitic nematodes requires the internal supply of dsRNA or the transformation of parasitic nematodes with expression constructs for *C. elegans* genes required for RNAi uptake and spread. Viney et al. (2008) suggest *C. elegans sid-1* as a candidate gene because *Drosophila* transfected with a *sid-1* expression construct were capable of dsRNA uptake, enabling RNAi by external supply of dsRNA and suggesting that animal parasitic nematodes may also be engineered in the same way to improve RNAi (Feinberg & Hunter, 2003).

The reason why *C. elegans* and plant parasitic nematodes are the only nematodes susceptible to RNAi from externally supplied dsRNA may be explained by the different lifestyles of the nematode species. It has been suggested that animal-parasitic nematodes receive greater exposure to viruses and other sources of foreign nucleic acids than plant-

parasitic nematodes, resulting in evolutionary pressure that selects those animal-parasitic nematodes incapable of taking up foreign RNA and unable to facilitate the spread of foreign RNA throughout the parasite upon infection (Knox et al., 2007; Viney et al., 2008). For RNAi in *C. elegans* to be an effective tool for investigating anthelmintic activity, identifying of novel anthelmintics, and understanding resistance, a more thorough analysis of the RNAi mechanisms present in parasitic nematodes is essential. As discussed in section 1.2.2, *C. elegans* is a useful model for parasitic nematodes, but the different selection pressures attributed to the free-living and parasitic life strategies will result in genetic differences that will necessitate validation of the results from *C. elegans* investigations in a parasitic model. Therefore, improvement to methodology and understanding of RNAi in parasitic nematodes is crucial and, if achieved, could become a vital tool for screening and validating new anthelmintics.

1.3 General nematode anatomy

Nematodes typically have a bilaterally symmetrical body shape consisting of a cylinder with tapered ends. Located at the extreme anterior of the animal is the opening of the buccal capsule, which is lined by cuticle. The sensory structures are also found anteriorly, and these may include a combination of glands, papillae, or bristles (reviewed in Bush et al, 2001). A highly schematic representation of basic nematode morphology is shown in figure 1.4, which also includes representations of both sexually mature female and male worms.

The nematode body wall consists of an outer epicuticle and, lying beneath this, the cuticle itself. A basement membrane then marks the division between the cuticle and the underlying epidermis, which is located above the longitudinal muscle of the worm. The highly stable cuticle, composed of mainly collagen and glycoproteins, antagonises the worm's longitudinal muscles to form a vital part of the animal's hydroskeleton. However, in parasitic nematodes, this structure also acts as a first line of defence against pathogens and anthelmintics, as well as protecting against the host immune system (Blaxter et al., 1992; Grieve, 1990). Additionally, the nematode cuticle has been proposed to play a role in the processes of worm nutrition and excretion (Sims et al., 1996).

Beneath the somatic musculature of the nematode is the pseudocoel: a cavity filled with the fluid hemolymph. The pseudocoel has two major functions in the worm: firstly, it is the primary component of the hydrostatic skeleton, and is therefore essential for nematode movement, and secondly, in the absence of a circulatory system, the pseudocoel is a crucial means of transporting solutes from tissue to tissue (reviewed in Bush et al., 2001; Johnstone, 1998).

The nematodes have a complete digestive system with two openings: the anterior mouth (stomodaeum) and posterior subterminal proctodaeum (anus in females, cloaca in males). The mouth leads directly into the buccal capsule, which then connects with the pharynx, and these structures are lined with cuticle.

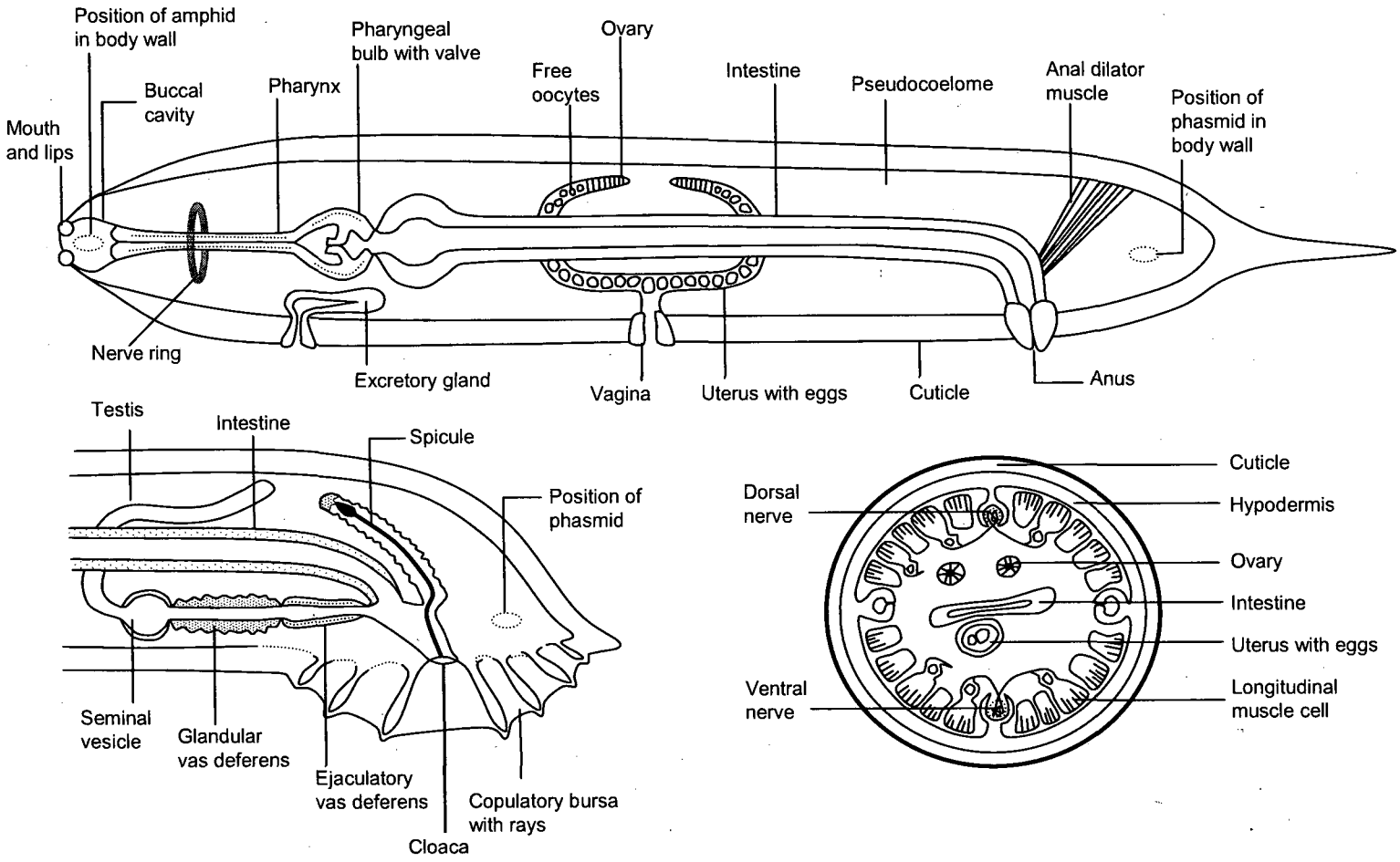

Figure 1.4: Schematic representation of nematode morphology
(Adapted from Whitfield, P. J. (1993) *Modern Parasitology* (Cox, F. ed)).
(a) A sexually mature female worm, (b) the posterior end of a sexually mature male worm, (c) transverse section through a female worm.

The nematode intestine consists of the foregut, which terminates in a valve and is followed by the midgut, and finally the hindgut. The nematode midgut is relatively unspecialised and does not possess muscle tissue; therefore propulsion of bacterial food down this intestinal region is thought to rely on pharyngeal pumping, high internal hydrostatic pressure and, possibly, worm locomotion. The nematode hindgut is essentially a tube lined with cuticle which connects the posterior intestine to the anus in females and cloaca in males. In male nematodes, the subterminal proctodaeum is named the cloaca because the vas deferens opens into the male rectum. Under experimental conditions, *C. elegans* empties its gut approximately every 45 seconds (reviewed in Bush et al., 2001).

Parasitic nematodes of animals are typically dioecious and often show sexual dimorphism. In *C. elegans*, the 'female' worms are, in fact, hermaphrodite, and are thus capable of self-fertilization. Male *C. elegans* do occur, but in much lower numbers than the hermaphrodites. Male nematodes are generally smaller than the females, and possess a single thread-like testis which merges into a seminal vesicle, followed by the vas deferens before terminating in the cloaca. The sperm of male nematodes do not possess flagella or cilia, and have been observed to move in a fashion similar to amoeboid locomotion using temporary pseudopodia (reviewed in Bush et al., 2001).

The female reproductive system in nematodes is often paired, with each proximally positioned thread-like ovary connecting to a slightly larger oviduct, which then merges with the uterus. The highly muscular distal ends of the uterus are often termed the oviprojectors, and from the two uteri these combine to form the short vagina that opens to the exterior environment via the vulva. The region at the junction of the oviduct and uterus forms the seminal receptacle, and is the site of fertilization (reviewed in Bush et al., 2001; Johnstone, 1998).

Unlike the platyhelminthes and arthropoda, the existence of specialized structures for the maintenance of position within an animal host is uncommon in the parasitic nematodes. However, there are exceptions, for example the tooth-like cuticle-derived structures of the hookworm and the preanal sucker on *Heterakis* species. The parasitic nematodes of animals are generally found in the tissue or gut of the host. Parasitic nematodes must resist being expelled from the host gut by muscular contraction and peristaltic movement. In addition to cuticle-derived attachment structures, it has been

proposed that secretions from the worm, including a 'vasoactive intestinal polypeptide-like protein', act as a 'biochemical holdfast' by reducing intestinal peristalsis (Lee, 1996).

1.3.1 The anatomy of the nematode pharynx

The nematode pharynx is a highly muscular organ responsible for generating sufficient pressure to suck food into the worm and propel it into and along the intestine. This force is necessary due to the higher pressure of the worm interior compared to the surrounding environment (Harris & Crofton, 1957). The nematode pharynx is tri-radiate in cross-section, and consists of up to three major regions: the corpus, isthmus, and bulb with tricuspid valve. Throughout the nematode groups, one or all of these regions are present, and within each group there may be further variations in the organisation of these pharyngeal regions. Associated with the pharynx is a dorsal gland and two subventral glands, and these may produce secretions important for digestive processes, such as anticoagulation (e.g. Blackburn & Selkirk, 1992; Pritchard et al., 1994).

C. elegans has been used extensively as a model organism to investigate the anatomy of the nematode pharynx. In this worm species, the pharynx is composed of 20 muscle cells, 9 epithelial cells, 5 gland cells, 20 neurons and 9 marginal cells (Albertson & Thomson, 1976). At the anterior of the pharynx is the corpus, which is composed of the procorpus and metacorpus, followed by the isthmus, and then the terminal bulb at the posterior. The position and structure of the pharynx in *C. elegans* is shown photographically and diagrammatically in figure 1.5.

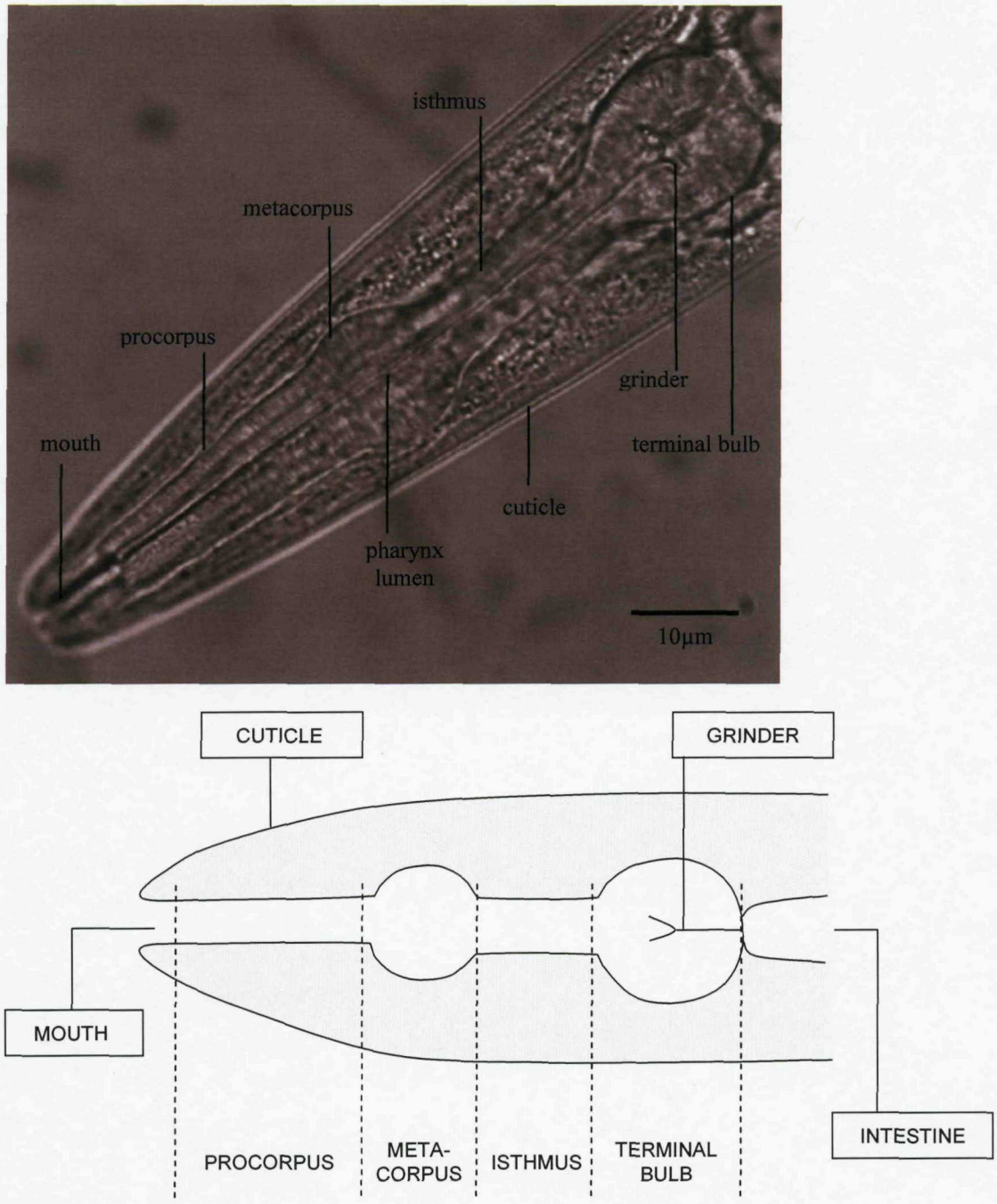

Figure 1.5 The pharynx of *C. elegans*
(a) Light microscopy image of a wild type (Bristol N2 strain) *C. elegans* pharynx.
(b) A simplified diagram enabling identification of the major regions of the pharynx shown in (a). The procorpus and metacorpus are often grouped together in the literature under the name corpus.

There are eight muscle layers in the *C. elegans* pharynx, with each layer consisting of one or three cells (Albertson & Thomson, 1976). Muscle layer m1 contains only one cell positioned at the extreme anterior of the pharynx, where it forms a thin muscle sheet completely surrounding the triangular lumen. Six thin processes project posteriorly from this cell, with each process joining to one other at a binucleate cell body in the nerve cords. Muscle layer m2 is positioned posterior to m1, and also forms a thin sheet around the pharynx lumen, but is composed of three cells. Each m2 cell has a projection terminating in a single nucleus in the nerve cords. Muscle layers m3, m4 and m5 are each formed from three wedge-shaped cells; each with two nuclei positioned either side of the nerve cord. Muscles m1, m2 and m3 together form the procorpus of the pharynx, with m4 forming the metacorpus, and m5 the isthmus. The muscles comprising the terminal bulb are m6, m7 and m8, with the three T-shaped m6 cells slotting into the three posteriorly positioned m7 cells. The m8 muscle layer is a single saucer-shaped cell which lines the extreme posterior wall of the pharynx. Figure 1.6 illustrates the structure of the *C. elegans* pharynx musculature.

Pharyngeal behaviour is composed of two motions: isthmus peristalsis and pumping (Avery & Horvitz, 1989). A pump consists of a nearly simultaneous contraction of the corpus, anterior isthmus and terminal bulb muscles, followed by their almost simultaneous relaxation. During pumping, the contraction of the radially oriented muscles of the corpus and isthmus opens the pharynx lumen, allowing liquid surrounding the worm to be sucked into the corpus where bacteria suspended in the liquid become trapped (Seymour et al., 1983). These bacteria are then propelled from the anterior isthmus to the terminal bulb by peristaltic contraction of the pm5 muscles, a motion called isthmus peristalsis (Doncaster, 1962). During the following pump, these bacteria are than processed through the grinder and propelled into the intestine by the contraction of the terminal bulb. Also during this pump, further bacteria are sucked into the anterior pharynx as a result of muscle contraction in the corpus and anterior isthmus.

The timing of muscle relaxation during pumping is thought to be crucial in ensuring that suspended bacteria that are engulfed during a pump become trapped in the corpus and are not expelled with the fluid during relaxation of the corpus and anterior isthmus (Avery, 1993). The timing of pumping and isthmus peristalsis is regulated by the nervous system of the pharynx, and is described in detail in section 1.4.5 (page 31).

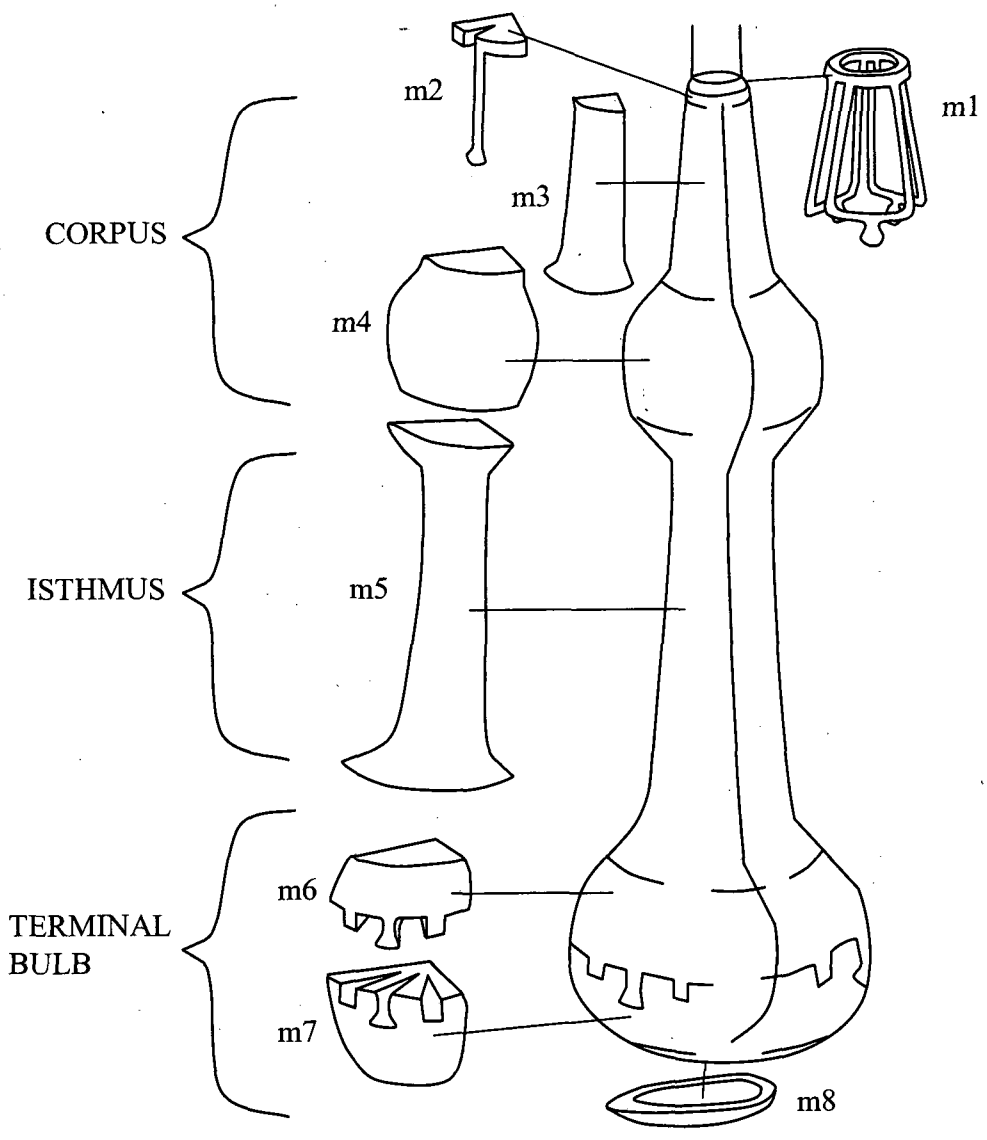

Figure 1.6 The musculature of the *C. elegans* pharynx.
(Adapted from Albertson & Thompson, 1976).

1.4 The nematode nervous system

Current understanding of the nematode nervous system was initially obtained from investigations using the parasitic nematode *Ascaris suum*, and later the free-living nematode *C. elegans*. A high degree of neuroanatomical similarity exists between these two nematode species, reinforcing the viability of *C. elegans* as a model for investigating the functioning of the parasitic nematode nervous system.

Approximately one-third of all the somatic cells in *C. elegans* form the nervous system of the worm, which has many similar and different properties to the vertebrate nervous system. Those gene systems conserved between worm and vertebrate include neurotransmitter biosynthetic enzymes, synaptic release mechanisms, neurotransmitter receptors (both ligand-gated ion channels and G protein-coupled receptors), most ion channels, and most second messenger pathways. However, *C. elegans* has a comparatively higher number of gene families with just one member, therefore supporting the theory that the mammalian genome underwent two large-scale duplications early in evolution (reviewed in Sidow, 1996).

1.4.1 The central nervous system

The nervous systems of *A. suum* and *C. elegans* are largely homologous in terms of neuronal types present, their morphology and arrangement within the worm. The circumpharyngeal nerve ring (sometimes called circumesophageal nerve ring) is located in the anterior of the worm, around which most of the nematode nervous system is organised. The nerve ring is often referred to as the nematode 'brain', and it contains almost all the interneurons and axons from most sensory neurons in the worm. A large number of processes in the nerve ring enter and leave ventrally, and these collectively form the ventral nerve cord (White et al., 1986). Half of all neurons in *C. elegans* are interneurons, one-quarter are sensory neurons, and one-quarter are motor neurons. Most of the sensory neurons are located in the head, projecting sensory dendrites to the nose tip, presumably because this is the first area of the worm to experience any environmental changes. The morphology of sensory neurons in nematodes suggests a chemosensory or mechanosensory role, but there is at least one thermosensory neuron called AFD (Gibbons, 2002).

1.4.2 The motor nervous system

There are thirty classes of nematode motor neuron, and these innervate the muscles of the body wall, pharynx, egg-laying apparatus, and anus (for defecation). The structure of the neuromuscular junctions (NMJs) in the worm is diverse, with pharyngeal and egg-laying NMJs at or near the end of motor axons or branches extending to the muscles. Innervation of the nematode body wall muscles is more complex than that for vertebrate skeletal muscle, with most muscle cells receiving synaptic input from three or more excitatory or inhibitory motor neurons. This may be responsible for graded muscle contraction in the worm, allowing a balance of graded excitation and inhibition by several classes of motor neuron (Gibbons, 2002).

From the anterior nerve ring, the ventral and dorsal nerve cords extend to the posterior of the worm, and are divided into five lateral segments, each containing eleven motor neurons located completely within that segment, and six interneurons that traverse the segments (Stretton et al., 1978). The motor neurons can be separated into seven distinct types: DI, DE1, DE2, DE3, VI, V-1 and V-2. The excitatory DE1, DE2 and DE3 and inhibitory DI innervate the dorsal muscle cells, whilst the excitatory V-1, V-2 and inhibitory VI innervate the ventral muscle cells (Walrond et al., 1985; Walrond & Stretton, 1985).

1.4.3 Molecular components of the *C. elegans* neuromuscular junction

1.4.3.1 Voltage-gated ion channels

Voltage-dependent currents for both calcium (Ca^{2+}) and potassium (K^+) have been obtained from neurons and muscle cells in *C. elegans*, implying the existence of voltage-gated Ca^{2+} and K^+ channels in this worm (Goodman et al., 1998; Lee et al., 1997).

The voltage-gated Ca^{2+} channels open in response to presynaptic depolarization, enabling Ca^{2+} entry and triggering presynaptic exocytosis and eventual muscle contraction or relaxation depending on the neurotransmitters released. In *C. elegans* this channel is composed of one $\alpha 1$ subunit, and accessory $\alpha 2$, δ, β, and γ subunits. There are five predicted $\alpha 1$ subunit genes in the worm genome, three of which are related to L-type channels, N/P/Q-type channels or T-type channels, as well as two $\alpha 1$ genes with

little similarity to any vertebrate channel genes, but with homology to a channel in the yeast *Schizosaccharomyces pombe* (Lee et al., 1997; Schafer & Kenyon, 1995).

C. elegans has approximately 80 predicted K^+ channel genes encoding three types of channel: inward rectifier channels (e.g. Fleischhauer et al., 2000), two pore or TWIK channels (e.g. De la Cruz et al., 2003), and voltage-regulated channels (e.g. Franks et al., 2002). The Ca^{2+} activated K^+ channel of *C. elegans* facilitates entry of K^+ into excitable cells such as neurons and muscle, and therefore this channel contributes to the regulation of the cell resting potential and excitability (e.g. Salkoff et al., 2006; Wang et al., 2001).

1.4.3.2 Neurotransmitters and neuropeptides

In the nematode, muscle activity is controlled by a number of different neurotransmitters and neuromodulators (Walker et al., 2000). A combination of experimental techniques have enabled the identification in *C. elegans* of the neurotransmitters acetylcholine (ACh; e.g. Ballivet et al., 1996), dopamine (e.g. Sulston et al., 1975; Wintle & Van Tol, 2001), 5-Hydroxytyptamine (5-HT, e.g. Desai et al., 1988; Horvitz et al., 1982), γ-aminobutyric acid (GABA; e.g. McIntire et al., 1993), glutamate (e.g. Hart et al., 1995; Maricq et al., 1995), and the invertebrate-specific biogenicamine octopamine (e.g. Horvitz et al., 1982). The distribution and physiological actions of these neurotransmitters are summarized in table 1.3. In *C. elegans*, the enzymes required for the synthesis of dopamine, 5-HT and octopamine, as well as enzymes essential to synaptic vesicular transport have been identified (e.g. Francis et al., 2005; Hare & Loer, 2004; Horvitz et al., 1982; Sakamoto et al., 2005).

The main excitatory and inhibitory transmitters that target nematode body wall muscle are ACh and GABA, respectively (Johnson & Stretton, 1985; Richmond & Jorgensen, 1999; Walker et al., 1992; Walrond et al., 1985). 5-HT also affects body wall muscle but not directly; instead 5-HT has been shown to inhibit ACh induced muscle contraction in *A. suum* (Trim et al., 2001). In the *C. elegans* pharynx, ACh and 5-HT increase pharyngeal pumping, whereas GABA, glutamate, octopamine and dopamine inhibit pumping (Avery & Horvitz, 1990; Lee et al., 1997; Pemberton et al., 2001; Raizen et al., 1995; Rogers et al., 2001).

Transmitter	Distribution	Physiological Actions			
		Somatic Muscle	**Nervous System**	**Pharyngeal muscle**	**Reproductive Muscle**
Acetylcholine	Excitatory motor neurons, sensory neurons e.g. amphids	Excitatory	Excitatory	Inhibitory	No effect
GABA	Inhibitory motor neurons and interneurons	Inhibitory	Inhibitory	Inhibitory	Not determined
Glutamate	Interneurons, M3 motor neurons (pharynx)	Modulatory	Excitatory	Inhibitory	Not determined
5-HT	ENS- pharyngeal, neurons in male tail, female reproductive system	Modulates ACh	Inhibitory	Stimulatory/ excitatory	Stimulatory (egg laying)
Dopamine	Sensory neurons in female reproductive system	Modulatory	Inhibitory	Inhibitory	Inhibitory
Octopamine		Modulatory		Inhibitory	Inhibitory

Table 1.3 The distribution and actions of 'classical' neurotransmitters in nematodes. (Adapted from Brownlee et al., 2000).

A number of neuroactive peptides have also been shown to cause the excitation or inhibition of body wall and pharyngeal muscle (Rogers et al., 2001). Neuropeptides have been found to play diverse roles in the nervous system of species throughout the animal kingdom, and the FaRPs (FMRFamide-related peptides) and FLPs (FMRFamine-like peptides) are the most widely studied family of invertebrate neuroactive peptides (Cowden et al., 1993; Stretton et al., 1991). Research has demonstrated that the immunoreactivity to neuropeptides is widespread in nematode nervous systems, suggesting that these molecules play a significant role in neurosignaling within these animals (Brownlee et al., 2000, 1993; Maule et al., 1996; Stretton et al., 1991).

The FMRF-amides are nematode neuropeptides which have been shown to have a role in numerous aspects of *C. elegans* physiology, including locomotion (Li et al., 1999; Nelson et al., 1998a, 1998b; Waggoner et al., 2000), response to nose touch (Li et al., 1999; Nelson et al., 1998b), response to environmental osmolarity (Nelson et al., 1998b), and egg laying behaviour (Li et al., 1999; Schinkmann & Li, 1992; Trent et al., 1983). Research in *C. elegans* has also demonstrated that specific FMRFamide peptides

can alter pharyngeal pumping rates, with an effectiveness similar to the classical transmitters 5-HT and octopamine. The peptides encoded by *flp-5*, *flp-6*, *flp-8* and *flp-14* were shown to increase pharyngeal pumping rate, whereas the FMRFamides encoded by *flp-1*, *flp-3*, *flp-9*, *flp-13* and *flp-16* appeared to inhibit pumping (Rogers et al., 2001).

1.4.3.3 Ligand-gated ion channels

C. elegans has approximately 100 genes encoding ligand-gated ion channels. These channels form neurotransmitter receptors in the worm because of their rapid opening and desensitization capabilities, thereby allowing short-term signaling. Within *C. elegans*, the excitatory receptors are sensitive to ACh and glutamate, and inhibitory receptors to GABA and glutamate. At both the nematode and vertebrate neuromuscular junction, excitatory motor neurons release ACh to produce muscle contraction (Stretton et al., 1985). In *C. elegans*, there are approximately 40 predicted ligand-gated (nicotinic) ACh receptor subunits, several of which have been identified as sensitive to the anthelmintic levamisole: *unc-29*, *unc-38*, and *lev-1*, *lev-8* and *unc-63* (Culetto et al., 2004; Fleming et al., 1997; Towers et al., 2005). The *C. elegans* excitatory glutamate receptors include six predicted receptors of the AMPA/kainate class and two predicted receptors of the NMDA class (Brockie et al., 2001; Hart et al., 1995). *C. elegans* also possess glutamate-gated chloride channels, which are one of the molecular targets for the ivermectins (Cully et al., 1994; Dent et al., 1997).

1.4.3.4 G protein-coupled receptors

G protein-coupled receptors, when compared to ligand-gated receptors, typically generate slower and longer-lasting alterations to neuronal excitability. G protein-coupled receptors have seven transmembrane domains, and are associated with a cytoplasmic heterotrimeric G protein consisting of an α, β, and γ subunit (reviewed in Heer, 1995). In *C. elegans* 20 different G protein α subunits have been identified, including one G_o-, G_q- and G_s-like protein, and 17 protein subunits from the G_i group. The G_o-, G_q-, and G_s-like proteins are all expressed in neurons; with mutation to G_o and G_q shown to affect locomotion and egg laying (Brundage et al., 1996; Mendel et al., 1995), and mutation to G_s shown to generate a lethal loss-of-function phenotype at early larval age (Korswagen et al., 1997). Three of the G_i proteins in *C. elegans* have been suggested to function in olfaction and pheromone sensation (Roayaie et al., 1998; Zwaal et al., 1997).

1.4.4 The neuronal control of nematode locomotion

Nematode locomotion is characterised by a sinusoidal pattern of movement, whereby "s-shaped bends" or "waves" travel down the worm body from anterior to posterior, propelling the worm forward (and vice versa for backward movement). This pattern of movement, described as sinusoidal, is achieved by the antagonistic contraction and relaxation of dorsal and ventral muscles under the control of excitatory and inhibitory motor neuron interactions.

There are 95 body wall muscle cells that participate in nematode locomotion, and these are arranged in four longitudinal bands, two of which are dorsal and two ventral. Each muscle cell contains three major components: the cell body, containing the nucleus and cytoplasmic organelles; multiple processes known as muscle arms, which extend to the dorsal or ventral nerve cords to receive synaptic input from the motorneurons; and the spindle, which contains the contractile myofilament lattice (reviewed in Waterston, 1988).

Forward and backward movement in *C. elegans* is modified by sensory input from the environment. A neuronal wiring diagram for the control of locomotion in response to sensory information has been established using electron micrographs of the worm nervous system as well as laser ablation of specific neurons and the production of genetically mutated worms (Chalfie et al., 1988; White et al., 1986; Zheng et al., 1999).

There are six major classes of motor neuron that innervate the body musculature in *C. elegans*; three innervate the dorsal muscles (DB, DD, and DA), and three innervate the ventral muscles (VB, VD, and VA; White et al., 1986).

Forward locomotion is mediated by the activation of the excitatory DB and VB motor neurons, which release the excitatory neurotransmitter ACh onto the muscles. DB and VB are activated by the forward command interneurons AVB and PVC, which receive input from sensory neurons. Backward movement is mediated by the activation of the excitatory DA and VA motor neurons, which release ACh on to the muscles. DA and VA are activated by the backward command interneurons AVA, AVD, and AVE, which receive input from sensory neurons.

The DD and VD motor neurons are inhibitory, releasing the neurotransmitter GABA, and receiving synaptic input from the other motor neurons rather than the command interneurons (McIntire et al., 1993). DD receives synaptic input from VB and VA, but synapses on to the muscles situated on the opposite side of those innervated by VB and VA. Consequently, activation of VB and VA stimulates ventral muscle contraction, and, via the activation of inhibitory DD, inhibits dorsal muscle contraction. The reverse situation is true for the VD motor neuron, which receives synaptic input from the DB and DA motor neurons, but synapses onto the ventral muscle to inhibit contraction of this muscle during dorsal muscle contraction. The alternate contraction of the dorsal and ventral muscles produces the characteristic sinusoidal waves in the worm body that enable forward and backward locomotion. Figure 1.7 shows schematically the neuronal circuitry controlling locomotion in *C. elegans*.

ALM and AVM are sensory neurons that detect touch to the anterior of the worm body, and the PLM sensory neuron detects touch to the posterior. These neurons extend projections to make synaptic connections onto the locomotory control interneurons. The polymodal sensory neuron ASH is involved in the coding of chemical, mechanical and osmotic input, and also makes synaptic contact onto AVA, AVB and AVD (Chalfie et al., 1988; Hart et al., 1999; Kaplan & Horvitz., 1993; White et al., 1986; Zheng et al., 1999).

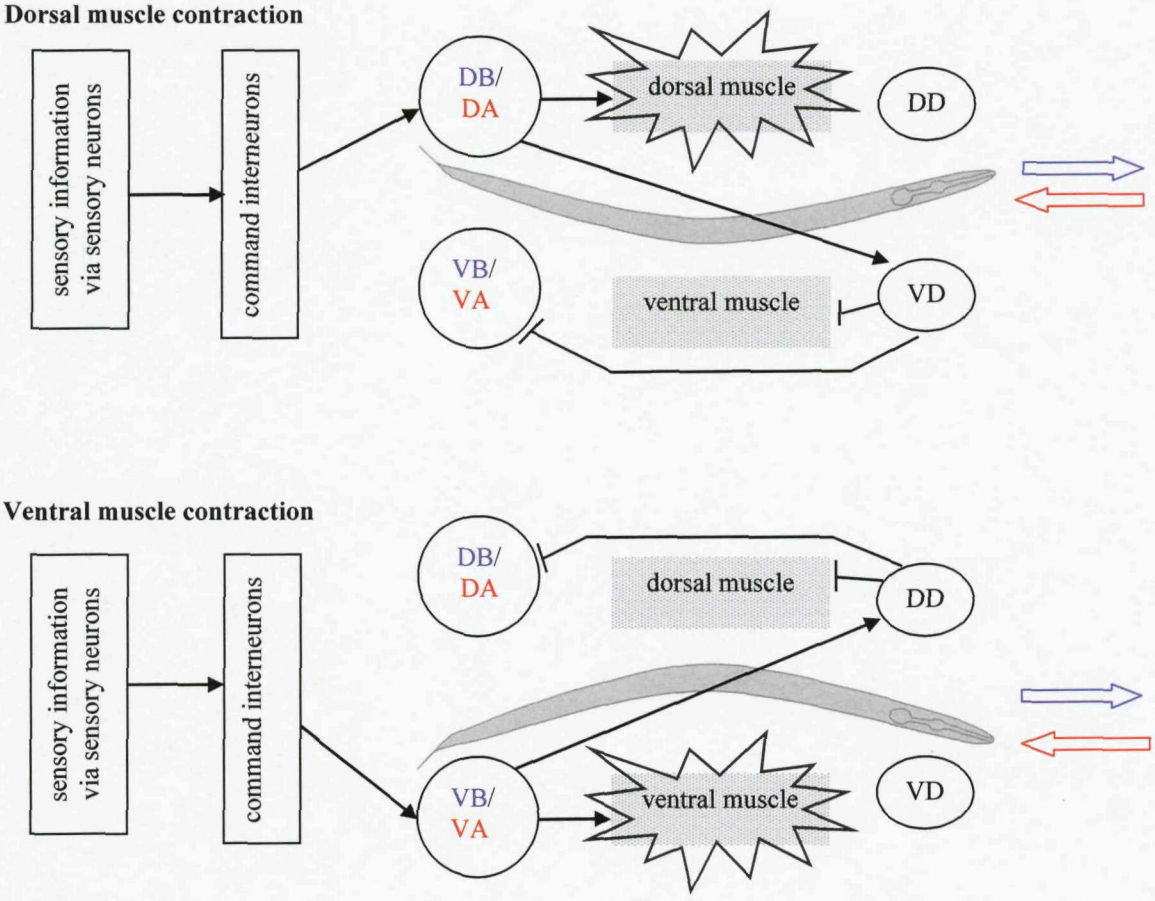

Figure 1.7 Schematic to show the circuitry of the *C. elegans* motor nervous system.
During forward locomotion, dorsal muscle contraction is produced by activated DB releasing ACh onto the dorsal muscle (inducing contraction) and VD, which releases GABA onto the ventral muscles and VB to inhibit ventral muscle contraction.
During forward locomotion, ventral muscle contraction is produced by activated VB releasing ACh onto ventral muscles (inducing contraction) and DD, which releases GABA onto the dorsal muscle and DB to inhibit dorsal muscle contraction.
During backward locomotion, dorsal muscle contraction is produced by activated DA releasing ACh onto the dorsal muscles (inducing contraction) and VD, which releases GABA onto the ventral muscles and VA to inhibit ventral muscle contraction.
During backward locomotion, ventral muscle contraction is produced by activated VA releasing ACh onto the ventral muscles (inducing contraction) and DD, which releases GABA onto the dorsal muscles and DA to inhibit dorsal muscle contraction.

1.4.5 Neurobiology of the nematode pharynx

The pharynx of *C. elegans*, and of parasitic nematodes, is the neuromuscular organ responsible for the ingestion of food, and therefore provides an excellent target for chemotherapy. Rhythmic contraction and relaxation of the pharynx pumps bacteria from the mouth of the worm to the intestine, and timing of this contraction-relaxation cycle is crucial for efficient feeding. Environmental conditions, such as the abundance of food, strongly influence the rate of pharyngeal contraction (Niacaris & Avery, 2003). The pharyngeal nervous system of *C. elegans* contains 20 neurons of 14 different types and functions independently from the extrapharyngeal nervous system. Table 1.4 lists the chemical and electrical connections between pharyngeal neurons. Communication between the pharyngeal and extrapharyngeal nervous systems is mediated via bilateral GAP junctions connecting the extrapharyngeal RIP neurons and the pharyngeal I1 neuron (Avery & Horvitz, 1989; Avery & Thomas, 1997; Franks et al., 2006).

Cell	Chemical synapse onto	Chemical synapse input from	Electrical synapse
M1	I3	I1, I2, I5, M1, M5	I2
M2	I1	I1	M1, M2, M3, M5
M3		I1, I3, I4, I5, M1, NSM	possibly MC
M4		I3, I5, I6	I6
M5		I5	possibly M2 and I5
I1	M2, M3, MC, NSM, I5		I5, RIP
I2	I4, I6, NSM, M1, possibly M2		M1, I1
I3	M3, NSM		possibly M2
I4	M1, M3, NSM	M1, I2	
I5	M1, M3, M4	I1	M5, I1
I6	M4	I2, I3, NSM	M4, M5
MI	M2, M3M MC, NSM, I5	M1	I3, I4, I5, M1, M2, M3, MC
NSM	I6, M3	I1, I2, I3, I4, I6	
MC	mc2	M1, I1	M2

Table 1.4 The chemical and electrical connections between the *C. elegans* pharyngeal neurons. (Adapted from Franks et al., 2006).

Avery & Horvitz (1989) have demonstrated the myogenic nature of the pharynx by showing that ablation of all 20 neurons of the pharyngeal nervous system does not fully inhibit pumping. Only three of the pharyngeal neurons appear important in the control of normal pharyngeal pumping: M4, M3 and MC (Avery & Horvitz, 1989; Raizen et al., 1995). The pharynx also contains nine marginal cells: the three mc1 cells extend from the anterior-most muscle cell to the level of the nerve ring in the metacorpus, the three mc2 cells extend from the nerve ring to the anterior of the terminal bulb, and the three mc3 cells are located in the terminal bulb (Albertson & Thomson, 1976). The marginal cells are believed to provide a fast conducting system, connecting particular pharyngeal neurons to muscles via gap junctions, and thereby contributing to co-ordination of the pharynx as a whole (reviewed in Franks et al., 2006). Table 1.5 shows which pharyngeal neurons chemically innervate which of the muscle cells, as well as showing where marginal cells enable neurons to innervate muscles via gap-junction activity.

Muscle cell type	Chemical innervation from	Gap-junction innervation from
pm1	M1	
pm2	M1	
pm3	M1	
pm4	M2, M3, MC	MC via mc2
pm5	M2, M3, M4, I5	
pm6	M5, possibly M4	M5 via mc3
pm7	M5	M5 via mc3
pm8		M5 via mc3

Table 1.5 The chemical and electrical innervation of the *C. elegans* pharyngeal muscles.
(Adapted from Franks et al., 2006).

In the pharynx, ACh and glutamate are the excitatory and inhibitory neurotransmitters, respectively (Albertson & Thomson, 1976). A number of genes encoding precursors for neuropeptides from the FLP and NLP families have been observed to be expressed in the pharyngeal neurons, suggesting that these peptides may contribute to the physiology of the pharynx (Kim & Li, 2004; Li, 2005; Nathoo et al., 2001). A number of FLP peptides have been found to have an excitatory or inhibitory effect on pharyngeal pumping, and two FLPs were shown to be highly potent (FLP-17A and FLP-13A) and expressed in several pharyngeal neurons, suggesting that these FLPs contribute to pharyngeal physiology (Papaioannou et al, 2005; Rogers et al., 2001). Table 1.6 shows the neurotransmitter released by each of the pharyngeal neurons, as well as listing the

neuropeptide precursor genes that have been shown to be expressed in each neuron and may therefore indicate that these peptides are used as transmitter molecules by specific neurons.

Pharyngeal Neuron	**Neurotransmitter released**	**Neuropeptide precursor genes expressed**
M1	ACh	*nlp-3*
M2	ACh	*nlp-3, nlp-13, flp-18, flp-21*
M3	Glutamate	*nlp-3, flp-13,* possibly *flp-18*
M4	ACh	*flp-5, flp-21,* possibly *flp-2*
M5	ACh	*flp-1, flp-13, flp-17*
I1		*nlp-3, flp-6*
I2		*nlp-3, nlp-8, flp-15*
I3		*nlp-3*
I4		*nlp-3, nlp-13, flp-5*
I5	Glutamate, 5-HT	*flp-2, flp-4, flp-13*
I6	ACh	*nlp-3, flp-4*
MI		
NSM	Glutamate, 5-HT	*nlp-13, nlp-18, flp-4, flp-19, nlp-3* (right-hand cell only)
MC	ACh	*flp-2, flp-21*

Table 1.6 The neurotransmitters and putative neuropeptide transmitters synthesized in the pharyngeal neurons. (Adapted from Franks et al., 2006).
It should be noted that the neuropeptide genes each encode a precursor that may be modified to form several protein products which are not listed here for reasons of clarity.

Experimental ablation of the MC motor neuron has shown it to be the major excitatory neuron required for fast pumping in the pharynx (Avery & Horvitz, 1989). The I5 interneuron and the two M3 motor neurons appear to be crucial for efficient transport of bacteria along the pharyngeal lumen (Avery, 1993). The sensory endings of the M3s, which are located at the corpus-isthmus boundary, act as mechanosensors for detecting contraction of the pharynx, and therefore, pharyngeal relaxation is stimulated via M3 motor output to the corpus and anterior isthmus (Albertson & Thomson, 1976). The M4 neuron, however, is important for enabling bacterial entry into the intestine by stimulating isthmus opening (Alfonso et al., 1994).

The ingestion of food by *C. elegans* consists of two separate processes: the first process is the synchronous contraction of the corpus, anterior isthmus and terminal bulb

(pharyngeal pumping), and the second process is peristalsis of the anterior isthmus (Avery & Horvitz, 1989). Generation of the pharyngeal action potential in *C. elegans* has been shown to be sodium-dependent, with indirect evidence suggesting that a voltage-gated sodium channel may have a role in the action potential (Franks et al., 2002).

The inhibitory glutamatergic M3 motor neurons of the pharynx are responsible for modulating the timing of pharyngeal relaxation and maintaining coordinated pumping (Li et al., 1997; Niacaris & Avery, 2003). The arrival of the action potential at the neuromuscular junction triggers the firing of these neurons, resulting in the release of the neurotransmitter glutamate (Li et al., 1997). The glutamate then acts on glutamate-gated chloride channels to produce inhibitory postsynaptic potentials (IPSPs), which promote repolarization of the pharyngeal muscle (Niacaris & Avery, 2003). Ablation of the M3 neurons increases the duration of pharyngeal contraction leading to inefficient feeding and eventual blockage of the pharyngeal lumen by lodged bacteria unable to move into the intestine. This supports a role for these neurons in coordinating effective pharyngeal pumping (Li et al, 1997; Niacaris & Avery, 2003).

The MC excitatory cholinergic motor neuron is also located in the pharynx and controls activation of the pharyngeal muscle and the frequency of pumping. Worms that possess a mutation in the *eat-18* gene (which encodes EAT-18 required for the functioning of pharyngeal nicotinic ACh receptors) demonstrate a reduction in pumping rate compared to wild type *C. elegans*. Firing of the MC neuron at the neuromuscular junction stimulates the release of ACh, which acts on postsynaptic nicotinic receptors to cause muscle contraction (Niacaris & Avery, 2003).

The I5 and NSM pharyngeal neurons have been shown to express the *tph-1* gene, which encodes tryptophan hydroxylase, necessary for the synthesis of 5-HT. In the presence of food, the rate of pharyngeal pumping in *C. elegans* increases, a process that can be mimicked by the addition of exogenous 5-HT (Avery & Horvitz, 1990). Conversely, the biogenic amine octopamine has been shown to inhibit pharyngeal pumping (Niacaris & Avery, 2003; Rogers et al., 2001). Reciprocal regulation of pharyngeal behaviour by 5-HT and octopamine has been suggested by Niacaris & Avery (2003) to form a mechanism for modulating the length of action potential in response to food availability. When food is abundant, 5-HT increases the speed and efficiency of *C. elegans* feeding,

however, when food has become exhausted, a decrease in 5-HT levels, possibly coupled with increasing octopamine levels, results in a reduction in pharyngeal pumping rate. Four 5-HT receptors have been identified in *C. elegans*: SER-1, SER-4, SER-7B and MOD-1, and the first three are found in specific pharyngeal neurons or muscle or both (Hamdan et al., 1999; Hobson et al., 2003; Olde & McCombie, 1997; Ranganathan et al., 2000). In the pharynx, *ser-1* is expressed in pharyngeal muscle cells pm1, pm2, pm3, pm5, pm7, whereas *ser-4* is expressed on an as-yet unidentified neuron. The *ser-7* gene is expressed in MC, M4, M5, I2 and I3 (Hobson et al., 2006). Loss-of-function mutation to *ser-7* produces *C. elegans* refractory to 5-HT-stimulation of pumping despite the continued presence of SER-1 in the pharyngeal muscles, suggesting that SER-1 receptors alone cannot confer pharyngeal sensitivity to 5-HT (Hobson et al., 2006). Significantly, *ser-7* mutants are capable of increasing their pumping rate in response to food, and 5-HT actually inhibits pumping in these worms. This suggests that the stimulation of pumping in response to food involves signals in addition to 5-HT, and the regulation of pumping rate in the presence of food involves a negative-feedback system in which 5-HT has a role (Hobson et al., 2006).

1.5 Anthelmintics and the problem of resistance

Anthelmintics have been found to function by targeting a variety of different receptors, ion channels and biochemical processes within the parasite (reviewed in Martin, 1997). Much of the research investigating the mechanism of action for these drugs has been stimulated by the increasing incidence of anthelmintic resistance, an occurrence stimulated by the heavy reliance on these drugs as a means of managing control of nematode parasites (Geary et al., 1999a; Sangster & Dobson, 2002; Sangster & Gill, 1999). Anthelmintic resistance has now spread to numerous parasitic helminth phyla, affecting humans and animals, and involving all the major chemical groups of anthelmintics (Geary et al., 1999a; Sangster & Dobson, 2002; Sangster & Gill, 1999; Waller, 1997).

Anthelmintic resistance occurs in parasitic nematode populations due to the process of selection; those parasites that survive anthelmintic treatment because of natural resistance conferred by random mutations in specific genes will reproduce and pass on those mutant alleles to their offspring (Geary et al., 1999a).

Receptors identified as targets for anthelmintics include the nicotinic ACh receptor, the GABA receptor, glutamate-gated chloride channels, and β-tubulin (reviewed in Martin et al., 1997). The following is a brief account of the commercially available anthelmintics that target these four molecular structures, including a description of the current research investigating how resistance to these drugs has occurred.

1.5.1 Anthelmintics that act on the nicotinic acetylcholine receptor (nAChR)

The imidothiazole and tetrahydropyrimidine anthelmintics have been shown to specifically target parasitic nematodes via their nAChRs; exploiting differences in the parasite and vertebrate nAChRs to avoid affecting the host itself (Ballivet et al., 1996; Harrow & Gration, 1985; Lewis & Berberich, 1992; Martin et al., 2003; Martin, 1997). In *A. suum*, the imidothiazole levamisole, and the tertrahydropyrimidines morantel and pyrantel mimic the action of ACh on the muscle cells: binding to nAChRs and opening non-selective cation channels in the muscle cell membrane. This results in an increased influx of sodium and potassium across the membrane and into the cell, and thereby produces sustained depolarization of the cell and spastic paralysis of the nematode

(Harrow & Gration, 1985). The length of time the cation channel remains open has been found to vary according to the anthelmintic used (Harrow & Gration, 1985).

The invertebrate nAChR is a pentameric structure composed of a combination of α and non-α subunits, forming hetromeric or homomeric channels (Karlin, 2002; Unwin, 1995). Each nAChR contains two α subunits, which are responsible for binding ACh (Changeux & Edelstein, 1998). In *C. elegans*, 29 nAChR subunits have been identified and have been categorized into five 'core' groups according to their sequence homology: the UNC-38 group, UNC-29 group, ACR-16 group, ACR-8 group and DEG-3 group. The ACR-16 group are homologous to the vertebrate α7 nAChR subunit, whilst the ACR-8 group and DEG-3 group represent nematode-specific receptor subtypes (Ballivet et al., 1996; Jones & Sattelle, 2004; Mongan et al., 2002). There are also 26 orphan subunits that exhibit nAChR homology but do not belong to any of the five groups. Of the levamisole-resistance loci generated by *C. elegans* mutagenesis experiments and then identified, five are genes encoding nAChR subunits: LEV-1, LEV-8 (also known as ACR-13), UNC-29, UNC-38 and UNC-63 (Culetto et al., 2004; Fleming et al., 1997; Towers et al., 2005). *C. elegans* highly resistant to levamisole possess mutations in the *lev-1* and *unc-29* genes that code for non α-subunits, whereas milder resistance to levamisole was conferred by mutation in the α-subunit encoded by *unc-38* (Fleming et al., 1997). Significantly, Francis et al. (2005) and Touroutine et al. (2005) have shown that the presence of the ACR-16 subunit confers insensitivity to levamisole. As ACR-16 resembles the vertebrate α7 nAChR subunit capable of forming homomeric receptors in *Xenopus* oocytes, it is possible that levamisole insensitivity may be attributed to nAChRs consisting only of ACR-16 (Ballivet et al., 1996; Raymond et al., 2000)

Resistance to the imidothiazoles and tetrahydropyrimidines has been reported in numerous parasitic helminth strains and in several host species, for example pyrantel resistance has been identified in species of small strongyles which infect horses, and imidothiazole resistance has been noted in *trichostrongyloid* species found in sheep (Sangster & Gill, 1999).

1.5.2 Anthelmintics that act on the GABA receptor

Piperazine acts as a GABA agonist, opening GABA receptor chloride channels on nematode body wall muscle cells, causing an increase in chloride ion conductance and a consequent hyperpolarization of the muscle membrane potential. This potentiation of the nematode GABA receptors produces muscle relaxation, and eventually causes flaccid paralysis of the animal (Del Castillo et al., 1963; Holden-Dye et al., 1989; Martin, 1997). Piperazine is primarily effective against large intestinal nematodes because flaccid paralysis of these parasites reduces their ability to maintain their position within the intestine, resulting in expulsion from the host (Martin, 1997).

1.5.3 Anthelmintics that act on glutamate-gated chloride channels

The macrocyclic lactones have been described as the most important group of currently available anthelmintics due to their high efficacy and broad spectrum, which includes the treatment of animal gastro-intestinal nematode infections and ectoparasite infestations, as well as human filarial nematode infections, such as onchocerciasis (McCavera et al., 2007; Omura & Crump, 2004; Wolstenholme & Rogers, 2005). The macrocyclic lactones target nematodes by paralysing movement and pharyngeal pumping (e.g. Brownlee et al., 1997; Geary et al., 1993; Kass et al., 1984). Although adult microfilariae are resistant to these effects, the macrocyclic lactones target microfilariae by reducing the production of new larvae, hence the success of the macrocyclic lactone ivermectin in the control of onchocerciasis (Campbell et al., 1983). Reports of nematode resistance to macrocylic lactones such as ivermectin are increasing, particularly in parasites of livestock (e.g. Jackson & Coop, 2000; Loveridge et al., 2003; Sangster & Gill, 1999). Continuing research using model organisms including *A. suum*, *C. elegans* and *H. contortus* has enabled the mechanism of action of macrocyclic lactones and the pathways of resistance to be investigated.

Initial research using *A. suum* demonstrated that the macrocyclic lactones target GABA-gated chloride (Cl^-) channels, opening the channels and increasing cell membrane Cl^- permeability (Holden-Dye & Walker, 1990; Holden-Dye et al., 1988; Martin & Pennington, 1989). However, the anthelmintic concentrations required to target GABA-gated Cl^- channels were not clinically relevant, therefore it was concluded that

macrocyclic lactones have at least one alternative target. In *C. elegans* the macrocyclic lactone ivermectin is lethal at clinically relevant concentrations, and by injecting *C. elegans* RNA into *Xenopus* oocytes it was found that ivermectin functions by producing a rapidly activating irreversible ivermectin-sensitive current (Arena et al., 1992, 1991). Subsequent RNA screening and *Xenopus* oocyte expression attributed this Cl^- current to glutamate-gated Cl^- (GluCl) channels formed from the α subunit (Arena et al., 1995; Cully et al., 1994). The *C. elegans* GluCl channel α subunits are encoded by a family of alternatively spliced genes, including *avr-15*, *avr-14*, *glc-1* and *glc-3* (Cully et al., 1994; Dent et al., 2000, 1997; Horoszok et al., 2001; Laughton et al, 1997; Yates et al., 2003). *C. elegans* possessing a null mutation in either *avr*-15, *avr-14* or *glc-1* were found not to possess significant resistance to macrocyclic lactones, but if two or all three of these genes were mutated, resistance was observed, suggesting that changes in multiple genes produce high-level target-site mediated resistance to macrocyclic lactones (Dent et al., 2000).

Other *C. elegans* proteins are believed to mediate sensitivity to macrocyclic lactones by interacting with the GluCl channel. For example, null mutations in *C. elegans unc-7* and *unc-9* genes (encoding the innexin gap junction subunits) have been found to confer ivermectin resistance, as well as enhancing the resistance of the *avr-15* null mutant when combined in a double mutant (Dent et al., 2000). Significantly, ivermectin was not found to bind UNC-7 or UNC-9, suggesting that these two genes contribute to ivermectin sensitivity indirectly, possibly by spreading the hyperpolarization induced by the opening of GluCl channels from cells expressing these channels to other excitable cells that do not possess them (Dent et al., 2000).

1.5.4 The benzimidazoles: anthelmintics that act via β-tubulin

The benzimidazoles, including albendazole, thiabendazole and mebendazole, act by specifically binding to parasite β-tubulin, a vital component of the microtubules inside nematode cells (e.g. Kwa et al., 1994; Lubega & Prichard, 1990). Mapping of the mutation producing benzimidazole resistance in *H. contortus* populations generated by *in vitro* selection revealed β-tubulin to be the anthelmintic target (Kwa et al., 1993). Later studies in *H. contortus* demonstrated that specific mutation of amino acid 200 in the β-tubulin protein produces benzimidazole resistance (Kwa et al., 1995, 1994), suggesting that this region of the β-tubulin forms a vital role in benzimidazole action. In

support of these findings, a mutagenesis screen for benzimidazole-resistant strains of *C. elegans*, revealed that a loss in expression of the β-tubulin isotype *ben-1* is strongly associated with resistance to benzimidazole anthelmintics (Driscoll et al, 1989; Geary et al., 1999a). The amino acid sequence of the *ben-1* β-tubulin isotype found in benzimidazole-susceptible *C. elegans* differs from the isotype found in the resistant worms (called *tub-1*) only at amino acid 200, with *ben-1* possessing a phenylalanine at this position, and *tub-1* a tyrosine instead (Driscoll et al., 1989).

β-tubulin is a crucial component of cellular microtubules, which perform numerous vital roles in the cell, including transport of cytoplasmic secretory vesicles (Wacker et al., 1997). Research has suggested that the benzimidazoles operate by inhibiting polymerization of microtubules via their binding to β-tubulin, resulting in major disruption to cellular integrity (Van den Bossche et al., 1982). In *A. suum*, a benzimidazole called mebendazole was shown to target the microtubules of intestinal cells, resulting in a loss of secretory vesicle transport and a consequent failure of glucose up-take by the intestinal cells. Therefore, following mebendazole application, the parasites starved (Van den Bossche et al., 1982).

1.6 The cyclodepsipeptides: potential as novel anthelmintics

The cyclic depsipeptides are a class of compound containing members which exhibit strong potential as new anthelmintics for veterinary applications (Geary et al., 1999a). One of the most active, and thus promising, of the new cyclodepsipeptide anthelmintics is PF1022A (Sasaki et al., 1992; Zahner et al., 2001a). In fact, the intrinsic activity of PF1022A is higher than the activity of any of the commercially available broad-spectrum anthelmintics (Samson-Himmelstjerna et al., 2000). It was in Japan that PF1022A was first isolated as a fermentation product of the fungus *Mycelia sterilia* which is found in the microflora of the plant *Camellia japonica* (Sasaki et al., 1992). The structure of PF1022A consists of four N-Methyl-L-leucines, two D-lactic acids and two-D-phenyllactic acids which are arranged as a cyclic octadepsipeptide with an alternating L-D-L-configuration (see figure 1.8; Harder et al., 2003)

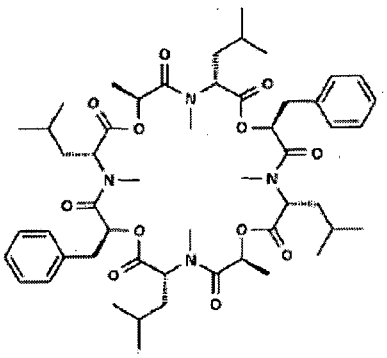

Figure 1.8 The structure of PF1022A (Harder et al., 2003)

Many *in vitro* and *in vivo* studies have taken place in an attempt to reveal the anthelmintic capacity of this compound, and the following is a summary of the major findings of this research.

1.6.1 The anthelmintic activity of PF1022A

PF1022A demonstrates strong anthelmintic properties as well as low toxicity, thereby making this compound one of the most promising anthelmintics to emerge since the discovery of the avermectins and milbemycins (Sasaki et al., 1992; Weckwerth et al., 2000). Since the discovery of PF1022A, research has shown that it possesses a broad spectrum of activity against a variety of nematodes in different companion and livestock animals (Nicolay et al., 2000). Early experiments demonstrated that PF1022A has *in vivo* activity against *Ascaridia galli* in chickens, and *Toxocara canis* and *Toxocara cati* in dogs (Sasaki et al., 1992; Terada, 1992). Further investigation has revealed that the

compound has anthelmintic capabilities against *Haemonchus contortus*, *Trichostrongylus colubriformis*, and *Ostertagia ostertagi* in gerbils (Conder et al., 1995). In mice, PF1022A has been shown to be effective against *Heligmosomoides polygyrus* and *Heterakis spumosa* after oral administration (Martin et al., 1996), and in rats the compound is fully effective against *Nippostrongylus brasiliensis* and *Strongyloides ratti* (Samson-Himmelstjerna et al., 2000). PF1022A also demonstrates effective anthelmintic activity against the lungworm *Dictyocaulus viviparous* in cattle, *Ancylostoma caninum* in dogs, small strongyles in horses, and *H. contortus* and *T. colubriformis* in sheep (Samson-Himmelstjerna et al., 2000). This novel anthelmintic has also been shown to be active against adult *Angiostrongylus cantonensis* stages which reside in the pulmonary arteries of rats and mice (Kachi et al., 1995, 1994).

Significantly, PF1022A has been shown to be fully effective against nematodes of sheep and cattle that are resistant to levamisole, ivermectin or the benzimidazoles. For example, the compound demonstrated strong anthelmintic activity against febantel- and ivermectin-resistant strains of *H. contortus* in sheep (Harder et al., 2003). Therefore, it appears that PF1022A possesses resistance-breaking properties in these instances, suggesting that it is operating anthelmintically via a novel pathway of action.

1.6.2 Emodepside: a derivative of PF1022A with potent anthelmintic capability

A variety of PF1022A derivatives have been synthesized, including the semi-synthetic derivative PF1022-221 or BAY44-4400, known as emodepside (Harder et al., 2003). Emodepside, the structure of which is shown in figure 1.9, demonstrates a high efficacy against a broad range of parasitic nematodes in a number of different host species. For example, this compound is highly effective against *N. brasiliensis* and *S. ratti* adult stages in the rat host, and against the mouse nematode *H. polygyrus*. Emodepside also exerts efficacy against *Acanthocheilonema viteae*, *Brugia malayi*, and *Litomosoides sigmodontis* as preadult worms, and as third and fourth stage larvae in infected *Mastomys coucha* (Harder et al., 2003; Zahner et al., 2001b). Just a single oral or spot-on application of emodepside has been shown to be effective against the microfilariae of all three of these parasite species, and, significantly, the drug can also induce severe pathological changes to the intrauterine stages of *L. sigmodontis* and *B. malayi*,

potentially leading to long-lasting reductions of microfilaraemia levels even if curative effects are unachievable (Harder et al., 2003).

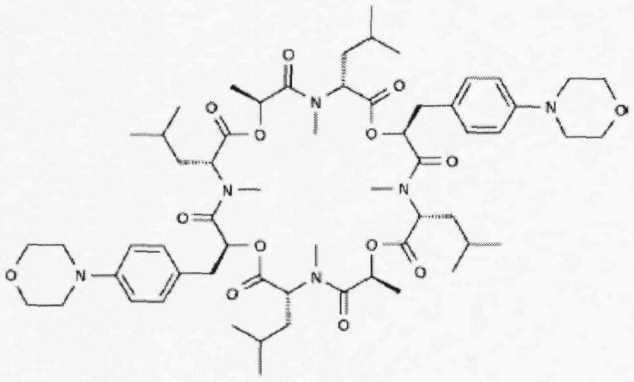

Figure 1.9 The chemical structure of emodepside (BAY44-4400 or PF1022-221). (Adapted from Harder et al., 2003).

Table 1.7 summarises the range of parasites against which emodepside has been shown to demonstrate anthelmintic activity. Importantly, emodepside has demonstrated an efficacy against *H. contortus* strains which are resistant to ivermectin and levamisole, as well as against ivermectin-resistant *Cooperia oncophora* isolates in cattle, and ivermectin-resistant *T. colubriformis* in sheep. This strongly suggests that the mechanism of action for emodepside is different to the neurobiological pathways employed by currently used anthelmintics (Harder et al., 2003).

Nematode	Host	Nematode	Host
• *Heligmosomoides polygyrus* • *Heterakis spumosa* • *Trichinella spiralis* • *Nippostrongylus muris* • *Strongyloides ratti* • *Brugia malayi* • *Litomosoides sigmodontis* • *Acanthocheilonema vitae*	Mice, rats, mastomys, chicken	• *Parascaris equorum* • Large strongyles • Small strongyles	Horse
• *Haemonchus contortus* • *Teladorsagia circumcincta* • *Ostertagia ostertagi* • *Trichostrongylus colubriformis* • *Trichostrongylus axei* • *Cooperia spp.* • *Trichuris ovis* • *Trichuris bovis* • *Dictyocaulus viviparus*	Sheep, cattle	• *Toxocara cati* • *Toxocara canis* • *Toxacaris leonine* • *Ancylostoma tubaeforme* • *Ancylostoma caninum* • *Uncinaria stenocephala* • *Trichuris vulpis*	Cat, dog

Table 1.7 The nematode species that emodepside is anthelmintically active against. The parasite hosts are also included. (Harder et al., 2003).

1.7 Investigations into the molecular mechanism of action of emodepside

The ability of emodepside to act against parasitic nematode strains resistant to currently available anthelmintics strongly supports a novel mechanism of action for this compound. The importance of emodepside as a new anthelmintic for breaking resistance has promoted detailed experimental investigations to establish the mechanism of its action against nematodes.

1.7.1 Emodepside binds to a latrophilin-like receptor

Immunoscreening of a cDNA library from the parasitic nematode *H. contortus* using the emodepside precursor PF1022A identified a 3539 base pair cDNA encoding a novel receptor. Named HC110-R, this novel receptor was subjected to database and phylogenetic analysis, and was revealed to have a high level of identity with human, bovine and rat latrophilin (Saeger et al., 2001). Emodepside was also shown to bind HC110-R when HEK-293 cells, transfected with myc/his-taged HC110-R, were lysed and transferred to a filter before being incubated with emodepside and investigated for binding using immunological probes (Saeger et al., 2001). To support this, emodepside was found to impair the response of HC110-R-transfected HEK-293 cells to α-latrotoxin, which is known to bind latrophilins to exert its toxic effects (Krasnoperov et al., 1997; Lelianova et al., 1997; Saeger et al., 2001). These results suggest that emodepside binds to a latrophilin-like receptor and this binding may be partly or wholly responsible for the anthelmintic effects of the compound. The native ligand for the latrophilins is currently unknown, but as mentioned previously, α-latrotoxin has been shown to bind to latrophilin to produce toxic effects; suggesting that emodepside and latrotoxin may share features of their mechanisms of action.

1.7.2 The mechanism of action of α-latrotoxin

α-Latrotoxin is a vertebrate specific neurotoxin and is the major component of black widow spider venom (reviewed in Henkel & Sankaranarayanan, 1999; Khvotchev & Südhof, 2000; Südhof, 2001). α-Latrotoxin has been shown to bind specifically to presynaptic neuronal membranes (Tzeng & Siekevitz, 1979; Valtorta et al., 1984), where it stimulates extensive neurotransmitter release (e.g. Augustin et al., 1999; Capogna et al., 1996; Grasso et al., 1980; Longenecker et al., 1970; Nicholls et al.,

1982). At the frog neuromuscular junction (NMJ), α-latrotoxin stimulates the fusion of small, clear synaptic vesicles docked at the active zone (the "readily releasable pool") with the presynaptic membrane (Matteoli et al., 1988). In chromaffin cells, pancreatic β-cells, and sensory neurons, α-latrotoxin stimulates exocytosis of dense-core vesicles (Barnett et al., 1996; De Potter et al., 1997; Lang et al., 1998). Three distinct membrane proteins that couple α-latrotoxin to cell secretion have been identified: the latrophilins (Krasnoperov et al., 1997; Lelianova et al., 1997), neurexin Iα (Geppert et al., 1998), and the receptor-like protein-tyrosine phosphatase σ (PTPσ; Krasnoperov et al., 2002a). It is possible that neurexin Iβ may also function as a receptor for α-latrotoxin, although the evidence for this is limited and suggests a lesser role for this protein compared to neurexin Iα (Sugita et al., 1999). The following is a brief description of the structural features of the proteins identified as α-latrotoxin receptors, followed by an explanation of how research has generated the current view on the mechanism of action of α-latrotoxin and the role of the identified receptors in this mechanism.

The neurexins constitute a highly polymorphic family of neuron-specific proteins located at the cell surface and, due to a sequence homology with the laminins, they are thought to mediate neuronal cell-cell recognition at the synapse (reviewed in Bittner, 2000; Südhof, 2001). Produced by three genes, each under the control of two promoters, the neurexins are subject to extensive alternative splicing, resulting in hundreds of isoforms (Ushkaryov et al., 1992). Neurexin Iα has been shown to constitute a specific high-affinity binding site for α-latrotoxin (Davletov et al. 1995; Geppert et al., 1998).

The latrophilins are G protein-linked receptors with large extra- and intracellular domains, and have been shown to act as receptors for α-latrotoxin (Krasnoperov et al., 1997; Lelianova et al., 1997). Structurally, latrophilin contains seven transmembrane (TM) domains, an intracellular region resembling a generic G protein-coupled receptor, and a large extracellular region containing lectin-like, olfactomedin-like and cysteine-rich regions (see figure 1.10; Krasnoperov et al., 1997; Sugita et al., 1998). The lectin- and olfactomedin-like domains have been suggested to fulfil a functional role in the coupling of cell adhesion to cell signaling by latrophilin (Sugita et al., 1998). Located between the cysteine-rich region and the first TM domain is a sequence of 19 amino acid residues called the G protein-coupled receptor proteolysis site (GPS), which is the signal site for post-translational proteolytic cleavage of the latrophilin precursor protein

to form the mature latrophilin (Krasnoperov et al., 2002b). Therefore, the mature protein is composed of two non-covalently bound fragments: p120 and p85.

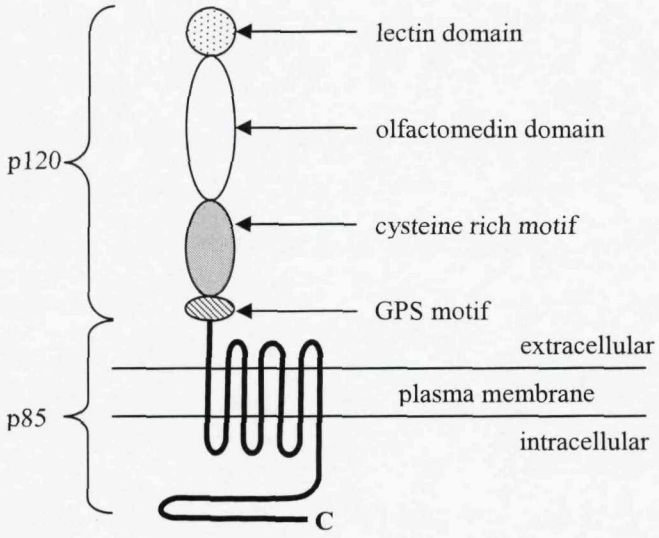

Figure 1.10: A schematic representation of the domain structure of latrophilin
(Adapted from Südhof, 2001; Krasnoperov et al., 2002b, 1997).

The vertebrate receptor-like protein-tyrosine phosphatase sigma (PTPσ) has been identified as a functional receptor for α-latrotoxin in the rat brain (Krasnoperov et al., 2002a). PTPσ is a member of a group of receptor-like protein-tyrosine phosphatases (RPTPs) which are leukocyte-common antigen related (LAR-like). The LAR-like RPTPs have been shown to be expressed in many epithelia and neural tissues, where they are important in regulating multiple developmental events, including neuronal development and axonal guidance during outgrowth (e.g. Den Hertog, 1999; Ensslen-Craig & Brady-Kalnay, 2004; Pulido et al., 1995).

Research has shown that when α-latrotoxin binds its receptor it inserts as a tetrameric structure into the membrane, resulting in the formation of a stable cation-permeable pore that mediates the influx of Ca^{2+} and the stimulation of exocytosis (Khvotchev & Südhof, 2000; Orlova et al., 2000; Wanke et al., 1986). Cation pore formation by α-latrotoxin appears to be sufficient to explain neurotransmitter release stimulated by the toxin when investigated in secretory cells such as neuroendocrine PC12 cells and chromaffin cells. For example, α-latrotoxin-stimulated release of dopamine or norepinephrine from PC12 cells is dependent on extracellular Ca^{2+}, suggesting that the

formation of cation channels, rather than direct intracellular signaling is operating (Grasso et al., 1980).

Neurexin Iα may also function as a Ca^{2+}-dependent α-latrotoxin receptor (Davletov et al., 1995; Geppert et al., 1998; Petrenko et al., 1990; Ushkaryov et al., 1992). For example, α-latrotoxin binding to synaptosomes prepared from mice possessing a null mutation in the neurexin Iα gene was reduced by 50% in the presence of Ca^{2+}. No reduction in α-latrotoxin binding was observed in the absence of Ca^{2+}, suggesting that neurexin Iα binding by the toxin is dependent on Ca^{2+} (Geppert et al., 1998). Interestingly, transient expression in PC12 cells of neurexin Iα and neurexin 1β significantly increased the sensitivity of these cells to secretion stimulated by α-latrotoxin, indicating that both of these neurexins can act as functional α-latrotoxin receptors (Sugita et al., 1999).

Latrophilin has also been shown to form a functional receptor for α-latrotoxin in many cell types. Significantly, α-latrotoxin was shown to be capable of stimulating vesicle exocytosis from PC12 cells transfected with truncated latrophilin lacking the G protein-coupled receptor-like domain that enables activation of cellular second-messenger signaling pathways by latrophilin. Therefore, in PC12 cells, α-latrotoxin-stimulated secretion does not appear to require stimulation of a second messenger cascade (Sugita et al., 1999). However, in specific intact presynaptic terminal cell systems, α-latrotoxin can stimulate neurotransmitter release in the absence of external Ca^{2+} and without observable release of Ca^{2+} from the intracellular stores (Capogna et al., 1996; Ceccarelli et al., 1979; Meldolesi et al., 1984; Misler & Hurlbut, 1979; Rosenthal et al., 1990). This suggests that α-latrotoxin can function without Ca^{2+}-influx via the cation pore, and must stimulate a second messenger system to cause vesicle exoctyosis. Supporting this, a form of α-latrotoxin capable of receptor-binding but not pore formation was shown to retain the ability to stimulate exocytosis, suggesting that α-latrotoxin can act via receptor-mediated signal transduction (Volynski et al., 2003).

A large body of evidence strongly supports a role for latrophilin as the receptor that mediates Ca^{2+}-independent neurotransmitter exocytosis by α-latrotoxin. Krasnoperov et al. (1997) have shown that chromaffin cell sensitivity to neurotransmitter exocytosis by α-latrotoxin is increased ten-fold by transfection of the cells with latrophilin cDNA. Importantly, these authors also found that latrophilin copurifies with syntaxin 1A, which

is a presynaptic plasma membrane protein that performs a fundamental role in neurotransmitter release (Richmond et al., 2001). Neurotransmitter release involves the docking of synaptic vesicles (containing neurotransmitters) at the presynaptic 'active zone', where they undergo 'priming' which prepares them for fusion with the synaptic membrane (e.g. Richmond & Broadie, 2002; Soller et al., 1993; Südhof, 1995). During the initial stages of priming, the activation of syntaxin enables it to recruit vesicles to the 'ready releasable pool' for exocytosis (Richmond et al., 2001). Therefore, the copurification of latrophilin with syntaxin by Krasnoperov et al. (1997) suggests that α-latrotoxin can stimulate neurotransmitter release via initiation of a second messenger cascade. Supporting this, Lelianova et al. (1997) have shown that latrophilin co-purifies with a 42kDa protein that reacts with antibodies raised against the G protein $G\alpha_o$. Vertebrate and invertebrate G proteins have been shown to function in second messenger pathways that can contribute to the control of neurotransmitter release (e.g. Brundage et al., 1996; Miller et al., 1996), and therefore it is likely that α-latrotoxin can stimulate neurotransmitter release by stimulation of a G protein-coupled second messenger pathway(s).

The most recent α-latrotoxin receptor to be identified is PTPσ (Krasnoperov et al., 2002a). The evidence for a α-latrotoxin receptor in addition to neurexin Iα and latrophilin was provided by double knock-out mice possessing inactive neurexin Iα and latrophilin genes. These mice were found to retain a physiological response to α-latrotoxin, and their brain membranes were shown to retain approximately 25% the α-latrotoxin binding of wild type mice (Tobaben et al., 2002). Subsequent investigation demonstrated that overexpression of PTPσ in chromaffin cells can increase the sensitivity of these cells to the stimulation of neurotransmitter release by α-latrotoxin, suggesting that PTPσ is another toxin receptor (Krasnoperov et al., 2002a). Structurally, PTPσ consists of a single transmembrane domain, an intracellular region containing the catalytic phosphatase domains, and a large extracellular region containing immunoglobulin (IgG) domains and fibronectin type 3 (FNIII) domains (Pulido et al., 1995). α-Latrotoxin has been shown to directly bind the extracellular region of PTPσ, including two fibronectin domains (Krasnoperov et al., 2002a). Importantly, the intracellular phosphatase domains of PTPσ were not required for the stimulation of neurotransmitter release from chromaffin cells by α-latrotoxin, suggesting that PTPσ-mediated intracellular signaling is not essential for toxin activity in these cells (Krasnoperov et al., 2002a). Therefore, Krasnoperov et al. (2002a) have proposed that

PTPσ may act as a targeting site to attract the toxin and facilitate its partial insertion into the chromaffin cell membrane, although the exact contribution of PTPσ to α-latrotoxin activity remains unclear.

1.7.3 Emodepside stimulates neuronal vesicle exocytosis in putative synaptic regions of the *C. elegans* pharynx

In section 1.7.1 (page 44), research was described that suggested emodepside can functionally bind to the latrophilin-like receptor HC110-R (Saeger et al., 2001). This suggested that latrophilin may be partly or wholly responsible for the anthelmintic effects of emodepside. As latrophilin is also a receptor for α-latrotoxin; an interaction that results in the stimulation of massive neurotransmitter release at the synapse (described in section 1.7.2, page 44), it is possible that emodepside binds to latrophilin and triggers excessive neurotransmitter release to produce its anthelmintic effects. In support of this hypothesis, emodepside has been shown to cause vesicle exocytosis in the neurons of the *C. elegans* pharynx. Using activity-dependent uptake of FM4-64 (rhodamine fluorescent marker) to label active synapses of the enteric neurons in the pharyngeal muscle, it was observed that 100nM emodepside caused a loss of FM4-64 fluorescence from these putative synaptic regions when compared to the control results (Willson et al., 2004). This suggests that emodepside can stimulate vesicular release, and may indicate a parallel between the molecular mechanisms utilized by emodepside and α-latrotoxin (Capogna et al., 1996; Willson et al., 2004). Importantly, 100nM emodepside was shown to paralyse the *C. elegans* pharyngeal response to 5-HT, suggesting that the stimulation of vesicle release by the anthelmintic is responsible for, or contributes to, the paralysis of the pharynx (Harder et al., 2003).

1.7.4 Emodepside inhibits muscle contraction in the parasitic nematode *A. suum*

Emodepside has been shown to irreversibly inhibit *A. suum* muscle contraction caused by ACh and the excitatory neuropeptide AF2, suggesting that emodepside functions at the neuromuscular junction (Willson et al., 2003). Removal of the nerve cords from *A. suum* somatic muscle preparations was shown to reduce emodepside-mediated inhibition of ACh response, suggesting that the major effect of emodepside is presynaptic (Willson et al., 2003). Supporting this, intracellular recordings from *A. suum* muscle cells revealed that emodepside, at concentrations which inhibited muscle

response to ACh, elicits a slow hyperpolarization of the muscle cells, suggesting that this effect is directly involved in the action of emodepside. Emodepside-stimulated hyperpolarization was irreversible upon drug washout, but significantly, it was reduced upon removal of Ca^{2+} from the external solution, and abolished by pre-treatment of the muscle cells with the K^+ channel blockers, 4-aminopyridine (4-AP) and tetraethylammonium (Willson et al., 2003). This suggests that in *A. suum*, emodepside affects Ca^{2+}-dependent neurotransmitter release, possibly by targeting Ca^{2+}-activated K^+ channels.

1.7.5 The latrophilins are involved in the mechanism utilized by emodepside to paralyse *C. elegans* locomotion and pharyngeal pumping

In the model organism *C. elegans*, emodepside has been found to immobilize mature adult worms and inhibit pharyngeal pumping, suggesting that the anthelmintic may target the neuromuscular junctions of the body wall and pharyngeal muscles (Willson et al., 2004). Based on the results of Saeger et al. (2001), which implicated a latrophilin-like receptor in the mechanism of action of emodepside, RNAi was performed targeting expression of *C. elegans lat-1* or *lat-2*, and the resultant worms were assayed for emodepside sensitivity. RNAi against either of the latrophilins was found to significantly reduce the emodepside sensitivity of *C. elegans* locomotion and pharyngeal pumping (Amliwala, 2005; Willson et al., 2004). These results suggest that the latrophilins are involved in the mechanism of action of emodepside.

1.7.6 The SLO-1 channel is involved in the mechanism utilized by emodepside to paralyse *C. elegans* locomotion

To identify further components of the mechanism of action of emodepside in *C. elegans*, a chemical mutagenesis screen was performed to generate *C. elegans* resistant to the effect of the anthelmintic on locomotion (Amliwala, 2005). Identification of the genes mutated in the resistant strains would therefore indicate components of the pathway(s) utilized by emodepside. The mutagenesis screen revealed that mutations in the *slo-1* gene produced worms with normal locomotion in the presence of 1μM emodepside, a concentration sufficient to cause maximal inhibition in wild-type (non-mutated) *C. elegans*. A role for SLO-1 in the mechanism utilized by emodepside was

further supported by identification of the resistance of the *C. elegans slo-1 (js379)* null mutant strain to emodepside-mediated paralysis of locomotion (Amliwala, 2005).

1.7.7 The *C. elegans* SLO-1 channel

The *C. elegans* SLO-1 channel belongs to the family of large conductance BK potassium (K^+) channels, which includes *Drosophila slowpoke* dSlo, and mammalian Slo channels. These channels **are distributed in both excitable and nonexcitable cells of vertebrates and invertebrates, where they are** activated by both intracellular calcium (Ca^{2+}) or voltage or synergistically by both (Magleby, 2003). As K^+ channels are the only ion-selective cation channel with an equilibrium potential near the typical cellular resting potential, they have been found to be crucial in determining the resting potential of most cells (Salkoff et al., 2006). The nature of BK channel activation means that they are ideally suited to a regulatory role in key physiological processes that involve an increase in intracellular Ca^{2+}, including muscle contraction and neurosecretion (e.g. Atkinson et al., 1991; Du et al., 2005; Elkins et al., 1986; Sausbier et al., 2004; Wang et al., 2001). Such an increase in Ca^{2+} concentration is achieved mostly via activation of voltage-dependent Ca^{2+} channels (VDCCs), which produces the electrical excitability that triggers processes like neurotransmitter release and muscle contraction. Importantly, the increase in intracellular Ca^{2+} is also thought to stimulate a negative feedback mechanism to depress this excitation and thereby provide a 'braking' mechanism for processes such as neurotransmitter release and muscle contraction. This 'braking' mechanism is though to involve the delayed opening of BK channels in response to increased intracellular Ca^{2+} (Latorre et al., 1982; Marty, 1981; McManus & Magelby, 1991; Pallota et al., 1981). BK channels have been found to functionally co-localize with VDCCs, which has been suggested to increase the efficiency of the negative feedback process (Marrion & Tavalin, 1998; Prakriya & Lingle, 1999).

In *C. elegans*, *slo-1* is expressed in the nerve ring, nerve cords, pharyngeal nervous system, body-wall muscle and vulval muscle (Wang et al., 2001). Structurally, the SLO-1 channel is a seven transmembrane domain protein with a large intracellular region containing four hydrophobic segments (S7-S10) and a region termed the 'calcium bowl' due to its Ca^{2+} sensing properties (see figure 1.11). The pore of the channel is located between the transmembrane S5 and S6, and the pore contains the K^+ selectivity filter (Wang et al., 2001). The RCK (regulator of conductance for K^+) domain, which

contains S7, possesses a site that works in conjunction with the Ca^{2+} bowl to regulate the channel in response to Ca^{2+}, and another site contributes to channel regulation in response to divalent cations (Xia et al., 2002).

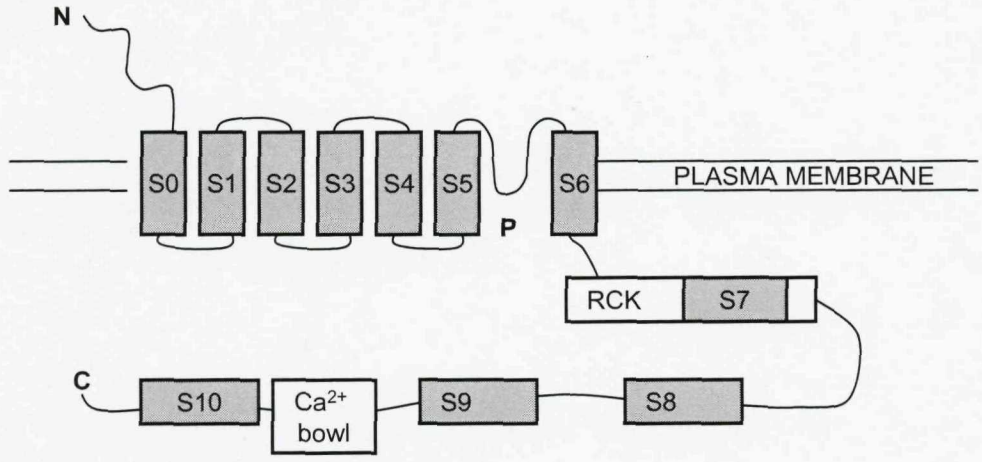

Figure 1.11 Predicted membrane topology of the SLO-1 channel. (Adapted from Wang et al., 2001; Xia et al., 2002).
SLO-1 possesses the major structural domains characteristic of BK channels: eleven hydrophobic regions (seven of these are transmembrane regions (S0-S6), and four are segments of the C-terminal cytosolic region (S7-S10)), the pore (P), the RCK domain, and the Ca^{2+} bowl.

In *C. elegans*, the SLO-1 channel is believed to be involved in the regulation of neurotransmitter release, with *slo-1* mutation found to suppress the lethargic phenotype of *unc-64* syntaxin mutants in which neurotransmitter release is restricted (Wang et al., 2001). Additionally, the *slo-1 (js379)* putative null mutant was shown to be aldicarb-hypersensitive, a phenotype attributed to enhanced ACh release (Wang et al., 2001). It has been suggested that SLO-1 channels contribute to the control of neurotransmitter release by opening in response to depolarization of the presynaptic membrane and the associated increase in Ca^{2+} levels within the presynaptic terminal. The consequent efflux of K^+ via SLO-1 acts to repolarize the presynaptic membrane and terminate neurotransmitter release (Wang et al., 2001). This is supported by the observed increase in the duration and amplitude of excitatory post-synaptic currents (EPSCs) at the neuromuscular junction (NMJ) of *C. elegans* lacking the SLO-1 channel; suggesting a loss of functional SLO-1 increases neurotransmitter release at the NMJ (Wang et al., 2001). Further supporting a role for SLO-1 in regulating neurotransmitter release, the channel is highly expressed in synaptic regions of the adult *C. elegans* nervous system, such as the nerve ring and body wall muscles (Wang et al., 2001).

Directed tissue-specific expression of *slo-1* (by injection of constructs containing *slo-1* placed behind a tissue-specific promoter) demonstrated that channel expression in neurons but not body wall muscle suppressed phenotypic paralysis in syntaxin mutants, suggesting a presynaptic functional location for SLO-1 (Wang et al., 2001). However, functional SLO-1 expression both pre- and postsynaptically has been shown to be important for the *C. elegans* response to ethanol (Davies et al., 2003). The *slo-1 (js118)* null mutant was found to be resistant to the intoxicating effects of ethanol on locomotion and egg laying. Restoration of *slo-1* expression in just the neurons was found to restore ethanol sensitivity for locomotion, but *slo-1* expression in the neurons, body-wall and vulval muscles was required to restore ethanol sensitivity in terms of egg-laying (Davies et al., 2003). Therefore, the role of *C. elegans* SLO-1 postsynaptically, presynaptically or both, is dependent on the specific physiological behaviour to which the channel contributes.

The BK channel Ca^{2+} bowl was suggested to be a region of high affinity Ca^{2+} binding as mutation to five highly conserved aspartate residues contained in the region produced a BK channel with reduced sensitivity to Ca^{2+} (Schreiber & Salkoff, 1997). However, BK channels in which the Ca^{2+} bowl was deleted were still capable of responding to physiologically relevant concentrations of Ca^{2+} (Xia et al., 2002), suggesting that there is more than one Ca^{2+}-binding site in the channel. It was subsequently shown that mutation of negative residues within a region of the BK channel called the regulator of conductance for K^+ (RCK) domain can reduce the high-affinity Ca^{2+}-sensitivity of the BK channel. Therefore, the RCK domain was suggested to be another high affinity Ca^{2+}-binding site (Bao et al., 2002; Jiang et al., 2001).

Although mutation of SLO-1 within the Ca^{2+} bowl produces a channel with reduced Ca^{2+} sensitivity, these channels retained the wild type sensitivity to cadmium ions (Cd^{2+}), suggesting that BK channels possess a least one binding site with a lower affinity for Ca^{2+} and the ability to bind other divalent cations (Schreiber & Salkoff, 1997). The presence within BK channels of multiple Ca^{2+} binding sites with differing Ca^{2+}affinities is believed to account for the large range of intracellular Ca^{2+} concentrations that regulates channel opening (Shi & Cui, 2001; Zhang et al., 2001). Therefore, over the physiological range of Ca^{2+} concentrations, relatively high affinity Ca^{2+} binding sites are suggested to mediate channel regulation. However, at much higher concentrations of intracellular Ca^{2+}, the sites with a lower affinity for Ca^{2+}

contribute to channel activation. The presence of low affinity Ca^{2+}-binding sites explains how BK channels can be activated in the absence of Ca^{2+} by the binding of divalent cations, such as Cd^{2+}, magnesium (Mg^{2+}), manganese, iron, cobalt and nickel, and also explains why binding by these divalent cations enhances the activation of BK channels already activated by Ca^{2+} (Oberhauser et al., 1988; Shi et al., 2002; Shi & Cui, 2001; Zeng et al., 2005; Zhang et al., 2001). Identification of the location of the low affinity sites was achieved by the creation of chimeric mammalian Slo channels composed of the transmembrane domains and extracellular regions of the mammalian Slo1 channel and the intracellular regions the Slo3 channel (Shi & Cui, 2001). Slo3 is a homologue of Slo1 and is a K^+ channel sensitive to pH and not Ca^{2+}, and therefore lacks the Ca^{2+} bowl within its intracellular regions (Moss & Magleby, 2001; Schreiber et al., 1998; Shi & Cui, 2001). It was found that these chimeric channels have a reduced Ca^{2+} sensitivity, but retained an ability to be activated by Mg^{2+}, suggesting that a low affinity Ca^{2+}-binding site is located in the RCK domains (Shi & Cui, 2001). To confirm these conclusions, the effect of point mutations to residues within the RCK domain on channel activation by Mg^{2+} was investigated, and resulted in the identification of two acidic amino acids that are crucial for Mg^{2+} binding to the RCK domain (Shi et al., 2002). Therefore, the RCK domain appears to contain both high affinity and low affinity Ca^{2+}-binding sites (Bao et al., 2002; Jiang et al., 2001; Shi et al., 2002). Recently, it has been proposed that BK channels, which consist of four channel subunits, possess two RCK domains per subunit, and that these RCK domains act as a gating ring in a similar way to the *M. thermoautotrophicum* K^+ (MthK) channel (Zeng et al., 2005). The gating ring of each MthK channel subunit is suggested to bind two Ca^{2+} ions, which results in a conformational change in the channel that expands the gating ring diameter and opens the channel pore (Jiang et al., 2002). Whether the BK channel also uses this mechanism is not yet proven, but the identification of two RCK domains within each BK channel subunit supports this hyothesis (Zeng et al., 2005).

The gating of BK channels by voltage is mediated by the voltage sensor located in the S4 region (Diaz et al., 1998). The activation of BK channels by both voltage and the binding of intracellular Ca^{2+} suggests that the channels possess two independent sensing mechanisms that converge near the gates of the pore located in the S6 region (Cox et al., 1997; Niu et al., 2004; Rothberg & Magelby, 2000). The synergistic action of the two types of sensors on channel gating is possible because the conformation changes that occur when the channel opens and closes are separate from conformational changes

associated with voltage sensor and Ca^{2+} sensor activation (Cox et al., 1997; Horrigan et al., 1999; Rothberg & Magleby, 1999). Each channel is composed of four subunits each with a voltage sensor and Ca^{2+} sensor. When the voltage sensors and Ca^{2+} sensors are not activated, the probability of channel opening is low. However, as more of the Ca^{2+} sensors and/or voltage sensors become activated, this increases the opening force on the gates, thereby leading an increase in the probability of channel opening. As up to four Ca^{2+} sensors can be activated along with up to four voltage sensors, this gives 25 different combinations of activated sensors. When the BK channel is in each of these 25 different states of sensor activation, the open probability of the channel is modified accordingly, but remains in equilibrium, so the channel continues to be in either an open or closed state. Therefore, for each of the 25 different states of sensor activation, the channel is open or closed, giving a two-tier allosteric model (Cui & Aldrich, 2000; Horrigan et al., 1999; Rothberg & Magleby, 2000, 1999). However, this model functions on the basis of there being only one Ca^{2+} sensor per BK channel subunit, and as previously discussed, at least two high-affinity Ca^{2+} binding sites and one low affinity Ca^{2+}/Mg^{2+}-binding site has been identified per subunit. Therefore, the allosteric model could be extended to account for a larger number of Ca^{2+} binding sites, resulting in a possible 1,250 channel states if there are three Ca^{2+}-binding sites per subunit (Salkoff et al., 2006).

1.8 PROJECT AIMS

Anthelmintic drugs are used to control parasitic nematodes, but continued heavy reliance on these compounds has led to the development of resistance in many species of parasite (Brownlee et al., 2000). Emodepside, a newly marketed anthelmintic, possesses efficacy against parasitic nematode species that are resistant to currently available anthelmintics, suggesting that emodepside utilizes a novel mechanism of action that could break the resistance problem (Harder et al., 2003).

The precise mechanism by which emodepside achieves anthelmintic efficacy is unknown, but recent research using the model organism *C. elegans* has suggested that emodepside can inhibit pharyngeal pumping and locomotion, possibly by the stimulation of excessive neurotransmitter release at the neuromuscular junction (Saeger et al., 2001; Willson et al., 2004, 2003). In this project, *C. elegans* was used to build upon this previous research by further investigating the effect of emodepside on worm physiology; revealing *C. elegans* behaviours affected by the compound, and identifying components of the pathway(s) involved in the mechanism of action for this drug. A combination of molecular techniques as well as behavioural and electrophysiological assays were used in the project to achieve these objectives.

Previous research has suggested that the *C. elegans* latrophilins have a significant role in the mechanism of action of emodepside (Amliwala, 2005; Willson et al., 2004). Therefore, one of key aims of this project was to further define the role of the latrophilins in the action of emodepside at the body wall and pharyngeal neuromuscular junctions.

Research has also suggested that the SLO-1 ion channel may be intimately involved in the activity of emodepside at the neuromuscular junction, with a functional loss of channel associated with strong drug resistance (Amliwala, 2005). Therefore, another key aim of this project was to extend this previous research by investigating how the SLO-1 ion channel operates as a component of pharyngeal neuromuscular junction as well as investigating its role in the mechanism of action for emodepside.

CHAPTER 2
MATERIALS AND METHODS

2.1 The culturing of *C. elegans*

C. elegans were grown on nematode growth medium (NGM) plates as described (Brenner, 1974). Composition of NGM (500ml) pre-autoclave: 1.5g NaCl, 10g Agar, 1.25g Peptone, 487.5ml distilled water. Post-autoclave: NGM medium supplemented with sterile 1M solutions: 0.5ml $CaCl_2$, 0.5ml $MgSO_4$, 12.5ml KH_2PO_4 and cholesterol. Wild type *C. elegans* used were Bristol, N2 strain. Hermaphrodite animals were fed and propagated on a bacterial lawn of *E. coli* OP50. The OP50 strain was used because it is a uracil-requiring mutant of *E. coli*, therefore uracil-limited NGM agar prevents OP50 overgrowth which would obscure *C. elegans* adults, larvae and eggs (Brenner, 1974).

2.2 *C. elegans* locomotion assays

2.2.1 Locomotion assay on emodepside-containing agar plates using synchronised *C. elegans* populations.

Emodepside or vehicle control (0.5% ethanol, v/v) was added to NGM media after autoclaving. Emodepside was freshly prepared as a 10^{-4}M stock in 100% ethanol, and appropriate quantities of stock were added to the NGM to generate drug concentration ranges on 9cm plates (10nM to 500nM emodepside). Plates used in the assay were prepared fresh for each experiment. 24 hours after the plates had been poured, 60μl OP-50 *E. coli* culture was spread onto each plate. These plates were incubated at room temperature for 48 hours to allow the growth of a robust bacterial lawn.

Eggs were isolated from gravid adult hermaphrodite worms by a modification of the alkaline hypochlorite method described by Lewis & Fleming (1995). Worms were harvested after three days growth at 20°C on NGM. Adults were floated off the plate in 5ml sterile M9 buffer, then transferred to a sterile 15ml screw-cap centrifuge tube and centrifuged for three minutes at 1500rpm using a Sorvall® Legend RT desktop centrifuge. The resultant pellet was washed twice in 5ml M9 buffer to remove contaminants and bacteria. Then 7ml of alkaline hypochlorite solution (2ml Clorox bleach in 5ml 1M NaOH) was added to dissolve the adult bodies. The solution was left for approximately five minutes, inverting gently and infrequently, to produce the egg solution. The alkaline hypochlorite solution was then diluted with M9 buffer (v/v), and centrifuged for two minutes at 1500rpm to collect the white egg pellet. The supernatant was removed, and the pellet resuspended in 10ml M9 buffer. The tube was inverted

several times, and centrifuged for two minutes at 1500rpm. This wash procedure was repeated a further three times to remove all the alkaline hypochlorite solution. The pellet was finally suspended in 0.5ml M9 buffer. 10μl of this solution was placed on a glass slide and viewed under a dissecting microscope to determine egg yield. Approximately 100 eggs were placed on each plate, and they were then incubated for five days at 20°C.

M9 buffer composition (g/litre): 6g Na_2HPO_4, 3g KH_2PO_4, 5g NaCl, 0.25g $MgSO_4.H_2O$. Alkaline hypochlorite composition: 2ml fresh Clorox bleach, 5ml 1M NaOH.

For analysis of locomotion, adult or L4 worms were transferred to plates with an identical agar composition to the plate that they had been developing on, but lacking bacterial food. Locomotion rate was quantified by counting the number of body bends produced by the worms in one minute. A body bend was counted each time the tip of the tail moved from the maximal upward deflection, to maximal downward deflection, and then returned to its original upward deflection. In separate assays, the time the worms spent moving was analysed by counting the number of seconds per minute the worms moved backward or forward regardless of how this movement was achieved by the worm (i.e. by sinusoidal or atypical body movements).

2.2.2 Locomotion assay on agar plates controlling for emodepside-exposure time

Emodepside (500nM) and ethanol (vehicle control) agar plates were made as described in section 2.2.1.

Adult and L4 *C. elegans* were transferred from NGM agar plates to emodepside or control plates with lawn of *E. coli* OP50 at zero hours. These worms were then incubated at 20°C for 18 hours. For analysis, adults and L4 worms were transferred to plates with an identical agar composition to the plate that they had been developing on, but without OP50. Locomotion rate was quantified by counting the number of body bends produced in one minute.

2.2.3 *C. elegans* thrashing assay

C. elegans adults or L4 were placed into a 3cm Petri dish containing Dent's saline supplemented with 1% bovine serum albumin (w/v). One worm was placed into each Petri dish. Thrashes produced by each worm in a 30 second period were counted after a two minute equilibration period. A thrash was defined as a change in direction of bending at the mid-body, as previously described (Miller et al., 1996). Emodepside was added to the Petri dish at zero minutes, and the thrashes produced by each worm in a 30 second period were counted 5, 10, 20, 30 and 60 minutes after emodepside was added to the saline. Emodepside was initially dissolved in ethanol vehicle to produce a stock solution, which was added to the Dent's saline to produce a final emodepside concentration of 10μM and a vehicle concentration of 0.1% (v/v). For the control experiments, ethanol vehicle was added to the Dent's saline at 0 minutes (final ethanol concentration was 0.1% (v/v), as in the emodepside experiments).

2.3 Assay to assess the effect of emodepside on *C. elegans* development

NGM agar plates containing emodepside (10-500nM) or ethanol (vehicle control) were made as described in section 2.2.1.

Synchronised populations of *C. elegans* (generated as described in section 2.2.1) were transferred as eggs to emodepside or control plates with a lawn of *E. coli* OP50 at zero hours. The development of these worm populations was assessed visually at 43 and 64 hours post-transferral. Worms were categorized as adults, larval stage four (L4), or larval stage one to three (L1-3) by looking for two key morphological characteristics: worm size and the development of the vulva. *C. elegans* development through the four larval stages to adulthood involves an increase in worm size. Larval stage four can be recognised by the developing vulva which does not yet create a passage from gonad to exterior, and can be identified as a clear, semi-circular region located in the middle (longitudinally) of the worm body. During the L4 moult to adulthood the developing vulva invaginates and then everts to form the mature vulva (Greenwald, 1997; Newman et al., 1996; Waterson, 1988), resulting in the disappearance of the clear region.

2.4 *C. elegans* egg laying assays

2.4.1 Assay to examine the effects of chronic exposure to emodepside on *C. elegans* egg laying

Measurement of the chronic effects of emodepside on egg laying behaviour was performed by modification of the method previously described by Bany et al. (2003). In this experiment, worms which had been transferred as eggs to plates containing emodepside at various concentrations were assayed at adulthood for the rate at which they laid eggs.

NGM agar plates containing emodepside (10-500nM) or ethanol (vehicle control plates) were made as described in section 2.2.1.

Worms were grown from synchronised egg populations on emodepside or control plates to early L4 stage, then ten worms were picked from each plate onto another plate with identical agar composition and food. 48 hours later egg laying rate was determined by transferring the adult *C. elegans* to a plate with an identical emodepside concentration for one hour and counting the number of eggs laid (one worm per plate). For each drug concentration tested, the assay was repeated a minimum of five times.

To investigate the reversibility of the impact of emodepside on egg laying, a modification of the assay described above was used. At early L4 stage, ten worms were taken from each emodepside plate and transferred onto control plates (one worm per plate). 48 hours later each worm was assayed for egg laying rate as described above. The assay was repeated a minimum of five times for each emodepside concentration.

To investigate whether emodepside exposure only during L4 and adulthood affects egg laying to the same extent as exposure from egg to adulthood, the assay described previously was modified again so that synchronised worm populations grown from eggs on control plates were transferred at early L4 stage to emodepside plates and then assayed 48 hours later for egg laying rate on emodepside. Again, for each drug concentration tested, the assay was repeated five times or more.

2.4.2 Assaying the effects of acute exposure to emodepside on *C. elegans* egg laying behaviour

The age-matched adult worms used in the acute emodepside assay were obtained by picking L4 stage hermaphrodites (grown on NGM agar) 44 hours before the assay and incubating these worms at 20°C on NGM agar.

For the assay, the age-matched adult worms were transferred initially to NGM agar plates (one worm per plate) and the number of eggs within the worm and the eggs laid in one hour were counted to ensure that all worms used in the assay were actively engaged in egg laying behaviour. These worms were then transferred to NGM plates containing either 500nM emodepside or the vehicle ethanol (at 0.5%, v/v), with one worm per plate. The number of eggs within each worm was then counted. One hour later the number of eggs laid on each plate and the number of eggs within each worm was counted. This procedure was repeated each hour for a total of four hours.

2.5 Assay to assess the acute effect of emodepside exposure on the timing of *C. elegans* egg hatching.

Ten gravid adult wild type *C. elegans* grown on NGM agar plates were transferred to an NGM plate with *E. coli* for one hour and then removed. The eggs laid on the plate were collected by floating them off in sterile M9 buffer (composition as described in section 2.2.1) and then centrifuged for two minutes at 2000g to collect the white egg pellet. The eggs were re-suspended by washing in fresh M9 buffer and then centrifuged and washed again to remove residual bacteria. The eggs were then transferred to NGM agar plates containing either 500nM emodepside or 0.5% (v/v) ethanol vehicle, and the number of eggs that hatched to produce active larvae were counted every two hours for twelve hours and then again at 22 hours.

2.6 Molecular genetics techniques

2.6.1 RNAi for *lat-1* using the feeding method

Exon rich fragments of *lat-1* were obtained by polymerase chain reaction (PCR) from *C. elegans* cDNA or genomic DNA. Oligonucleotides were produced by Invitrogen Ltd. Primer design and PCR were performed by J. Willson and K. Amliwala as described in Willson et al. (2004). The *lat-1* fragments (all ~1kb in length) were cloned into the L4440 feeding vector (Pdp129.36), and the resulting plasmids were transformed into competent HT115 (DE3) *E. coli* (as detailed in Willson et al., 2004). Single colonies of HT115 bacteria that had been successfully transformed with the L4440 plasmid were picked and grown in culture in LB with 100μg/ml ampicillin (amp) and 12.5μg/ml tetracycline. Bacteria grown for eight hours were then seeded directly onto NGM plates containing 1mM isopropyl-β-D-thiogalactopyranoside (IPTG) and 50μg/ml amp. Seeded plates were allowed to dry at room temperature and induction proceeded at room temperature overnight. Single L4 hermaphrodite worms (*rrf-3 (pk1426)* strain) were placed onto the NGM + amp plates containing seeded bacteria expressing *lat-1* dsRNA and were incubated for 40-60 hours at 20°C. Following incubation, three F2 worms were transferred onto plates seeded with the same bacteria and were allow to populate the plate. The adult progeny from these F2 worms were assayed for emodepside sensitivity.

2.6.2 Generation of transgenic *C. elegans* in which *slo-1* is expressed in pharyngeal muscle

A construct to drive expression of *slo-1* in the pharyngeal muscles was made by placing the *slo-1* sequence (from the pBK3.1 plasmid; Wang et al., 2001; kindly provided by L. Salkoff) behind the *myo-2* promoter of the pPD30-69 plasmid (kindly provided by A. Fire).

Initially, the *slo-1* sequence (splice variant *slo-1a*) was digested from the pBK3.1 plasmid using a triple restriction digest with the restriction enzymes XbaI, ApaI and NheI. The following reaction mix and procedure was used:

Reagent	Volume µl
pBK3.1	5
Apa1	1
BSA (100x)	0.5
Buffer (10x)	5
Water (ddH_2O)	33.5
Incubated for 17 hours at 25°C, then added:	
Nhe1	1
Xba1	1
Incubated for 6 hours at 37oC, then added:	
Shrimp alkaline phosphatase	3
Incubation for 1 hour at 37°C, then the mix was put at 65°C for 20 minutes to inactivate the enzymes and phosphatase.	

Shrimp alkaline phosphatase was added to remove phosphate groups from the 5'-ends of the linearized DNA fragments and prevent re-ligation.

Following the digest, the pBK3.1 fragment containing the *slo-1a* sequence was isolated by agarose gel electrophoresis. Gel composition: 1.4g agarose, 140ml buffer, 5µg ml^{-1} ethidium bromide. 12.5µl loading buffer was added to the 50µl digest solution, and then loaded into the gel with a DNA ladder for reference. The gel was run for three hours at 100 volts. The DNA band corresponding in size to the pBK3.1 fragment containing the *slo-1a* and GFP sequences was cut from the gel and purified using the Qiagen™ QIquick™ gel purification kit.

The pPD30-69 plasmid containing the *myo-2* promoter sequences and the ampicillin-resistance gene was digested using the enzymes Apa1 and Nhe1 to remove the *unc-53* untranslated (UTR) sequence, thereby enabling the pBK3.1 *slo-1a* fragment to be ligated into pPD30-69 behind the *myo-2* promoter sequences. The double restriction enzyme digest of pPD30-69 was performed as follows:

Reagent	Volume µl
pPD30-69	2
Apa1	1
BSA (100x)	0.5
Buffer (10x)	5
Water (ddH_2O)	36
Incubated for 2 hours at 25°C, then added:	
Nhe1	1
Incubated for 2 hours at 37oC, then placed at 65°C for 20 minutes to inactivate the enzymes.	

The fragment of pPD30-69 containing the *myo-2* promoter sequences and ampicillin-resistance gene was isolated by agarose gel electrophoresis (gel composition as before). 11µl of loading buffer was added to the mixture from the pPD30-69 digest and then loaded into the gel with a DNA ladder for reference. The gel was run for two hours at 100 volts. The DNA band corresponding in size to the pPD30-69 fragment containing the *myo-2* promoter sequence was cut from the gel and purified using the Qiagen™ QIquick™ gel purification kit.

The pBK3.1 *slo-1a* fragment was ligated behind the *myo-2* promoter sequences of the pPD30-69 fragment by incubating the following mixture for 17 hours at 15°C:

Reagent	Volume µl
Linearized pPD30-69	3
slo-1a/gfp sequences	41.5
Ligase	1
Buffer (10x)	3
PCR-grade water	1.5

To increase the quantity of plasmid generated by the ligation, DH5α bacterial cells were transformed with the newly constructed plasmid and allowed to proliferate. For the transformation, 1µl of the mixture from the ligation was added to 25µl of DH5α cells and then incubated on ice for 30 minutes. The bacteria were then heat shocked at 42°C for 45 seconds to enable the transformation. Immediately following the heat shock the

bacteria were placed on ice for two minutes. Following this, 100µl of LB (Luria-Bertani) medium (at room temperature) was added and the mixed continuously for one hour at 37°C. LB medium composition: 10g tryptone, 5g yeast extract, 5g NaCl, 1ml of 1M NaOH, 1 litre distilled water (LB medium was autoclaved prior to use). Following the one hour incubation of the bacteria, 20µl and 100µl aliquots of this solution were spread onto LB ampicillin agar plates. These plates were prepared by the addition of 15g bacteriological agar per litre of standard LB medium and autoclaved. Following cooling to below 50°C (to prevent loss of antibiotic function), 50µg/ml ampicillin was added, thereby allowing only bacterial cells expressing the newly constructed plasmid (which contains the ampicillin-resistance gene) to culture.

The plates were then cultured overnight at 37°C and individual colonies picked and transferred separately to 10ml aliquots of LB medium containing ampicillin (50µg/ml). These colonies were then incubated for 18 hours at 37°C and were continuously shaken during the incubation to maximise colony growth.

Cultures were then spun at 13,000rpm to isolate the bacterial cells. The supernatant was decanted off and the bacterial cells resuspended. DNA was extracted from the cells using the Qiagen™ QIAPrep Miniprep kit. The resuspended cells were lysed using NaOH/SDS buffer, which was then neutralized in a high salt buffer to precipitate any cellular debris, denatured proteins, chromosomal DNA and SDS. The resulting lysate was centrifuged for ten minutes at 13,000rpm to separate the precipitated matter from the supernatant containing the DNA. This supernatant was pipetted onto a 1ml spin column containing a silica gel membrane and centrifuged for one minute at 13,000rpm, leaving the DNA bound to the column membrane. Subsequent washing of the membrane with alkali buffer removed any salts, ensuring that only DNA was bound to the membrane. RNAse-free water was then applied to the membrane and the column was centrifuged for one minute at 13,000rmp to elute the DNA.

The cells produced from each colony originally picked from the LB/ampicillin plates were kept separate and therefore separate Minipreps were performed for each. This method produced 18-21µg/ml of DNA for all the solutions.

To check that the DNA samples obtained from the Minipreps contain only the new construct, a restriction digest was performed on a small sample of DNA from each Miniprep using the enzyme HindIII. The digestion mixture was as follows:

Reagent	**Volume µl**
DNA from Miniprep	5
HindIII	1
BSA (100x)	0.5
Buffer (10x)	5
Water (ddH_2O)	38.5

The digestion mix was incubated at 37°C for 17 hours, and then the enzymes were inactivated by 20 minutes at 65°C. Visualization of the DNA fragments produced from the digest was achieved by agarose gel eletrophoresis (gel composition as before). 12.5µl of loading buffer was added to the 50µl solution from the digest and then loaded onto the gel. A DNA ladder was also loaded on the gel (but separated from the digestion mix), to enable the size of the bands produced to be ascertained. The gel was run for four hours at 100 volts.

The HindIII digest confirmed which of the DNA solutions from which of the original DH5α colonies picked from the LB/ampicillin plates contained the plasmid and could be used for injection into *C. elegans*.

C. elegans were injected with two constructs: the new plasmid containing the *slo-1a* sequence under the control of the *myo-2* promoter (*myo-2::slo-1*), as well as the reporter construct containing the *gfp* sequence under the control of the *myo-2* promoter. For the injections, young gravid adult *slo-1 (js379) C. elegans* were transferred to an agarose pad covered with a thin layer of mineral oil. Agarose pads were prepared from a solution of 2% (w/v) agarose in water, which was melted (60-95°C) and then a drop was placed on a glass slide and flattened using a cover slip to produce a thin, even layer of agarose. Once the worms had stuck to the agarose pad, they were ready for injection.

The solution for injection was as follows:

Reagent	Volume µl
Injection buffer (5x): ▪ 10ml 1M K_2HPO_4, pH7.5 ▪ 5ml 300mM potassium citrate pH7.5 ▪ 10g polyethylene glycol ▪ 35ml water (ddH_20)	4
Marker plasmid (500ng/µl)	4
myo-2::slo-1 plasmid (125ng/µl)	5
Water (ddH_2O)	7

The injection solution was centrifuged at 13,000rpm before each use to minimize undesired particulate matter blocking the injection needle.

Microinjection needles were pulled on a Sutter Flamin-Brown P2080 from alluminosilicate glass capillaries with an outer diameter of 1.0mm. These needles were filled with the injection solution, and the tip of the needle was broken against a coverslip to allow the solution to flow out. The loaded needle was placed into an instrument holder attached to a controllable pressure source (Eppendorf microinjection controller), and the needle assembly was mounted into a remote-controlled instrument manipulator (Narashige). The needle assembly was positioned over the stage of an inverted microscope. A glass slide possessing a worm mounted on an agarose pad was placed on the microscope stage and the injection needle was positioned next to the worm at the level of the syncytial gonad. The needle was pushed against the worm cuticle until a slight indentation was observed. A gentle tap was then applied to the micromanipulator to allow the needle to penetrate the worm. The DNA solution was then injected into the worm gonad using the Eppendorf microinjection controller. Filling of the gonad was visible as an inflation of the structure, and filling was only ceased when the gonad had inflated completely along its length. Both gonads were injected in each worm.

After the injection, the worms were floated off the agarose pad with M9 buffer (see section 2.2.1 for composition) and transferred to agar plates (prepared with *E. coli*) for culturing. Each injected worm was placed on a separate agar plate.

The progeny of the injected worms were examined under UV illumination for GFP fluorescence in the pharyngeal muscles. Of the 50 worms injected, one produced progeny demonstrating GFP fluorescence. These progeny were transferred to a new

plate for further culturing. The incidence of plasmid inheritance was approximately 20% of the progeny produced by the transgenic worms. When the food had been depleted on an agar plate, fluorescent worms were identified and transferred individually to a new plate to prevent loss of the strain.

2.7 Electrophysiological techniques

2.7.1 Extracellular recordings: electropharyngeograms (EPGs)

Extracellular recordings were performed using previously described methods as a basis from which modifications appropriate for the current investigation were made (Davis et al., 1995; Raizen and Avery, 1994; Willson et al., 2004).

Adult hermaphrodites were transferred into 3ml Dent's Saline supplemented with 1% (w/v) bovine serum albumin, and were then cut just posterior to the terminal bulb of the pharynx with a surgical blade.

Dissected worm heads were then transferred to a custom built chamber (volume 500μl) on a glass cover slip. Suction pipettes were pulled from borosilicate glass (Harvard instruments, diameter 1mm). The diameter of the pipette tip varied according to the size of the dissected head, but typically ranged between 20 and 40μm. The suction pipette was mounted in a holder with a tubing port through which suction was applied. The pipette was lowered into the chamber containing Dent's saline, and suction was applied to fill the pipette with saline solution. The pressure within the pipette was then allowed to equilibrate with atmospheric pressure for three minutes before the dissected head was placed into the chamber. The pipette was manoeuvred close to the nose of the worm head, and then suction was applied to capture the worm.

The suction pipette contained a silver electrode, which was connected to a HS2 head-stage (Axon Instruments), which in turn was connected to an Axoclamp 2B-recording amplifier. A glass capillary filled with 4% (w/v) agarose gel containing 3M KCl was used to connect the recording bath to a KCl solution containing a silver electrode connected to the HS2 head-stage (see figure 2.1A). Data were acquired using axoscope (Axon Instruments). Recordings were done at ambient temperature (21-26°C).

When the pharyngeal preparation is sucked into the suction pipette, two electrical compartments are created, and these are separated by the seal between the cuticle of the preparation and the pipette wall. Therefore, voltage transients produced by currents flowing out of the preparation 'mouth' (R_o, see figure 2.1B) and across the resistance formed at the junction between the cuticle and pipette (R_s, see figure 2.1B) can be recorded (Raizen & Avery, 1994).

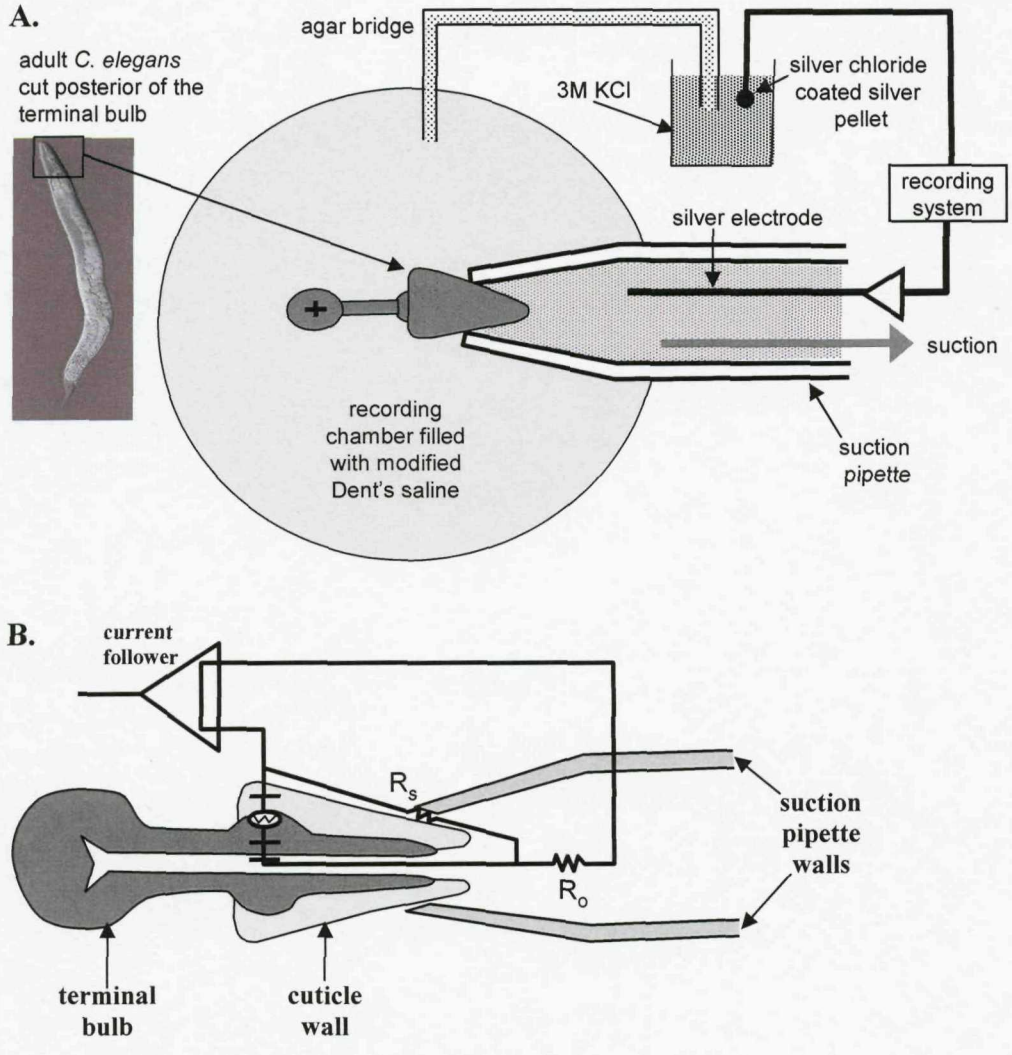

Figure 2.1 Experimental set-up for EPG recording from the *C. elegans* pharynx.
A. Diagram to show how the apparatus for recording EPGs is arranged. **B.** Diagram to show the circuit that is set up to record extracellular electrical activity from the pharynx. R_o is the current flowing from the 'mouth' of the head preparation. R_s is the resistance formed at the junction of the pipette wall and cuticle of the head preparation.

Dimethyl sulphoxide (DMSO) was used as the vehicle for each of the novel anthelmintic compounds tested in the electropharyngeogram assay (except where specified). The DMSO concentration in all experiments was 0.01% (v/v final concentration) except where specified. Control experiments were performed for each of the *C. elegans* strains used in the EPG assays to establish whether DMSO at 0.01% had any effect on pharyngeal activity. The protocol used for this investigation first exposed the pharyngeal preparations to 500nM 5-HT for two minutes to obtain a sufficient pumping rate for analysis. This was followed by a wash in Dent's saline to remove the 5-HT, and then application of a 0.01% DMSO solution for ten minutes (with no 5-HT present). Finally, the pharynx was washed to remove the DMSO, and then 500nM 5-HT was applied for a further two minutes. For each pharynx, the pumping rate in 5-HT following DMSO exposure was expressed as a percentage of the pumping rate in 5-HT before DMSO was applied. This is the same protocol employed when DMSO is being used as a vehicle for the anthelmintic compounds, and will therefore allow DMSO to be tested in the context of the protocol used for anthelmintic testing.

No strains were found to have significantly altered response to 500nM 5-HT following exposure to 0.01% DMSO for ten minutes (see figure 2.2). Therefore, DMSO was a suitable vehicle for the anthelmintic compounds tested.

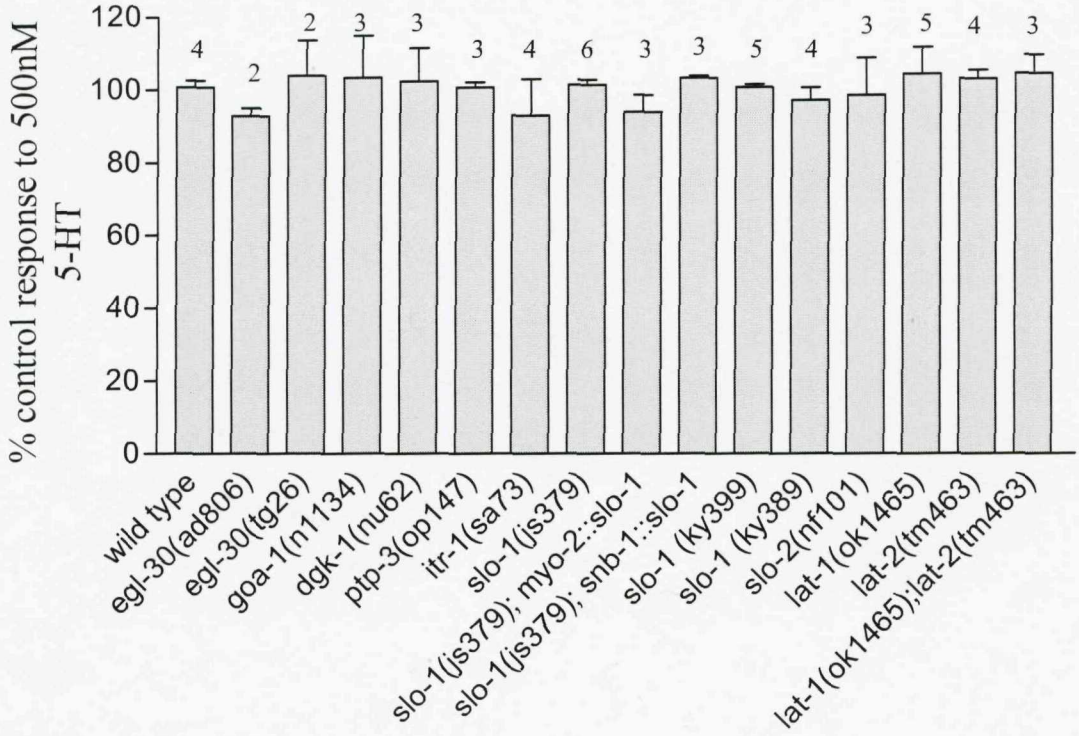

Figure 2.2 The effect of 0.01% DMSO on the pharyngeal response to 500nM 5-HT in each of the worm strains used in this project.
Each bar is the mean ± S.E.Mean of (n) pharyngeal preparations. The n numbers are given above each bar. '% control response to 500nM 5-HT' is the pharyngeal pumping rate in 5-HT following DMSO exposure as a percentage of the pumping rate in 5-HT prior to DMSO exposure.

2.7.2 Preparation of the anthelmintic compounds for use in the EPG assay

The compound JES-737 was initially dissolved in DMSO to make a 'stock solution' of 1mM, which was then diluted to produce a solution of 1μM JES-737 (0.01% DMSO, v/v) for use in the electropharyngeogram experiments.

The novel compound HLR8090-3-4 was provided in a resinous formulation of unknown concentration, and the density of the compound was also not provided. Therefore, it was assumed that 1μl of the resinous formulation is equal to 1mg of the compound. As the molecular weight of HLR8090-3-4 is 171.4, then a 1M solution would be:

HLR8090-3-4 molecular weight = 171.4

Therefore 171.4 g/litre = 1M

171.4 mg/ml = 1M

Assume 1μl = 1 mg (actual density unknown)

Then 171.4 μl/ml = 1M or 17.1% solution

A 20% solution would be approximately 1M

Therefore 200μl of the resinous formulation was dissolved in 800μl of DMSO to produce a 1M solution

The 1M stock solution was then diluted to produce a solution of 1μM HLR8090-3-4 (0.01% DMSO vehicle) for use in the electropharyngeogram experiments.

The cyclooctadepsipeptide compounds, emodepside, verticilide, PF1022-888 and PF1022-222 were initially prepared as 10mM stock solutions in DMSO, and then diluted to achieve the required concentration of compound (0.01% DMSO).

2.7.3 The use of 5-HT in the protocol for the EPG assay

To examine the effect of novel anthelmintics on pharyngeal activity using the EPG preparation, a variety of protocols were used and are described for each individual experiment. Except where specified, a protocol involving the use of 5-HT was adopted to stimulate a regular pumping rate in the preparation, enabling a more accurate analysis of the effect of specific compounds on pharyngeal activity. This is because the wild type pharyngeal preparation pumps at only one Hertz or less in Dent's saline (Rogers et al., 2001), which could lead to subtle effects of the tested compounds on pumping rate being obscured.

It was noticed that when the EPG pharynx preparation was exposed to 5-HT for the first time, it often demonstrates a "naïve response", in which pumping rate is stimulated to a less-than-maximal rate for that concentration of 5-HT. Subsequent washing of the preparation in Dent's saline, followed by a 'recovery' period of two minutes in Dent's saline (not wash solution), and the reapplication of 5-HT (at same concentration as used in the initial application) was found to result in a faster pumping rate in 5-HT (see figure 2.3). Consequently, during the testing of novel compounds using a 5-HT

protocol, an increase in pumping rate in 5-HT following exposure to a compound may be due to a sub-maximal initial response to 5-HT rather than a specific stimulatory effect of the compound. To counter this, each pharynx preparation treated with the 5-HT protocol underwent a pre-recording repeated exposure to 5-HT (at the concentration and for the time length used in the protocol) to ensure that the preparation would reach its maximal pumping rate when the 5-HT was applied during recording. Each preparation was exposed to 5-HT repeatedly until two sequential applications elicited a pump rate difference of 2% or less (if the response to 5-HT began to decline upon repeated 5-HT application, then the preparation was discarded). 39% of wild type *C. elegans* reached maximum 5-HT response upon the third application, 34% upon the second application, 16% upon the first application, and 11% required four or more applications (from a total of 64 wild type *C. elegans*). These results suggest that dissected wild type *C. elegans* pharyngeal preparations vary in the length of 5-HT exposure time required to reach maximal response, with 89% requiring longer than 2 minutes exposure and the majority of worms requiring between four and six minutes. It is possible that this variation occurs naturally in the intact worm or is a result of variable levels of damage incurred during the dissection process. Future investigation could establish whether such variation in the time scale for maximal response to 5-HT exists in intact wild type *C. elegans*.

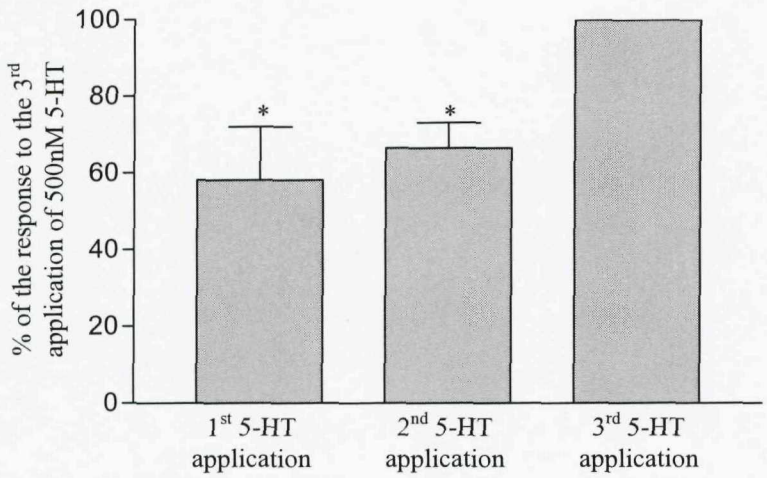

Figure 2.3 The effect of repeated application of 500nM 5-HT on wild type *C. elegans* pharyngeal pumping rate.
Each bar is the mean ± S.E.Mean of 7 pharyngeal preparations. Statistical significance (Student's t-test) relates to a comparison of the mean pumping rate in the 1st or 2nd 5-HT applications with the pumping rate in the 3rd 5-HT application. Each 5-HT application was for 2 minutes duration. The pharynx was washed in Dent's saline following each 5-HT application and allowed to recover in Dent's saline for 2 minutes before 5-HT was reapplied.

2.7.4 Whole cell patch clamp recording

Whole cell currents were recorded from the muscle cells of the *C. elegans* pharynx terminal bulb. The head of each worm was dissected as described in the EPG protocol (see section 2.7.1), and then transferred to a recording chamber where a suction pipette (filled with chamber medium) was attached to the cut edge of the cuticle and used to gently hold the preparation in position against the base of the recording chamber. The solution in which the dissection takes place and the bath solution in the recording chamber are both composed of 10mM Hepes, 140mM NaCl, 5mM KCl, 6mM $CaCl_2$, 5mM $MgCl_2$, pH adjusted to 7.4 (Carre-Pierrat et al., 2006).

An enzymatic digest was then used to remove the basement membrane of the pharynx which will interfere with seal formation and obtaining whole cell access. Firstly, a preparation of 1mg/ml trypsin in bath solution was applied for 30 seconds, and then the pharynx was washed thoroughly but gently in bath solution. This was followed by application of a solution containing 0.23mg/ml protease type XIV and 0.63mg/ml collagenase P in bath solution for two minutes, and then the pharynx was washed again to remove all enzymes.

Patch electrodes for whole cell recordings were pulled from alluminosilicate glass capillaries to a resistance of 4-8MΩ using a Sutter Flamin-Brown P2080. The pulled capillaries were filled with internal solution containing 10mM Hepes, 140mM KCl, 0.1mM $CaCl_2$, 5mM $MgCl_2$, pH adjusted to 7.40 (Carre-Pierrat et al., 2006). The capillary was mounted in the holder of a headstage connected to an Axopatch 2A amplifier. The capillary holder contained a silver electrode which was inserted into the capillary lumen when mounted in the holder. The headstage was held in a mechanical manipulator allowing the patch electrode to be manoeuvred to enable formation of a GΩ seal with the plasma membrane of a terminal bulb muscle cell of the digested pharynx. A small electrical current was then applied through the electrode to break the membrane spanning the lumen of the electrode tip, thereby achieving whole cell access. A voltage step-protocol was applied in which the cell was held at -80mV for 200 ms, followed by 10mM steps from -100mV to 90mV for 100 ms at each voltage. Data were acquired using Clampex 9.2 (Axon Instruments). A glass capillary filled with 4% (w/v) agarose gel containing 3M KCl was used to connect the recording bath to a KCl solution

containing a silver electrode connected to the head-stage. Recordings were done at ambient temperature (21-26°C).

2.8 Visual counting method to examine pharyngeal pumping in intact *C. elegans*

Intact *C. elegans* were placed into the recording bath used for the EPG assays and the anterior tip ('nose') of a worm was sucked into a glass capillary pulled to a fine diameter in exactly the same way as the recording electrode for the EPG assays. The glass capillary was held in a mechanical manipulator which allowed the worm to be positioned very gently against the base of the recording chamber to reduce thrashing behaviour. Pharyngeal pumps were counted over 30 second periods. Drugs were applied to the recording chamber in exactly the same fashion as in the EPG assay (without perfusion).

2.9 Measuring ethanol concentration using the Randox™ alcohol testing kit

Ethanol concentration of samples was analysed using the Randox™ blood, serum and urine alcohol testing kit. The procedure used was the serum/urine assay (non-cellular), which is based on the oxidation of blood alcohol to acetaldehyde using the enzyme alcohol dehydrogenase (ADH), as shown below:

$$C_2H_5OH + NAD^+ \xrightarrow{ADH} CH_3CHO + NADH + H^+$$

NAD^+ is the oxidised form of NAD (nicotinamide adenine dinucleotide), and NADH is the reduced form of NAD. The corresponding increase in NADH is measured from the change in solution absorbance.

A reagent blank was used a control for the contribution of the buffer and NAD to the absorbance reading in the spectrophotometer. Five standard solutions were made using a known concentration of ethanol (100, 200, 300, 400, 500mM). This enabled a calibration graph to be made, in which the absorbance of these five solutions was plotted against their ethanol concentration. Using this graph the ethanol concentration of sample solutions was calculated from their absorbance reading.

Solutions were prepared using the compositions given in the table below.

	Reagent Blank	Standard (solution of known ethanol concentration)	Sample (solution of unknown ethanol concentration)
Buffer (Solution 1)	4.8ml	4.8ml	4.8ml
NAD+ (Solution 2)	0.1ml	0.1ml	0.1ml
Double distilled water	0.01ml		
Standard ethanol solution		0.01ml	
Sample ethanol solution			0.01ml

These solutions were mixed well and then 0.02ml of ADH was added to each tube, and these solutions were then incubated in a water bath at 37°C for 25 minutes. The absorbance of the solutions was then read against the blank using a spectrophotometer.

Figure 2.4 shows the calibration graph that was constructed from the absorbance reading of five solutions of known ethanol concentration (zeroed against the reagent blank).

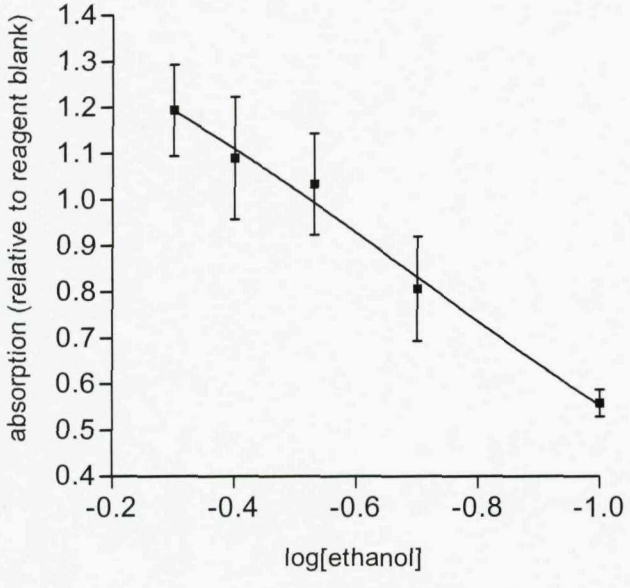

Figure 2.4 Calibration graph constructed from the absorbance reading of five solutions of known ethanol concentration (zeroed against the reagent blank).

The protocol for the pharyngeal assay examining the impact of ethanol on the *C. elegans* pharynx involved the application of a 1ml ethanol solution for ten minutes. Therefore, five 1ml solutions of known ethanol concentration (100, 200, 300, 400, 500mM) were left for ten minutes in the exact conditions that would be used in the pharyngeal assay, and then the ethanol concentration of each solution following the ten

minutes was calculated form the absorbance using the calibration graph shown in figure 2.4. This experiment was repeated five times to obtain a mean absorbance value for each of the solutions. The results are shown in the table below.

Original ethanol concentration before 10 minutes exposure (mM)	**Mean absorbance (against reagent blank) following 10 minutes exposure (n=5)**	**Log[ethanol] calculated from calibration graph**	**Actual ethanol concentration following 10 minutes exposure (mM)**
100	0.475	-1.08	83
200	0.752	-0.8	158
300	-.856	-0.67	214
400	1.035	-0.49	324
500	1.071	-0.44	363

From these results it can be seen that up to 29% of the ethanol evaporated from a 1ml solution over a ten minute period. Therefore, it was decided that a perfusion system was required for the pharyngeal assay using ethanol.

2.10 Statistical analysis

Data are presented as the mean: with 95% confidence interval for 'n' experiments. Inhibition curves were fitted to the modified logistic equation using Graph Pad Prism computer software (version 3.0, San Diego California). Statistical significance was determined using Student's t-test (unpaired test used, significance level set at $P<0.05$). Concentration response curves were fitted using the nonlinear regression sigmoidal dose-response (four-parameter logistic) equation. The Graph Pad Prism program was used to analyse the data and fit the curve. The regression model is based on the following equation:

Y = Bottom + (Top-Bottom) / (1+10^ (logEC50-X)*HillSlope))

Bottom is the Y value at the bottom plateau of the curve (set as a constant 0), and Top is the Y value at the top plateau of the curve (set as a constant 100). The logEC50 is the log of the X value when the response is halfway between Bottom and Top (also referred to as the IC50 when the data demonstrates inhibitory activity). The HillSlope is the steepness of the curve and is fitted by this Prism program. All curves were analysed using these parameters, the only exceptions being the pharyngeal response of the *slo-1 (js379)* strain and *slo-1 (js379); myo-2::slo-1* strain to emodepside. For these two *C. elegans* strains, pharyngeal inhibition did not reach the IC50 within the range of

emodepside concentrations used. Therefore, for the nonlinear regression equation, the value Bottom was not set to a constant of zero.

CHAPTER 3
INVESTIGATING THE EFFECTS OF SEVEN NOVEL ANTHELMINTIC COMPOUNDS ON WILD TYPE (BRISTOL N2 STRAIN) *C. elegans*

3.1 Introduction

The rising incidence of parasite resistance to anthelmintics has stimulated increased investment in the search for new anthelmintics that operate via novel biological pathways. In this chapter, seven novel compounds identified as potential anti-nematodal drugs (provided by Bayer AG) are tested for anthelmintic activity in *C. elegans*.

JES-737 (also known as HLR8068-3-3; molecular weight 216.2) and HLR8090-3-4 (molecular weight 317.34) are novel compounds with anthelmintic potential, and their structures are shown in figure 3.1.

Emodepside, a novel anthelmintic compound, has been shown to possess anthelmintic activity against a range of parasitic nematodes, including strains that are resistant to currently used anthelmintics (Harder et al., 2003; Zahner et al., 2001b). Therefore, emodepside appears to utilize a novel mechanism of action against parasitic nematodes, suggesting that this drug possesses resistance-breaking capability. Emodepside is derived from the compound PF1022A by addition of a morpholino group to each of the two PhLac moiety side-chains attached to the main cyclic 'backbone' of PF1022A (Jeschke et al., 2005; see figure 3.1). Further modification to the morpholino groups of emodepside has produced the derivative bis-dimethyl-morphonyl-PF1022 (see figure 3.1).

PF1022A and emodepside share potent anthelmintic capabilities against parasitic nematodes *in vivo*, attributed to their structural similarity (Jeschke et al., 2005). Therefore, the common structural features of emodepside and its derivative bis-dimethyl-morphonyl-PF1022 suggest that this compound may also share the anthelmintic properties previously exhibited for emodepside in *C. elegans* (Harder et al., 2003; Willson et al., 2004, 2003).The molecular weight of bis-dimethyl-morphonyl-PF1022 is 1100.

PF1022-888 and PF1022-222 are derivatives of the emodepside-precursor PF1022A, and were created by the addition of structures to the two PhLac moiety side-chains attached to the main cyclic 'backbone' of PF1022A (see figure 3.1; Jeschke et al., 2005). PF1022-888 and PF1022-222, like PF1022A and emodepside, have been shown to be active *in vivo* against the parasitic nematodes *H. contortus* and *T. colubriformis*.

Significantly, Jeschke et al. (2005) have demonstrated that PF1022-888 has greater potency against *H. contortus* than both emodepside and PF1022A, and its potency against *T. colubriformis* is greater than PF1022A although less than emodepside. It was also shown by Jeschke et al. (2005) that PF1022-222 is more potent than PF1022A but less potent than emodepside against *H. contortus*. Against *T. colubriformis*, PF1022-222 and emodepside are equally potent (Jeschke et al., 2005). This suggests that PF1022-888 and PF1022-222, like the PF1022A-derivative emodepside, may have anthelmintic activity in *C. elegans*. PF1022-888 and PF1022-222 have molecular weights of 1141 and 1091.42, respectively, and their structures are shown in figure 3.1.

Verticilide (FKI-1033) is another derivative of PF1022A, however, unlike PF1022A and the previously described derivatives, verticilide does not possess the PhLac moiety and instead has a carbon/hydrogen chain shown in figure 3.1 (d). Verticilide has a molecular weight of 853.1.

(a) JES-737

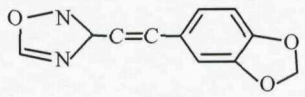

(b) HLR8090-3-4

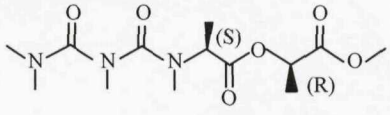

(c) PF1022A

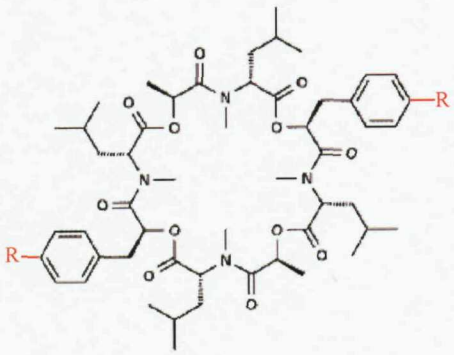

(d) Verticilide

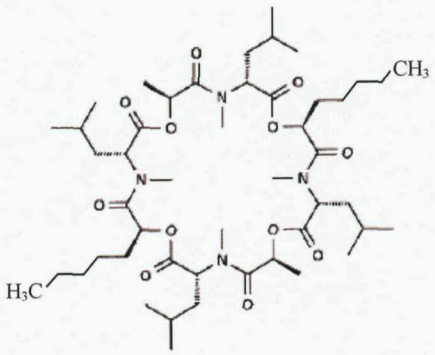

(e)

Novel anthelmintic	(PF1022A) + R group
emodepside	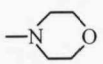
Bis-Dimethy-Morphonyl-PF1022	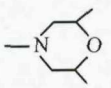
PF1022-222	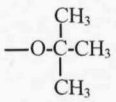
PF1022-888	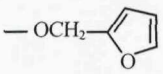

Figure 3.1 The chemical structures of the seven novel compounds investigated in this chapter as well as the octacyclodepsipeptide 'parent' compound PF1022A (provided for structural reference). Structural information provided by Bayer AG.
The structures of **(a)** JES-737, **(b)** HLR8090-3-4, **(c)** PF1022A: the structure of PF1022A forms the 'core' of the anthelmintics listed in (e). The R group is not present in PF1022A itself, but is an additional group attached to the PhLac moitety in the derivatives. **(d)** The structure of verticilide is identical to PF1022A, except that it has -CH2-CH2-CH2-CH3 in place of the PhLac moitety **(e)** The R group modifications to PF1022A that create emodepside, Bis-Dimethyl-Morphonyl-PF1022, PF1022-222 and PF1022-888.

Many of the commercially available anthelmintics function by inhibiting nematode motility, feeding, reproduction, defence against the host immune system or a combination of these physiological functions (reviewed in Martin, 1997). Electrophysiological techniques have provided insight into the mechanism of action of anthelmintics (e.g. Martin et al., 1996). In *C. elegans*, electrophysiological recordings from the pharynx, the organ responsible for feeding behaviour, have been previously used to demonstrate the potent activity of the anthelmintic cyclooctadepsipeptide PF1022A and its derivative emodepside (Harder et al., 2003; Willson et al., 2004). This suggests that testing emodepside, bis-dimethyl-morphonyl-PF1022, HLR8090-3-4, JES-737, and the PF1022A derivatives verticilide, PF1022-888 and PF1022-222 in the *C. elegans* pharynx using electrophysiological recordings would enable identification of anthelmintic capability and allow the potency of all the compounds to be compared.

As previous research has demonstrated that emodepside can inhibit wild type *C. elegans* locomotion (Willson et al., 2004), those of the seven novel compounds demonstrating the most potent anthelmintic activity in the pharynx were also examined for any activity on *C. elegans* locomotion. This would reveal whether those selected compounds are capable of acting at more than one site in the nematode; an ability that could increase the potency of the compounds when used as commercial anthelmintics.

3.2 Identification of novel compounds with anthelmintic activity in the wild type *C. elegans* pharynx

To investigate the effect of the seven novel compounds on the *C. elegans* pharynx, extracellular recordings of pharyngeal activity upon exogenous application of the compounds were achieved using the EPG (Davis et al., 1995; Raizen & Avery, 1994; Willson et al., 2004). For EPG recordings, a dissected preparation of the *C. elegans* head, including the pharyngeal muscles and nervous system, is immersed in solution (which can be changed) and held in position by a suction-recording electrode (see chapter 2, section 2.7.1, page 69 for a detailed method description). A typical example of a wild type *C. elegans* pharyngeal pump is shown in figure 3.2.

Each wild type EPG pump in Dent's saline consistently contains an excitatory or contraction phase (E2 on figure 3.2) reflecting depolarization of the pharyngeal muscle cells, and an inhibitory or relaxation phase (R1 on figure 3.2) associated with repolarization of the corpus muscle. An initial excitatory phase (E1 on figure 3.2) associated with the activation of the MC motor neuron may be present prior to the main depolarization phase (Franks et al., 2006). E1 is typically smaller than E2, and may be separated distinctly from E2, or may be partially merged with the larger depolarization spike as in figure 3.2 (in wild type recordings in Dent's saline, the partial merging of E1 and E2 was more commonly observed). The absence of E1 from the EPG trace may be due to it being masked by E2 of the same pump or by the close temporal proximity of the previous pump (Franks et al., 2006). A second relaxation or inhibitory phase (R2 on figure 3.2) may also be present following the R1 spike, and is thought to be a reflection of terminal bulb repolarization (Franks et al., 2006). R2 is typically smaller than R1, and the two spikes can be distinct (as in figure 3.2) or can be partially merged. The absence of R2 may be due to it being masked by the R1 spike. During the EPG, inhibitory potentials of varying amplitude and in vary number are often observed (I in figure 3.2). These potentials are suggested to be the result of glutamate being released from the M3 neuron and the consequent activation of ligand-gated chloride channels (Dent et al., 1997; Li et al., 1997).

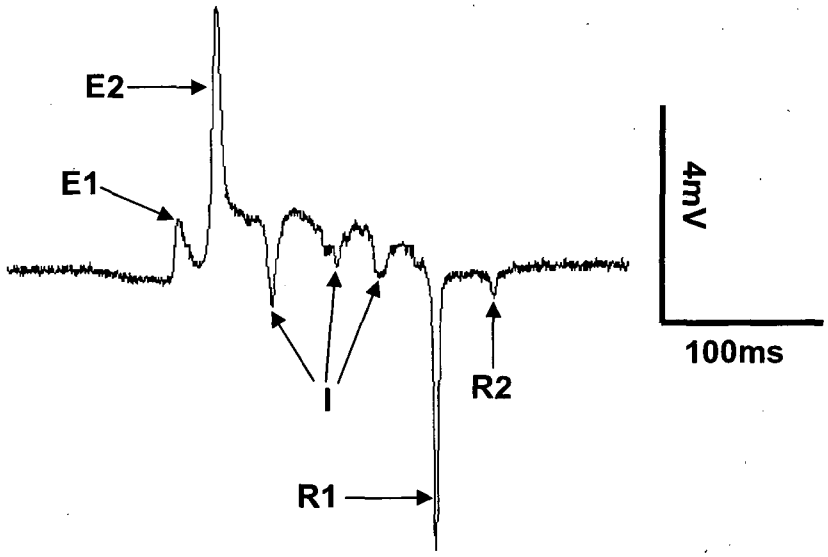

Figure 3.2 An example of an EPG trace, a single pump from a wild type *C. elegans* (modified from Franks et al., 2006)
For this recording the pharyngeal preparation was immersed in Dent's saline. The EPG consists of several components. E1: associated with activation of the MC motor neuron. E2: depolarization of the muscle cells. R1: repolarization of corpus muscle. R2: associated with terminal bulb repolarization. I: inhibitory potentials.

The form of an individual pump recorded by the EPG can vary between animals (even animals from the same strain) partly due to the relative position of the recording electrode to the pharynx (Franks et al., 2006). To enable more reliable interpretation of recordings, electrode position for each preparation was maintained as accurately as possible half-way between the tip of the worm nose and the anterior-most part of the metacorpus. Nonetheless, recordings between worm preparations of the same strain still varied in individual pump shape, and therefore, shape changes upon drug application were interpreted with caution. Instead, pump rate was used as the indicator of drug activity, as this is a more consistent and reliable indicator, and has been used successfully in previous research to identify the anthelmintic activity of PF1022A and emodepside (Willson et al., 2004).

3.2.1 The effect of JES-737 and HLR8090-3-4

EPG recordings were employed to examine the response of the pharynx to exogenous application of JES-737 or HLR8090-3-4. Each pharynx preparation was initially 'primed' to reach maximal response to 1μM 5-HT by repeated application of 1μM 5-HT for three minutes interspersed with a three minute wash in Dent's saline until a 5-HT application elicited a pump rate within two percent of the rate in the previous 5-HT application (see chapter 2, section 2.7.3, page 73). Following 'priming', the pharynx was washed in Dent's saline for three minutes, followed by the recording protocol (in order of application): three minutes 1μM 5-HT, wash (Dent's saline), ten minutes of either 1μM HLR8090-3-4 (0.01% DMSO vehicle, no 5-HT), or JES-737 at 1μM or 10μM (0.01% DMSO vehicle, no 5-HT) or a control solution containing only 0.01% DMSO (no 5-HT), followed by a wash (Dent's saline), then three minutes 1μM 5-HT. Each change in solution included a wash in Dent's saline to remove as much of the initial solution before application of the next. For the analysis, the response of the pharynx to 5-HT following exposure to JES-737 or HLR8090-3-4 was calculated as a percentage of the response of that worm to 5-HT immediately prior to drug exposure.

Exposure for ten minutes to a 1μM solution of JES-737 produces only a 5% (mean ± 4) decrease in pharyngeal response to 1μM 5-HT (see figure 3.3(a)). To establish whether this result demonstrated a weak ability of the compound to suppress the 5-HT response, EPG recordings were repeated using a 10μM solution of JES-737. The higher concentration of JES-737 did not produce a further suppression in pharyngeal response to 5-HT (see figure 3.3(a)). This suggests that the compound does not affect functioning of the pharynx at pharmacologically relevant concentrations.

Exposure for ten minutes to 1μM HLR8090-3-4 produces no significant change in pharyngeal response to 1μM 5-HT (see figure 3.4(a) and compare (b) and (c)), suggesting that the compound does not affect functioning of the pharynx at a pharmacologically relevant concentration.

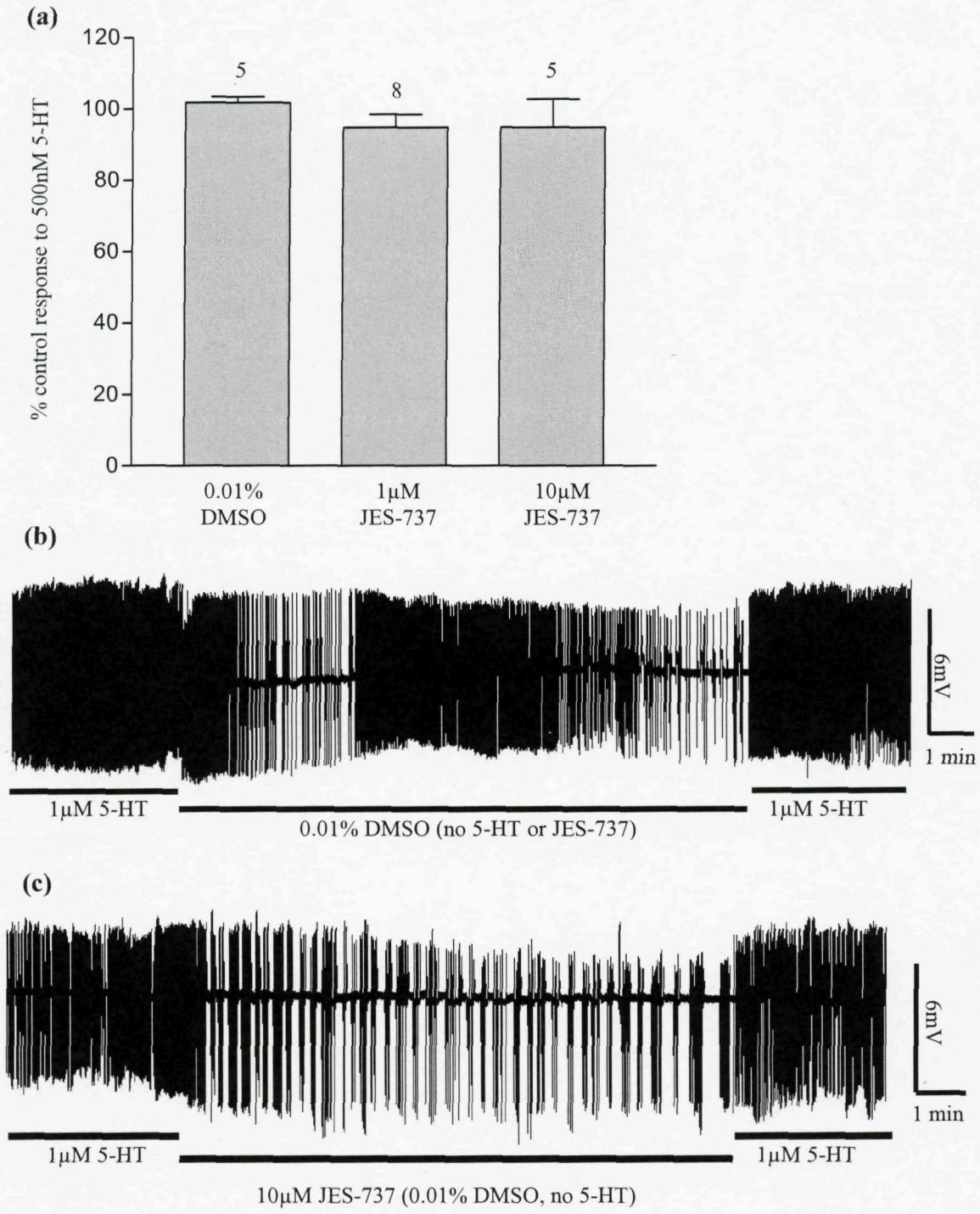

Figure 3.3 The impact of JES-737 on pharyngeal pumping in wild type (N2) *C. elegans*.
(a) Graph showing the effect of JES-737 on pharyngeal response to 1μM 5-HT. '% control response to 5-HT' is the pharyngeal pump rate response to 5-HT following drug exposure expressed as a percentage of the 5-HT response prior to drug application. Each bar is the mean ± S.E. Mean of (n) pharyngeal preparations, n numbers are given above each bar. **(b-c)** Example EPG recordings showing the effect of either (b) 0.01% DMSO (vehicle control) or (c) 10μM JES-737 on the stimulation of pharyngeal pumping by 1μM 5-HT. Each vertical line represents the electrical activity associated with a single pharyngeal pump. Notice the rapid pumping rate of both pharynx preparations when initially exposed to 1μM 5-HT, and the similarity of 5-HT response following exposure to either 0.01% DMSO or 10μM JES-737, indicating minimal anthelmintic activity of the novel compound.

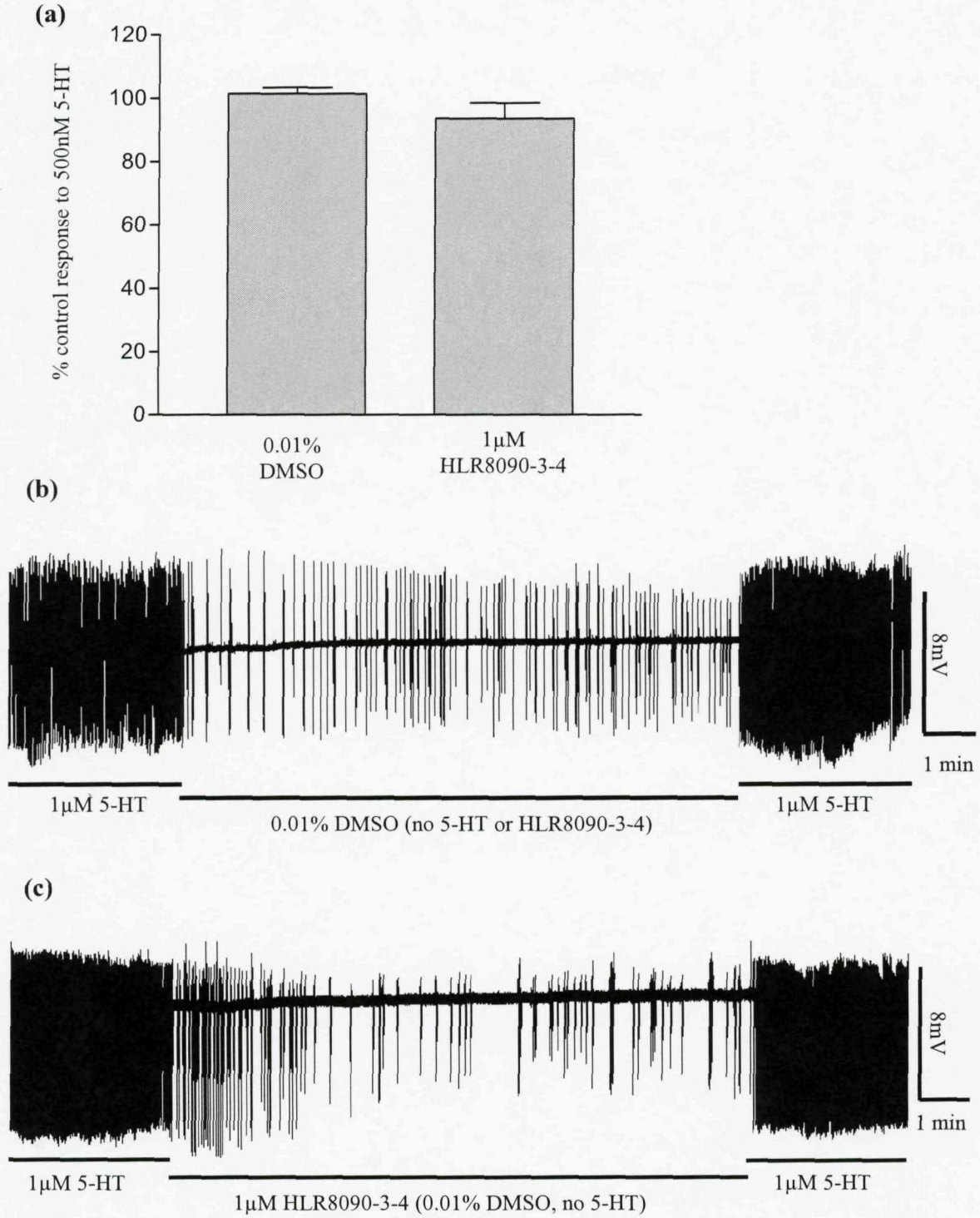

Figure 3.4 The Impact of HLR8090-3-4 on pharyngeal pumping in wild type (N2) *C. elegans*.
(a) Graph showing the effect of HLR8090-3-4 on pharyngeal response to 1μM 5-HT. '% control response to 5-HT' is the pharyngeal pump rate response to 5-HT following drug exposure expressed as a percentage of the 5-HT response prior to drug application. Each bar is the mean ± S.E. Mean of 5 pharyngeal preparations. **(b-c)** Example EPG recordings showing the effect of (b) 0.01% DMSO (vehicle control) or (c) *1μM HLR8090-3-4* on pharyngeal response to *1μM 5-HT*. By comparing the pumping rate in 5-HT before and after exposure to HLR8090-3-4 or DMSO it can be seen that HLR8090-3-4 has minimal anthelmintic effect on pharyngeal response to 5-HT.

3.2.2 The effect of emodepside

To investigate whether emodepside is capable of effecting pharyngeal pumping using the EPG assay, each pharynx preparation was initially 'primed' with 500nM 5-HT as described in section 3.2.1. Priming was followed by the recording protocol (in order of application): three minutes 500nM 5-HT, wash (Dent's saline), ten minutes 1μM emodepside, wash (Dent's saline), three minutes 500nM 5-HT. For each worm tested, the response of the pharynx to 5-HT following exposure to emodepside was calculated as a percentage of the response of that worm to 5-HT (immediately prior to emodepside application).

When applied to the pharyngeal preparation, 1μM emodepside completely abolished the pumping response to 5-HT in wild type *C. elegans* (see figure 3.5(a)). Consequently, a comparison of the pump rate in 500nM 5-HT following application of 1μM emodepside and application of only 0.01% DMSO (vehicle control) revealed the rates to be highly significantly different ($P<0.001$).

To investigate whether emodepside maintains such a high potency at lower concentrations, the experimental protocol was repeated but using 100nM or 10nM emodepside instead of 1μM. Exposure to 100nM or 10nM emodepside reduced the response of the pharynx to 500nM 5-HT by 99% (± 1) and 65% (± 4), respectively (see figure 3.5(a)). Comparison of the pump rate in 500nM 5-HT following exposure to 100nM or 10nM emodepside and exposure to only 0.01% DMSO (vehicle control) revealed the rates to be highly significantly different for both concentrations of emodepside ($P<0.001$).

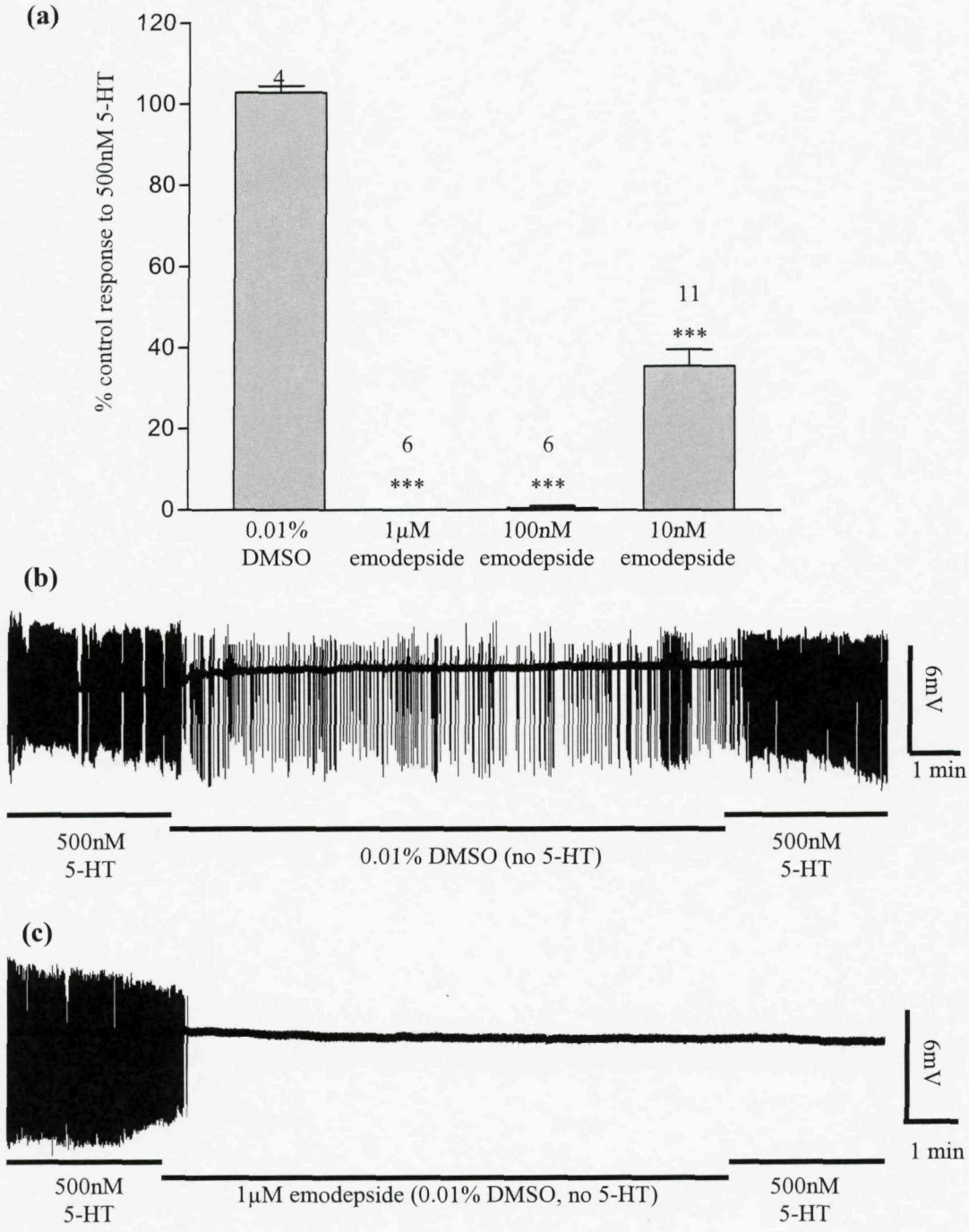

Figure 3.5 The effect of emodepside on the wild type *C. elegans* pharyngeal response to 5-HT. **(a)** Graph showing the effect of emodepside on pharyngeal response to 500nM 5-HT. '% control response to 5-HT' is the pharyngeal pump rate response to 5-HT following drug exposure expressed as a percentage of the 5-HT response prior to drug application. Each bar is the mean ± S.E. Mean of (n) pharyngeal preparations. Significance (Student's t-test) relates to a comparison of the effect of emodepside on the 5-HT response with the effect of only DMSO, ***P<0.001, n numbers given above each bar. **(b-c)** Example EPG recordings showing the effect of (b) 0.01% DMSO (vehicle control), and (c) 1μM emodepside on the pharyngeal response to 500nM 5-HT. Notice the rapid cessation of pumping following emodepside application in (c), and the failure of the pharynx to respond to the second 5-HT application.

To investigate whether emodepside can inhibit pharyngeal pumping in Dent's saline without the presence of 5-HT, a second protocol was used in which the preparations were exposed to Dent's saline for four minutes, then 100nM emodepside was applied for ten minutes, followed by exposure to Dent's saline for a further four minutes. Constant perfusion of the Dent's saline or emodepside solution at 4ml per minute was used in the absence of 5-HT to stimulate a rate of pumping that would be sufficient to reveal any inhibitory effect of emodepside. The mean number of pumps per 30 seconds during the initial four minutes of Dent's saline application was then compared to the mean number of pumps during the second exposure to Dent's saline, after application of emodepside.

Exposure to 100nM emodepside for ten minutes was found to reduce the mean number of pumps per 30 seconds in Dent's saline by 99% (± 1; see figure 3.6(a)), which was a statistically significant reduction in pump rate ($P<0.05$). This is in agreement with the results of the previous EPG assay using 5-HT which demonstrated a 99% reduction in pump rate in 500nM 5-HT following exposure to 100nM emodepside for ten minutes.

Examination of the number of pumps per minute throughout the entire EPG recording, including perfusion of the emodepside as well as the Dent's saline, reveals that during the sixth minute of emodepside application (minute eleven of the full recording) the mean number of pumps had reduced to 65% (± 31) when compared the mean number of pumps per minute during the initial four minutes of perfusion in Dent's saline (see figure 3.6(c)). During the seventh minute of emodepside exposure (minute twelve of the full recording) the mean number of pumps had reduced to 48% (± 26), indicating that 100nM emodepside can reduce pharyngeal pumping by 50% within six to seven minutes of application to the cut preparation. During the tenth minute of emodepside application all pharyngeal preparations used had ceased to pump. There was minimal recovery of pumping during the second perfusion of Dent's saline: just one of the pharynx preparations pumped twice during this time.

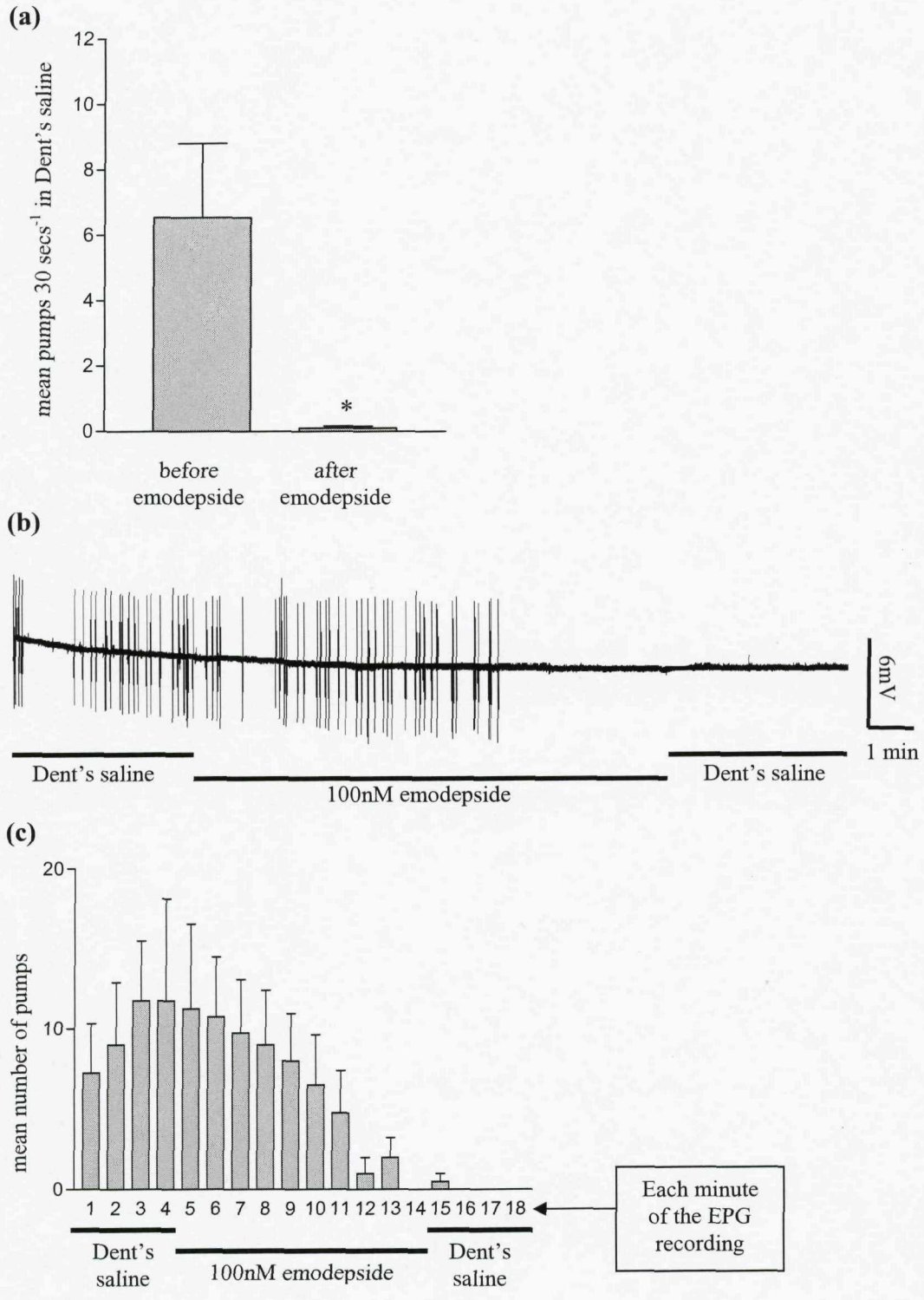

Figure 3.6 The effect of 100nM emodepside on pharyngeal pumping without stimulation by 5-HT
(a) Graph showing the effect of 100nM emodepside on pharyngeal pumping in Dent's saline (perfusing at 4ml/minute). Each bar is the mean ± S.E.Mean of 4 pharyngeal preparations. Statistical significance (Student's t-test) is a comparison of the mean pump rate in Dent's saline before and after emodepside application, * $P<0.05$, $n = 4$. **(b)** An example EPG recording demonstrating the reduction in pharyngeal pumping during emodepside application. Notice that this pharynx ceases to pump at approximately the seventh minute of emodepside exposure, and does not pump during the second application of Dent's saline. **(c)** Graph showing a profile for the pumping activity of the pharynx throughout the experimental protocol. During the initial four minutes of exposure to Dent's saline, the mean number of pumps per minute was 10. Notice that the mean number of pumps in the sixth minute of emodepside exposure (minute 11 of the EPG recordings) was less than 50% of the mean pumps/minute in Dent's saline.

Emodepside is soluble in DMSO and ethanol, and both compounds can be used as vehicles for the anthelmintic. A brief investigation was performed to establish whether ethanol and DMSO are equally as effective when used as emodepside vehicles in the EPG assay, or whether one compound is preferable to the other. For the EPG recordings, the wild type *C. elegans* pharynx was dissected and then 'primed' with 500nM 5-HT as described in section 3.2.1. 'Priming' was followed by the recording protocol (in order of application): two minutes 500nM 5-HT, wash (Dent's saline), 10nM or 100nM emodepside for ten minutes using either DMSO or ethanol as vehicle, wash (Dent's saline), two minutes 500nM 5-HT. The pharyngeal pumping rate in the second 5-HT application was expressed as a percentage of the rate in 5-HT immediately prior to emodepside exposure.

Ethanol, at a concentration of 0.1%, has been previously employed successfully as an emodepside vehicle when investigating the activity of the novel anthelmintic on the *C. elegans* pharynx (Harder et al., 2003; Willson et al., 2004). Therefore, for the current investigation ethanol was also used at 0.1%. However, DMSO had to be used at a lower concentration of 0.01% because 0.1% was found to impair pharyngeal pumping in control experiments where the vehicle was applied in the absence of emodepside (see figure 3.7). Pharyngeal pumping during application of 0.1% DMSO did not appear to be affected, but during the second exposure to 5-HT pumping rapidly deteriorated, with the shape of the pump grossly altered. During the second 5-HT application only the depolarization spike (E2 phase) of each pump remained, and the repolarization spikes (R1 and R2) and the inhibitory potentials (IPs) were not evident (see figure 3.7 and compare (b) and (c)).

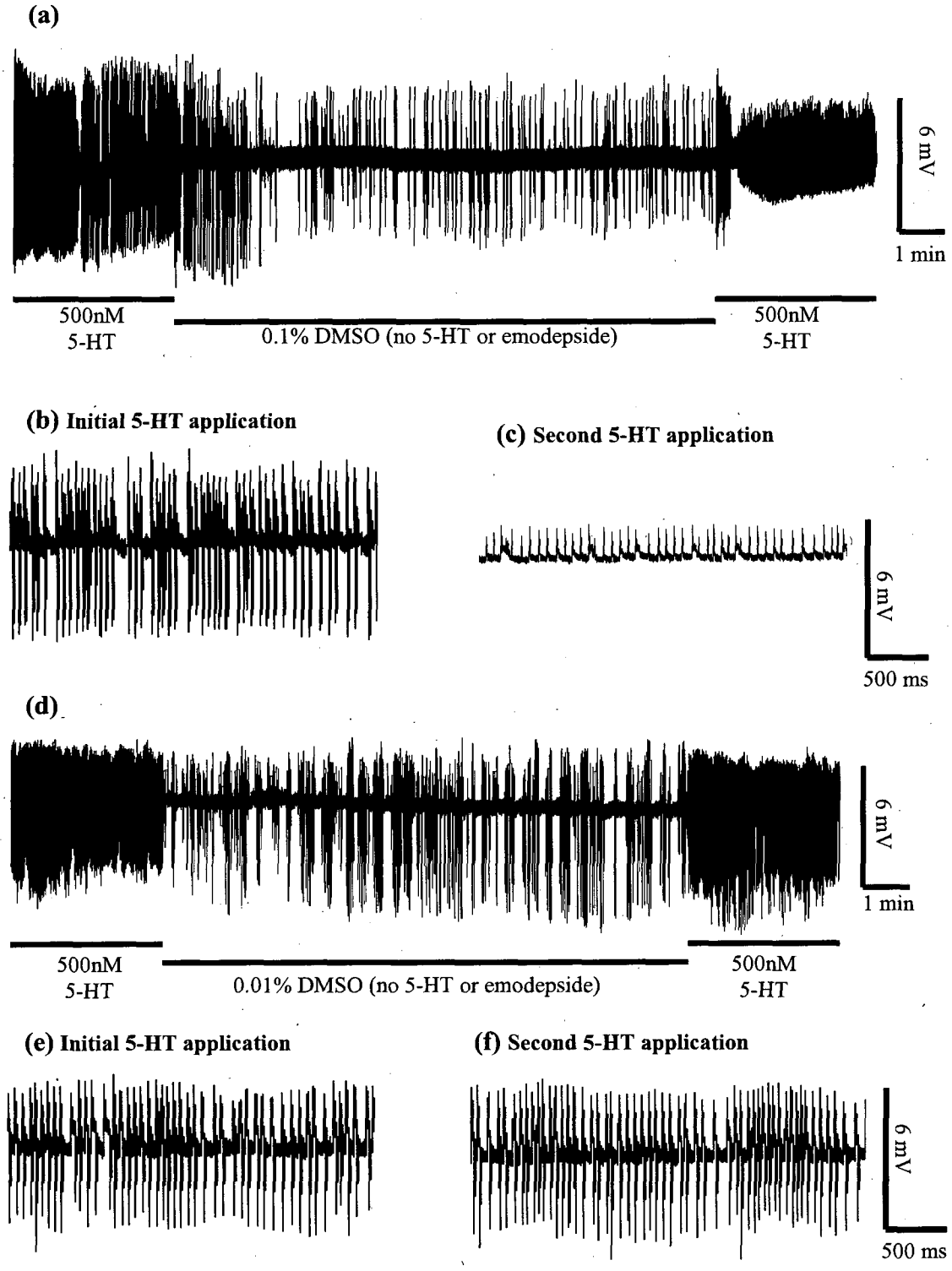

Figure 3.7 The effect of 0.1% and 0.01% DMSO on pharyngeal pumping in wild type *C. elegans*. **(a)** An example EPG recording demonstrating the effect of 0.1% DMSO on pharyngeal response to 500nM 5-HT. This can be seen more clearly by comparing **(b)** and **(c)**, which are enlarged sections of the recording shown in (a). **(d)** An EPG recording showing the effect of 0.01% DMSO on pharyngeal response to 500nM 5-HT. This can be seen more clearly by comparing **(e)** and **(f)**, which are enlarged sections from the recording shown in (d). Notice that 0.1%, but not 0.01%, DMSO changes the shape of the pumps during the second application of 5-HT; reducing them to small depolarization spikes approximately 2mV in size (shown in (c)).

At 10nM, emodepside inhibited pharyngeal pumping by 65% using 0.01% DMSO as the vehicle, and by 55% using 0.1% ethanol as the vehicle. At 100nM, emodepside inhibited pharyngeal pumping by 99% and 87% using DMSO and ethanol as vehicles, respectively (see figure 3.8). Student's t-test confirmed no significant difference between the efficacies of the two vehicle compounds.

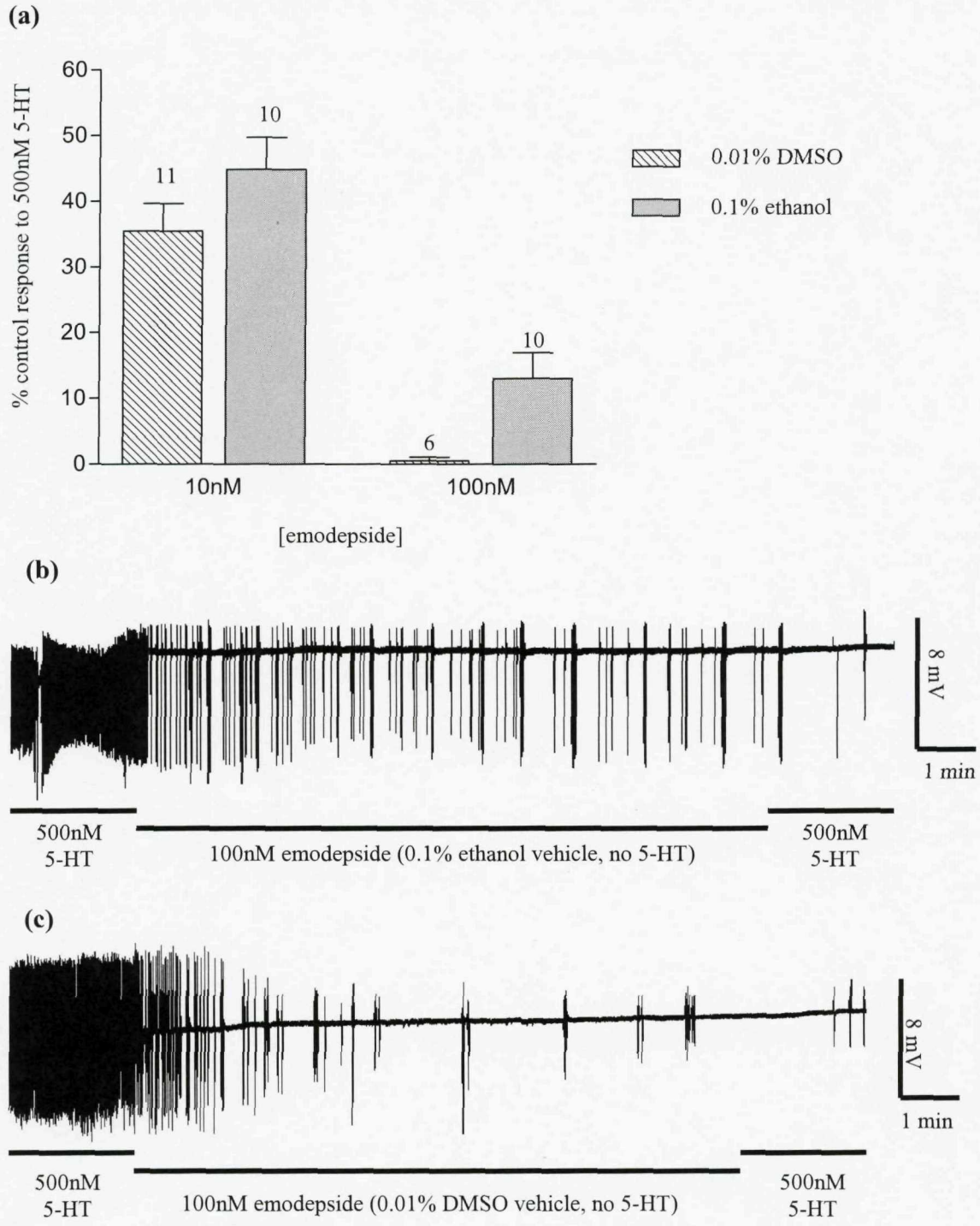

Figure 3.8 Comparison of DMSO and ethanol as emodepside vehicles.
(a) Graph showing the effect of emodepside on pharyngeal response to 500nM 5-HT when using two different drug vehicles: ethanol and DMSO. '% control response to 500nM 5-HT' is the pharyngeal pump rate response to 5-HT following drug exposure expressed as a percentage of the 5-HT response prior to drug application. Each bar is the mean ± S.E. Mean of (n) pharyngeal preparations, n numbers given above each bar. **(b-c)** Example EPG recordings showing the effect of 100nM emodepside on pharyngeal response to 500nM 5-HT when using the vehicle (b) ethanol, and (c) DMSO. Notice that the potency of emodepside in inhibiting pumping response to 5-HT was very similar when using either of the vehicles.

3.2.3 The effect of verticilide

EPG recordings were employed to examine the response of the pharynx to 500nM 5-HT following exogenous application of verticilide. Control experiments in which emodepside was tested were performed alongside the verticilide experiments to enable accurate comparison of the two PF1022A derivatives. Each dissected pharynx was initially 'primed' with 500nM 5-HT as described in section 3.2.1, followed by the recording protocol (in order of application): three minutes 500nM 5-HT, wash (Dent's saline), ten minutes verticilide or emodepside at 10nM, 100 nM or 1μM (0.01% DMSO vehicle, no 5-HT), wash (Dent's saline), three minutes 500nM 5-HT. The response of each preparation to 5-HT following exposure to verticilide (or emodepside) was calculated as a percentage of the 5-HT response immediately prior to verticilide application. Additional control experiments were performed using the same protocol described above, the only alteration being the substitution of the verticilide or emodepside solution with a vehicle control solution containing 0.01% DMSO.

Following ten minutes exposure to 1µM verticilide, the response of the wild type *C. elegans* pharynx to 500nM 5-HT was reduced by 94% (± 1) when compared to the pump rate in 500nM 5-HT prior to drug exposure. In comparison, 1µM emodepside completely abolished all pumping in 500nM 5-HT after ten minutes exposure to the novel compound, a difference in potency that is significantly different ($P<0.01$, see figure 3.9(a)). This significant difference in potency between the two anthelmintic candidates was increased when applied at 100nM. Following ten minutes exposure to 100nM verticilide, the pharyngeal response to 500nM 5-HT was reduced by 41% (± 10), compared to a reduction of 99.8% (± 0.2) following exposure to 100nM emodepside ($P<0.001$, see figure 3.9(a)). Application of 10nM verticilide or emodepside reduced pharyngeal response to 5-HT by 12% (± 5) or 48% (± 7), respectively, a difference in potency that is significant ($P<0.01$, see figure 3.9(a)).

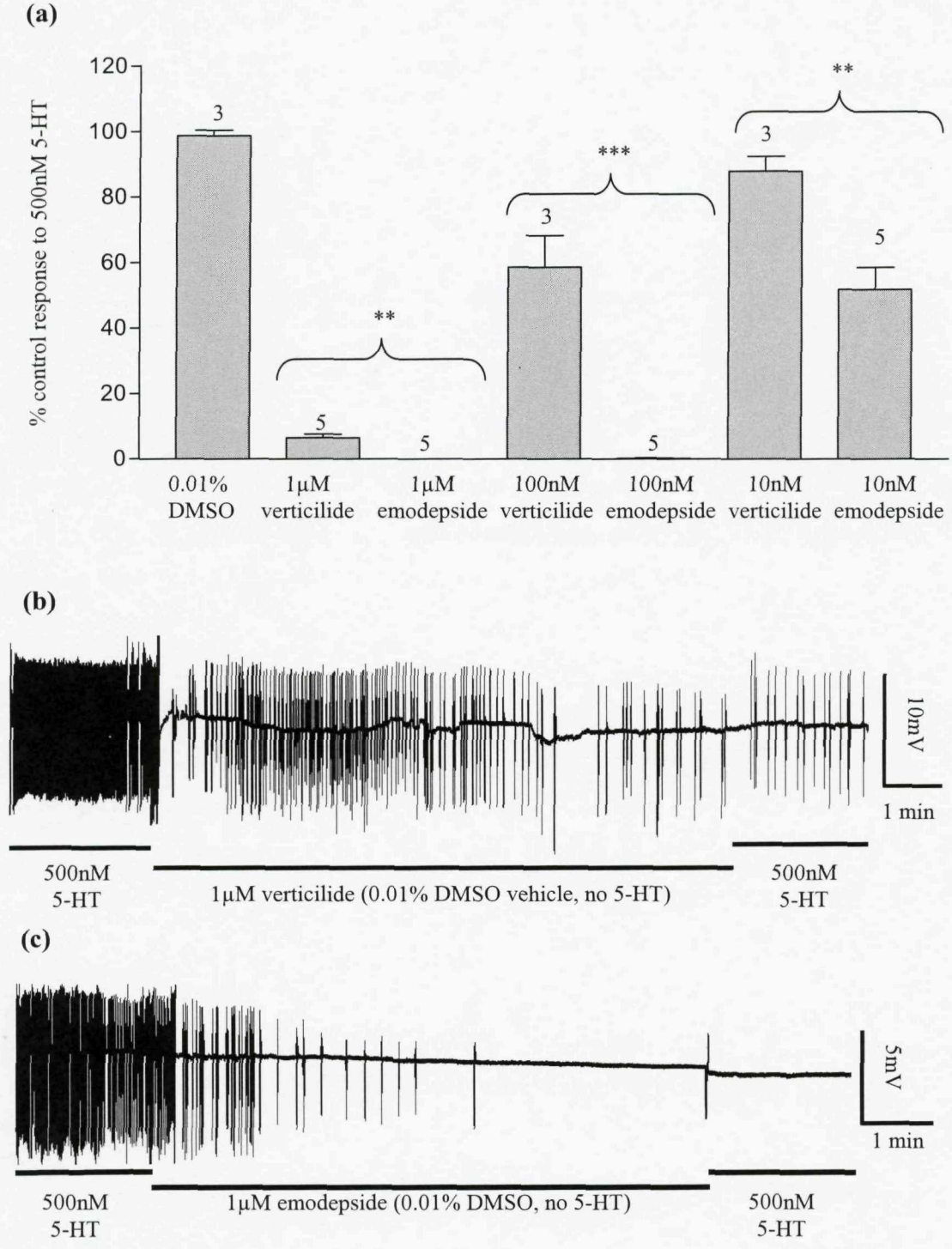

Figure 3.9 The effect of verticilide on pharyngeal pumping in wild type *C. elegans*.
(a) Graph showing the effect of verticilide on pharyngeal response to 500nM 5-HT. '% control response to 5-HT' is the pharyngeal response to 500nM 5-HT following verticilide or emodepside exposure as a percentage of the initial response to 5-HT (prior to anthelmintic application). Each bar is the mean ± S.E.Mean of (n) determinations. Significance (Student's t-test) relates to a comparison of the effect of emodepside and verticilide at the same concentration on the 5-HT response, ** $P<0.01$, *** $P<0.001$, n numbers are given above each bar. **(b-c)** Example EPG recordings showing the effect of: (b) 1μM verticilide, and (c) 1μM emodepside on pharyngeal response to 500nM 5-HT. Notice that verticilide inhibits the 5-HT response, but that emodepside completely abolishes pumping during the second application of 5-HT.

3.2.4 The effect of bis-dimethyl-morphonyl-PF1022A

To examine the effect of exogenous application of bis-dimethyl-morphonyl-PF1022 on the response of the pharynx to 500nM 5-HT, the EPG technique was employed. Bis-dimethyl-morphonyl-PF1022 is a derivative of emodepside and might therefore be expected to share the anthelmintic potency of emodepside on the pharynx. Consequently, emodepside was tested separately but at the same time and at the same concentration as bis-dimethyl-morphonyl-PF1022 to enable accurate comparison of the compounds. Each dissected pharynx was initially 'primed' with 500nM 5-HT as described in section 3.2.1, followed by the recording protocol (in order of application): 2 minutes 500nM 5-HT, wash (Dent's saline), ten minutes application of 100nM bis-dimethyl-morphonyl-PF1022 or emodepside (0.01% DMSO vehicle, no 5-HT), wash (Dent's saline), two minutes 500nM 5-HT. The response of each pharyngeal preparation to 5-HT following exposure to the anthelmintic was calculated as a percentage of the 5-HT response immediately prior to drug application. Additional control experiments were performed using the same protocol described above, the only alteration being the substitution of the verticilide or emodepside solution with a vehicle control solution containing 0.01%DMSO.

Figure 3.10 demonstrates that ten minutes exposure to 100nM bis-dimethyl-morphonyl-PF1022 inhibited the response of the wild type *C. elegans* pharynx to 500nM 5-HT by 77% (± 10), which is a significant reduction in pumping when compared to the DMSO controls ($P<0.01$). However, 100nM emodepside significantly inhibited the pharyngeal response to 500nM 5-HT by 96% (± 3; $P<0.001$, comparison with DMSO controls).

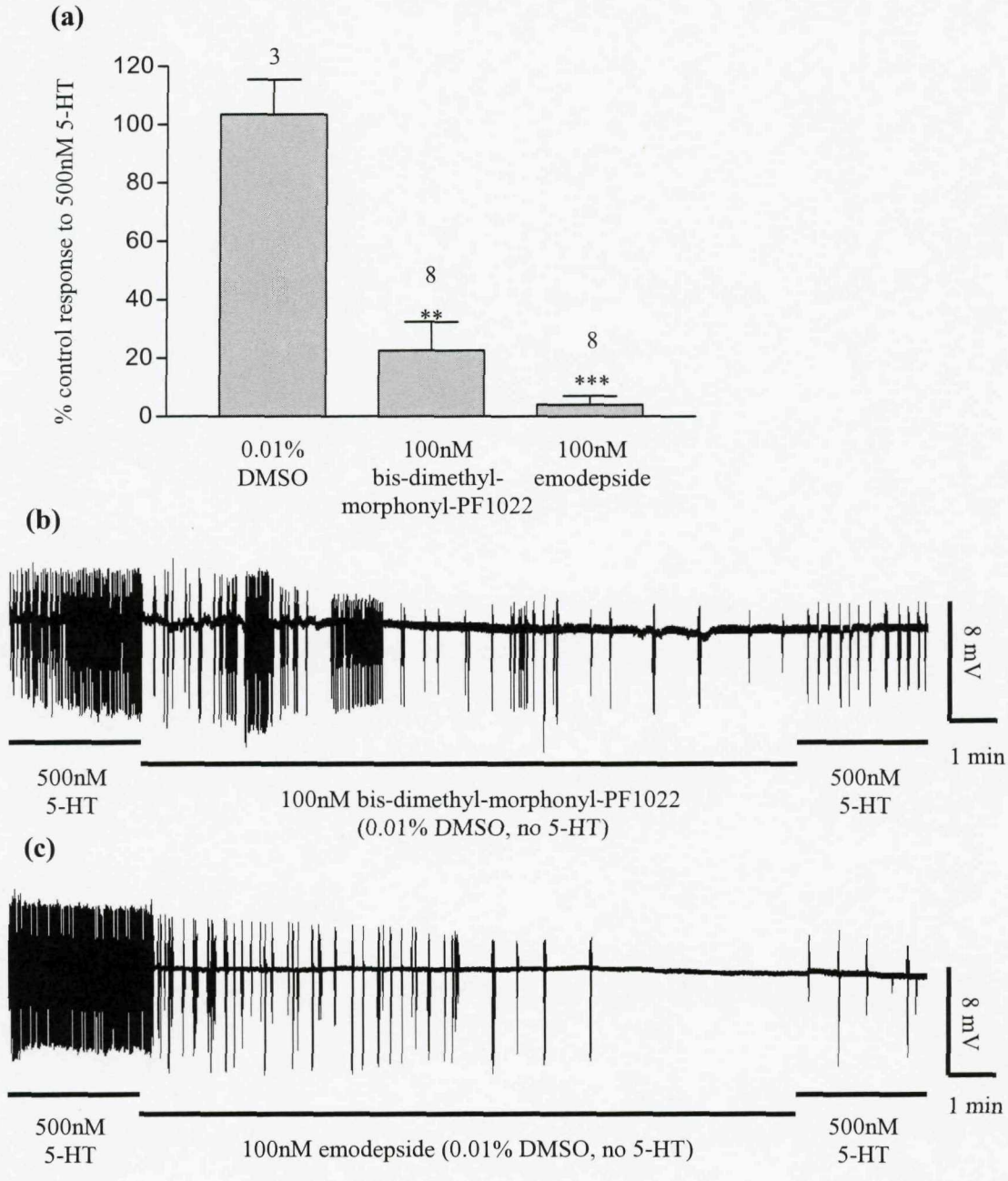

Figure 3.10 The effect of bis-dimethyl-morphonyl-PF1022 on the pharyngeal response to 5-HT in wild type *C. elegans*.

(a) Graph showing the effect of bis-dimethyl-morphonyl-PF1022 on pharyngeal response to 500nM 5-HT. '% control response to 5-HT' is the pharyngeal response to 500nM 5-HT following bis-dimethyl-morphonyl-PF1022 or emodepside exposure as a percentage of the initial response to 5-HT (prior to anthelmintic application). Each bar is the mean ± S.E.Mean of (n) determinations. Significance (Student's t-test) relates to a comparison of the effect of 0.01% DMSO (vehicle control) and either emodepside or bis-dimethyl-morphonyl-PF1022, ** $P<0.01$, *** $P<0.001$, n numbers are given above each bar. **(b-c)** Example EPG recordings showing the effect of: (b) 100nM bis-dimethyl-morphonyl-PF1022, and (c) 100nM emodepside on pharyngeal response to 500nM 5-HT. Notice that bis-dimethyl-morphonyl-PF1022 inhibits the 5-HT response, but emodepside is more potent.

3.2.5 The effect of PF1022-888 and PF1022-222

PF1022-888 and PF1022-222 are derivatives of the emodepside-precursor PF1022A, suggesting that these two new compounds may share with emodepside an ability to inhibit pharyngeal pumping significantly at 10nM. To investigate this using the EPG assay, each pharynx preparation was initially 'primed' with 500nM 5-HT as described in section 3.2.1, followed by the recording protocol (in order of application): two minutes 500nM 5-HT, wash (Dent's saline), ten minutes application of either PF1022-888, PF1022-222 or emodepside (all at 10nM, with 0.01% DMSO, no 5-HT), or a control solution of 0.01% DMSO (no 5-HT), followed by a wash (Dent's saline), then two minutes 500nM 5-HT. For each worm tested, the response of the pharynx to 5-HT following exposure to the novel anthelmintics or vehicle control was calculated as a percentage of the initial response of that worm to 5-HT (prior to drug application).

Figure 3.11 and 3.12 show that ten minutes exposure to 10nM PF1022-888 or PF1022-222 significantly inhibited the response of the wild type *C. elegans* pharynx to 500nM 5-HT by 38% (± 7) or 57% (± 12), respectively ($P<0.01$, comparison with vehicle control: 0.01% DMSO). As a comparison, 10nM emodepside significantly inhibited the pharyngeal response to 500nM 5-HT by 54% (± 4; $P<0.001$, comparison with vehicle control 0.01% DMSO).

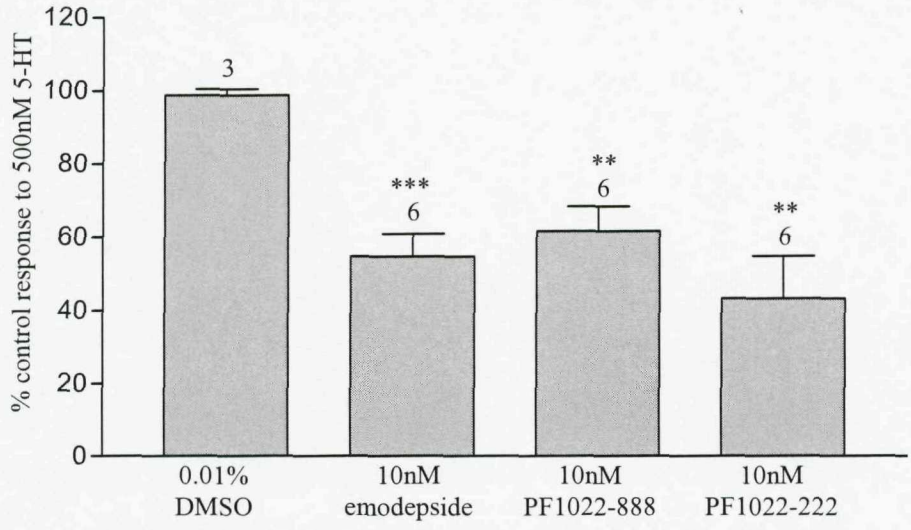

Figure 3.11 Graph comparing the effect of PF1022-222, PF1022-888 and emodepside on the response of the wild type pharynx to 500nM 5-HT.
'% control response to 5-HT' is the response to 500nM 5-HT following drug exposure as a percentage of the initial response to 5-HT (prior to drug application). Each bar is the mean ± S.E.Mean of (n) determinations. Significance (Student's t-test) relates to a comparison of the effect of 0.01% DMSO (vehicle control) and one of the anthelmintics, ** $P<0.01$, *** $P<0.001$, n numbers are given above each bar.

(a) 10nM emodepside on wild type

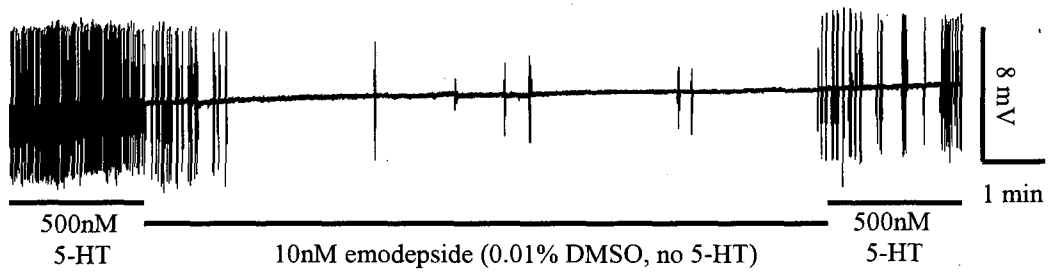

(b) 10nM PF1022-222 on wild type

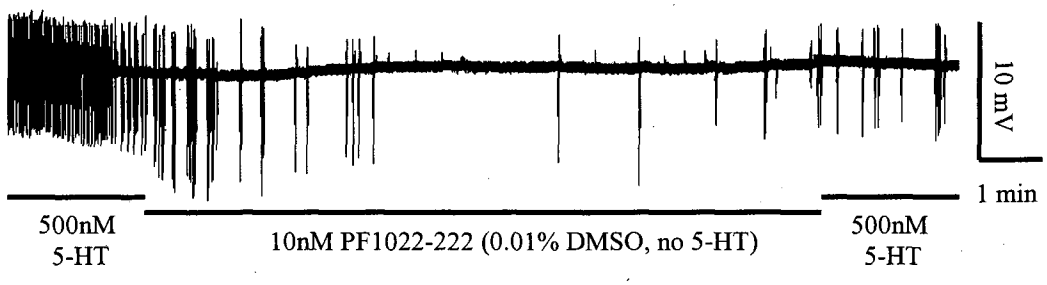

(c) 10nM PF1022-888 on wild type

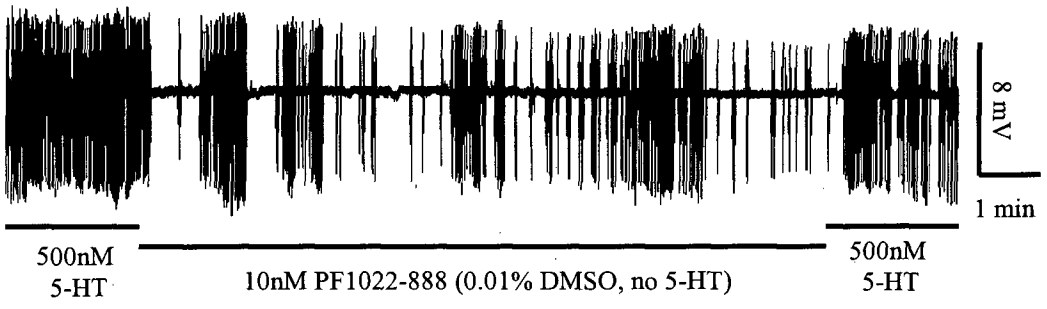

Figure 3.12 The effect of PF1022-222 and PF1022-888 on the response of the wild type pharynx to 500nM 5-HT.
Example EPG recordings showing the effect of: **(a)** 10nM emodepside, **(b)** 10nM PF1022-222, and **(c)** 10nM PF1022-888 on pharyngeal response to 500nM 5-HT. In each of the recordings, compare the pumping in 5-HT before and after drug application, and notice that PF1022-222 is the most potent of the three anthelmintics, followed by emodepside and then PF1022-888.

3.3 Identification of novel compounds with anthelmintic activity on wild type *C. elegans* locomotion

Previous research has demonstrated that emodepside can inhibit locomotion in wild type *C. elegans* (Willson et al., 2004). To accurately determine the acute impact of emodepside on worm locomotion, a thrashing assay was performed. *C. elegans* produces a characteristic thrashing movement when placed in liquid and this behaviour can be used to quantify subtle locomotion defects, because, unlike worm movement on a solid substrate, thrashing is both continuous and high frequency (Miller et al., 1996). In Dent's saline, wild-type *C. elegans*, in the absence of drug, demonstrate a remarkably constant 'thrashing' movement at a frequency of between 50 and 70 body bends per 30 seconds. A body bend is counted each time the tip of the tail moves in the opposite direction and then returns to its original position. To assess the ability of emodepside to cause paralysis of *C. elegans* locomotion, a time-dependent assay was employed in which adult worms were transferred to Dent's saline and at specific time points after addition of the anthelmintic these worms were analysed for 'thrashing motion'. Thrashing was recorded immediately before addition of emodepside (or 0.1 % ethanol (vehicle control)) and recorded again following 5, 10, 20, 30 and 60 minutes exposure to emodepside or ethanol.

Wild type *C. elegans* thrashing behaviour was increasingly inhibited during the 60 minutes of emodepside exposure (see figure 3.13). A significant 20% (± 5) reduction in thrashing behaviour ($P<0.05$) was observed just five minutes after commencement of emodepside exposure, although this inhibition appeared to stabilize by ten minutes, before a further and more significant 34% (± 9) reduction in thrashing was seen 20 minutes after emodepside was applied ($P<0.01$). After 60 minutes exposure to emodepside, thrashing had been reduced by 84% (±9), which was highly significant ($P<0.001$) when compared to vehicle control results.

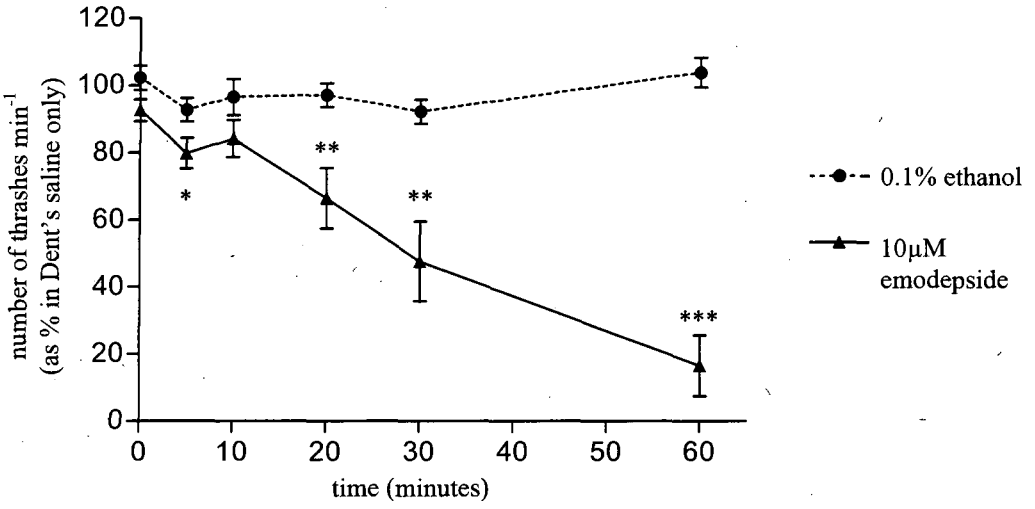

Figure 3.13 The effect of emodepside on adult wild type *C. elegans* thrashing behaviour. Graph showing the effect of 10μM emodepside on the thrashing behaviour of adult *C. elegans*. At each time point data were analysed as the number of thrashes min^{-1} in emodepside or ethanol as a % of thrashes min^{-1} in Dent's saline before application of either compound (0 mins). Each datum point is the mean ± S.E.Mean of (n) *C. elegans*. Significance (Student's t-test) relates to a comparison of thrashing behaviour by *C. elegans* in 0.1% ethanol and worms in 10μM emodepside, ***P<0.001, **P<0.01, * P<0.05, n numbers: 9 (emodepside exposed), 10 (ethanol exposed).

Bis-dimethyl-morphonyl-PF1022 is a derivative of emodepside, and both compounds potently inhibit *C. elegans* pharyngeal pumping (see section 3.2.5). Suggesting that bis-dimethyl-morphonyl-PF1022 may also share the ability of emodepside to inhibit *C. elegans* locomotion. To examine this, the previous thrashing assay was repeated, but using bis-dimethyl-morphonyl-PF1022 instead of emodepside.

Wild type *C. elegans* thrashing behaviour was increasingly inhibited during the 60 minutes of bis-dimethyl-morphonyl-PF1022 exposure (see figure 3.14). A significant 13% (± 6) reduction in thrashing behaviour (P<0.05) was observed just five minutes after bis-dimethyl-morphonyl-PF1022 exposure commenced, with a further and highly significant 39% (± 8) inhibition of thrashing seen at ten minutes (P<0.01). Thrashing had been reduced by 96% (± 2) after 60 minutes exposure to bis-dimethyl-morphonyl-PF1022, which was highly significant (P<0.001) when compared to vehicle control results.

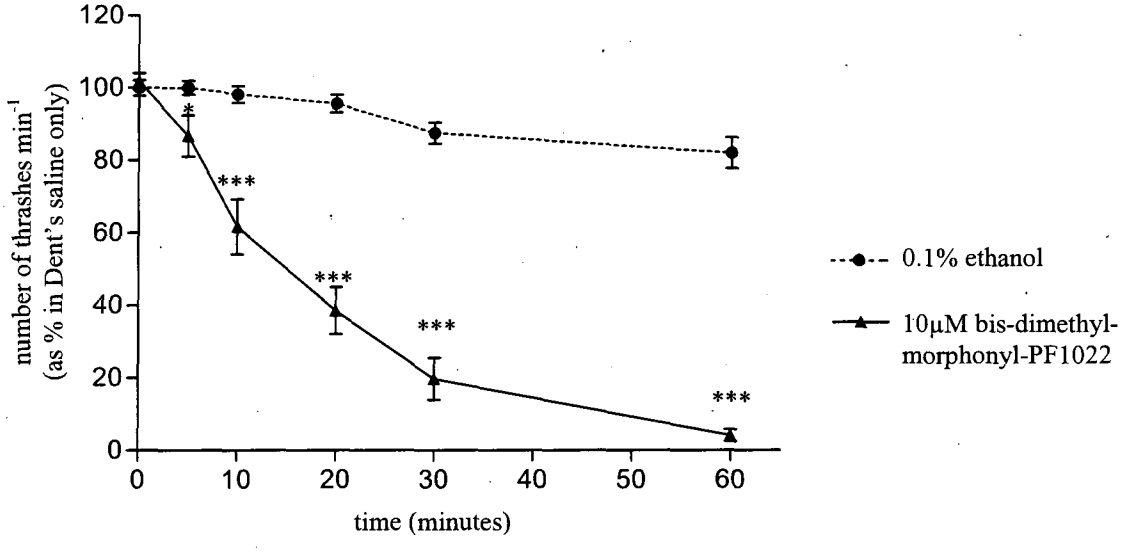

Figure 3.14 The effect of bis-dimethyl-morphonyl-PF1022 on adult wild type *C. elegans* thrashing behaviour.

Graph showing the effect of 10μM bis-dimethyl-morphonyl-PF1022 on the thrashing behaviour of adult *C. elegans*. At each time point data were analysed as the number of thrashes min^{-1} in bis-dimethyl-morphonyl-PF1022 or ethanol as a percentage of thrashes min^{-1} in Dent's saline before application of either compound (0 mins). Each datum point is the mean ± S.E.Mean of 30 *C. elegans*. Significance (Student's t-test) relates to a comparison of thrashing behaviour by *C. elegans* in 0.1% ethanol and in 10μM bis-dimethyl-morphonyl-PF1022, ***P<0.001, * P<0.05, n = 30.

3.4 Discussion

The increased occurrence of anthelmintic resistance has become a global problem in terms of human, animal and plant health, and has consequently sèrious economic ramifications (reviewed in Geary and Thompson, 2003). Therefore, the development of novel anthelmintics that can overcome the resistance problem is vital, and in this chapter the results from examination of seven novel compounds for anthelmintic activity in the model nematode *C. elegans* are shown and their potential will now be discussed.

JES-737 and HLR8090-3-4 were found to have minimal or no discernable impact on wild type *C. elegans* pharyngeal pumping in response to 5-HT. However, it is worth considering the possibility that the formulation of these two drugs and the protocol used to examine their activity may have obscured their anthelmintic capabilities. JES-737 was a highly static powder, and HLR8090-3-4 was a resinous formulation, which made both compounds difficult to weigh accurately, and when they were dissolved in DMSO and then added to Dent's saline to achieve the desired concentration, they required sonication before each use to retain them in solution, presumably due to a high level of insolubility. Additionally, the high concentration of 5-HT used in the protocols examining the activity of JES-737 and HLR8090-3-4 may have masked any effect of the drugs on pharyngeal pumping because the pharynx was being stimulated at such a high level. Further investigation into the potential of these two compounds should employ a lower 5-HT concentration of 500nM or 200nM, or alternatively, a perfusion system could be set up to remove the need to use 5-HT altogether. Of course, it is possible that JES-737 and HLR8090-3-4 do not produce their anthelmintic effects via inhibition of pharyngeal pumping at all, but may instead have a detrimental impact on other *C. elegans* behaviours such as locomotion, egg laying or chemotaxis response to stimuli. Therefore, future investigation could examine the effect of the two drugs on other aspects of *C. elegans* physiology using a thrashing assay (such as that used in this chapter), an egg laying assay (such as that used by Bany et al., 2003), or by assessment of worm response to nose-touch or to aversive or attractive stimuli (e.g.Chalfie & Sulston, 1981; Kaplan & Horvitz, 1993; Ward, 1973; Wicks & Rankin, 1997).

In agreement with previous research (Willson et al., 2004), emodepside was shown in this chapter to inhibit wild type *C. elegans* pharyngeal pumping in Dent's saline and in

response to 5-HT. The potency of the PF1022A derivative verticilide and the emodepside derivative bis-dimethyl-morphonyl-PF1022 were less than that of emodepside. However, the PF1022A derivatives PF1022-222, PF1022-888 and emodepside demonstrated an equal efficacy at inhibiting wild type *C. elegans* pharyngeal pumping response to 5-HT.

The structural similarity between emodepside, verticilide, bis-dimethyl-morphonyl-PF1022, PF1022-222 and PF1022-888 may explain the ability of all five to inhibit wild type *C. elegans* pharyngeal pumping, suggesting that they all work via a mechanism of action involving some or all of the same components. The structural differences between the compounds may explain their varying potency. PF1022A and emodepside have both been shown to bind the *H. contortus* latrophilin-like receptor (Saeger et al., 2001), which suggests that different cyclooctadepsipepides may share common components of their mechanism of action. However, differences in the structure of these compounds could affect their ability to bind receptors, resulting in the variation in potency observed in the results shown in this chapter.

As emodepside has been previously shown to inhibit locomotion in wild type *C. elegans* (Willson et al., 2004), the ability of the compound to affect thrashing behaviour in the worms was examined along with bis-dimethyl-morphonyl-PF1022, which was the most potent of the emodepside derivatives in the pharyngeal assay. Emodepside and bis-dimethyl-morphonyl-PF1022 were found to inhibit thrashing behaviour over a 60 minute period, with both compounds producing a significant reduction in thrashing just five minutes after they were applied ($P<0.05$). During the following 55 minutes of the assay, bis-dimethyl-morphonyl-PF1022 appeared to inhibit wild type *C. elegans* thrashing more rapidly and significantly than emodepside, with the former anthelmintic producing a 96% reduction in thrashing after 60 minutes, compared with the 84% produced by emodepside. This suggests that bis-dimethyl-morphonyl-PF1022, in comparison with emodepside, functions as an anthelmintic to more potently paralyse *C. elegans* locomotion, whereas emodepside activity is more potently directed at paralysis of the worm pharynx. It is possible that a combination of these two compounds within a commercial anthelmintic would prove a more effective treatment by achieving the maximum potency at multiple physiological targets in the parasite.

In conclusion, emodepside, bis-dimethyl-morphonyl-PF1022, verticilide, PF1022-222 and PF1022-888 all demonstrate anthelmintic activity in the pharynx, with emodepside and bis-dimethyl-morphonyl-PF1022 also anthelmintically active at the body wall muscle NMJ. The results shown in this chapter also demonstrate that emodepside is the most consistently potent at inhibiting *C. elegans* pharyngeal pumping, as well as achieving rapid paralysis of worm locomotion. Consequently, a more detailed investigation into the effect of emodepside on *C. elegans* physiology was performed and the results of this are shown in chapter 4. The pharmacological results of this chapter are summarized in table 3.1.

Novel anthelmintic	**Inhibition of pharyngeal pumping response to 5HT by an anthelmintic concentration of:**			
	10μM	**1μM**	**100nM**	**10nM**
JES-737	5% (not significant)	5% (not significant)	-	-
HLR8090-3-4	-	5% (not significant)	-	-
Emodepside	-	100%	99%	65%
Verticilide	-	94%	41%	12%
Bis-dimethyl-morphonyl-PF1022A	-	-	77%	-
PF1022-888	-	-	-	38%
PF1022-222	-	-	-	57%
	Inhibition of pharyngeal pumping in Dent's saline by an anthelmintic concentration of:			
	10μM	**1μM**	**100nM**	**10nM**
Emodepside	-	-	99%	-
	Inhibition of thrashing behaviour after exposure to 10μM anthelmintic for:			
	5 minutes	**10 minutes**	**20 minutes**	**30 minutes**	**60 minutes**
Emodepside	20%	16%	34%	52%	84%
Bis-dimethyl-morphonyl-PF1022A	13%	39%	62%	81%	96%

Table 3.1 A summary of the pharmacological results shown in chapter 3.

CHAPTER 4
DEFINING THE ACTION OF EMODEPSIDE ON *C. elegans* DEVELOPMENT AND BEHAVIOUR

4.1 Introduction

Emodepside possesses anthelmintic activity against parasitic nematode strains that are resistant to currently available anthelmintics, suggesting that emodepside utilizes a novel mechanism of action and has resistance-breaking capability (Harder et al., 2003; Zahner et al., 2001b). The results from chapter 3, in agreement with previous research (Harder et al., 2003; Willson et al., 2004), have demonstrated that emodepside paralyses *C. elegans* locomotion and pharyngeal pumping. Taken together, these results suggest that emodepside acts at the *C. elegans* neuromuscular junction (NMJ) to paralyse the pharyngeal and body wall muscles.

When examining the effect of emodepside on pharyngeal pumping and locomotion (results shown in chapter 3), it was also noticed that the anthelmintic affects *C. elegans* egg laying behaviour and development, suggesting that it targets a range of biological processes and physiological behaviours to render the worms unviable. It was also noticed that the locomotion of L4 worms is substantially affected by emodepside, but less severely than that observed in the adults. It is important to fully characterise and quantify these additional observations of emodepside activity in *C. elegans* as it will provide additional insight into the mechanisms utilized by the compound to paralyse the worms. For example, if emodepside does inhibits L4 locomotion less potently than in the adult, then this could be the result of adult and L4 *C. elegans* possessing differential expression of one or more components of the molecular pathway utilized by emodepside to paralyse the body wall muscles, or it could be due to the differential permeability of the adult and L4 cuticle to the drug, or a combination of both factors. The *C. elegans* cuticle consists of a layered internal structure with surface specializations and is known to change in both composition and structure during the life-cycle of the worm (reviewed in Kramer, 1997). One of the major features of the fourth larval moult is the larva-to-adult switch (L/A switch) involving the formation of adult cuticle, which differs from that of L4 *C. elegans* in both its molecular composition and organisation of constitutive components (Ambros, 1989; Kramer, 1997). It is possible that such an alteration in cuticle structure may contribute to, or be responsible for, the difference in emodepside-sensitivity of L4 and adult *C. elegans*. If the cuticle does not act as a barrier to emodepside activity in the L4, then this suggests that the reduced sensitivity of these worms to the anthelmintic is due to differential expression

in the adult and L4 worm of proteins utilized by emodepside to exert its effects. Such knowledge would help in the quest to identify further proteins involved in the pathways activated by emodepside by focusing investigation on those that show altered expression patterns in adult and L4 *C. elegans*.

To investigate the role of the cuticle in forming a barrier to emodepside activity, a pharyngeal assay was performed on dissected pharyngeal preparations (where the cuticle is no longer a barrier for drug access) as well as intact worms. The results of these assays are shown in this chapter.

4.2 The effect of chronic exposure to emodepside on locomotion

C. elegans locomotion is achieved by reciprocal contraction and relaxation of the dorsal and ventral body wall muscles, producing a sinusoidal wave of movement that propagates along the length of the worm body, generating a body bend which propels the animal forward or backward (Barnes et al., 1993).

Preliminary observations indicated that emodepside could disrupt worm locomotion at two levels: firstly, locomotion via sinusoidal body bend generation, and secondly, the ability of the worms to move per se (via normal or atypical body movement). Quantification of the former was achieved by measuring body bends per minute, and the latter was quantified by measuring the amount of time the worms spent moving forward or backward per minute regardless of whether this was via body bend production or an atypical body movement. For the latter assay, the time that the animals were stationary was not counted.

Emodepside was found to reduce body bend generation in mature fertile adult *C. elegans* in a concentration-dependent manner (IC_{50} 4nM; 95% confidence limits 3 to 4nM, see figure 4.1). Body bend generation by *C. elegans* at the fourth larval stage (L4) was also inhibited by emodepside in a concentration-dependent manner, but with a lower potency that in adult worms (IC_{50} 13nM; 95% confidence limits 12 to 15nM, see figure 4.1).

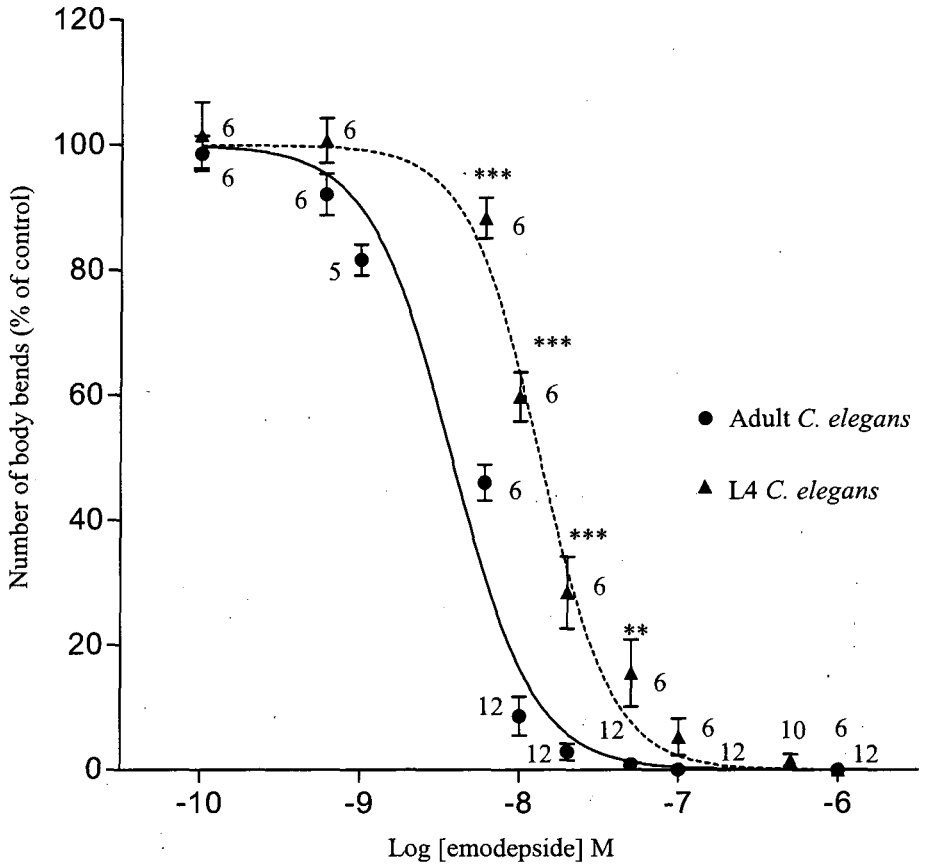

Figure 4.1 Concentration response curve demonstrating the effect of emodepside on body bend generation in wild type *C. elegans* adults and L4.
Synchronised populations of *C. elegans* were grown from eggs on agar plates containing emodepside (100pM to 1μM). 'number of body bends (% of control)' is the body bends per minute produced by adult and L4 worms on emodepside plates as a % of the body bends per min produced by adult and L4 *C. elegans* grown on control plates (0.5% ethanol). Each datum point is the mean ± S.E.Mean of (n) *C. elegans*. Significance (Student's t-test) relates to a comparison of body bend generation in adult and L4 *C. elegans* exposed to the same concentration of emodepside, ***P<0.001, ** P<0.01, n numbers are given beside each datum point. To clarify, n numbers at 100nM emodepside: 12 (adult), 6 (L4), at 500nM: only L4 assayed (10 worms), and at 1μM: 12 (adult), 6 (L4). The curves were fitted using the nonlinear regression four-parameter logistic equation described in chapter 2, section 2.10.

The inhibition of body bend generation by emodepside in adult *C. elegans* was accompanied by a reduction in the time the worms spent moving; an effect that was not observed in L4 worms (figure 4.2(a)). L4 worms exposed to emodepside and demonstrating a loss in body bend generation were still capable of locomotion via shallow and irregular sinusoidal movement restricted to the posterior region of the worm. The anterior region of these L4 worms appeared incapable of flexing to generate sinusoidal wave contraction, and maintained a "rod-like" appearance as the worm moved forward or backward (figures 4.2(b), (c)), which produced characteristic tracks on the agar plates (figures 4.2(d), (e)).

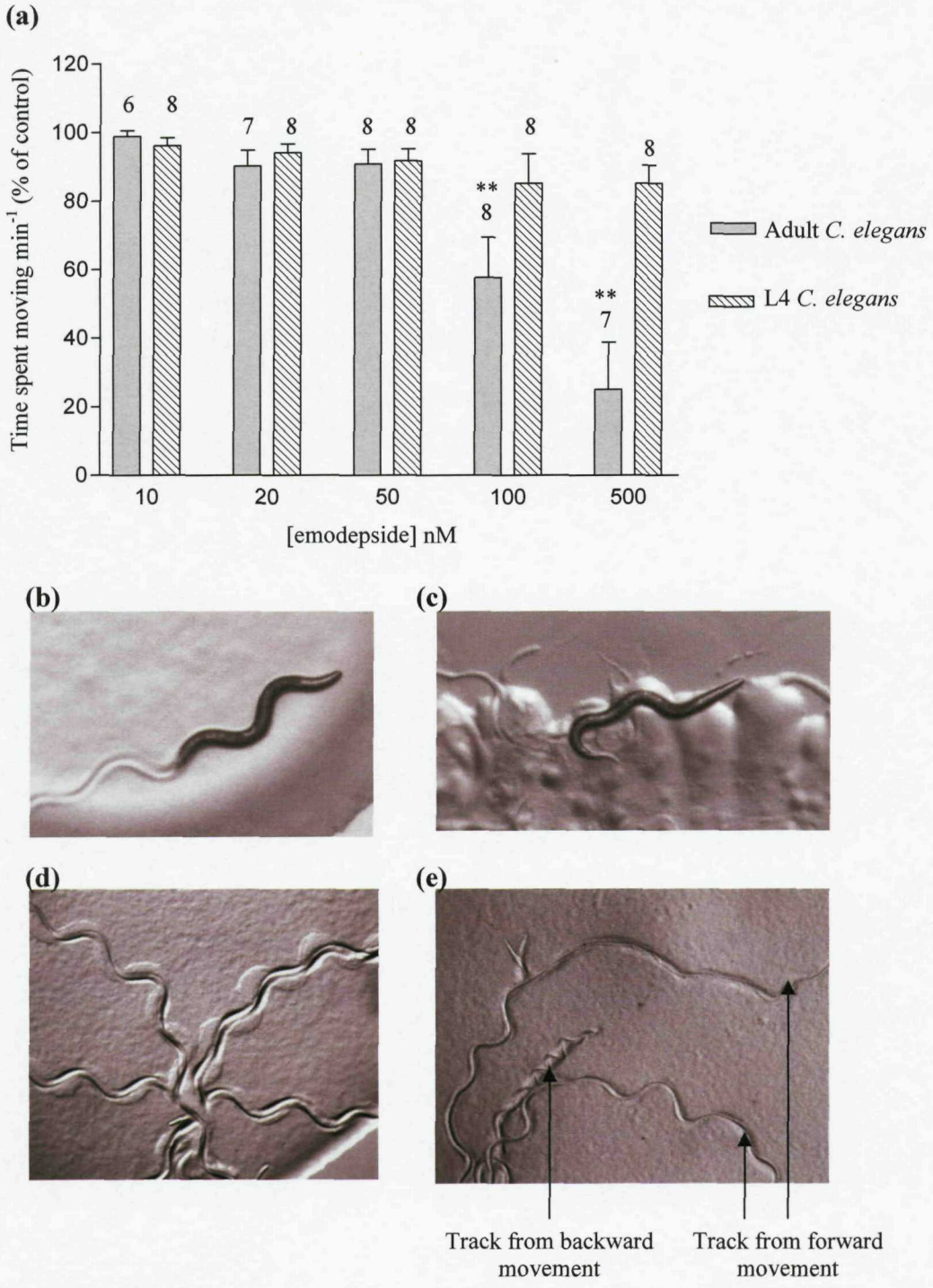

Figure 4.2 The effect of emodepside on the locomotion of adult and L4 wild type *C. elegans*.
(a) Graph showing the effect of emodepside on the time *C. elegans* adults and L4 spend moving. Each bar is the mean ± S.E.Mean of (n) *C. elegans*. Significance (Student's t-test) relates to a comparison of the time spent moving per minute of adult and L4 *C. elegans* exposed to the same emodepside concentration, **P<0.01, n numbers given above each bar. **(b)** A typical *C. elegans* grown on control plates (0.5% ethanol). Note the sinusoidal "wave-like" shape of the worm body. **(c)** A typical *C. elegans* L4 grown on 500nM emodepside plates. Note the "rod-like" anterior region of the worm (where localized paralysis was observed) and the curved shape of the posterior region (which remained capable of sinusoidal movement). During forward locomotion, the L4 appeared to push the anterior region along via sinusoidal movement (often shallow and irregular) in the posterior. **(d)** *C. elegans* L4 grown on vehicle control agar plates (0.5% ethanol) produced sinusoidal tracks on the agar, which were similar when moving backward or forward. **(e)** *C. elegans* L4 grown on 500nM emodepside plates produced very distinct tracks when moving forward, as indicated. These worms were also capable of reverse locomotion via exaggerated body bends, leaving characteristic tracks on the agar, also indicated.

It is possible that the locomotory paralysis produced by emodepside in adult and L4 *C. elegans* differed because the worms were at different developmental stages or because the adult worms had been in contact with emodepside for longer than the L4 larvae when analysed. To determine whether the latter possibility is correct, body bend production by adult and L4 *C. elegans* was analysed after both had been exposed to 500nM emodepside for 18 hours (prior to analysis). Figure 4.3 shows that the differential paralysis of adult and L4 *C. elegans* by emodepside is maintained even when exposed to the drug for the same length of time.

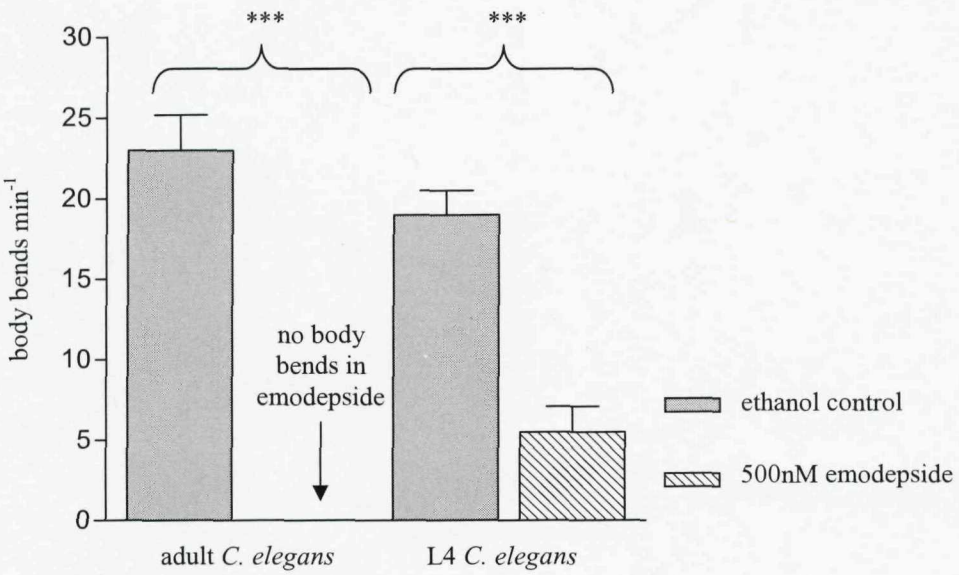

Figure 4.3 A graph showing the effect of acute exposure to 500nM emodepside on body bend generation in wild type *C. elegans* adults and L4.
Each bar is the mean of ± S.E.Mean of 10 *C. elegans*. Significance (Student's t-test) relates to a comparison of body bend generation by either adult or L4 *C. elegans* exposed to 500nM emodepside and control worms of the same age, ***P<0.001, n = 10 worms.

4.3 The effect of acute exposure to emodepside on locomotion

To determine the acute impact of emodepside on worm locomotion, a thrashing assay was performed on adult and L4 worms. *C. elegans* produces a characteristic thrashing movement when placed in liquid and this behaviour can be used to quantify subtle locomotion defects, because, unlike worm movement on a solid substrate, thrashing is both continuous and high frequency (Miller et al., 1996). The thrashing behaviour of L4 *C. elegans* exposed to 10μM emodepside was significantly reduced 60 minutes after commencement of drug exposure when compared to vehicle control (figure 4.4(b)). However, adult worms were paralysed faster, with a highly significant reduction ($P<0.01$) in thrashing behaviour at 20 minutes when compared with adults exposed to the vehicle (figure 4.4(a)). These results suggest that adult *C. elegans* are more sensitive to emodepside in terms of thrashing behaviour than L4 worms.

(a) Adult *C. elegans*

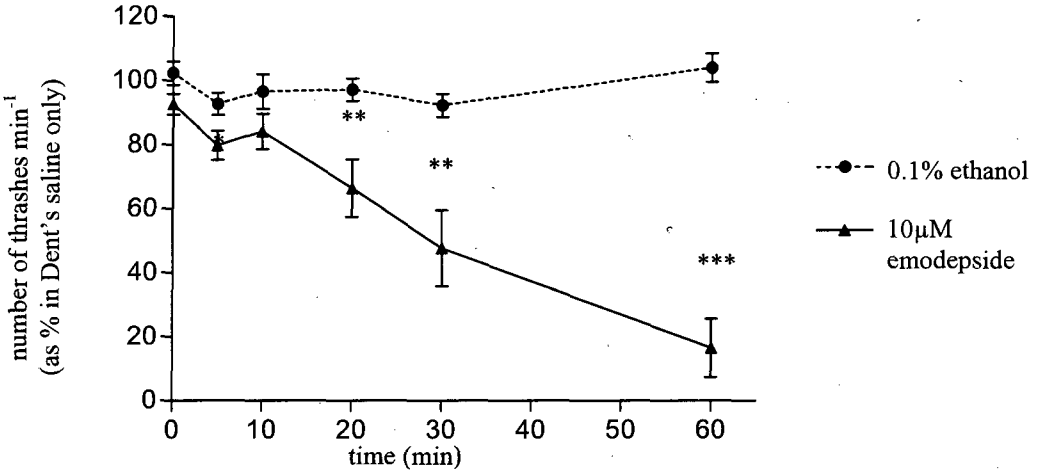

(b) L4 *C. elegans*

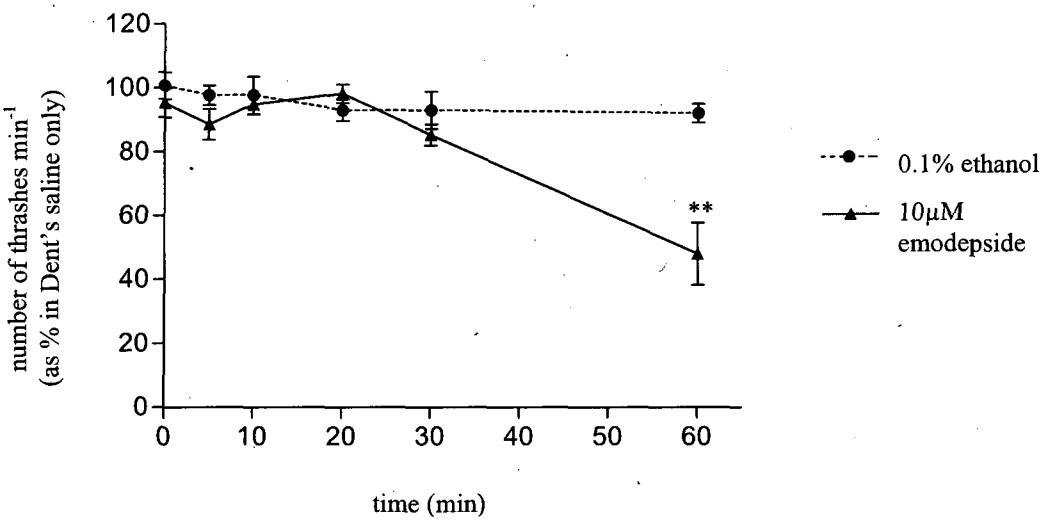

Figure 4.4 The effect of emodepside on adult and L4 wild type *C. elegans* thrashing behaviour. Graphs showing the effect of 10μM emodepside on the thrashing behaviour of **(a)** adult *C. elegans* and **(b)** L4 *C. elegans*. At each time point data were analysed as the number of thrashes per minute in emodepside or ethanol as a % of thrashes per minute in Dent's saline at the corresponding time point. Each datum point is the mean ± S.E.Mean of 12 *C. elegans*. Significance (Student's t-test) relates to a comparison of thrashing behaviour by *C. elegans* in 0.1% ethanol and worms in 10μM emodepside, ***P<0.001, **P<0.01, * P<0.05, n = 12.

4.4 The effect of emodepside on development

It was observed that when *C. elegans* were grown from egg to adulthood on agar plates containing emodepside at 10nM or higher, emodepside retarded the speed of worm development.

C. elegans populations assayed 43 hours after the transfer of eggs to agar plates containing emodepside (various concentrations tested) demonstrated an alteration in the percentage of worms that had reached L4 (figure 4.5(a)). Even the lowest concentration of emodepside tested in this assay was capable of producing a change in the timing of worm development, with just 10% of the worms on 10nM emodepside at the L4 stage, compared to 61% for the control worms. *C. elegans* populations exposed to 50nM, 100nM and 500nM emodepside consisted of 97% L3 stage or younger, compared to just 38% for control worms, with the remaining worms at L4 stage. 64 hours after the transferral of *C. elegans* eggs to the agar plates, the control worm population consisted of 92% adults. However, *C. elegans* populations exposed to 500nM emodepside possessed only 1% adult worms, and still consisted of 52% L3 worms or younger (figure 4.5(b)). This was not a complete arrest in development as emodepside treated worms could become adults, albeit over a much prolonged time-course.

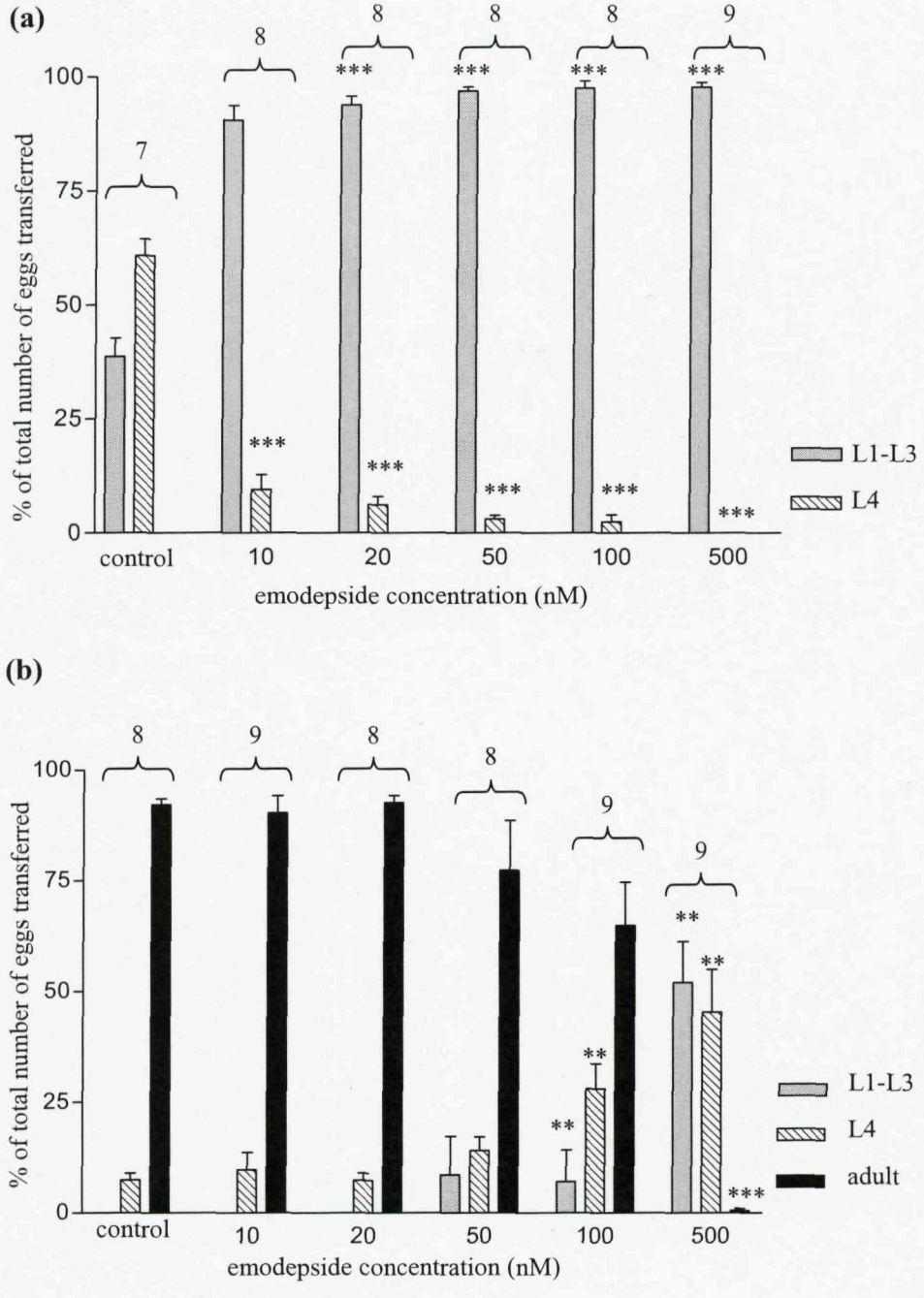

Figure 4.5 The effect of emodepside on wild type *C. elegans* development.
(a) Graph showing *C. elegans* populations assayed 43 hours after being transferred as eggs to agar plates containing emodepside (10-500nM). **(b)** Graph showing *C. elegans* populations assayed 64 hours after being transferred as eggs to agar plates containing emodepside (10- 500nM). For both (a) and (b), each bar is the mean ± S.E.Mean of (n) worm populations. Significance (Student's t-test) relates to a comparison of the proportion of each population at a particular developmental stage on a specific emodepside concentration with the proportion of the control population at the same time, ***P<0.001, **P<0.01, n numbers are given above each emodepside concentration.

4.5 The effect of acute exposure to emodepside on the timing of egg hatching

The results shown in section 4.4 demonstrate that emodepside retards the speed of *C. elegans* development to adulthood. However, these results do not elucidate whether this delay occurs continuously throughout worm development or only at specific stages, such as certain larval stages, at moulting or egg hatching. To investigate whether the developmental delay caused by emodepside includes an alteration to the timing of egg hatching, eggs that were laid in one hour by *C. elegans* grown on NGM agar were transferred to plates containing either 500nM emodepside or 0.5% ethanol vehicle (control) and the timing of hatching was followed. Figure 4.6 shows that emodepside did not significantly alter the timing of egg hatching when compared to controls, indicating that exposure to emodepside after eggs have been laid does not effect hatching times, suggesting that the delay in worm development caused by emodepside exposure is post-hatching.

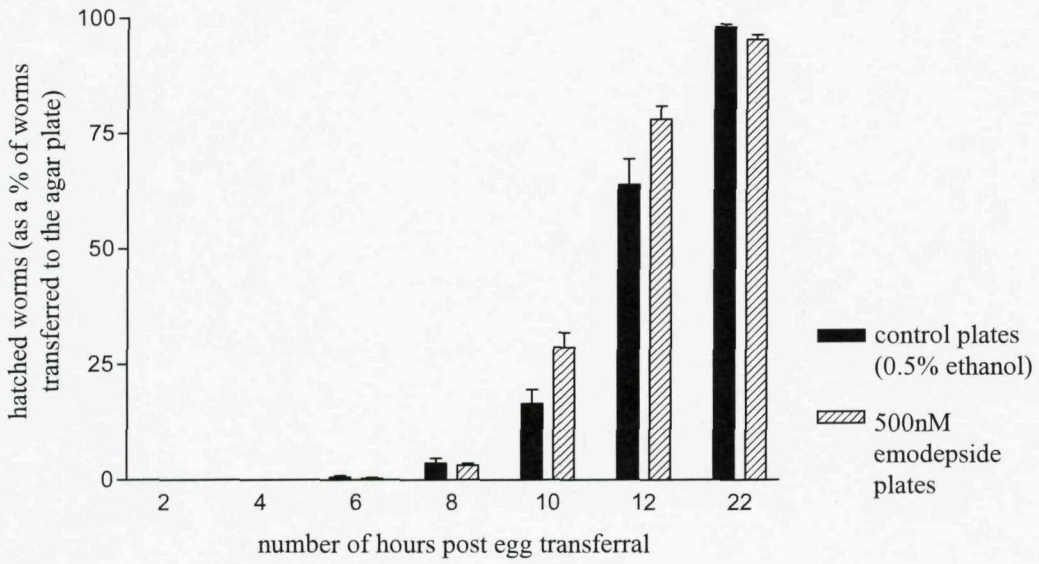

Figure 4.6 The effect of acute exposure to emodepside on the timing of wild type *C. elegans* egg hatching.
Graph showing the number of worms that hatched from a synchronized population of eggs at specific time points after transferral to agar plates containing 500nM emodepside or vehicle (0.5% ethanol). Each bar is the mean ± S.E..Mean of 5 egg populations (50-150 eggs per population).

4.6 The effect of emodepside on egg laying behaviour

C. elegans transferred as eggs to agar plates containing 100nM emodepside or more became bloated with eggs when they reached fertile adulthood, and at 500nM emodepside, adult *C. elegans* frequently contained hatched larvae and often ruptured due to the hatching of progeny within the parent worm. To quantify these observations, the chronic effect of emodepside on egg laying behaviour was measured by transferring *C. elegans* eggs onto plates containing emodepside at various concentrations and then assaying the worms at adulthood for the number of eggs laid in one hour (figure 4.7(a), protocol 1). Emodepside at concentrations of 20nM to 500nM was shown to significantly inhibit *C. elegans* egg laying behaviour in a concentration-dependent manner ($P<0.001$): an increasing emodepside concentration corresponded with a reduction in the number of eggs laid (figure 4.7(b), black bars on graph).

However, if *C. elegans* eggs were transferred to plates containing emodepside at concentrations capable of inhibiting egg laying as part of protocol 1 (20nM to 500nM), but were then removed at early L4 stage and transferred to plates containing only 0.5% ethanol vehicle (figure 4.7(a), protocol 2), they did not demonstrate the inhibition in egg laying (figure 4.7(b), hatched bars on the graph). In fact, there is a slight but significant increase ($P<0.05$) in egg laying behaviour in worms exposed to 20nM or 50nM emodepside from egg to L4.

C. elegans that were grown from egg to L4 stage on agar plates containing only vehicle (0.5% ethanol) and then transferred to emodepside-containing plates (see figure 4.7(a), protocol 3), demonstrated an inhibition of egg laying behaviour that was dependent on emodepside concentration (figure 4.7(b), white bars). Interestingly, all emodepside concentrations tested (1nM to 500nM) as part of protocol 3 elicited a significant reduction in egg laying behaviour ($P<0.001$). This is different from the results of protocol 1, where emodepside concentrations of 20nM and above were required to suppress egg laying behaviour significantly.

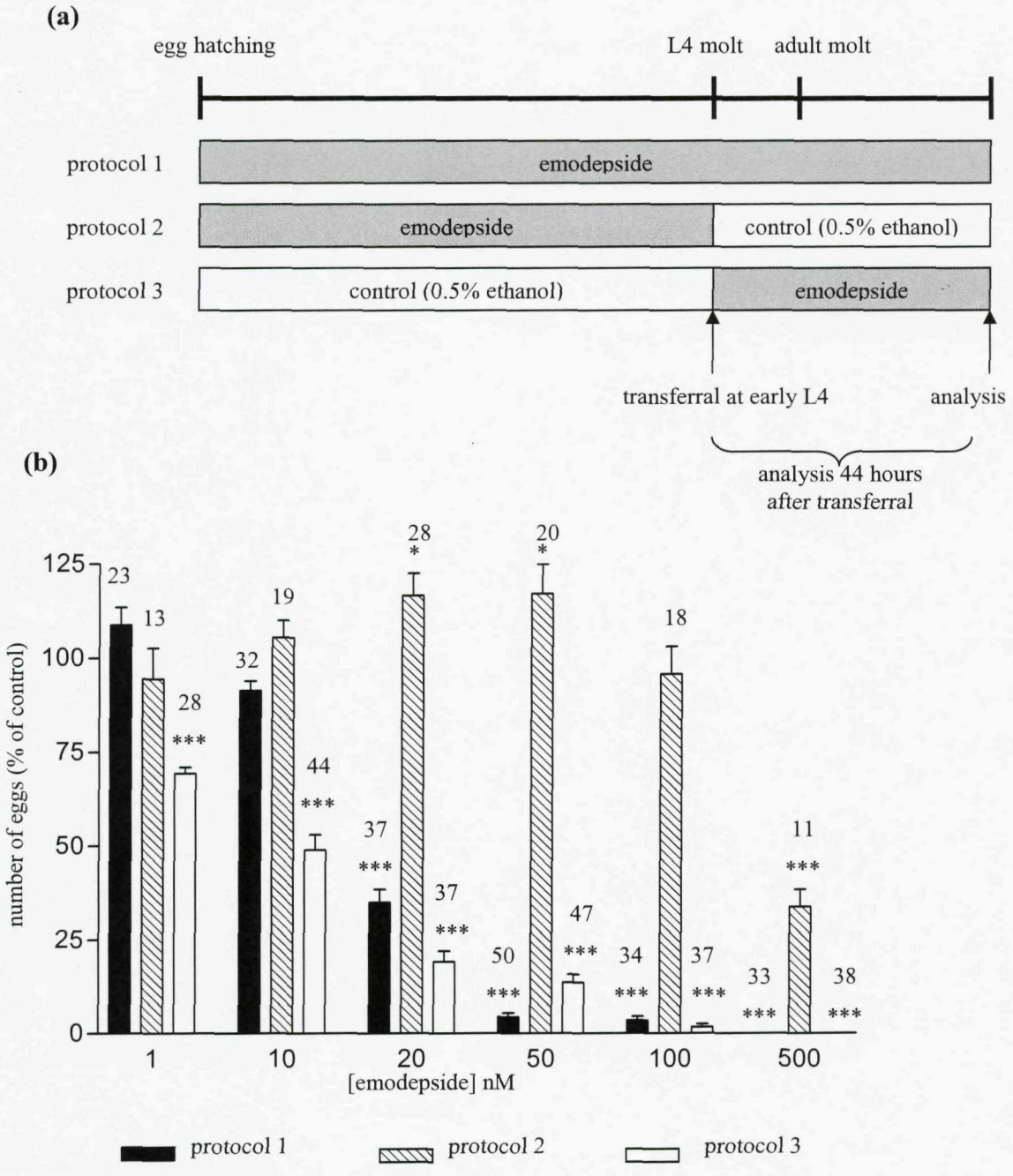

Figure 4.7 The effect of chronic exposure to emodepside on the egg laying behaviour of wild type *C. elegans*.

(a) A schematic to show the three protocols employed to investigate whether exposure to emodepside at different points of the *C. elegans* life cycle affects the potency of the drug's effect on egg laying behaviour. **(b)** A graph showing the egg laying behaviour of *C. elegans* exposed to varying concentrations of emodepside using the three protocols shown in (a). Each bar is the mean ± S.E.Mean of (n) *C. elegans*. 'number of eggs (% of control)' refers to the control worms grown throughout the entire lifecycle on plates containing only vehicle (0.5% ethanol). Significance (Student's t-test) relates to a comparison of egg-laying behaviour in *C. elegans* exposed to emodepside and control results (worms exposed to 0.5% ethanol only), ***P<0.001, **P<0.01, *P<0.05, n numbers are given above each bar.

It is possible that the observed impact of emodepside on the speed of *C. elegans* development may result in a delay in the onset of egg laying behaviour, and this could be responsible for the reduction in the number of eggs laid by drug-exposed worms compared to control worms at the time of analysis. To control for this possibility, experiments were performed to investigate the acute affect of emodepside on *C. elegans* egg laying. When age-matched adult *C. elegans* grown on NGM agar and actively engaged in egg laying behaviour were transferred to agar plates containing 500nM emodepside, egg laying behaviour was almost entirely abolished within the first hour, and no further eggs were laid for the following three hours of the assay (figure 4.8). In comparison, age-matched control *C. elegans* transferred to agar plates containing vehicle (0.5% ethanol) but not emodepside continued to lay a mean number of nine eggs during each hour of the assay.

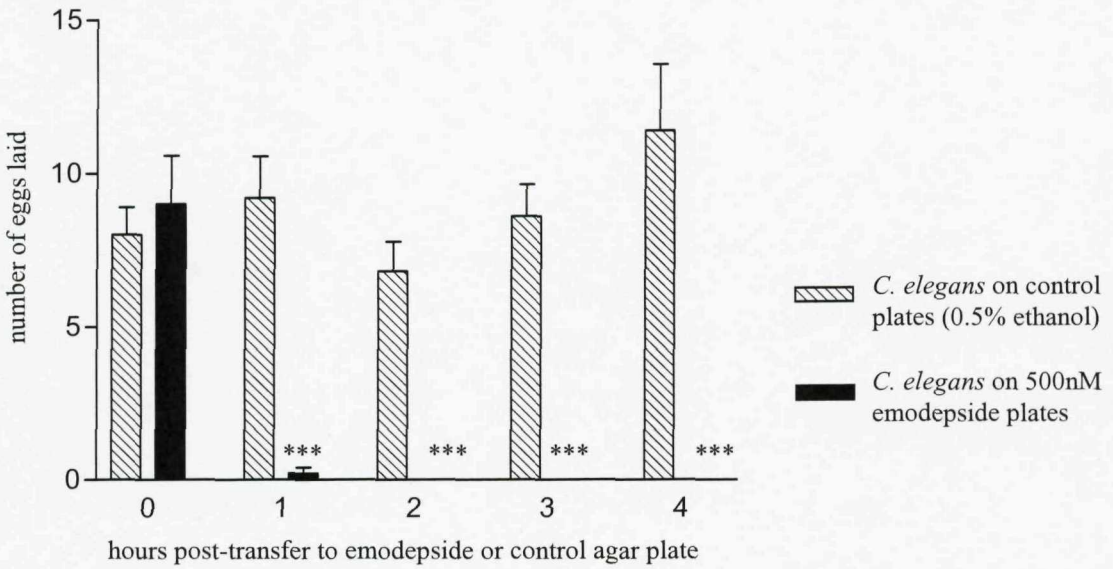

Figure 4.8 Graph showing the effect of acute exposure to 500nM emodepside on wild type *C. elegans* egg laying.
Each bar is the mean ± S.E.Mean of 5 *C. elegans*. Significance (Student's t test) relates to the number of eggs laid by the worms exposed to emodepside and the control worms (transferred to 0.5% ethanol vehicle plates rather than emodepside) at each time point, ***P<0.001, **P<0.01, *P<0.05, n = 5.

Importantly, when the number of eggs inside the worms was counted each hour of the assay, the *C. elegans* exposed to emodepside demonstrated an accumulation of eggs throughout the assay, whereas each control worm contained a relatively consistent number of eggs throughout. By counting the number of eggs laid and the number of eggs inside each worm every hour of the assay, the number of eggs produced by each worm per hour could be counted. For example, if a worm contained 12 eggs at the beginning of the assay, and one hour later had laid 10 and contained 11, then the worm produced 9 eggs in that hour. If, however, the worm contained 12 eggs at the start of the assay, and one hour later had laid none and contained 23, then the worm produced 11 eggs. Using this analysis revealed that the number of eggs produced per hour by *C. elegans* exposed to emodepside and the control worms were not significantly different (figure 4.9). Therefore, because the egg laying behaviour of the emodepside-exposed *C. elegans* was inhibited, these worms accumulated eggs (see figure 4.10(a)), with some containing more than 40 eggs by the end of the assay. Figure 4.10 (b-d) show examples of *C. elegans* in the presence and absence of emodepside, illustrating the accumulation of eggs within the emodepside-exposed worms. These results provide evidence that emodepside can directly inhibit *C. elegans* egg laying behaviour, which the drug may achieve by interfering with neuromuscular control of the egg laying muscles.

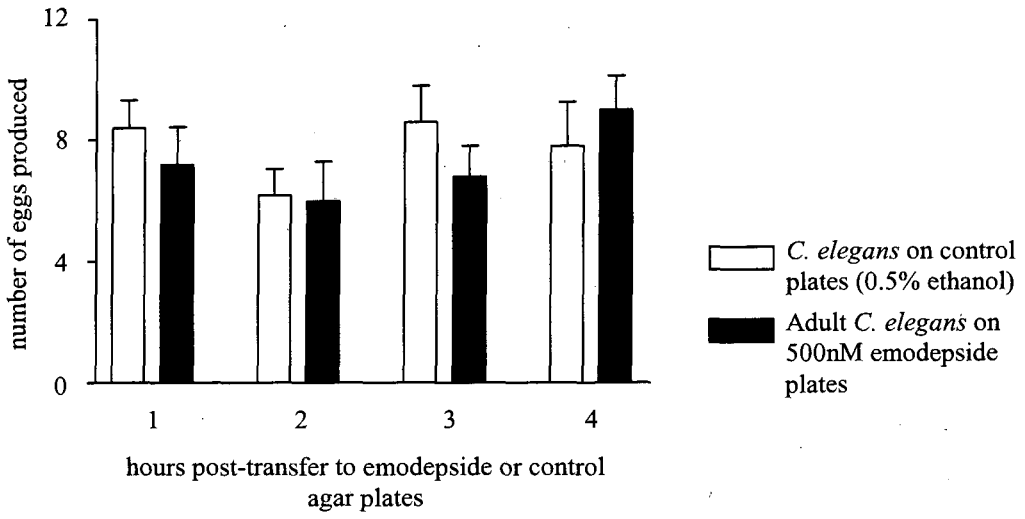

Figure 4.9 The effect of acute exposure to emodepside on egg production by wild type *C. elegans*. Graph to show the number of eggs produced by the worms each hour after exposure to emodepside or vehicle (0.5% ethanol) commenced. Each bar is the mean ± S.E.Mean of 5 *C. elegans*.

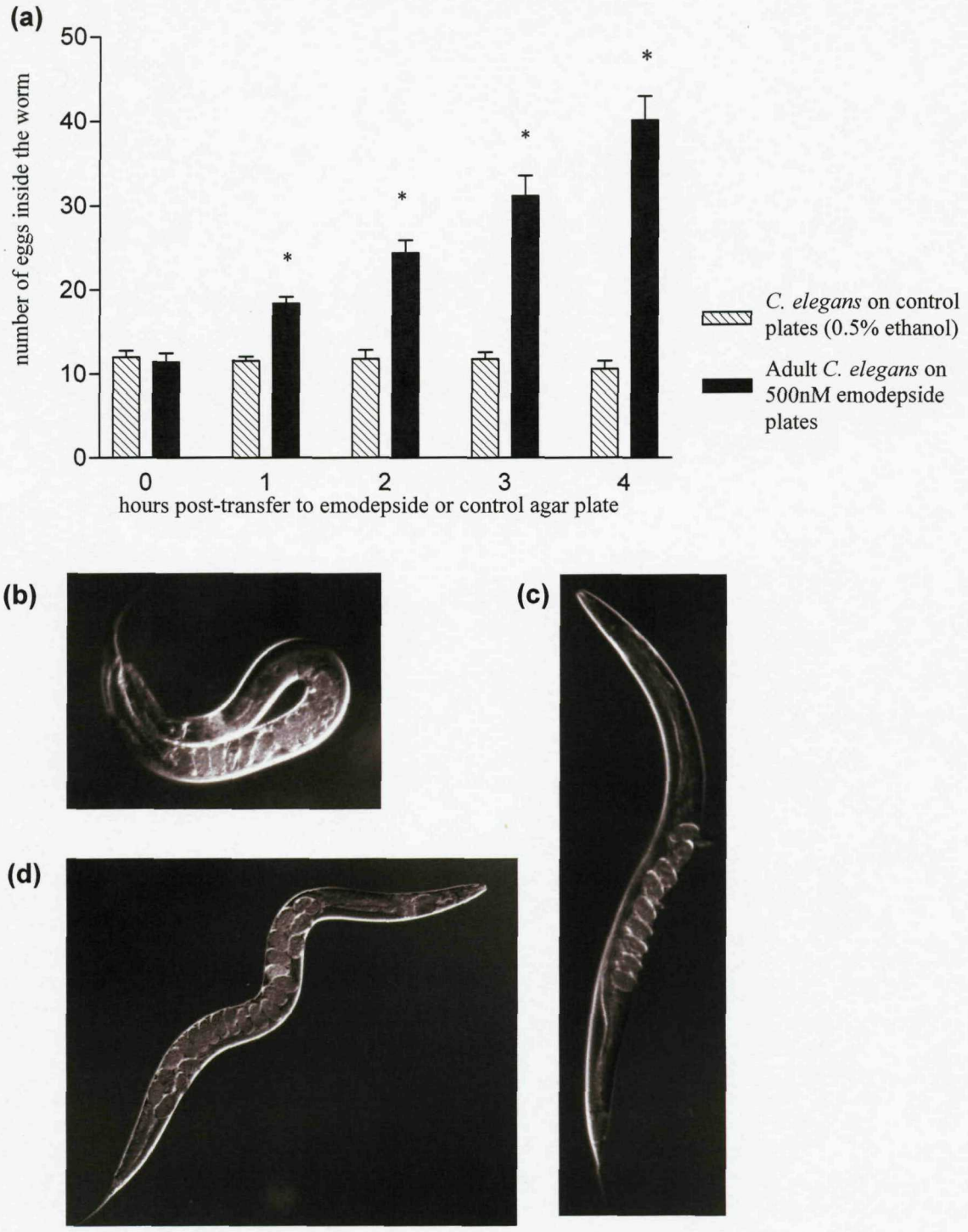

Figure 4.10 The effect of acute exposure to emodepside on egg accumulation in wild type *C. elegans*. **(a)** Graph to show the number of eggs within the worms each hour after exposure to emodepside or vehicle (0.5% ethanol) commenced. Each bar is the mean ± S.E.Mean of 5 *C. elegans*. Significance (Student's t-test) relates to comparison of egg production by *C. elegans* exposed to emodepside and ethanol, ***P<0.001, **P<0.01, *P<0.05, n = 5. **(b)** A typical *C. elegans* grown on NGM agar (0.5% vehicle control) at the start of the acute egg laying assay (44 hours post-late L4 stage). The worm contains 10 eggs. **(c)** A typical control *C. elegans* 4 hours after the start of the assay (exposed to only 0.5% ethanol vehicle) containing 9 eggs. At the start of the assay the worm contained 13 eggs, and laid 17 eggs in the first two hours of the assay and 25 eggs in the last two hours. Therefore, this worm produced 20 eggs during the 4 hours of the assay. **(d)** A typical *C. elegans* after 4 hours exposure to 500nM emodepside. This worm contains 24 eggs, compared to 10 eggs at the start of the assay. No eggs were laid by this worm during the 4 hour assay. Therefore, this worm produced 14 eggs during the 4 hours of the assay.

The accumulation of eggs within *C. elegans* exposed to 500nM emodepside resulted in the 'bagging' phenotype; with worms becoming first bloated with unlaid eggs and then with hatched larvae. This effect can be seen in figure 4.11, which shows an adult worm treated with 500nM emodepside as part of the acute egg laying assay and then allowed to remain on the emodepside-containing plate for 18 hours after the 4 hour assay was completed.

(a)

(b)

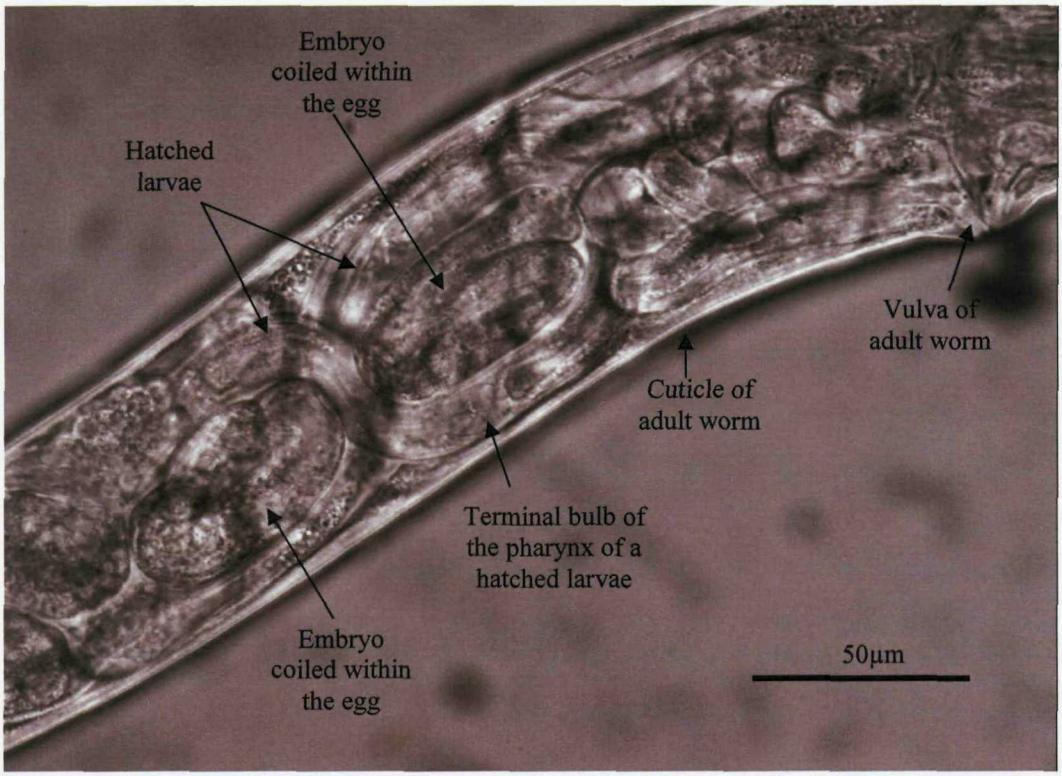

Figure 4.11 *C. elegans* exposed to 500nM emodepside exhibit the 'bagging' phenotype.
(a) An adult *C. elegans* 22 hours after transferral to an agar plate containing 500nM emodepside. The worm was grown from egg to adulthood on NGM agar, and was actively engaged in egg laying behaviour before transferral to the emodepside plate. The black square indicates the magnified view of this worm shown in **(b)**. Notice that both unhatched eggs and hatched larvae are present within the adult worm.

4.7 The impact of emodepside on pharyngeal pumping in *C. elegans*

In chapter 3 (section 3.2.2, page 90) emodepside at 1μM, 100nM and 10nM was shown to be capable of paralysing the pharyngeal muscles using the EPG technique. To extend these earlier studies, a broader range of emodepside concentrations were examined for their effect on pharyngeal response to 500nM 5-HT using the EPG, enabling an IC_{50} value to be obtained.

Each pharynx preparation was initially 'primed' with 500nM 5-HT as described in section 3.2.1 (page 87), followed by the recording protocol (in order of application): three minutes 500nM 5-HT, wash (Dent's saline), ten minutes emodepside at a range of concentrations, wash (Dent's saline), three minutes 500nM 5-HT. Each change in solution included a wash in Dent's saline to remove as much of the initial drug as possible before applying the next. For each worm tested, the response of the pharynx to 5-HT following exposure to emodepside was calculated as a percentage of the response of that worm to 5-HT immediately prior to emodepside application.

Emodepside inhibits pharyngeal pumping in wild type *C. elegans* in a concentration-dependent manner, with an IC_{50} of 9nM (95% confidence limits 6 to 12nM) (see figure 4.12). No change in pump shape or duration was seen during emodepside application.

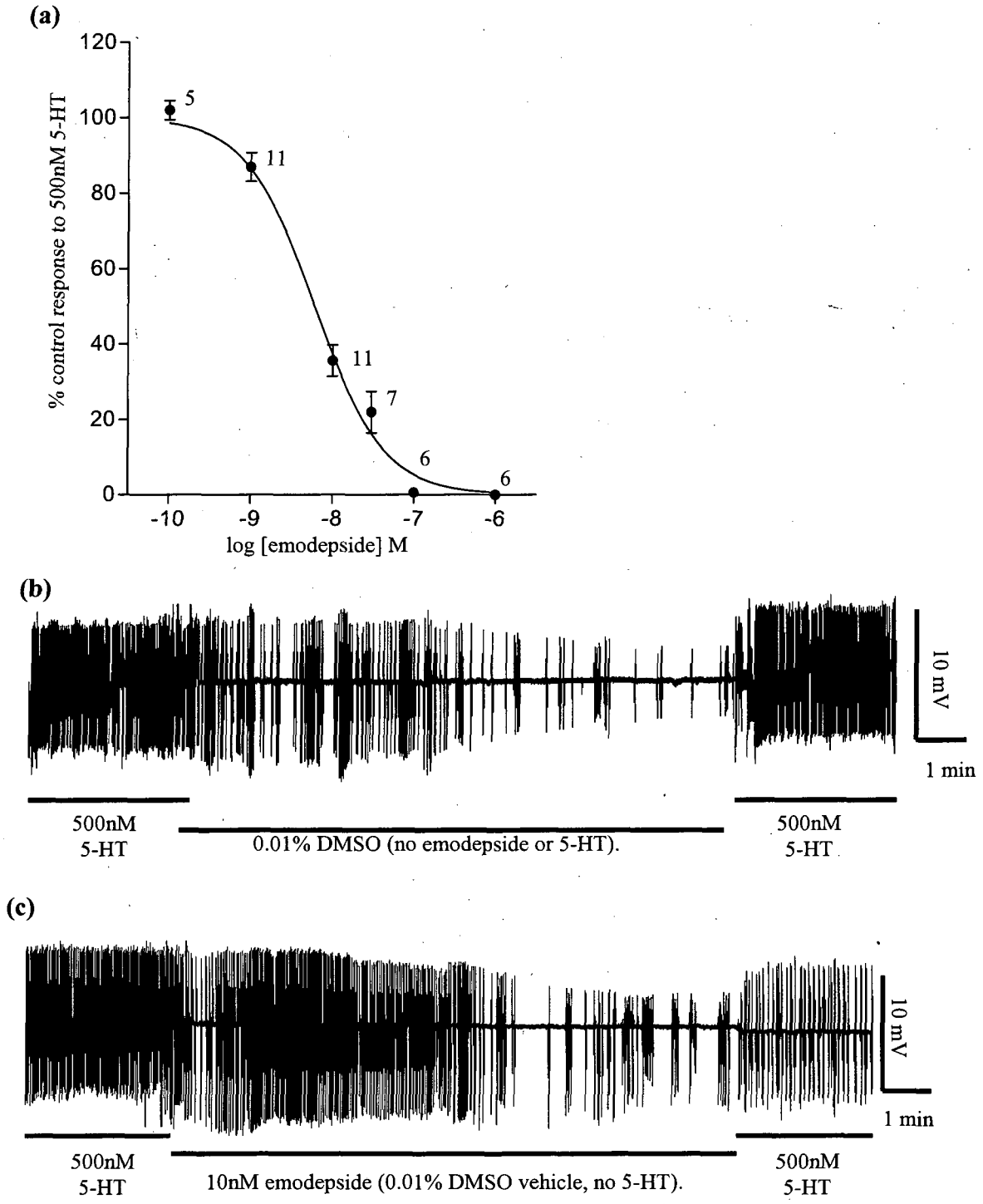

Figure 4.12 The effect of emodepside on pharyngeal pumping in wild type *C. elegans*.
(a) Concentration response curve demonstrating the effect of emodepside on the response of the *C. elegans* pharynx to 500nM 5-HT. Each datum point is the mean ± S.E.Mean of (n) pharyngeal preparations, n numbers are given beside each datum point. '% of control response to 5-HT' was calculated by expressing the pharyngeal response to 500nM 5-HT following exposure to emodepside as a percentage of the initial response to 5-HT (prior to emodepside application). The curve was fitted using the nonlinear regression four-parameter logistic equation described in chapter 2, section 2.10. **(b)** An example EPG recording for a control experiment demonstrating that 0.01% DMSO has no effect on pharyngeal response to 5-HT. Each vertical line represents the electrical activity associated with a single pharyngeal pump. **(c)** An EPG recording showing the effect of 10nM emodepside on pharyngeal pumping. Note the reduced pumping response to 5-HT following emodepside application.

Section 4.2 and 4.3 suggested that L4 wild type *C. elegans* are less sensitive to emodepside than adult worms. To investigate whether *C. elegans* age also affects pharyngeal sensitivity to emodepside, the response of the L4 and adult pharynx to 500nM 5-HT following exposure to 100nM emodepside was examined using the EPG technique. The protocol used was modified slightly from the previous assay on adult *C. elegans* because of the greater fragility of the L4 pharynx preparation, therefore, adults were assayed at the same time as L4 using the new protocol for both to ensure accurate comparison of the emodepside response. Worms were 'primed' using two minute repeated applications of 500nM 5-HT interspersed with three minutes in Dent's saline (as described in section 3.2.1, page 87). This was followed by the recording protocol (in order of application): two minutes 500nM 5-HT, wash (Dent's saline), ten minutes 100nM emodepside, wash (Dent's saline), two minutes 500nM 5-HT.

100nM emodepside inhibited adult and L4 *C. elegans* pharyngeal response to 5-HT by 98% (± 2) and 97% (± 1), respectively, suggesting that adult and L4 worms are equally sensitive to the effect of 100nM emodepside on pharyngeal pumping (see figure 4.13).

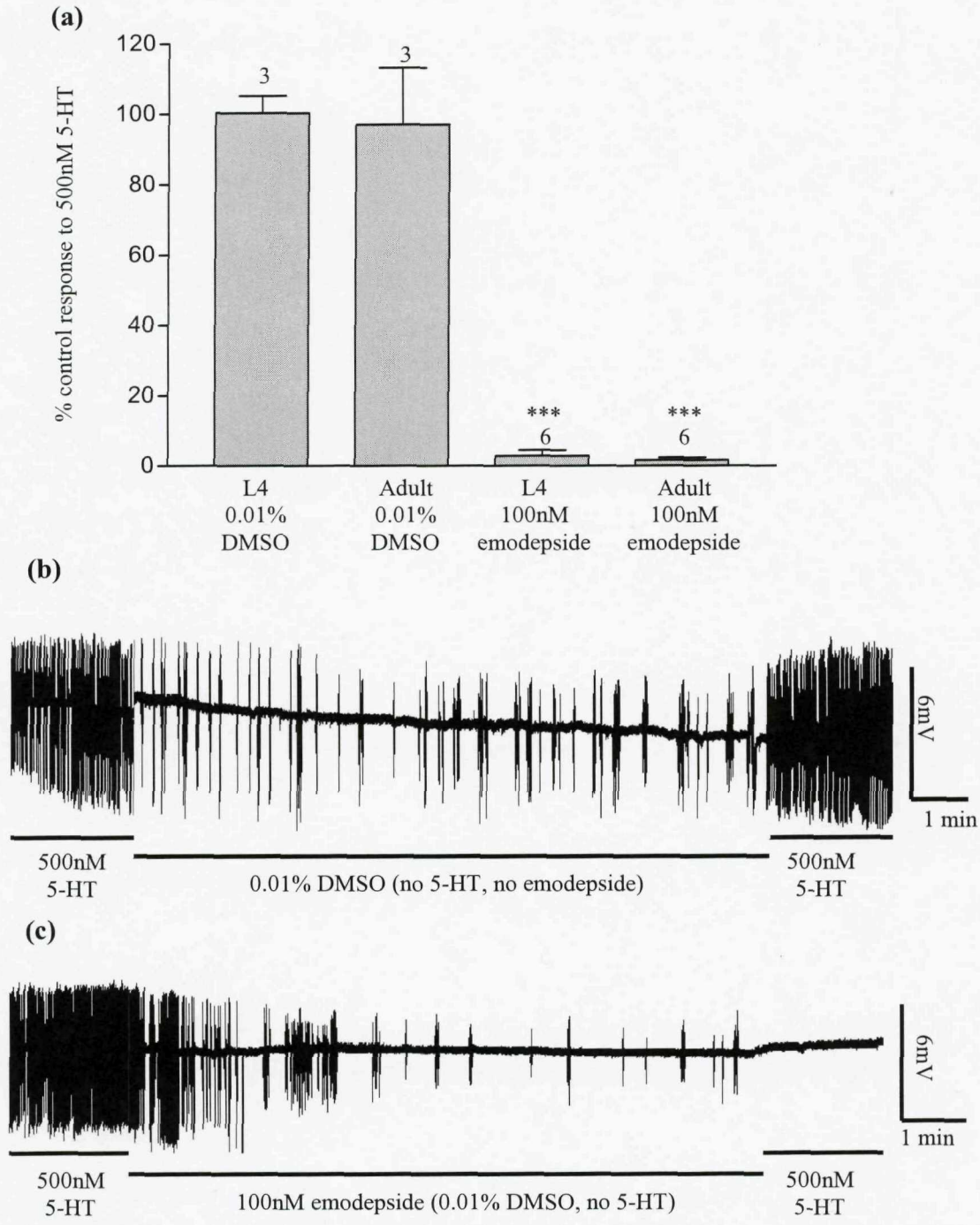

Figure 4.13 The effect of 100nM emodepside on L4 *C. elegans* pharyngeal pumping in 500nM 5-HT. **(a)** Graph showing the response of the L4 and adult pharynx to 500nM 5-HT following exposure to 100nM emodepside or 0.01% DMSO (vehicle control). Each bar is the mean ± S.E.Mean of (n) pharyngeal preparations. '% control response to 500nM 5-HT' was calculated by expressing the pharyngeal response to 500nM 5-HT following exposure to emodepside as a percentage of the initial response to 5-HT (prior to emodepside application). Significance (Student's t-test) relates to a comparison of either adult or L4 pharyngeal response to 5-HT following application of emodepside and application of only DMSO, ***P<0.001, n numbers are given above each bar. **(b-c)** Example EPG traces of L4 pharyngeal response to 5-HT following exposure to: (b) 0.01% DMSO only, (c) 100nM emodepside. Note that the pharyngeal pumping in (b) is stimulated by 5-HT to an equal extent before and after DMSO exposure, but the pharynx in (c) fails to respond to 5-HT following exposure to 100nM emodepside, in a manner very similar to the adult pharynx.

As discussed in section 4.1, it is possible that the difference in L4 and adult sensitivity to emodepside-induced paralysis of locomotion is associated with the cuticle, which is known to alter during the larva-to-adult switch at the fourth larval moult (Ambros, 1989; Kramer, 1997). Therefore, the L4 may be less sensitive to emodepside in the locomotion assays because of the presence of a less drug-permeable cuticle. In the EPG assay shown previously, the sensitivity of the L4 and adult pharynx to 100nM emodepside was not significantly different, but this assay used a cut preparation of the pharynx, which removes the cuticle as a barrier to emodepside action. It is possible that with the cuticle present, the sensitivity of the L4 and adult *C. elegans* pharynx to emodepside may differ in a manner similar to locomotion. If so, then this would support a role for the cuticle in determining the potency of emodepside for its effect on both the pharynx and locomotion. However, if the pharyngeal sensitivity of L4 and adult *C. elegans* remains the same in the presence of the cuticle, then this suggests that the mechanism of action for emodepside at the pharyngeal NMJ, and possibly at the body wall muscle NMJ as well, is partially dependent on constitutive components that are differentially expressed in the adult and L4 worm.

To investigate the possible involvement of the *C. elegans* cuticle in determining the potency of emodepside at the pharynx, a visual counting method was used to measure pharyngeal activity in intact worms (see chapter 2, section 2.8, page 76 for a detailed method description). The protocol used was identical to that used in the previous EPG assay which examined emodepside activity on cut pharyngeal preparations from L4 and adult *C. elegans*. Figure 4.14 demonstrates a significant difference in the potency of 100nM emodepside on L4 and adult pharyngeal response to 5-HT ($P<0.01$, red stars on figure 4.14), with the L4 5-HT response inhibited by 65% (± 9) compared with adult inhibition of 91% (± 3). Adult pharyngeal response to 5-HT was more significantly inhibited than L4 response when compared to worms of a corresponding age exposed to only the vehicle (adult $P<0.001$; L4 $P<0.01$; black stars on figure 4.14).

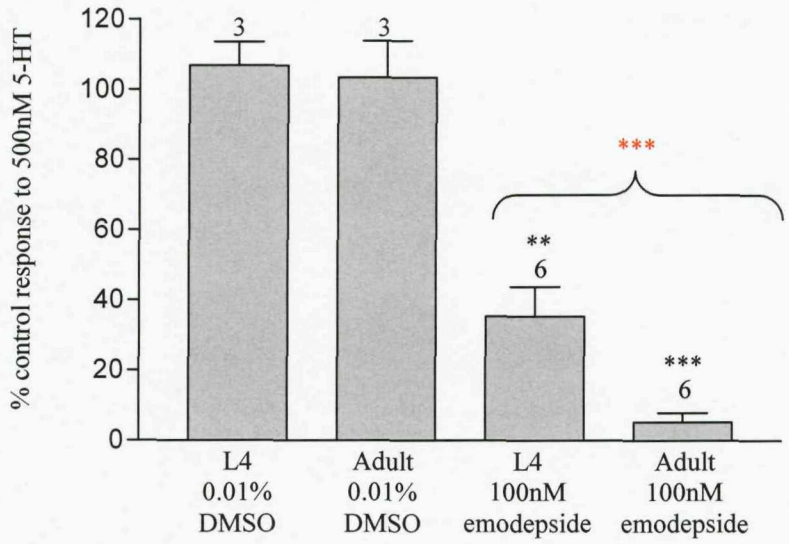

Figure 4.14 The effect of 100nM emodepside on L4 *C. elegans* pharyngeal pumping in 500nM 5-HT using intact animals.

Graph showing the response of the L4 and adult pharynx to 500nM 5-HT following exposure to 100nM emodepside or 0.01% DMSO (vehicle control). Each bar is the mean ± S.E.Mean of (n) pharyngeal preparations. '% control response to 500nM 5-HT' was calculated by expressing the pharyngeal response to 500nM 5-HT following exposure to emodepside as a percentage of the initial response to 5-HT (prior to emodepside application). Significance (Student's t-test) relates to (for the black stars) a comparison of either adult or L4 pharyngeal response to 5-HT following application of emodepside and application of only DMSO, ***P<0.001, **P<0.01, and (for the red stars) a comparison of L4 and adult response to 5-HT following emodepside exposure, n numbers are given above each bar.

4.8 Discussion

To investigate the action of emodepside on *C. elegans* development and behaviour, a wide range of concentrations, from 10nM to 10μM, were used. Significantly, the effect of emodepside on sinusoidal movement on solid media, egg laying behaviour, pharyngeal pumping and development were observed at concentrations of 500nM or less which is consistent with the previously proposed hypothesis that emodepside can function via one or more high affinity receptors (Willson et al., 2004). Emodepside, like latrotoxin, has been shown to stimulate *C. elegans* neurotransmitter release by a pathway involving latrophilin, suggesting that there are parallels between the mechanisms utilized by these two compounds (Willson et al., 2004). Latrotoxin is believed to function by specific stimulation of presynaptic secondary messenger pathways via binding to latrophilin, as well as mediating a less specific mechanism via formation of a nonselective cation channel (Khvotchev & Südhof, 2000; Krasnoperov et al., 1997; Lelianova et al., 1997; Volynski et al., 2000). Therefore, the effects of emodepside observed at concentrations greater than 500nM may be the result of a less specific mechanism involving the formation of nonselective ion channels in a manner similar to latrotoxin.

Emodepside inhibits wild type *C. elegans* locomotion on solid and in liquid media, but the extent of this paralysis appears to be dependent on the developmental stage of the worm when exposed to the anthelmintic. A comparison of body bend generation and thrashing behaviour in adult and L4 *C. elegans* exposed to emodepside suggests that the drug inhibits L4 less potently than the adult, and that the fourth larval stage is a transitional period to full emodepside sensitivity in terms of worm locomotion. This could be a result of adult and L4 *C. elegans* possessing differential expression of one or more components of the molecular pathway utilized by emodepside to paralyse the body wall muscles, or it could be due to the differential permeability of the adult and L4 cuticle to the drug, or a combination of both factors. Supporting a substantial role for the permeability of the cuticle in determining emodepside sensitivity in the pharynx, pumping by dissected L4 pharyngeal preparations is inhibited by 100nM emodepside to a similar extent as adult preparations, however, pharyngeal pumping in the intact L4 worm is inhibited less significantly than in the intact adult. This suggests that L4 pharyngeal sensitivity to emodepside is reduced by the presence of the cuticle, and it is possible that this is also true for the reduced emodepside sensitivity of L4 locomotion.

Significantly, emodepside has been previously shown to have a variable efficacy against the larval and adult forms of specific parasitic nematodes species *in vivo*. Against adult *Heligmosomoides polygyrus* emodepside is highly active *in vivo*, however, the larval stages of this parasite, found in the intestinal mucosa of the host mouse, were shown to be only partially affected by the drug suggested to be due to the encysted larvae being relatively impermeable to the compound (Harder & von Samson-Himmelstjerna, 2001). It was also demonstrated *in vivo* that emodepside is only effective against the microfilarae of *Brugia malayi* and *Litomosoides sigmodontis*, with only moderate or low efficacy against the adult worms of these two parasite species (Zahner et al., 2001a). However, emodepside has been shown to be effective against both the adult and larval stages of *Nippostrongylus brasiliensis*, *Strongyloides ratti* and *Acanthocheilonema viteae* (Harder & von Samson-Himmelstjerna, 2001; Zahner et al., 2001b). These previous findings, coupled with the results shown in this chapter, suggest that the efficacy of emodepside is dependent on both the parasitic nematode species targeted and the developmental stage of the parasite when exposed to the drug. It is likely that the permeability of the cuticle is a major determinant of *C. elegans* sensitivity to emodepside, although other factors, such developmental variation in the expression of proteins constituent to the mechanism of action for the drug, may also play a role. It is noteworthy that variation in anthelmintic sensitivity between larval *C. elegans* and adults is not uncommon and has been previously observed for drugs such as mebendazole (Bernt et al., 1998).

Wild type *C. elegans* exposed to emodepside throughout their development take longer to reach adulthood as the drug concentration increases. Emodepside is not unique as an anthelmintic capable of disrupting normal *C. elegans* development, as this has also been observed for ivermectin (Dent et al., 2000). It is unclear whether the effect of emodepside on the rate of development is directly due to the drug or is possibly an indirect result of the inhibition of worm locomotion by emodepside, which may decrease the ability of the worms to forage effectively for food. Additionally, emodepside, like ivermectin, inhibits pharyngeal pumping, which would be expected to restrict worm feeding (Bernt et al., 1998). Previous research has indicated that dietary restriction in *C. elegans* slows worm development as well as increasing lifespan, although whether these two effects are linked remains controversial (Walker et al., 2005). Therefore, it is possible that emodepside slows worm development via its impact on locomotion and pharyngeal pumping. Significantly, acute exposure of laid eggs to

emodepside does not significantly alter the timing of hatching, suggesting that the effect of emodepside on the rate of worm development is a post-hatching event, possibly because the egg is impermeable to the drug, or because the effect of emodepside on development is due to its impact on worm locomotion and pharyngeal pumping or a combination of both factors. However, the experiments shown in this chapter do not exclude the possibility that emodepside is capable of altering the speed of embryonic development or disrupting embryonic development if the parent worm is subjected to emodepside treatment, and it is possible that eggs laid by emodepside-exposed parent worms may demonstrate altered timing of hatching and may also show further changes in their development, behaviour and reproductive capability. Significantly, the emodepside-precursor PF1022A has also been shown to slow the rate of *C. elegans* development (Bernt et al., 1998). When these authors removed newly fertilized eggs from adult *C. elegans* and allowed them to undergo embryonic development in the presence of PF1022A, no effect of the drug on embryogenesis or on eventual hatching of the eggs was observed (Bernt et al., 1998). Not only do these results show that emodepside and its precursor PF1022A share an ability to target *C. elegans* pharyngeal pumping, locomotion, egg hatching and development, but also suggests that emodepside may share the inability of PF1022A to affect embryogenesis. This would support the conclusion that the effect of emodepside on development is post-hatching.

Wild-type *C. elegans* chronically exposed to emodepside throughout their life demonstrate a concentration-dependent reduction in egg laying; with worms exposed to 100nM emodepside or more exhibiting the 'bagging' phenotype. In support of these findings, acute exposure of adult *C. elegans* to 500nM emodepside almost entirely inhibits egg laying behaviour within the first hour, but does not inhibit egg production, thereby resulting in an accumulation of eggs in the uterus and, eventually, the 'bagging' phenotype. These results suggest that emodepside inhibits egg laying behaviour but not actual egg production. It is possible therefore that the vulval neuromuscular junction is another synaptic site of emodepside action. In support of these findings, it has been previously shown that the emodepside-precursor PF1022A can inhibit egg laying, resulting in the accumulation of eggs within the parent worm (Bernt et al., 1998).

C. elegans exposed to 20, 50, 100 and 500nM emodepside only from egg to early L4 stage do not demonstrate an inhibition in egg laying behaviour when they become adult worms. Indeed, emodepside must be present from late L4 in order for this inhibition to

be observed. Development of the egg laying system is completed when the final morphogenesis steps occur during late L3 to the larva-to-adult moult when the developing vulva invaginates and then everts to form the mature vulva (Greenwald, 1997; Newman et al., 1996; Waterson, 1988). The normal egg laying behaviour of worms exposed to emodepside before early L4 stage suggests that emodepside cannot persist within the worm from early L4 to the gravid adult when the egg laying system is in place and is active.

Egg laying behaviour in *C. elegans* is activated by signaling through the G protein $G\alpha_q$, and is inhibited by $G\alpha_o$ (Bany et al., 2003; Desai et al., 1988; Dong et al., 2000; Wilkie, 2000). Activation of egg laying depends on the two serotonergic hermaphrodite-specific neurons (HSNs), which stimulate the contraction of 16 egg laying muscle cells to push eggs through the uterus and out of the vulva (Desai et al., 1988). Acetylcholine (ACh) released at the vulval muscle NMJ is capable of binding to both muscarinic and nicotinic G protein-coupled receptors at the post-synaptic membrane, and the signalling pathways stimulated by these two types of receptor produce antagonistic effects on egg-laying behaviour. The binding of ACh to the nicotinic receptors stimulates egg laying, whereas binding to muscarinic receptors inhibits egg laying (Bany et al., 2003). However, the application of aldicarb has been found to produce an overall effect of inhibition of egg laying, suggesting that the release of a large quantity of ACh at the vulval muscle NMJ would inhibit egg laying (Bany et al., 2003). Previous research has suggested that emodepside functions in *C. elegans* by binding latrophilin, which is a G protein-coupled receptor, and stimulating neurotransmitter release (Willson et al., 2004). Therefore, it could be hypothesised that emodepside reduces egg laying behaviour by stimulating vesicular exocytosis of ACh from the presynaptic terminals of the vulval muscle NMJ, resulting in a spastic paralysis of the vulval muscles.

In conclusion, it has previously been shown that emodepside has a potent inhibitory action on *C. elegans* locomotion and pharyngeal pumping (Harder et al., 2003; Willson et al., 2004). The investigations in this chapter further characterise the effect of emodepside on locomotion and demonstrate that the adult is more sensitive to emodepside than the larval stages, possibly due to drug accessibility to its target site. The inhibitory action of emodepside on pharyngeal pumping also appeared dependent on larval stage, but only in the presence of the intact cuticle, suggesting that this is a major determinant of worm sensitivity to emodepside. The inhibitory effect of

emodepside on *C. elegans* locomotion and pharyngeal pumping may be responsible wholly, or partially, for the reduction in the speed of worm development in the presence of the drug. Finally, emodepside has been shown to elicit a concentration-dependent inhibition of egg laying, suggesting that emodepside affects at least three fundamental physiological processes: egg laying, feeding and locomotion by interfering with signaling through a pathway that is common to the vulval, pharyngeal and body wall neuromuscular junctions.

CHAPTER 5
IDENTIFICATION OF *C. elegans* MUTANTS WITH ALTERED SENSITIVITY TO EMODEPSIDE, VERTICILIDE, PF1022-888 AND PF1022-222

5.1 Introduction

In chapter 3, candidate anthelmintic compounds were examined for their effect on pharyngeal pumping and locomotion in wild type *C. elegans*. Four of these compounds demonstrated potent inhibitory activity in the pharynx and are of specific interest as potential commercial anthelmintics (A. Harder, personal communication). These compounds are emodepside, verticilide, PF1022-888 and PF1022-222, and all four are structurally derived from the cyclodepsipeptide PF1022A. It is possible that the structural relationship between these compounds may also be reflected in the mechanism by which they exert their anthelmintic activity; sharing common components of the pathways they utilize. Emodepside is the best characterized of the four anthelmintics, with the results from chapter 4 showing that it can inhibit wild type *C. elegans* locomotion, pharyngeal pumping and egg laying; findings which are in agreement with and extend the results of previous research (Willson et al., 2004). To identify components of the mechanism of action for emodepside at the neuromuscular junction (NMJ) of the pharyngeal and body wall muscles, the thrashing assay and electropharyngeogram (EPG) techniques were used to assess the sensitivity of *C. elegans* mutants to emodepside in comparison with wild type. The results of these investigations are shown in this chapter.

The *C. elegans* latrophilins (LAT-1 and LAT-2) were the initial focus point for studying the mechanism of action for emodepside because they have been previously shown by RNA interference (RNAi) to have a significant role in the activity of the drug in the pharynx and body wall muscles of *C. elegans* (Willson et al., 2004). To further define the role of LAT-1 in emodepside action at the body wall muscle NMJs, a *C. elegans lat-1* putative null strain was assayed using the thrashing assay to reveal the emodepside sensitivity of this strain (section 5.2). In contrast to previous research, showing that RNAi directed against *lat-1* reduces the emodepside sensitivity of *C. elegans* locomotion (Willson et al., 2004), the *lat-1* null mutants demonstrated a wild type response to emodepside in the thrashing assay. The *lat-1* RNAi procedures used by Willson et al. (2004) were repeated, and the results again demonstrated a reduction in thrashing sensitivity to emodepside in *C. elegans* treated with *lat-1* RNAi (section 5.3). Based on these results, which suggested that the RNAi procedure may not specifically target the *lat-1* gene, only the *lat-1* null mutant was used to investigate the role of LAT-1 in the action of emodepside at the pharyngeal NMJ (section 5.4.1).

Based on the results of the pharyngeal and thrashing assays using the *lat-1* null *C. elegans*, which demonstrated a role for LAT-1 in emodepside action at the pharyngeal NMJ but not the body wall muscle NMJ, it was decided that in this project the pharynx would be the focus site for further investigation into emodepside activity. The mechanism by which emodepside inhibits locomotion should be investigated independently due to the apparent differences in the molecular pathways utilized by emodepside at the pharyngeal and body wall muscle NMJs. The availability of a *lat-2* null mutant and a double mutant for both *lat-1* and *lat-2* enabled investigation into the importance of LAT-2 alone, as well as in conjunction with LAT-1, in the activity of emodepside on the pharynx using the EPG technique.

The latrophilins have been identified as receptors for latrotoxin (Krasnoperov et al., 1997; Lelianova et al., 1997; Sugita et al., 1999), which causes excessive neurotransmitter release at the neuromuscular junction via stimulation of synaptic vesicle exocytosis (Krasnoperov et al., 1997). Emodepside is also thought to function by stimulating neurotransmitter release at the neuromuscular junction via latrophilin (Willson et al., 2004), suggesting that the anthelmintic and the toxin may share common features of their mechanism of action in addition to the latrophilins. Human receptor-like protein-tyrosine phosphatase sigma (PTPσ) has been identified as a receptor of α-latrotoxin (Krasnoperov et al., 2002a). By binding directly to PTPσ, latrotoxin has been shown to stimulate insulin secretion from MIN6 β-cells via a pathway involving activation of phospholipase and alteration to ion channel functioning, including the reduction of repolarizing currents produced by large-conductance (BK) potassium channels (Lajus et al., 2006). It is possible that emodepside may not only function via the latrophilin receptor, but also the *C. elegans* ortholog of the PTPσ receptor.

The human type IIa family of receptor protein tyrosine phosphatases (RPTPs) includes the leukocyte-common antigen related (LAR)-like RPTPs called PTPδ and PTPσ. The *C. elegans* PTP-3 is the worm ortholog of the LAR-like RPTPs (Harrington et al., 2002). An independent BLASTp search (http://www. wormbase.org/db/searches/ blast_blat) of the *C. elegans* proteins with the PTPσ protein sequence, confirmed this by identifying the two PTP-3 splice variants (PTP3a and PTP3b) as having the closest sequence similarity with PTPσ. Both PTP-3 splice variants are highly expressed in the adult *C. elegans* nervous system (Harrington et al. 2002), with PTP3a predominantly localized to

presynaptic domains, and PTP3b found extrasynaptically within neurons and in the pharyngeal epithelium (Ackley et al., 2005). Therefore, to identify if PTP-3 has a role in the mechanism of action for emodepside in the pharynx, the PTP-3 loss-of-function mutant *C. elegans ptp-3 (op147)* was assayed for emodepside sensitivity using the EPG technique.

Latrophilin is a G protein-coupled receptor, and has been shown to couple to $G\alpha_q$, a G protein shown to activate a signaling pathway leading to neurotransmitter release (Rahman et al., 1999; Brundage et al., 1996). Consequently, if the physiological effects of emodepside on *C. elegans* are due to latrophilin-binding and resultant neurotransmitter release, it is possible that $G\alpha_q$ is involved in the pathway.

At the *C. elegans* NMJ, $G\alpha_q$ stimulates release of acetylcholine (ACh) via activation of phospholipase Cβ (PLCβ) (Brundage et al., 1996), which then hydrolyses phosphatidylinositol-4,5-bisphosphate (PIP2) to produce diacylglycerol (DAG) and inositol-1,4,5-triphosphate (IP3) (Lee et al., 1992; Taylor & Exton, 1991). DAG binds to the UNC-13 protein (Ahmed et al., 1992; Kazanietz et al., 1995), allowing the latter to prime synaptic vesicles for release via syntaxin activation (Richmond et al., 2001). Syntaxin, located at the presynaptic plasma membrane, performs a fundamental role during vesicle fusion, but it must achieve the open conformation before it can take part in vesicular exocytosis (Richmond et al., 2001). Activated syntaxin increases the number of vesicles in the 'ready releasable pool' at the presynaptic 'active zone'. These vesicles are then ready to complex with the vesicle-localized protein synaptobrevin (VAMP) and SNAP-25 to form the SNARE complex, which facilitates vesicle fusion with the presynaptic membrane and release of vesicle contents via exocytosis (e.g. Rizo & Südhof, 2002; Soller et al., 1993; Sutton et al., 1998).

At the *C. elegans* NMJ, hydrolysis of PIP2 by PLCβ is negatively regulated by the protein $G\alpha_o$, and therefore, this protein provides a pathway for the inhibition of neurotransmitter release (Miller et al., 1999; Nurrish et al., 1999). The reciprocal effects of $G\alpha_q$ and $G\alpha_o$ on neurotransmitter release contribute to the control mechanism for muscular contraction in the worm. Importantly, a loss-of-function mutation to the *dgk-1* gene, which encodes diacylglycerol kinase DGK-1, produces *C. elegans* with hyperactive locomotion and resistance to 5-HT-induced slowing of locomotion. These are similar

behavioural defects to *goa-1* mutants (*goa-1* encodes $G\alpha_o$), suggesting involvement of the two proteins in a common molecular pathway (Nurrish et al., 1999). Gain-of-function mutation to *goa-1* partially rescues the 5-HT insensitivity caused by *dgk-1* loss-of-function, suggesting that DGK-1 acts downstream or in parallel with the $G\alpha_o$ protein (Nurrish et al., 1999). DGK-1 phosphorylates DAG to produce phosphatidic acid (PA), and the *dgk-1* gene is expressed in most neurons of *C. elegans*, including motor neurons (Nurrish et al., 1999). In a model proposed by Nurrish et al. (1999), DGK-1 regulates the abundance of presynaptic DAG at the neuromuscular junction, thereby acting as a critical second messenger in the $G\alpha_o$ pathway that contributes to the control of ACh release. The *goa-1* and *dgk-1* genes are ubiquitously expressed in the worm nervous system (Nurrish et al., 1999), and *goa-1* is also expressed in the pharyngeal muscles and the pharyngeal neuron NSM (Segalat et al., 1995), suggesting that $G\alpha_o$ and DGK-1 could function as part of the mechanism of action for emodepside in the pharynx.

Emodepside is thought to paralyse *C. elegans* locomotion and pharyngeal pumping by stimulating excessive neurotransmitter release via activation of the presynaptic $G\alpha_q$ pathway negatively regulated by $G\alpha_o$ (Willson et al., 2004), therefore, a loss of functional $G\alpha_q$ (encoded by the *egl-30* gene) would be predicted to prevent or reduce emodepside-stimulated muscle paralysis, whereas a loss of functional $G\alpha_o$ or DGK-1 would be predicted to promote emodepside activity. To investigate this, four *C. elegans* mutant strains were assayed using the EPG technique for pharyngeal emodepside sensitivity: *egl-30 (ad806)* reduction-in-function, *egl-30 (tg26)* gain-of-function, *goa-1 (n1134)* loss-of-function, and *dgk-1* (*nu62*) loss-of-function.

The $G\alpha_q$ pathway generates IP3 as a by-product of PIP2 cleavage, and the only known action of IP3 is to induce calcium (Ca^{2+}) release from intracellular stores via activation of IP3 receptors (Berridge, 1993). The *C. elegans* IP3 receptors, all encoded by the *itr-1* gene, are Ca^{2+} release channels localized to the endoplasmic reticulum (ER) and strongly expressed in the pharynx (Baylis et al., 1999). IP3 receptor activation opens the channel, allowing Ca^{2+} efflux from the ER to the cytoplasm. These Ca^{2+} ions can then bind to neighbouring IP3 receptors to facilitate further Ca^{2+} release, a positive-feedback process called Ca^{2+}-induced Ca^{2+} release (Bezprozvanny et al., 1991). In *C. elegans*, the IP3 signaling pathway involving the IP3 receptor ITR-1 is required for the stimulation of pharyngeal pumping in response to food (Walker et al., 2002). The *itr-1 (sa73)* reduction-

in-function mutant demonstrates a significantly reduced rate of pumping in the presence of food (Walker et al., 2002). The results shown in chapter 3 and 4 suggest that emodepside can inhibit the stimulation of pharyngeal pumping in response to exogenous 5-HT application, with such stimulation interpreted as analogous to the response to food (Walker et al., 2002). These results, coupled with previous research showing that emodepside operates via the $G\alpha_q$ pathway that generates IP3 (Willson et al., 2004), suggests the possibility that emodepside action targets the IP3/ITR-1 pathway. If this was true, emodepside might be predicted to inhibit IP3 signaling to reduce pharyngeal pumping rate, possibly by disrupting the $G\alpha_q$ pathway upstream of IP3, or by inhibiting the ITR-1 receptor itself. To investigate whether a loss-of-function in *itr-1* affects the potency of emodepside, the *itr-1 (sa73)* reduction-of-function mutant pharynx was assayed using the EPG technique for emodepside sensitivity in comparison with wild type *C. elegans*. The results of this investigation are shown in this chapter.

In a screen of *C. elegans* subjected to chemical mutagenesis, Amliwala (2005) identified five strains resistant to locomotory paralysis by 1 μM emodepside whose mutations map (by snip-SNP mapping) closely to the *slo-1* locus. Supporting these findings, the *slo-1 (js379)* null *C. elegans* was found to be resistant to emodepside-stimulated locomotory paralysis, suggesting a role for the SLO-1 channel in the mechanism of action for this novel anthelmintic at the body wall muscle NMJ (Amliwala, 2005).

Expression of *slo-1* in the *C. elegans* nervous system including the pharyngeal neurons (Wang et al., 2001), suggests that the channel may have a role in the pharyngeal paralysis caused by emodepside as well as the inhibition of locomotion previously demonstrated (Amliwala, 2005; Guest et al., 2007). The importance of the SLO-1 channel in the mechanism of emodepside-stimulated pharyngeal paralysis was investigated in this project using the *slo-1 (js379)* putative null *C. elegans* and two gain-of-function mutants: *slo-1 (ky399)* and *slo-1 (ky389)*. The results of these experiments are shown in this chapter.

The SLO-2 channel was also investigated for a role in emodepside activity in the pharynx because it has an expression pattern closely overlapping that of *slo-1*, suggesting that the two channels may be involved in the same physiological processes including the regulation of cellular excitability (Yuan et al., 2000). SLO-2 is a high-conductance

potassium channel, and can be activated by voltage, as well as both calcium and chloride, but not calcium or chloride independently (Yuan et al., 2000). Using a GFP fusion construct, the *slo-2* gene has been shown to be widely expressed in *C. elegans*, including the nervous system, pharyngeal-intestinal valve muscles, and possibly the pharyngeal muscles (Yuan et al., 2000). A role for SLO-2 in the mechanism of action for emodepside in the pharynx was investigated using the *slo-2 (nf101)* loss-of-function mutant, and the results are shown in this chapter.

The results shown in chapter 3 demonstrate that the novel anthelmintics emodepside, verticilide, PF1022-222 and PF1022-888 all inhibit pharyngeal pumping in wild type *C. elegans*, although the potency of the four compounds differs. As all four compounds are derived from the same precursor molecule (PF1022A), it is possible that they share some or all of the proteins involved in their mechanisms of action in the pharynx. To investigate this possibility, the *lat-1 (ok1465)* loss-of-function mutant and the *slo-1 (js379)* null mutant were assayed for their sensitivity to verticilide, PF1022-222 and PF1022-888. The results of these experiments are shown in this chapter.

5.2 Effect of emodepside on thrashing behaviour in *lat-1 (ok1465)* loss-of-function *C. elegans*

RNAi directed against *lat-1* expression in wild type *C. elegans* has been previously shown to reduce the sensitivity of *C. elegans* to emodepside-induced locomotory paralysis (Amliwala, 2005). However, the availability of a *lat-1 (ok1465)* putative null *C. elegans* shortly after completion of these previous RNAi investigations provided an excellent opportunity to support the findings of the RNAi work, facilitating a more definite conclusion regarding the contribution of LAT-1 to the mechanism of action for emodepside to be made.

The *lat-1 (ok1465)* strain (VC965) contains a 2209 base pair in-frame deletion in the *lat-1* gene that removes exons 3, 4 and 5 and inserts an AT. This is predicted to encode a truncated protein lacking the first transmembrane domain as well as the G protein-coupled receptor proteolytic site domain and is likely to result in loss of LAT-1 function. Due to a larval arrest phenotype, *lat-1(ok1465)* is balanced by *mIn-1* (Edgley & Riddle 2001), which is an inverted sequence that prevents recombination in this region and contains *dpy-10* (a recessive mutation resulting in a dumpy appearance) and *gfp* (encoding green fluorescent protein (GFP), driven by a pharyngeal muscle promoter). Heterozygous *ok1465 C. elegans* have weak pharyngeal GFP expression and a non-dumpy phenotype, whereas homozygous *ok1465* worms exhibit no GFP expression or dumpy phenotype, and *C. elegans* not carrying *ok1465* have strong GFP expression and a dumpy phenotype. Approximately 99% of the homozygous *lat-1(ok1465)* worms demonstrated developmental arrest at L1, however, 1% of the worms developed normally to adulthood and a stable line was generated from these animals (strain XA3726) (Guest et al., 2007). The XA3726 strain was used in this investigation.

lat-1 (ok1465) C. elegans were assayed for sensitivity to 10μM emodepside by examining thrashing behaviour for 60 minutes following commencement of drug exposure. The inhibition of thrashing behaviour by emodepside in the wild type and *lat-1 (ok1465) C. elegans* was not found to be significantly different during the time-course of the assay (see figure 5.1). Exposure to 10μM emodepside for 60 minutes reduced wild type thrashing by 97% and *lat-1 (ok1465)* thrashing by 94%.

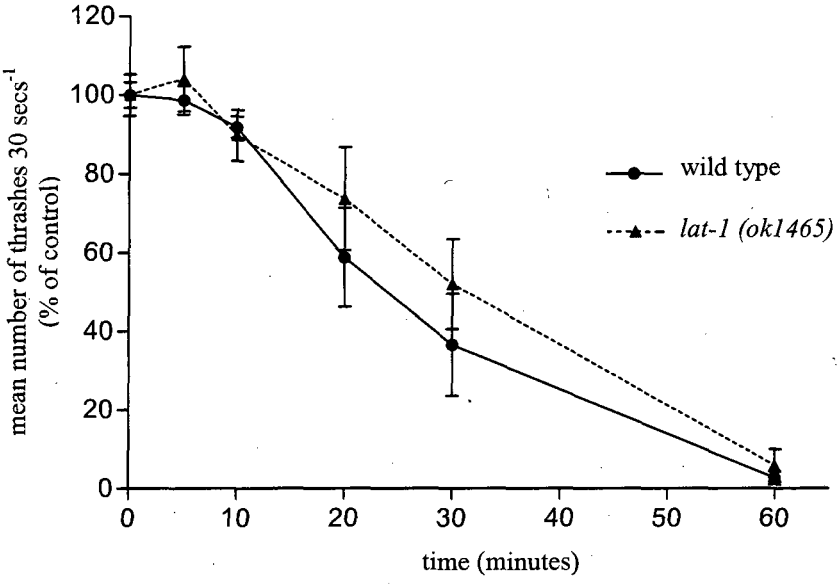

Figure 5.1 The effect of emodepside on the thrashing behaviour of wild type and *lat-1 (ok1465) C. elegans*.
Each datum point is the mean ± S.E.Mean of (n) *C. elegans*, where (n) is 5 (wild type) and 6 (*lat-1*). Emodepside was added after the first count of thrashing behaviour at 0 minutes. 'Mean number of thrashes 30 $secs^{-1}$ (% of control)' is the thrashing rate at each time point as a percentage of the thrashing rate of the same worm strain at the beginning of the assay (0 minutes, when exposed to only Dent's saline).

These results appear to contradict the results of the earlier *lat-1* RNAi experiments performed by Amliwala (2005). Therefore, to verify the results of the previous work, the *lat-1* RNAi assay was repeated and the effect of emodepside on thrashing behaviour was examined.

5.3 The effect of *lat-1* RNAi on the emodepside sensitivity of *C. elegans* thrashing behaviour

RNA interference (RNAi) by bacteria feeding was used to reduce functional expression of *lat-1* in *rrf-3 (pk1426) C. elegans*. Briefly, HT115 (DE3) *E. coli* were transformed with a L4440 plasmid vector containing a portion of the *lat-1* sequence, and successfully transformed bacteria were fed on by *rrf-3(pk1426)* worms, leading to expression of *lat-1* double-stranded RNA (dsRNA) in the worms and predicted interference in the transcription of the *lat-1* (for a detailed method description see chapter 2, section 2.6.1, page 63).

As the RNAi investigation was performed on RNAi sensitive *rrf-3 (pk1426) C. elegans*, it was initially important to rule out any independent effect of the *rrf-3* mutation on the emodepside sensitivity of locomotion in these worms compared to wild type *C. elegans*. To assess this, a thrashing assay was performed in which both worm strains were exposed to 10μM emodepside and their thrashing behaviour analysed at regular intervals for the following 60 minutes. As a control, both *C. elegans* strains were exposed to the vehicle ethanol (0.1%). Thrashing behaviour of wild type and *rrf-3 (pk1426) C. elegans* at each time point after exposure to emodepside or ethanol began, was expressed as a percentage of the mean thrashing rate by the same worm strain at the beginning of the assay (when exposed to only Dent's saline).

There was no significant difference between the inhibition of wild type and *rrf-3 (pk1426) C. elegans* thrashing behaviour by emodepside at any of the analysis time points during the 60 minute assay (see figure 5.2 (a)). Therefore, the *rrf-3* mutation does not appear to affect the emodepside sensitivity of *C. elegans* thrashing behaviour, and consequently, any effects of RNAi directed against functional *lat-1* expression cannot be attributed to the use of *rrf-3 (pk1426) C. elegans* instead of wild type worms.

The effect of emodepside on locomotion in RNAi-treated *C. elegans* was analysed by the thrashing assay used previously. Control worms were *rrf-3 (pk1426) C. elegans* fed on bacteria transformed with the L4440 vector but with no *lat-1* gene insert. Both the RNAi-treated and control vector-fed *C. elegans* were either exposed to 10μM emodepside or the

vehicle ethanol at 0.1%, and their thrashing behaviour assessed a specific time points in the 60 minutes following commencement of emodepside exposure. Thrashing behaviour at each time point was expressed as a percentage of the mean thrashing rate of the same worm strain at the beginning of the assay (when exposed to only Dent's saline).

An emodepside concentration of 10μM paralysed the control vector-fed *rrf-3 (pk1426) C. elegans*, with a 77% inhibition in body bends after 60 minutes exposure to the drug (see figure 5.2 (b)). However, RNAi for the latrophilin-like receptors resulted in a loss of emodepside-sensitivity in the worms, with only an 11% inhibition of body bends after 60 minutes exposure to emodepside. A significant difference in the thrashing rate between the control vector-fed *C. elegans* and RNAi-treated worms was observed after 20 minutes of emodepside exposure ($P<0.001$).

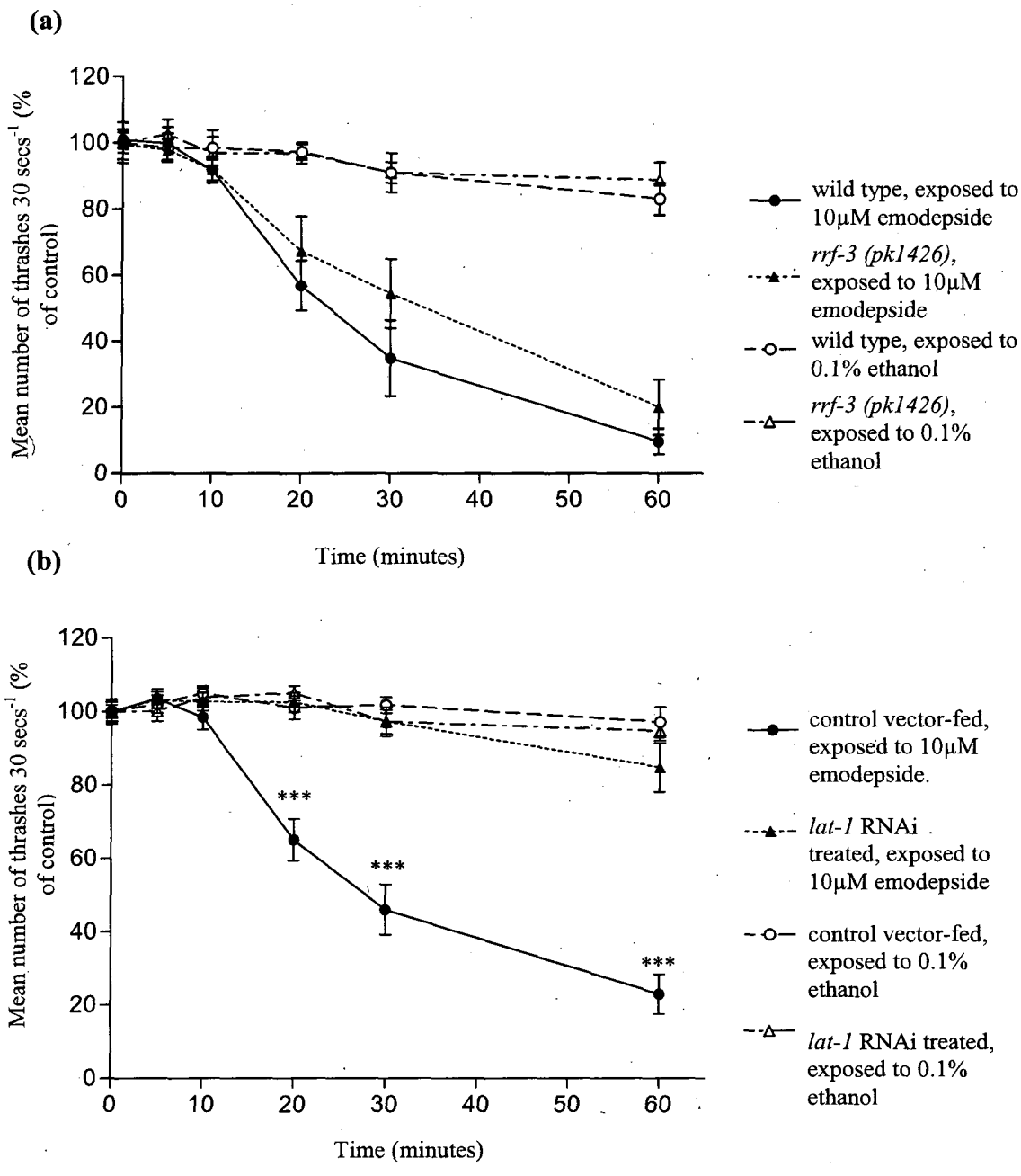

Figure 5.2 Investigating the role of *lat-1* in the mechanism by which emodepside inhibits *C. elegans* thrashing behaviour using RNAi.

(a) Graph comparing the effect of 10μM emodepside on the thrashing behaviour of wild type and *rrf-3 (pk1426) C. elegans*. Each datum point is the mean ± S.E.Mean of 8 *C. elegans*. 'Mean number of thrashes 30 secs^{-1} (% of control)' is the thrashing rate at each time point as a percentage of the thrashing rate of the same worm strain at the beginning of the assay (0 minutes, when exposed to only Dent's saline). **(b)** Graph showing the effect of 10μM emodepside on the thrashing behaviour of *rrf-3 (pk1426) C. elegans* fed on bacteria transformed with either the *lat-1* vector or the control vector. Each datum point is the mean ± S.E.Mean of (n) *C. elegans*, where (n) is: 39 (control vector-fed, exposed to 10μM emodepside), 40 (control vector-fed, exposed to 0.1% ethanol vehicle), 16 (*lat-1* RNAi-treated, exposed to emodepside), 16 (*lat-1* RNAi-treated, exposed to 0.1% ethanol vehicle). 'Mean number of thrashes 30 secs^{-1} (% of control)' is the thrashing rate at each time point as a percentage of the thrashing rate of the same worm strain at the beginning of the assay (0 minutes, when exposed to only Dent's saline). Significance (Student's t-test) relates to a comparison of control vector-fed and *lat-1* RNAi treated *C. elegans* thrashing rate at a specific time point after emodepside exposure began; ***P<0.001.

The results of the repeated RNAi assay agree with the previous findings of Amliwala (2005). However, the reduction in emodepside sensitivity demonstrated by *C. elegans* treated with *lat-1* RNAi was not shown by the *lat-1 (ok1465)* mutants (section 5.2).

5.4 The role of the latrophilins in the emodepside sensitivity of the *C. elegans* pharynx.

To investigate the role of *lat-1* in the mechanism by which emodepside inhibits pharyngeal pumping, the response of the pharynx from the *lat-1 (ok1465)* mutant (strain XA3750) to emodepside application was compared to the wild type response using the electropharyngeogram (EPG) technique.

Previous research has shown that LAT-2 as well as LAT-1 may be involved in the mechanism of action for emodepside (Willson et al., 2004). Therefore, the emodepside sensitivity of the *lat-2 (tm463)* pharynx was investigated using the EPG assay. The *lat-2* allele *tm463* (*C. elegans* strain VC158) has a deletion spanning exon 4 to intron 9 and is predicted to encode a truncated protein consisting of only of the N-terminal lectin C-type domain. The VC158 strain was previously out-crossed five times into the Bristol N2 strain and renamed strain XA3727 (Guest et al., 2007), which was used for the EPG assay.

To investigate the effect of emodepside, 5-HT was applied before and after emodepside exposure to stimulate pumping so that any effect of emodepside on pump rate could be seen. Prior to the assay 'recording' protocol, each pharynx preparation was 'primed' with 500nM 5-HT (see chapter 2, section 2.7.3, page 73) by repeated application of 5-HT for two minutes interspersed with two minutes recovery in Dent's saline until a 5-HT application produced a pump rate within 2% of the previous rate in 5-HT. Following priming, each pharynx preparation was allowed to recover for three minutes in Dent's saline before commencing the recording protocol (in order of application): two minutes 500nM 5-HT, wash (Dent's saline), ten minutes emodepside (at 1nM-1μM, 0.01% DMSO vehicle, no 5-HT), wash (Dent's saline), two minutes 500nM 5-HT. Each change in solution included a wash of the pharyngeal preparation in Dent's saline to remove as much of the remaining drug solution before application of the next. Wild type *C. elegans*

pharynx preparations were assayed at the same time as the mutant strains to enable an accurate comparison of the emodepside sensitivity.

5.4.1 Effect of emodepside on pharyngeal pumping in *lat-1 (ok1465)* loss-of-function *C. elegans*

Emodepside appeared to inhibit *lat-1(ok1465) C. elegans* pharyngeal pumping in response to 5-HT in a concentration-dependent manner (see figure 5.3). However, the *lat-1 (ok1465)* pharynx was less sensitive to the inhibitory effect of emodepside than the wild type pharynx, with a *lat-1 (ok1465)* IC_{50} value of 21nM (95% confidence limits 15 to 29nM) compared to a wild type IC_{50} of 9nM (95% confidence limits 8 to 10nM). Inhibition of the wild type and *lat-1 (ok1465)* pharyngeal response to 5-HT was significantly different when emodepside was applied at 10 to 100nM ($P<0.01$), with the *lat-1 (ok1465)* pharynx always exhibiting reduced anthelmintic sensitivity (see figure 5.3).

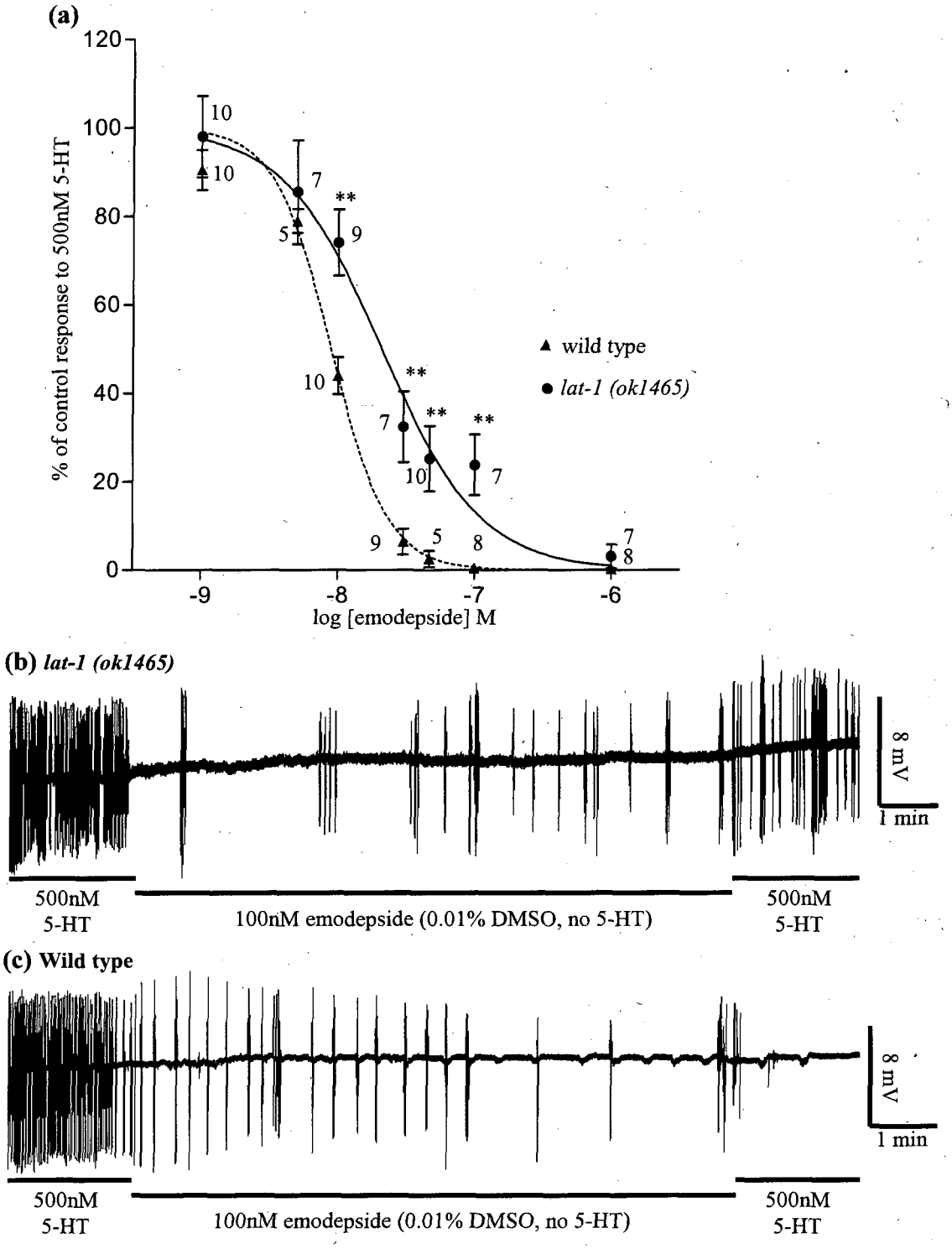

Figure 5.3 The effect of emodepside on the response of the *lat-1 (ok1465)* pharynx to 500nM 5-HT. **(a)** Concentration response curve comparing the effect of emodepside on the response of the wild type and *lat-1 (ok1465)* pharynx to 500nM 5-HT. '% control response to 500nM 5-HT' is the pharyngeal response to 5-HT after emodepside exposure as a % of the response before application of the drug. Each datum point is the mean ± S.E.Mean of (n) pharynx preparations. Significance (Student's t-test) relates to a comparison of wild type and *lat-1* response to 500nM 5-HT following exposure to each emodepside concentration tested, **P<0.01, n numbers given beside each datum point. The curves were fitted using the nonlinear regression four-parameter logistic equation described in chapter 2, section 2.10. **(b-c)** Example EPG recordings from (b) a *lat-1 (ok1465)* pharynx, and (c) a wild type pharynx. Notice that the *lat-1* pharynx, but not the wild type pharynx, pumps in 5-HT following emodepside exposure, though at a lower rate than prior to drug application.

5.4.2 Effect of emodepside on pharyngeal pumping in *lat-2 (tm463)* loss-of-function *C. elegans*

Emodepside appeared to inhibit *lat-2(tm463) C. elegans* pharyngeal pumping in response to 500nM 5-HT in a concentration-dependent manner not significantly different to the wild type *C. elegans* response (see figure 5.4). Consequently, the IC_{50} values of the two worm strains are similar, with a *lat-2 (tm463)* IC_{50} of 10nM (95% confidence limits 8 to 12nM) and a wild type IC_{50} of 8nM (95% confidence limits 8 to 10nM).

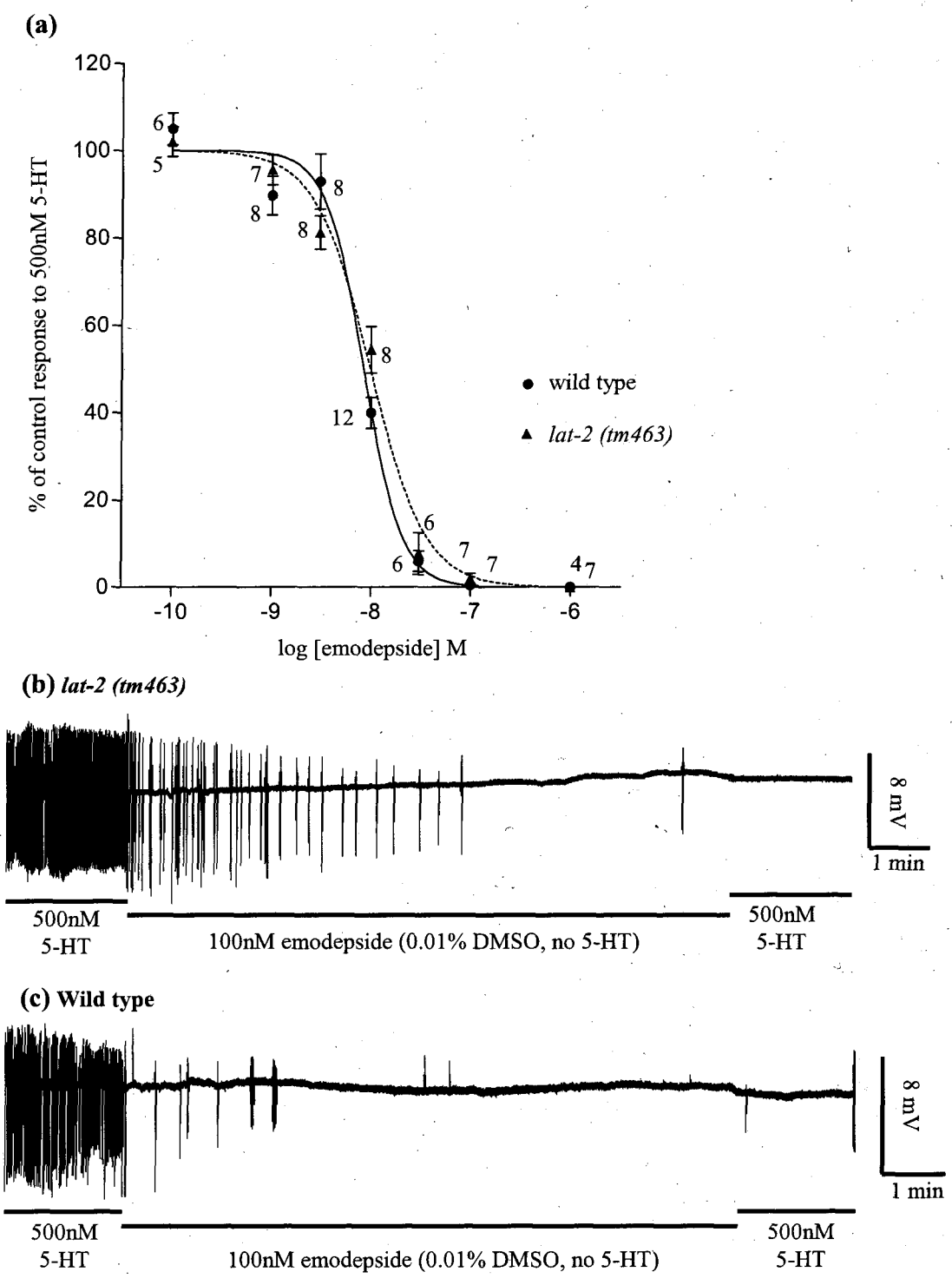

Figure 5.4 The effect of emodepside on *lat-2(tm463) C. elegans* pharyngeal response to 500nM 5-HT. **(a)** Concentration response curve comparing the effect of emodepside on the response of the wild type and *lat-2 (tm463)* pharynx to 500nM 5-HT. '% control response to 500nM 5-HT' is the pharyngeal response to 5-HT after emodepside exposure as a % of the response before application of the drug. Each datum point is the mean ± S.E.Mean of (n) pharynx preparations. n numbers are given beside each datum point. To clarify, n numbers at 1μM emodepside: 4 (*lat-2*), 7 (wild type). Curves were fitted using the nonlinear regression four-parameter logistic equation described in chapter 2, section 2.10. Solid curve: wild type. Dotted curve: *lat-2*. **(b-c)** Example EPG recordings showing the effect of 100nM emodepside on the response to 5-HT by (b) the *lat-2(tm463)* pharynx, and (c) wild type pharynx.

5.4.3 Effect of emodepside on pharyngeal pumping in *lat-1 (ok1465); lat-2 (tm463)* double loss-of-function *C. elegans*

The wild type response of the *lat-2 (tm463)* pharynx to emodepside suggests that LAT-2 in isolation does not have a significant role in the mechanism of action for emodepside at the pharyngeal neuromuscular junction. However, it is possible that the function of LAT-2 may be compensated for in the null mutant by the activity of LAT-1. Therefore, the *lat-1(ok1465); lat-2(tm463)* double loss-of-function mutant (strain XA3749; Guest et al., 2007), was assayed for the effect of emodepside on the pharyngeal response to 500nM 5-HT. The recording protocol, 5-HT 'priming' procedure, and data analysis were as described in section 5.4.

Emodepside appeared to inhibit *lat-1(ok1465); lat-2 (tm463) C. elegans* pharyngeal pumping in response to 5-HT in a concentration-dependent manner (see figure 5.5). However, the *lat-1 (ok1465); lat-2 (tm463)* pharynx was less sensitive to the inhibitory effect of emodepside than the wild type pharynx, with an IC_{50} value of 25nM (95% confidence limits 17 to 37nM) for the double mutant, compared to a wild type IC_{50} of 11nM (95% confidence limits 10 to 13nM). Inhibition of the wild type and *lat-1 (ok1465); lat-2 (tm463)* pharyngeal response to 5-HT was significantly different only when emodepside was applied at 30nM ($P<0.05$), with the pharynx of the double mutant exhibiting reduced anthelmintic sensitivity (see figure 5.5).

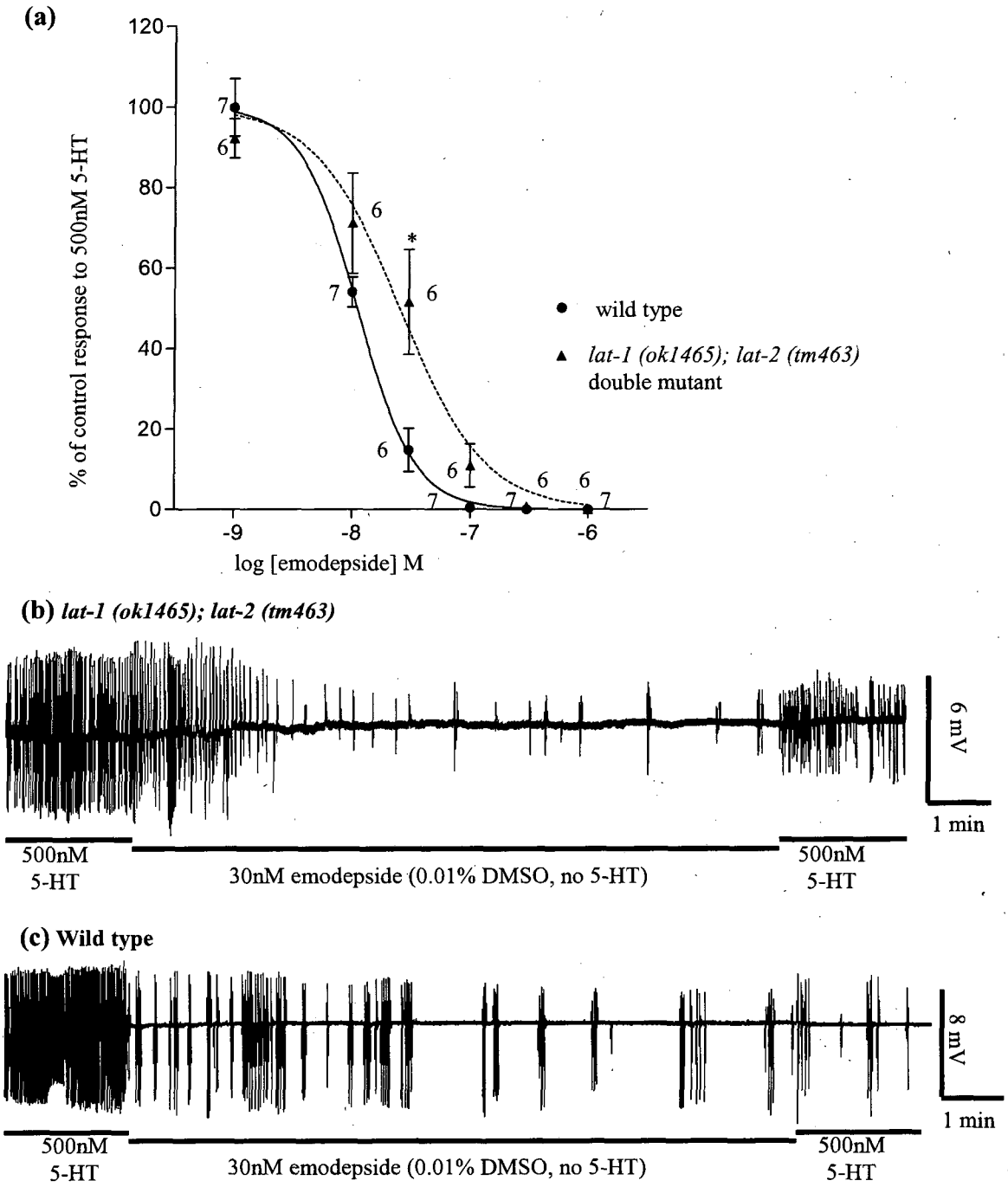

Figure 5.5 The effect of emodepside on the response of the *lat-1 (ok1465); lat-2 (tm463)* pharynx to 500nM 5-HT. (a) Concentration response curve comparing the effect of emodepside on the response of the wild type and *lat-1 (ok1465); lat-2 (tm463)* pharynx to 500nM 5-HT. '% control response to 500nM 5-HT' is the pharyngeal response to 5-HT after emodepside exposure as a % of the response before application of the drug. Each datum point is the mean ± S.E.Mean of (n) pharynx preparations. Significance (Student's t-test) relates to a comparison of wild type and *lat-1; lat-2* response to 500nM 5-HT following exposure to each emodepside concentration tested, *P<0.05, n numbers given beside each datum point. To clarify, n numbers at an emodepside concentration of 300nM: 7 (wild type), 6 (*lat-1; lat-2*), and at 1μM: 7 (wild type), 6 (*lat-1; lat-2*). Curves were fitted using the nonlinear regression four-parameter logistic equation described in chapter 2, section 2.10. **(b-c)** Example EPG recordings from (b) a *lat-1 (ok1465); lat-2 (tm463)* pharynx, and (c) a wild type pharynx. Comparing the pharyngeal pumping rate of each pharynx in 5-HT before and after emodepside exposure shows that the mutant pharynx in (b) is not inhibited to the same extent as the wild type pharynx in (c).

5.5 The effect of emodepside on pharyngeal pumping in *C. elegans ptp-3 (op147)* loss-of-function *C. elegans*.

To identify if PTP-3 has a role in the mechanism of action for emodepside in the pharynx, the strong PTP-3 loss-of-function mutant *C. elegans ptp-3 (op147)* (strain CZ540, obtained previously out-crossed ten times) was assayed for emodepside sensitivity using the EPG technique. The *op147* allele is a transposon insertion in the phosphatase domain present in PTP-3a and PTP-3b, which is predicted to disrupt catalytic activity of the protein (Harrington et al, 2002).

The 5-HT 'priming' procedure and the recording protocol used to compare the emodepside sensitivity of wild type *C. elegans* and the *ptp-3 (op147)* mutant was identical to that described in section 5.4, as was the method of data analysis.

Emodepside appeared to inhibit *ptp-3 (op147)* pharyngeal pumping in response to 5-HT in a concentration-dependent manner not significantly different to that observed in the wild type pharynx (see figure 5.6 (a)). The IC_{50} value for both the wild type and *ptp-3 (op147) C. elegans* was 12nM (95% confidence limits: 8 to 18nM for the wild type, 9 to 16nM for the mutant).

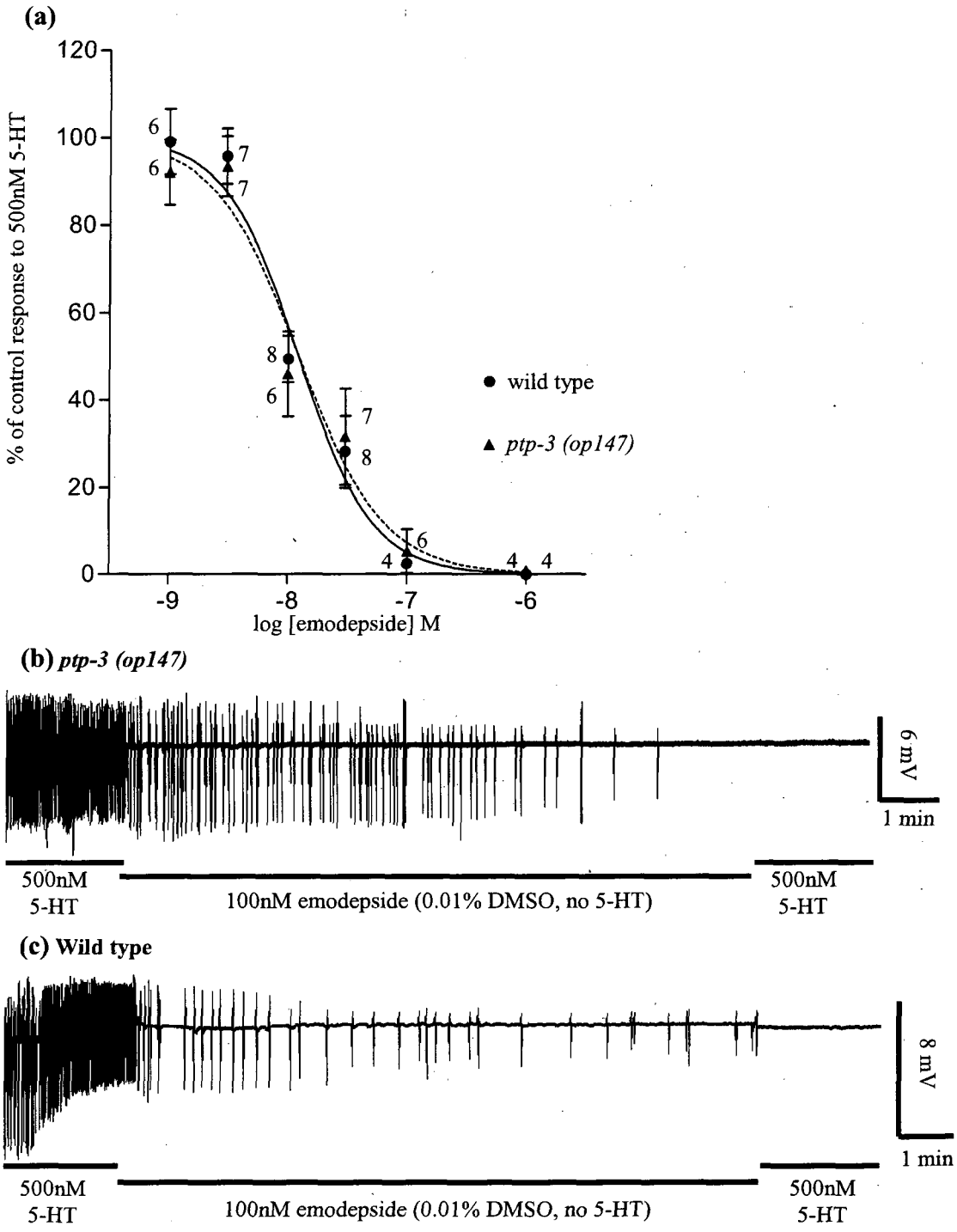

Figure 5.6 The effect of emodepside on the response of the *ptp-3 (op147)* pharynx to 500nM 5-HT. **(a)** Concentration response curve comparing the effect of emodepside on the response of the wild type and *ptp-3 (op147)* pharynx to 500nM 5-HT. '% control response to 500nM 5-HT' is the pharyngeal response to 5-HT after emodepside exposure as a % of the response before application of the drug. Each datum point is the mean ± S.E.Mean of (n) pharynx preparations. n numbers given beside each datum point. To clarify, n numbers at an emodepside concentration of 100nM: 4 (wild type), 6 (*ptp-3*) Curves were fitted using the nonlinear regression four-parameter logistic equation described in chapter 2, section 2.10. Solid curve: wild type. Dotted curve: *ptp-3*. **(b-c)** Example EPG recordings from (b) a *ptp-3* pharynx, and (c) a wild type pharynx. Notice that wild type and *ptp-3* pharyngeal pumping in 500nM 5-HT is completely inhibited by exposure to 100nM emodepside for 10 minutes.

5.6 The role of the $G\alpha_q$ signaling pathway in the emodepside sensitivity of the *C. elegans* pharynx

The results from section 5.4.1 suggest that *C. elegans* LAT-1 has a functional role in the mechanism of action for emodepside at the pharyngeal neuromuscular junction. LAT-1 is a G protein-coupled receptor (Krasnoperov et al., 1997; Lelianova et al., 1997), which couples with $G\alpha_q$ (Rahman et al., 1999). This suggests that emodepside may mediate neurotransmitter release by regulating the $G\alpha_q$ pathway via binding to the LAT-1 receptor. $G\alpha_q$ itself is found in the nervous system and the pharyngeal muscle of adult *C. elegans* (Bastiani et al., 2003), and therefore, the protein is in the appropriate location to function in emodepside-mediated paralysis of pharyngeal pumping. To investigate the role of $G\alpha_q$ in the mechanism of action for emodepside in the pharynx, the sensitivity of two $G\alpha_q$ mutants to emodepside was assayed using the EPG technique. An *egl-30* loss-of-function strain cannot be used because such mutants are subviable and arrest early in development, precluding analysis of adult pharyngeal pumping (Brundage et al., 1996). Therefore, the *egl-30 (ad806)* reduction-of-function strain was used because these worms can develop to adulthood and posses only a mild phenotype, including moderate bloating with eggs, and slow atypical locomotion (Brundage et al., 1996). The *ad806* allele contains a point mutation that converts a highly conserved serine residue to phenylalanine, and is predicted to disrupt the association of $G\alpha_q$ with the Gβ and Gγ subunits crucial for G protein functioning (Lambright et al., 1996).

The *egl-30 (tg26)* gain-of-function mutant was also assayed for pharyngeal emodepside sensitivity using the EPG assay. The *tg26* allele is a missense point mutation at highly conserved arginine residue required for inactivation of the $G\alpha_q$ protein (Doi & Iwasaki, 2002; Natochin & Artemyev, 2003). The α-subunit of heterotrimeric G proteins functions as a molecular switch, alternating between an active state when bound to guanosine 5'-triphosphate (GTP), and an inactive state when bound to guanosine 5'-diphosphate (GDP) and associated with the β and γ subunits. G protein inactivation is controlled by regulators of G protein signaling (RGS), which bind to activated Gα subunits and facilitate GTP hydrolysis to GDP (Berman & Gilman, 1998; Ross & Wilkie, 2000). The mutation in the *tg26* allele is thought to uncouple Gα from the RGS protein, inhibiting inactivation of Gα, and resulting in a gain-of-function phenotype (Natochin & Artemyev, 2003).

As $G\alpha_o$ as been shown to act as a negative regulator of the $G\alpha_q$ pathway, the role of the $G\alpha_o$ protein in the mechanism of action for emodepside in the pharynx was investigated using the *goa-1 (n1134)* loss-of-function mutant. The *n1134* allele contains a missense point mutation in codon 1 of the *goa-1* gene, which produces truncation of four amino acids at the NH_2-terminal of $G\alpha_o$ that results in an inability of the protein to associate with the Gβ and Gγ subunits and a consequent loss of $G\alpha_o$ function (Segalat et al., 1995).

The possibility that emodepside targets the $G\alpha_q$ pathway via the IP3 receptor was investigated by assaying the emodepside sensitivity of the 5-HT response of the *itr-1 (sa73)* mutant pharynx. The *itr-1 (sa73)* allele is a cytosine to tyrosine (wild type to mutant) substitution in the open reading frame at residue 1525, located in the central modulatory region of the protein and adjacent to the Ca^{2+} binding site. The *sa73* allele is thought to disrupt Ca^{2+} binding to ITR-1, and thereby affect the positive-feedback mechanism that facilitates Ca^{2+} release upon initial activation of ITR-1 receptors, which is important for the stimulation of pharyngeal pumping in response to food (Dal Santo et al., 1999).

To investigate if emodepside targets neurotransmitter release via the negative regulator of the $G\alpha_q$ pathway DGK-1, the *dgk-1 (nu62)* mutant pharyngeal response to 5-HT was also assayed for emodepside sensitivity. The *dgk-1 (nu62)* allele is a cytosine to tyrosine (wild type to mutant) substitution in the coding exon, resulting in a stop codon at amino acid 167, and premature truncation of the *dgk-1* protein, producing a predicted *dgk-1* null mutant (Jose & Koelle, 2005; Nurrish et al., 1999).

The 5-HT 'priming' procedure, recording protocol and data analysis methods used to compare the emodepside sensitivity of the wild type *C. elegans* pharynx and the pharynxes of the *egl-30 (ad806)*, *egl-30 (tg26)*, *goa-1 (n1143)*, *itr-1 (sa73)* and *dgk-1 (nu62)* mutants were as described in section 5.4.

5.6.1 Effect of emodepside on pharyngeal pumping in $G\alpha_q$ reduction-of-function *egl-30 (ad806) C. elegans*

Emodepside appeared to inhibit *egl-30 (ad806)* pharyngeal pumping response to 5-HT in a concentration-dependent manner (see figure 5.7 (a)). A significant difference between the wild type and *egl-30 (ad806)* response to emodepside exposure was observed when 10nM of the anthelmintic was applied, with the *egl-30 (ad806)* pharynx demonstrating marginally increased sensitivity. No significant difference between the mutant and wild type emodepside sensitivity was observed when 1nM and 100nM of the anthelmintic was applied. The IC_{50} value for *egl-30 (ad806)* was 8nM (95% confidence limits 6 to 10nM), and the wild type IC_{50} was 11nM (95% confidence limits 9 to 13nM).

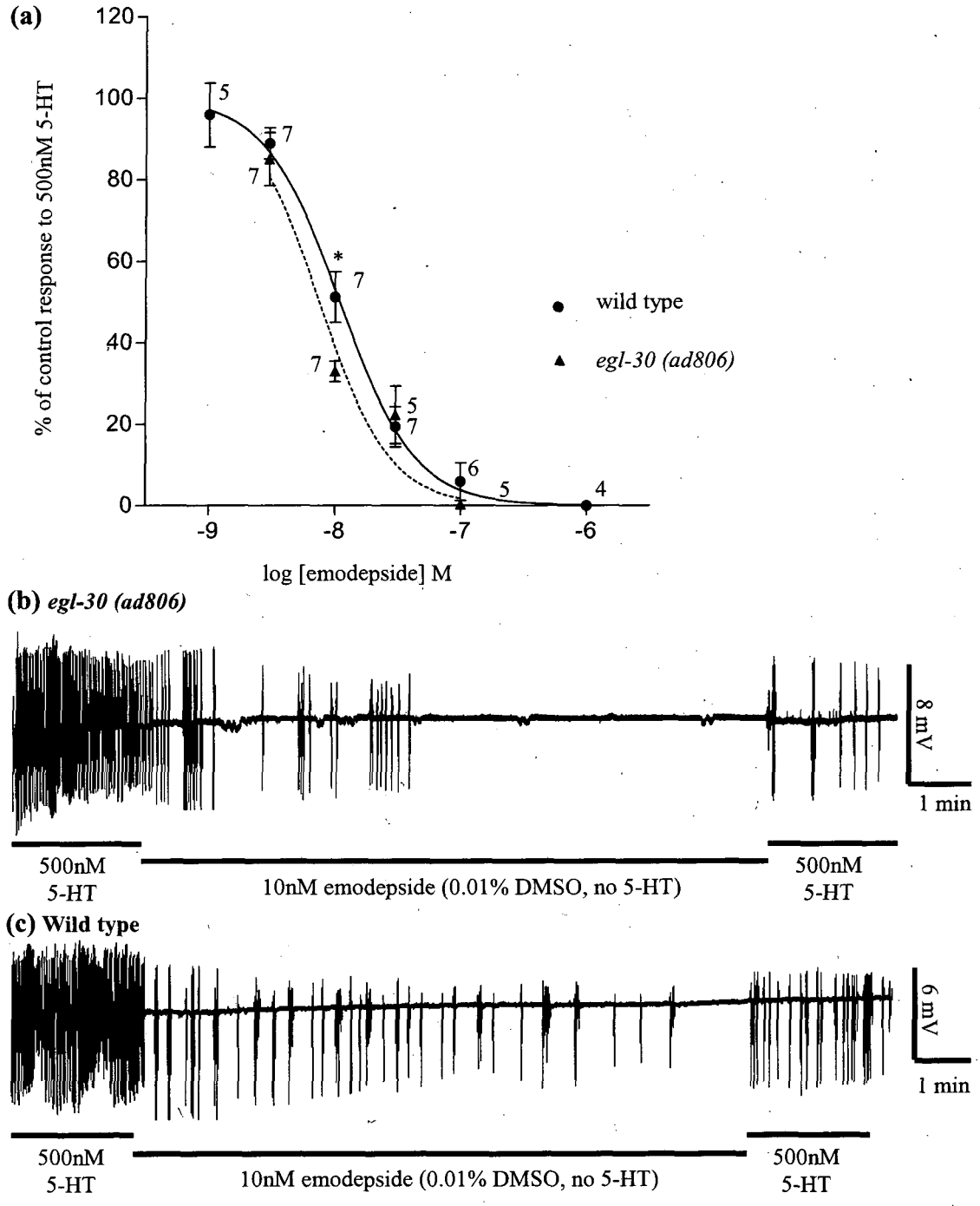

Figure 5.7 The effect of emodepside on the response of the *egl-30 (ad806)* pharynx to 500nM 5-HT. **(a)** Concentration response curve comparing the effect of emodepside on the response of the wild type and *egl-30 (ad806)* pharynx to 500nM 5-HT. '% control response to 500nM 5-HT' is the pharyngeal response to 5-HT after emodepside exposure as a % of the response before application of the drug. Each datum point is the mean ± S.E.Mean of (n) pharynx preparations. Significance (Student's t-test) relates to a comparison of wild type and *egl-30* response to 500nM 5-HT following exposure to each emodepside concentration tested, *P<0.05, n numbers given beside each datum point. To clarify, n numbers at 30nM emodepside: 7 (wild type), 5 (*egl-30*), and at 100nM: 6 (wild type), 5 (*egl-30*). Curves were fitted using the nonlinear regression four-parameter logistic equation described in chapter 2, section 2.10. Dotted curve: *egl-30*. Solid curve: wild type. **(b-c)** Example EPG recordings from (b) an *egl-30* pharynx, and (c) a wild type pharynx. Comparing the pumping rate of each pharynx in 5-HT before and after emodepside exposure shows that the mutant pharynx in (b) is inhibited to a greater extent than the wild type pharynx in (c).

5.6.2 Effect of emodepside on pharyngeal pumping in $G\alpha_q$ gain-of-function *egl-30 (tg26) C. elegans*

The response of the *egl-30 (tg26)* pharynx to 5-HT appeared to be inhibited by emodepside in a concentration-dependent manner (see figure 5.8(a)). The *egl-30 (tg26)* response to emodepside was significantly different to that of wild type when 30nM of the anthelmintic was applied, with the mutant demonstrating decreased sensitivity. The IC_{50} value for *egl-30 (tg26)* was 36nM (95% confidence limits 19 to 69nM), and the wild type IC_{50} was 12nM (95% confidence limits 9 to 14nM), suggesting decreased sensitivity of the mutant to the inhibition of the 5-HT response by emodepside.

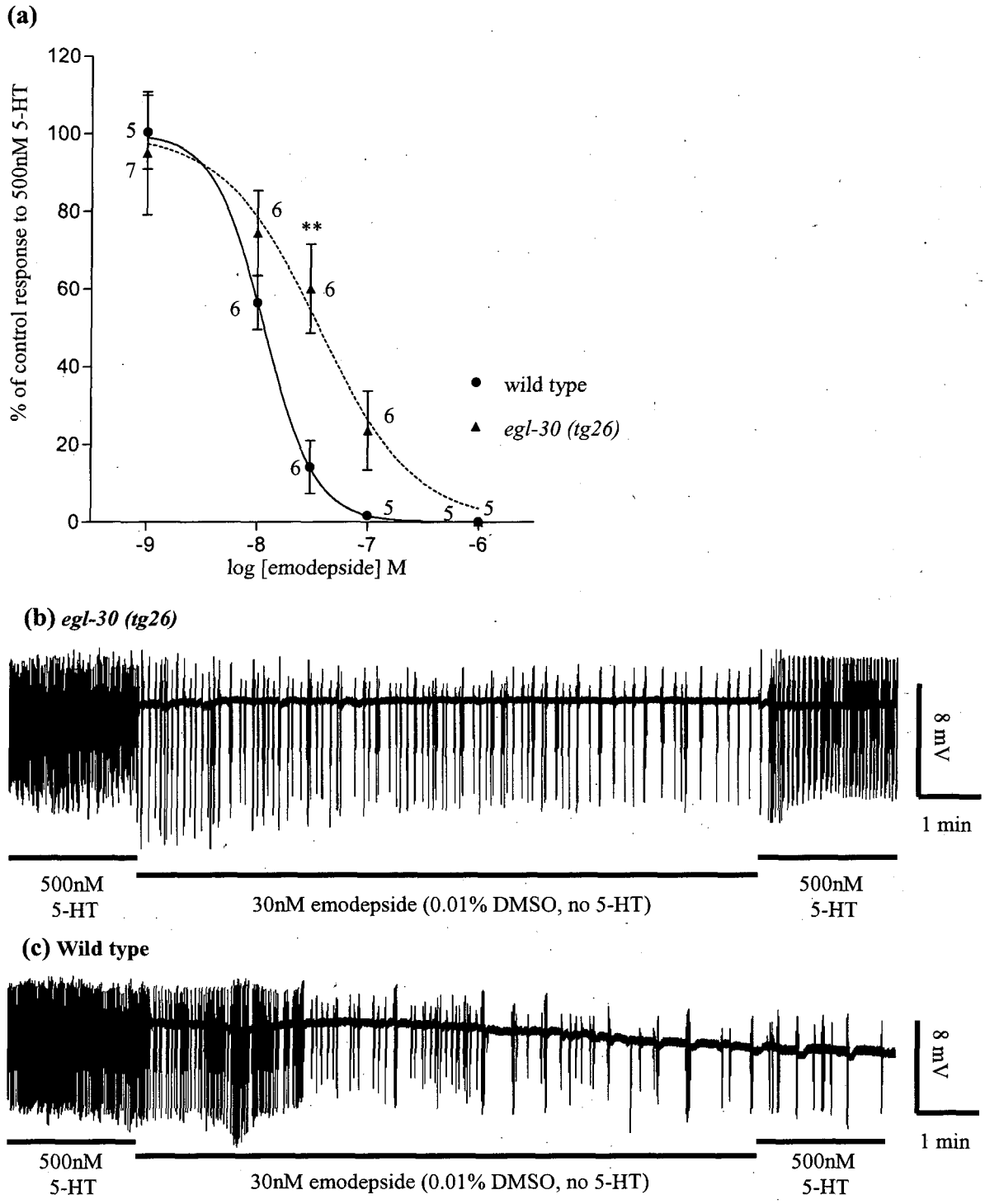

Figure 5.8 The effect of emodepside on the response of the *egl-30 (tg26)* pharynx to 500nM 5-HT.
(a) Concentration response curve comparing the effect of emodepside on the response of the wild type and *egl-30 (tg26)* pharynx to 500nM 5-HT. '% control response to 500nM 5-HT' is the pharyngeal response to 5-HT after emodepside exposure as a % of the response before application of the drug. Each datum point is the mean ± S.E.Mean of (n) pharynx preparations. Significance (Student's t-test) relates to a comparison of wild type and *egl-30* response to 500nM 5-HT following exposure to each emodepside concentration tested, **P<0.01, n numbers given beside each datum point. Curves were fitted using the nonlinear regression four-parameter logistic equation described in chapter 2, section 2.10. **(b-c)** Example EPG recordings from (b) an *egl-30 (tg26)* pharynx, and (c) a wild type pharynx. Comparing the pharyngeal pumping rate of each pharynx in 5-HT before and after emodepside exposure shows that the mutant pharynx in (b) is inhibited to a lesser extent than the wild type pharynx in (c).

5.6.3 Effect of emodepside on pharyngeal pumping in $G\alpha_o$ loss-of-function *goa-1 (n1134) C. elegans*

The response of the *goa-1 (n1134)* pharynx to 5-HT appeared to be inhibited by emodepside in a concentration-dependent manner (see figure 5.9(a)). The *goa-1 (n1134)* response to emodepside was significantly different to that of wild type when 10nM of the anthelmintic was applied, with the mutant demonstrating decreased sensitivity. The IC_{50} value for *egl-30 (tg26)* was 33nM (95% confidence limits 22 to 50nM), and the wild type IC_{50} was 13nM (95% confidence limits 10 to 16nM), suggesting decreased sensitivity of the mutant to the inhibition of the 5-HT response by emodepside.

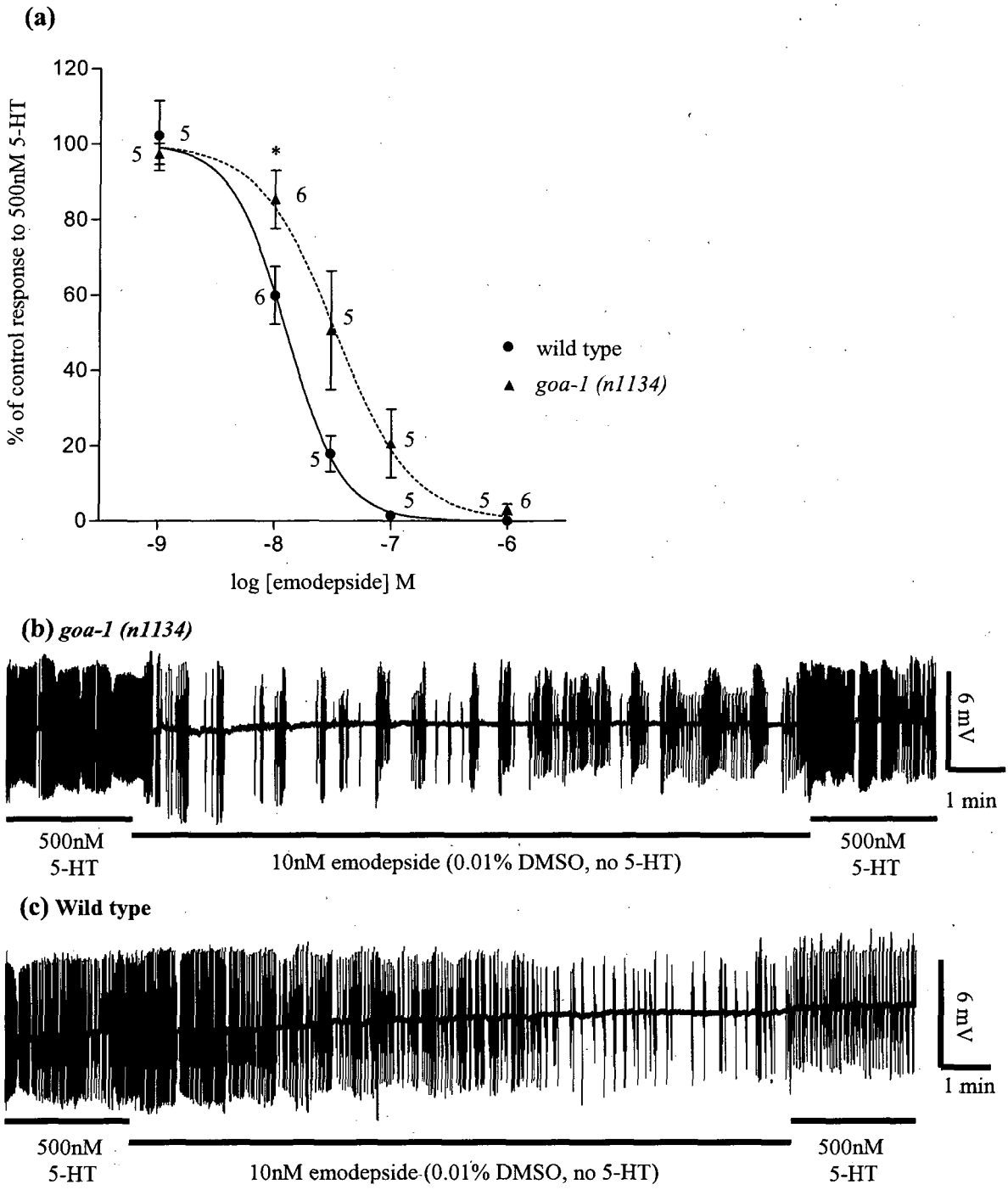

Figure 5.9 The effect of emodepside on the response of the *goa-1 (n1134)* pharynx to 500nM 5-HT. **(a)** Concentration response curve comparing the effect of emodepside on the response of the wild type and *goa-1 (n1134)* pharynx to 500nM 5-HT. '% control response to 500nM 5-HT' is the pharyngeal response to 5-HT after emodepside exposure as a % of the response before application of the drug. Each datum point is the mean ± S.E.Mean of (n) pharynx preparations. Significance (Student's t-test) relates to a comparison of wild type and *goa-1* response to 500nM 5-HT following exposure to each emodepside concentration tested, *P<0.05, n numbers given beside each datum point. To clarify, n numbers at 1μM emodepside: 6 (wild type), 5 (*goa-1*). Curves were fitted using the nonlinear regression four-parameter logistic equation described in chapter 2, section 2.10. **(b-c)** Example EPG recordings from (b) a *goa-1 (n1134)* pharynx, and (c) a wild type pharynx. Comparing the pharyngeal pumping rate of each pharynx in 5-HT before and after emodepside exposure shows that the mutant pharynx in (b) is inhibited to a lesser extent than the wild type pharynx in (c).

5.6.4 Effect of emodepside on pharyngeal pumping in ITR-1 reduction-in-function *itr-1 (sa73) C. elegans*

The response of the *itr-1 (sa73)* pharynx to 5-HT was inhibited by emodepside in a concentration-dependent manner that was not significantly different to the wild type response at any of the emodepside concentrations tested (see figure 5.10). The *itr-1 (sa73)* IC_{50} was 12nM (95% confidence limits 7 to 21nM) compared to the wild type IC_{50} 15nM (95% confidence limits 11 to 21nM).

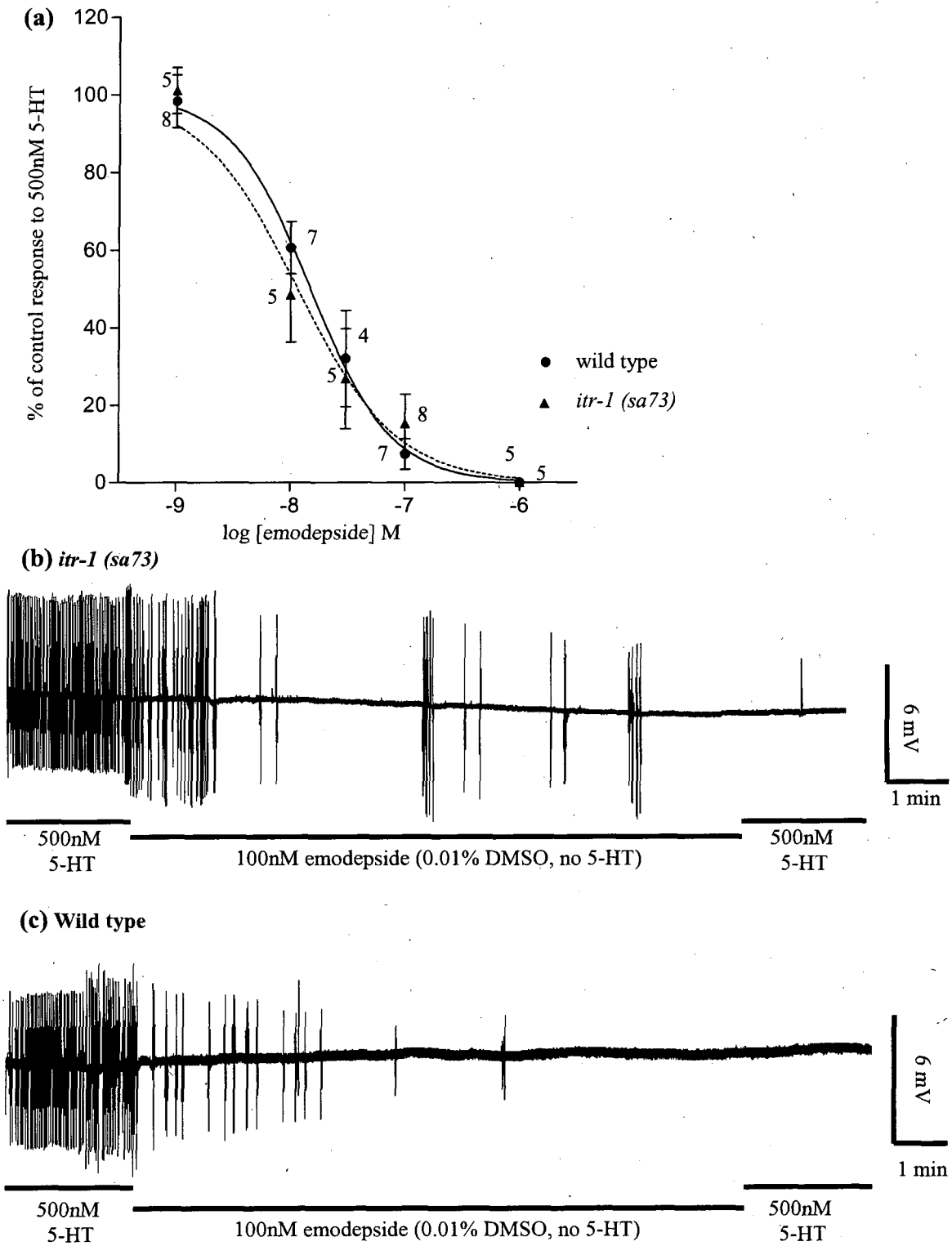

Figure 5.10 The effect of emodepside on the response of the *itr-1 (sa73)* pharynx to 500nM 5-HT. **(a)** Concentration response curve showing the effect of emodepside on the pharyngeal response to 500nM 5-HT in wild type and *itr-1 (sa73) C. elegans*. '% of basal response to 5-HT' is the pharyngeal response to 5-HT after emodepside exposure as a % of the response before application of the drug. Each datum point is the mean ± S.E.Mean of (n) pharynx preparations. n numbers are given beside each datum point. Curves were fitted using the nonlinear regression four-parameter logistic equation described in chapter 2, section 2.10. Solid curve: wild type. Dotted curve: *itr-1*. **(b-c)** Example EPG recordings from (b) an *itr-1* pharynx and (c) a wild type pharynx. Notice that wild type and *itr-1* pharyngeal pumping in 500nM 5-HT is completely inhibited by exposure to 100nM emodepside for 10 minutes.

5.6.5 Effect of emodepside on pharyngeal pumping in DGK-1 loss-of-function *dgk-1 (nu62) C. elegans*

The response of the *dgk-1 (nu62)* pharynx to 5-HT was inhibited by emodepside in a concentration-dependent manner that was not significantly different to the wild type response at any of the emodepside concentrations tested (see figure 5.11). The *dgk-1 (nu62)* IC_{50} was 7nM (95% confidence limits 3 to 13nM) compared to the wild type IC_{50} 7nM (95% confidence limits 5 to 10nM).

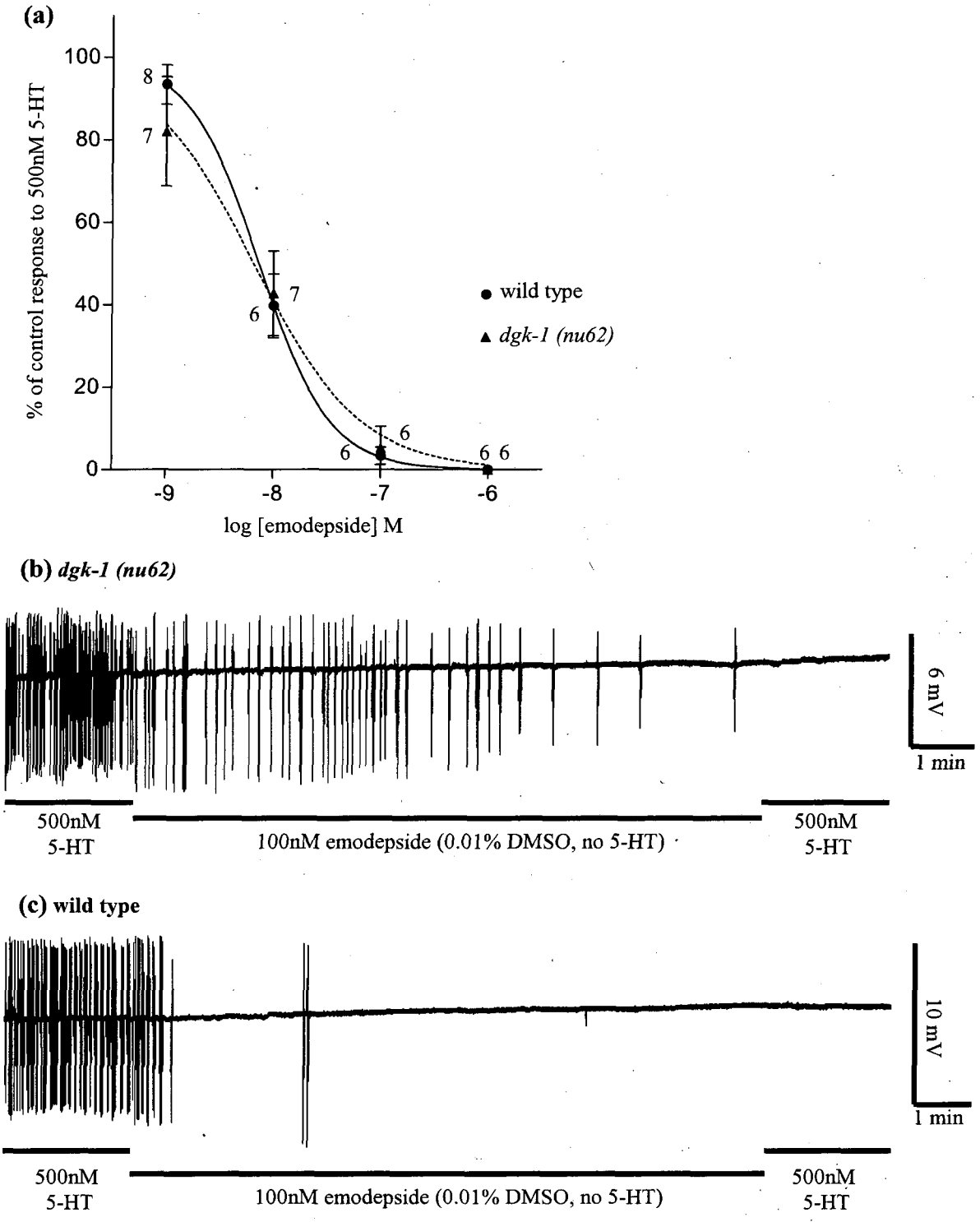

Figure 5.11 The effect of emodepside on the response of the *dgk-1 (nu62)* pharynx to 500nM 5-HT. **(a)** Concentration response curve showing the effect of emodepside on the pharyngeal response to 500nM 5-HT in wild type and *dgk-1 (nu62) C. elegans*. '% of basal response to 5-HT' is the pharyngeal response to 5-HT after emodepside exposure as a % of the response before application of the drug. Each datum point is the mean ± S.E.Mean of (n) pharynx preparations. n numbers are given beside each datum point. To clarify, n numbers at 10nM emodepside: 6 (wild type), 7 (*dgk-1*). Curves were fitted using the nonlinear regression four-parameter logistic equation described in chapter 2, section 2.10. Solid curve: wild type. Dotted curve: *dgk-1*. **(b-c)** Example EPG recordings from (b) a *dgk-1* pharynx and (c) a wild type pharynx. Notice that wild type and *dgk-1* pharyngeal pumping in 500nM 5-HT is completely inhibited by exposure to 100nM emodepside for 10 minutes.

5.7 The role of the SLO-1 and SLO-2 potassium channels in the emodepside sensitivity of the *C. elegans* pharynx

To investigate the role of SLO-1 and SLO-2 in the mechanism of action for emodepside in the pharynx, the *slo-1 (js379)* null mutant, the *slo-1 (ky399)* and *(ky389)* gain-of-function mutants, and the *slo-2 (nf101)* loss-of-function mutant were assayed using the EPG technique, with the recording protocol, 5-HT 'priming' procedure and data analysis the same as described in section 5.4.

The *slo-1 (js379)* mutation is a nonsense lesion early in the gene, corresponding to a protein termination in the fourth transmembrane domain. As the gene lesion occurs prior to the ion-conducting channel pore, this is expected to preclude formation of a functional channel and is therefore a putative null mutation (Wang et al., 2001).

The *slo-1* gain-of-function allele *(ky399)* contains a missense mutation at amino acid 350, which is located in the conserved seventh transmembrane domain of the protein. Amino acid substitutions at an analogous position in other voltage-gated potassium channels have been shown to alter the kinetics of channel activation, deactivation, and recovery from deactivation (Jerng et al., 1999; Lees-Miller et al., 2000). Phenotypically, *slo-1 (ky399)* mutants are aldicarb resistant, suggesting a decrease in acetylcholine release predicted to be due to the increase in SLO-1 activity (Davies et al., 2003). Additionally, the *slo-1 (ky399)* mutants demonstrated an increase in SLO-1-dependent currents as shown in whole cell recordings for CEP neurons, again indicating increased SLO-1 channel activity (Davies et al., 2003).

The *slo-1 (ky389)* allele contains a threonine to isoleucine substitution at amino acid 1001 located in the S10 segment, which is a region that appears important in the Ca^{2+} sensitivity of the mouse Slo channel (Schreiber et al., 1998), and it is predicted to have a similar function in *C. elegans* SLO-1 (Davies et al., 2003). Supporting this, the *slo-1 (ky389)* has been found to possess a depressed locomotion rate and egg laying behaviour, consistent with an increase in SLO-1 activity (Davies et al., 2003).

The *slo-2* allele *nf101* encodes a loss-of-function deletion mutant, where the SLO-2 protein is terminated prematurely at amino acid 489, resulting in a truncated protein

lacking most of the cytoplasmic carboxyl domain, including the predicted chloride and calcium sensing region (Santi et al., 2003). The *nf101* allele is therefore a predicted loss-of-function (Santi et al., 2003).

5.7.1 Effect of emodepside on pharyngeal pumping in *slo-1 (js379)* loss-of-function *C. elegans*

The *slo-1(js379)* mutant demonstrated an extremely high level of resistance to the inhibitory impact of emodepside on pharyngeal pumping, with an IC_{50} greater than 1μM compared to a wild type IC_{50} of 8nM (95% confidence limits 6 to 10nM) (see figure 5.12 (a)). After exposure to 1μM emodepside, pharynx preparations from the *slo-1 (js379)* mutant exhibited only a 12% reduction in response to 5-HT, compared to a 100% reduction for wild type *C. elegans*.

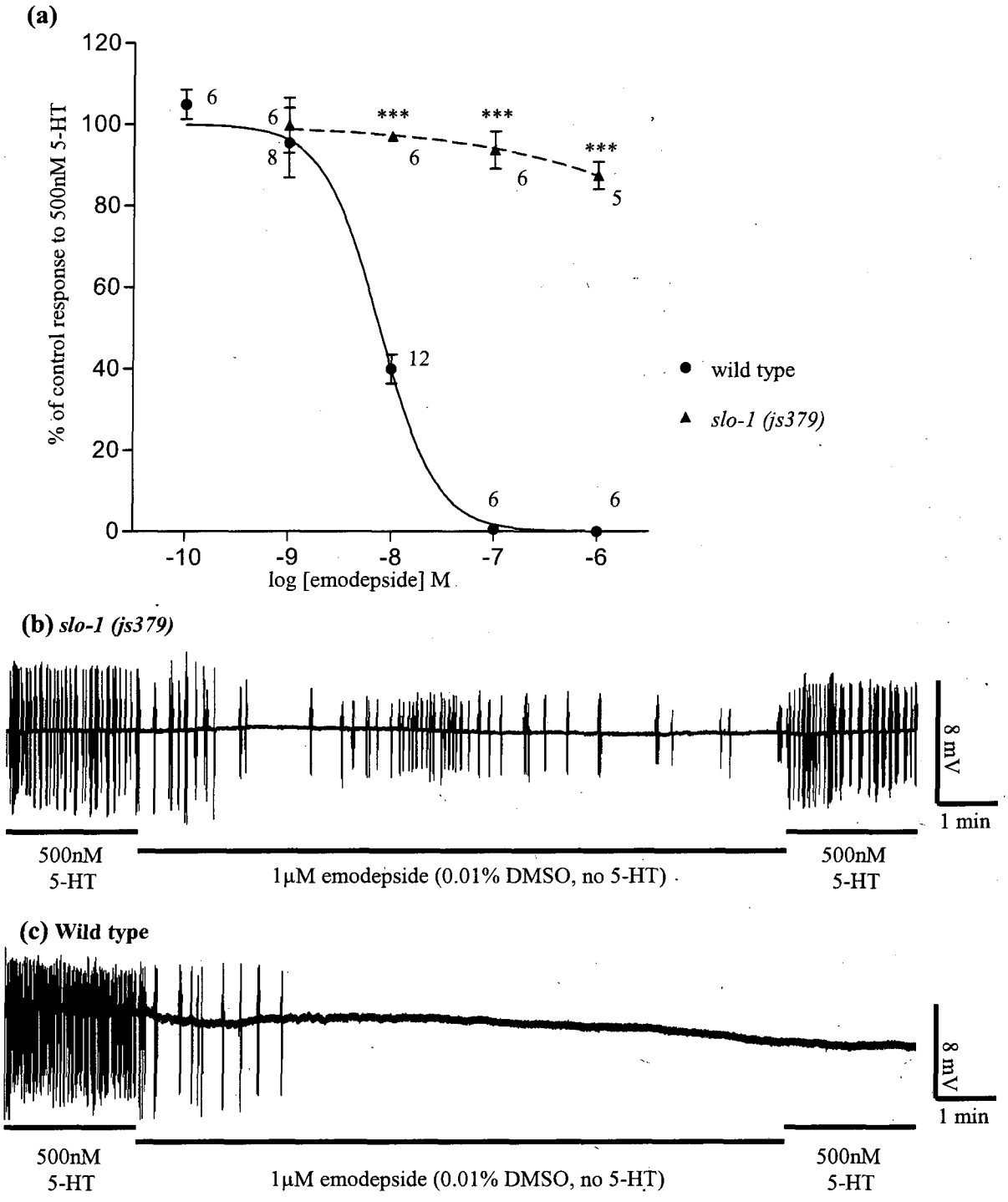

Figure 5.12 The effect of emodepside on the response of the *slo-1 (js379)* pharynx to 500nM 5-HT. **(a)** Concentration response curve showing the effect of emodepside on the pharyngeal response of wild type and *slo-1 (js379) C. elegans* to 500nM 5-HT. '% of basal response to 5-HT' was calculated by expressing the pharyngeal response to 500nM 5-HT following exposure to emodepside as a percentage of the basal response to 5-HT (prior to emodepside application). Each datum point is the mean ± S.E.Mean of (n) pharyngeal preparations. Significance (Student's t-test) relates to a comparison of wild type and *slo-1* response to 500nM 5-HT following exposure to each emodepside concentration tested, *** $P<0.001$, n numbers given beside each datum point. Curves were fitted using the nonlinear regression four-parameter logistic equation described in chapter 2, section 2.10. **(b-c)** Example EPG recordings from (b) a *slo-1* pharynx and (c) a wild type pharynx. Notice that the pharyngeal pumping rate of *slo-1* in 5-HT before and after emodepside exposure is almost the same, however, the wild type pharynx is rapidly paralysed during application of emodepside and does not pump when 5-HT is applied again.

5.7.2 Effect of emodepside on pharyngeal pumping in *slo-1 (ky399)* gain-of-function *C. elegans*

Emodepside inhibited the 5-HT response of the *slo-1 (ky399)* pharynx in a concentration-dependent manner (see figure 5.13 (a)). The *slo-1 (ky399)* mutants did not exhibit a sensitivity to emodepside significantly different to that of wild type *C. elegans* at any of the emodepside concentrations used in the pharyngeal assay. The IC_{50} for *slo-1 (ky399)* was 7nM (95% confidence limits 5 to 10nM) compared to wild type *C. elegans* IC_{50} of 8nM (95% confidence limits 6 to 10nM).

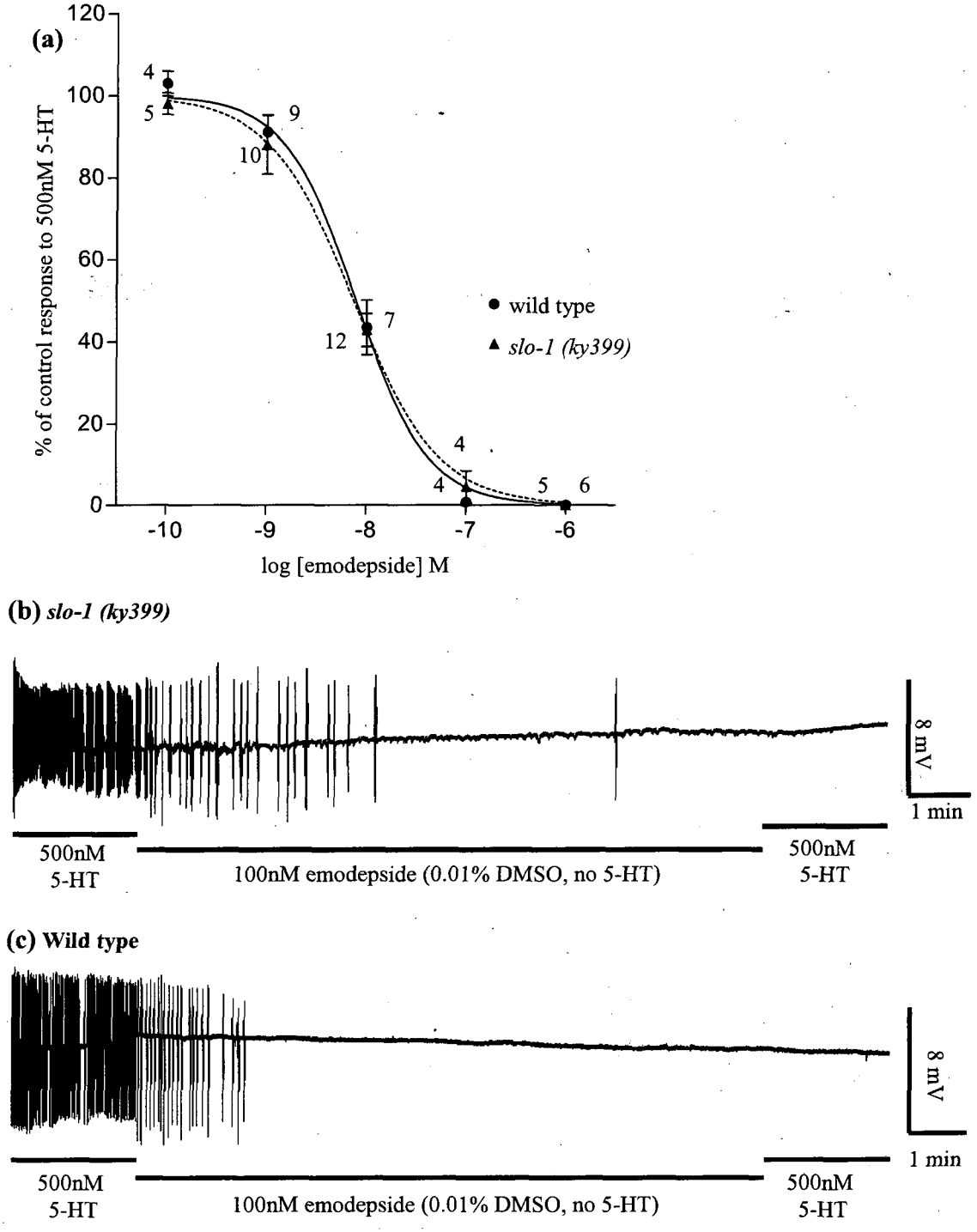

Figure 5.13 The effect of emodepside on the response of the *slo-1 (ky399)* pharynx to 500nM 5-HT. **(a)** Concentration response curve showing the effect of emodepside on the pharyngeal response to 500nM 5-HT in wild type and *slo-1 (ky399) C. elegans*. '% of basal response to 5-HT' is the pharyngeal response to 5-HT after emodepside exposure as a % of the response before application of the drug. Each datum point is the mean ± S.E.Mean of (n) pharynx preparations, n numbers are given beside each datum point. To clarify, n numbers at 10nM emodepside: 7 (wild type), 12 (*slo-1*), and at 1μM: 6 (wild type), 5 (*slo-1*). Curves were fitted using the nonlinear regression four-parameter logistic equation described in chapter 2, section 2.10. Solid curve: wild type. Dotted curve: *slo-1*. **(b-c)** Example EPG recordings from (b) a *slo-1* pharynx and (c) a wild type pharynx. Notice that the wild type and *slo-1* pharyngeal pumping in response to 500nM 5-HT is completely inhibited in these recordings by exposure to 100nM emodepside for 10 minutes.

5.7.3 Effect of emodepside on pharyngeal pumping in *slo-1 (ky389)* gain-of-function *C. elegans*

At 10nM, emodepside inhibited the 5-HT response of the *slo-1 (ky389)* pharynx by 84%, which is significantly different to a wild type inhibition of 52%, ($P<0.001$; see figure 5.14 (a)). DMSO at 0.01% did not effect the 5-HT response of the *slo-1 (ky389)* or wild type pharynx.

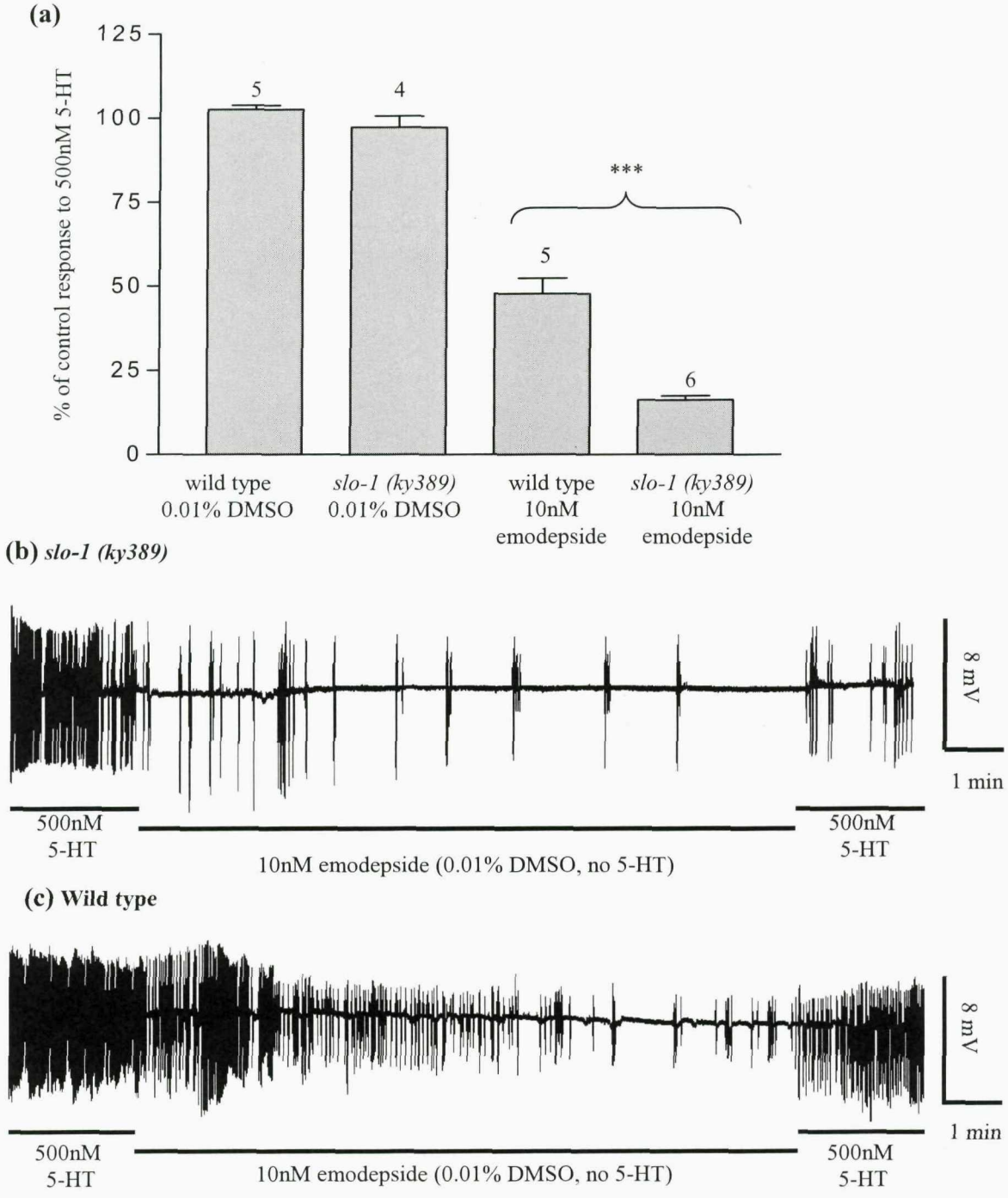

Figure 5.14 The effect of 10nM emodepside on the response of the *slo-1 (ky389)* pharynx to 500nM 5-HT.

(a) Graph showing the effect of emodepside on the pharyngeal response of wild type and *slo-1 (ky389) C. elegans* to 500nM 5-HT. '% of basal response to 5-HT' was calculated by expressing the pharyngeal response to 500nM 5-HT following exposure to emodepside as a percentage of the basal response to 5-HT (prior to emodepside application). Each bar is the mean ± S.E.Mean of (n) pharyngeal preparations. Significance (Student's t-test) relates to a comparison of wild type and *slo-1* response to 500nM 5-HT following exposure to 10nM emodepside, *** $P<0.001$, n numbers given above each bar. **(b-c)** Example EPG recordings from (b) a *slo-1* pharynx and (c) a wild type pharynx. Notice that the pharyngeal pumping rate of *slo-1* in 5-HT is more severely inhibited after exposure to emodepside than the wild type pharynx.

5.7.4 Effect of emodepside on pharyngeal pumping in *slo-2 (nf101)* loss-of-function *C. elegans*

Emodepside inhibited the 5-HT response of the *slo-2 (nf101)* pharynx in a concentration-dependent manner (see figure 5.15 (a)). The *slo-2 (nf101)* mutants did not exhibit a sensitivity to emodepside significantly different to that of wild type *C. elegans* at any of the emodepside concentrations used in the pharyngeal assay. The IC_{50} for *slo-2 (nf101)* was 13nM (95% confidence limits 9 to 21nM) compared to wild type *C. elegans* IC_{50} of 10nM (95% confidence limits 8 to 13nM).

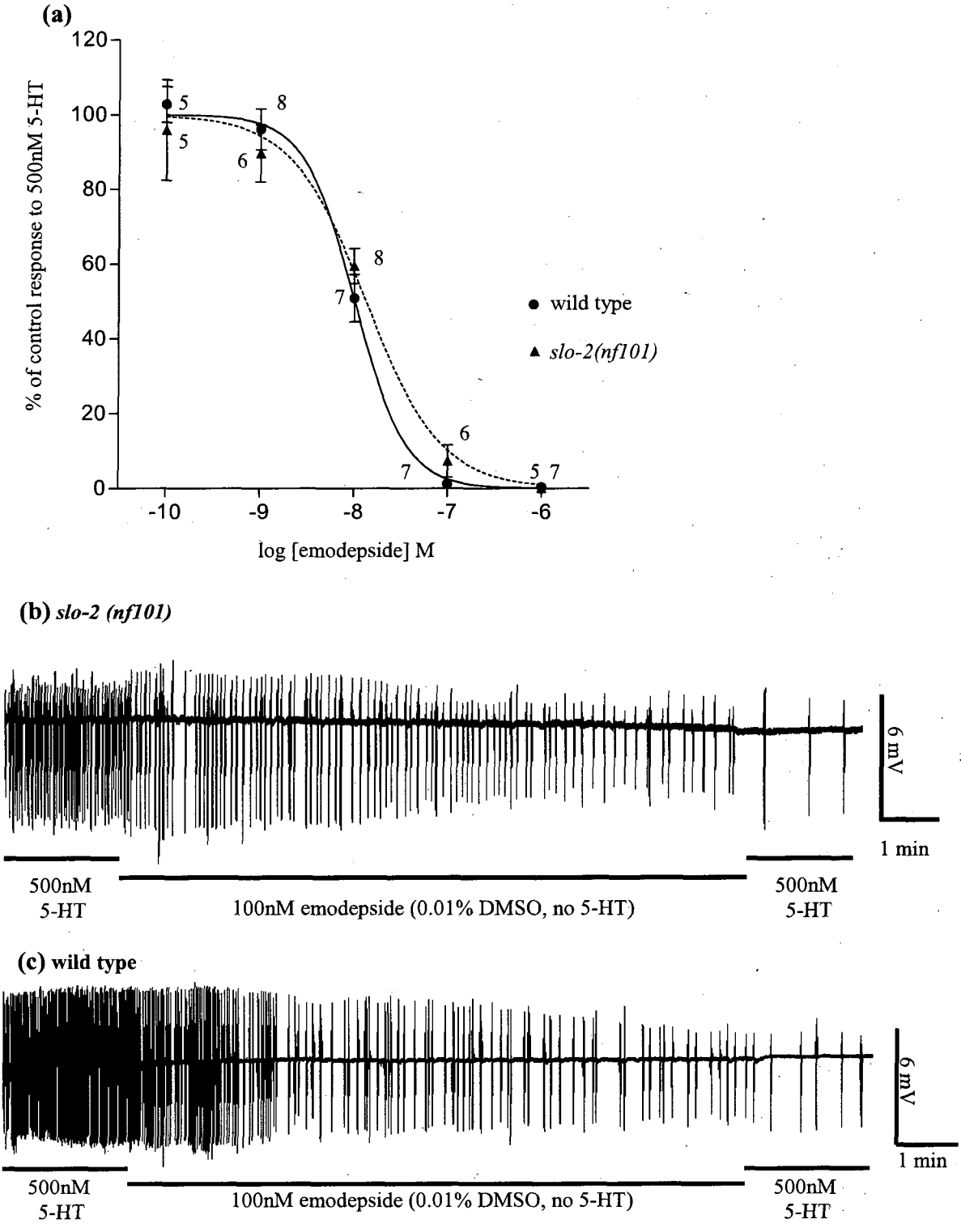

Figure 5.15 The effect of emodepside on the response of the *slo-2 (nf101)* pharynx to 500nM 5-HT. **(a)** Concentration response curve showing the effect of emodepside on the pharyngeal response to 500nM 5-HT in wild type and *slo-2 (nf101) C. elegans*. '% of basal response to 5-HT' is the pharyngeal response to 5-HT after emodepside exposure as a % of the response before application of the drug. Each datum point is the mean ± S.E.Mean of (n) pharynx preparations, n numbers are given beside each datum point. To clarify, n numbers at 1μM emodepside: 7 (wild type), 5 (*slo-1*). Curves were fitted using the nonlinear regression four-parameter logistic equation described in chapter 2, section 2.10. Solid curve: wild type. Dotted curve: *slo-2*. **(b-c)** Example EPG recordings from (b) a *slo-2* pharynx and (c) a wild type pharynx. Notice that wild type and *slo-1* pharyngeal pumping in 500nM 5-HT is similarly inhibited in these two recordings by exposure to 100nM emodepside for 10 minutes.

5.8 Investigating the mechanism of action of other novel anthelmintics in the *C. elegans* pharynx.

The results shown in sections 5.4.1, 5.7.1 and 5.7.3 suggest that LAT-1 and SLO-1 are involved in the inhibitory pathways utilized by emodepside in the pharynx. As the three novel anthelmintics verticilide, PF1022-222 and PF1022-888 can also inhibit pharyngeal pumping in wild type *C. elegans*, and they are structurally related to emodepside, it is possible that their mechanisms of action also involve LAT-1 and SLO-1. To investigate this, the *lat-1 (ok1465)* loss-of-function mutant and the *slo-1 (js379)* null mutant were assayed for the sensitivity of their 5-HT response to the three novel anthelmintics.

5.8.1 The effect of verticilide on pharyngeal pumping in *slo-1 (js379)* null *C. elegans* and *lat-1 (ok1465)* loss-of-function *C. elegans*

Wild type *C. elegans* were assayed at the same time as the *lat-1 (ok1465)* and *slo-1 (js379)* mutants to increase reliability when comparing the verticilide sensitivity of the strains. Each pharyngeal preparation was 'primed' to reach maximum response to 500nM 5-HT by repeated application for three minutes interspersed with three minutes in Dent's saline (see chapter 2, section 2.7.3, page 73). This was followed by three minutes recovery in Dent's saline, and then the recording protocol was applied (in order of application): three minutes 500nM 5-H, wash (Dent's saline), ten minutes verticilide (at 100nM or 1μM, 0.01% DMSO vehicle, no 5-HT), wash (Dent's saline), three minutes 500nM 5-HT. The pharyngeal pumping rate in response to 5-HT following verticilide application was calculated as a percentage of the pharyngeal response to 5-HT prior to drug exposure.

The 5-HT response of the wild type pharynx, but not the *lat-1 (ok1465)* and *slo-1(js379)* pharynx, was inhibited significantly by 100nM verticilide when compared to DMSO control experiments ($P<0.05$, figure 5.16 (a): black stars). The *lat-1 (ok1465)* and *slo-1 (js379)* pharyngeal preparations appear to have reduced sensitivity to the effect of 100nM verticilide; demonstrating only a 10% and 6% inhibition in 5-HT response (respectively), which is significantly different to the 34% inhibition observed in the wild type ($P<0.05$, figure 5.16 (a): red stars). When exposed to 1μM verticilide, the 5-HT response of the wild type and *lat-1 (ok1465)* pharynx is significantly inhibited by 94% and 81%, respectively ($P<0.001$, figure 5.16 (b): black stars, and figure 5.17). However the *slo-1*

(js379) pharynx exhibited only a 22% inhibition of 5-HT response when exposed to 1μM verticilide, which is a significant reduction in anthelmintic sensitivity when compared to the wild type (P<0.001, figure 5.16 (b): red stars, and figure 5.17).

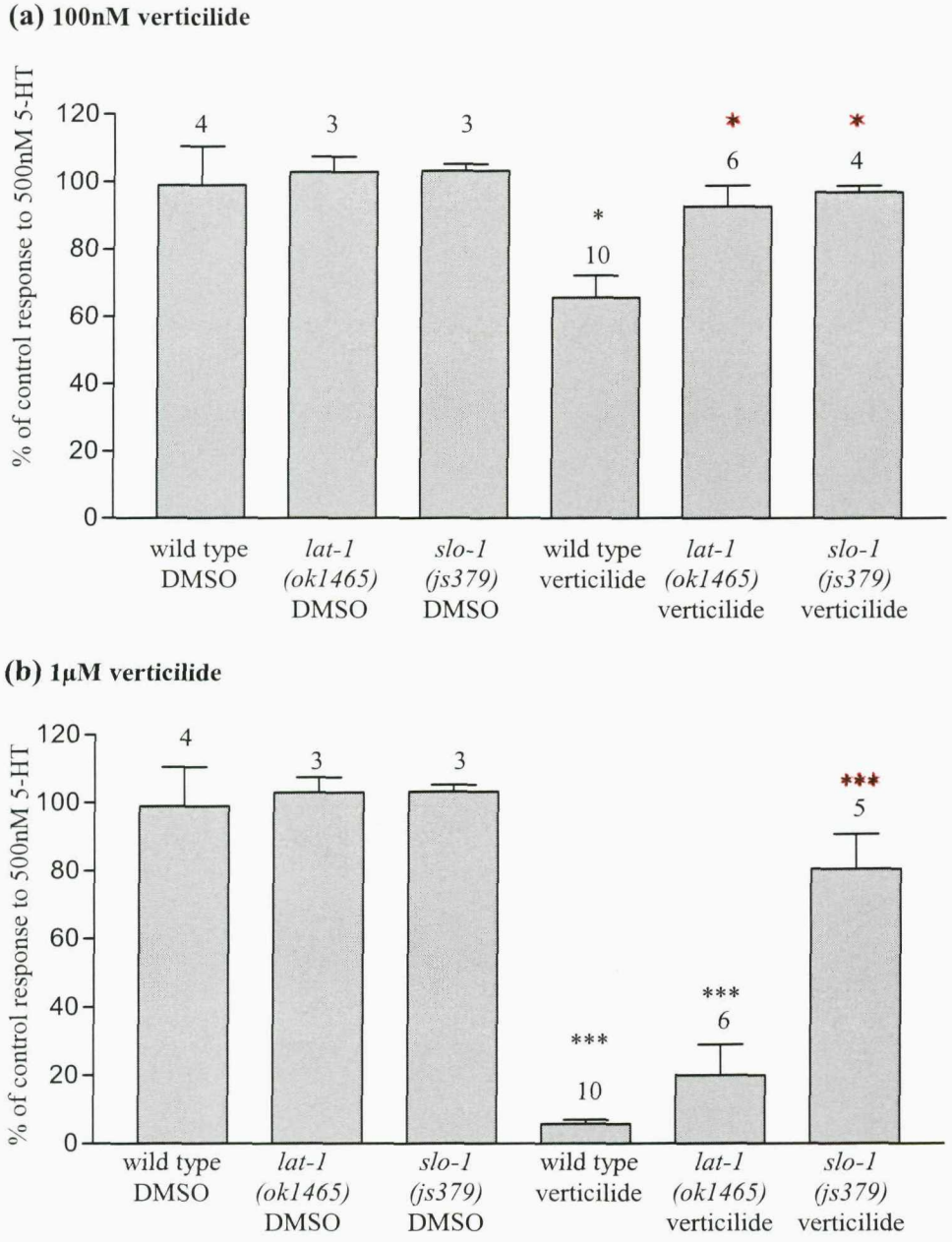

Figure 5.16 Graphs showing the effect of verticilide on the 5-HT response of the wild type, *lat-1 (ok1465)*, and *slo-1 (js379)* *C. elegans* pharynx.
The effect of 100nM and 1μM verticilide on the pharyngeal response of the three worm strains to 500nM 5-HT is shown in **(a)** and **(b)**, respectively. DMSO was applied as a 0.01% solution in Dent's saline. '% of control response to 5-HT' is the pharyngeal response to 5-HT after verticilide or DMSO exposure as a % of the response before application of the compound. Each bar is the mean ± S.E.Mean of (n) pharynx preparations. Significance (Student's t-test) relates to a comparison of: (for the red stars) the effect of 100nM or 1μM verticilide on wild type and mutant 5-HT response, *** P<0.001, *P<0.01, and (for the black stars) the effect of DMSO and either 100nM or 1μM verticilide on one of the *C. elegans* strains tested, ***P<0.001, *P<0.05, n numbers are given above each bar.

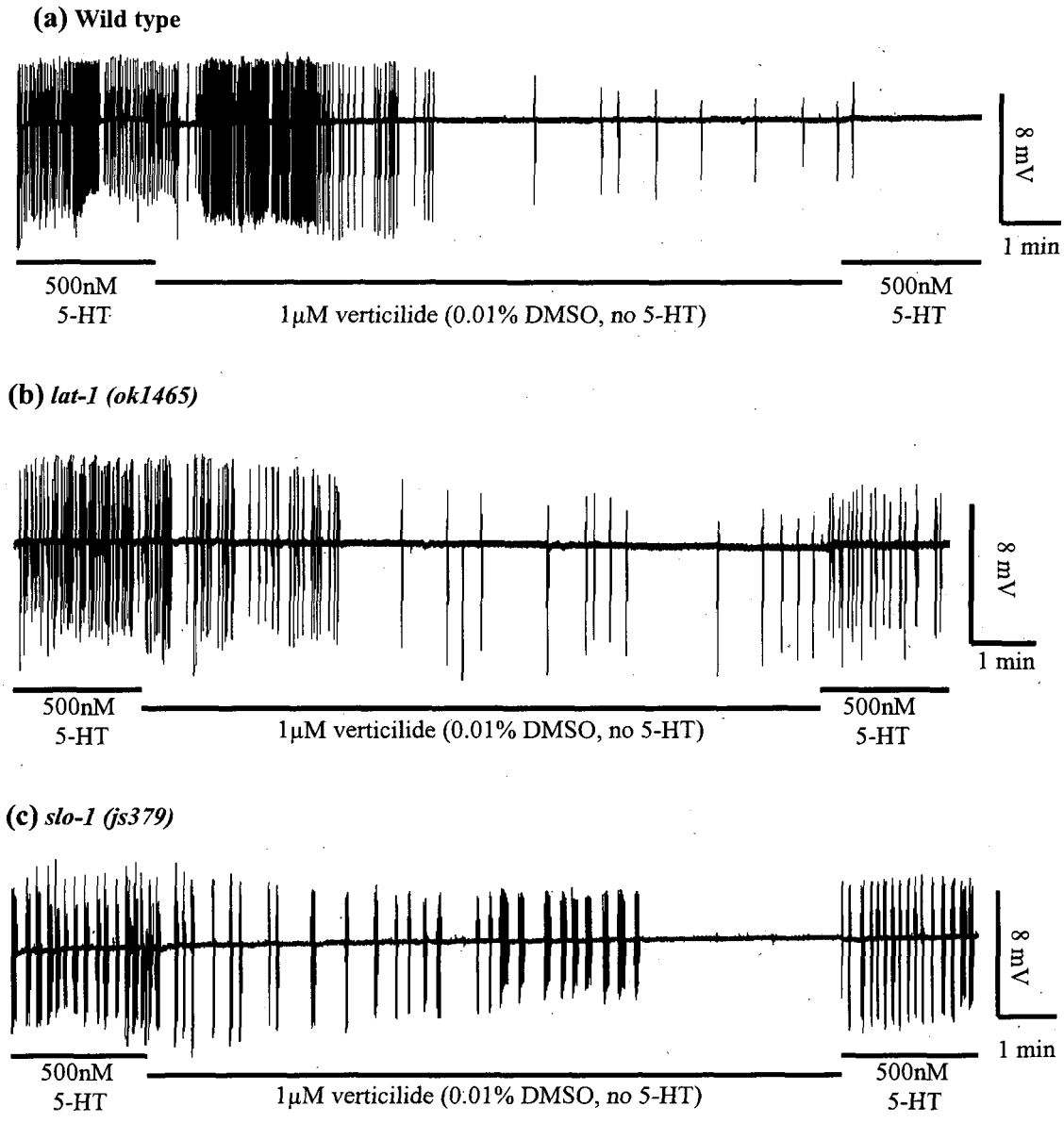

Figure 5.17 The effect of 1μM verticilide on the response of the *lat-1 (ok1465)* and *slo-1 (js379)* pharynx to 500nM 5-HT.
Example EPG recordings showing the effect of 1μM verticilide on the 5-HT response of pharyngeal preparations from **(a)** wild type, **(b)** *lat-1 (ok1465)*, and **(c)** *slo-1(js379) C. elegans*. Notice that wild type pharyngeal pumping in 500nM 5-HT is almost totally abolished by exposure to 1μM verticilide for 10 minutes. However, the *lat-1 (ok1465)* pharynx continues to pump in 5-HT following verticilide exposure, albeit at a lower frequency than before drug exposure. The *slo-1 (js379)* pharyngeal pumping rate in 5-HT after verticilide exposure is reduced compared to the rate before drug application, but not to the extent of the *lat-1 (ok1465)* mutant.

5.8.2 The effect of PF1022-888 and PF1022-222 on pharyngeal pumping in *slo-1 (js379)* null *C. elegans* and *lat-1 (ok1465)* loss-of-function *C. elegans*

Wild type *C. elegans* were assayed at the same time as the *lat-1 (ok1465)* and *slo-1 (js379)* mutants to increase reliability when comparing the anthelmintic sensitivity of the strains. Each pharyngeal preparation was 'primed' with 500nM 5-HT as described in section 5.4, followed by the recording protocol (in order of application): two minutes 500nM 5-HT, then wash (Dent's saline), ten minutes of either PF1022-222, PF1022-888, or emodepside (all at 10nM, 0.01% DMSO vehicle, no 5-HT) or a control solution of only 0.01% DMSO (no anthelmintics or 5-HT), wash (Dent's saline), two minutes 500nM 5-HT. The pharyngeal pumping rate in response to 5-HT following application of one of the anthelmintics or DMSO was calculated as a percentage of the pharyngeal response to 5-HT prior to drug exposure.

In the wild type pharynx, emodepside, PF1022-222 and PF1022-888 all significantly inhibited the 5-HT response ($P<0.01$, figure 5.18), with PF1022-222 producing mean inhibition of 57%, compared to 54% for emodepside and 38% for PF1022-888. When analysed using Student's t-test, no significant difference was found between the levels of inhibition caused by the three compounds in the wild type pharynx. In the *slo-1 (js379)* pharynx, only PF1022-888 inhibited the 5-HT response significantly when compared to the DMSO control ($P<0.05$, figure 5.18). However, pharyngeal inhibition by PF1022-888 was reduced in *slo-1 (js379)* compared to inhibition in the wild type, with the *slo-1 (js379)* response inhibited by 20%, compared to 38% in the wild type. In the *lat-1 (ok1465)* mutant, only PF1022-222 significantly inhibited the 5-HT response ($P<0.05$, figure 5.18). However, PF1022-222 only inhibited *lat-1 (ok1465)* pharyngeal 5-HT response by 35%, which was less than the 57% inhibition caused by the compound in the wild type pharynx.

In summary, emodepside, PF1022-222 and PF1022-88 all significantly inhibited the 5-HT response of the wild type pharynx, and the pharynx of the *slo-1 (js379)* and *lat-1 (ok1465)* mutants demonstrated decreased sensitivity to all three compounds. Representative EPG recordings for the effect of PF1022-222 and PF1022-888 on the three *C. elegans* strains are shown in figure 5.19 (PF1022-222) and figure 5.20 (PF1022-888).

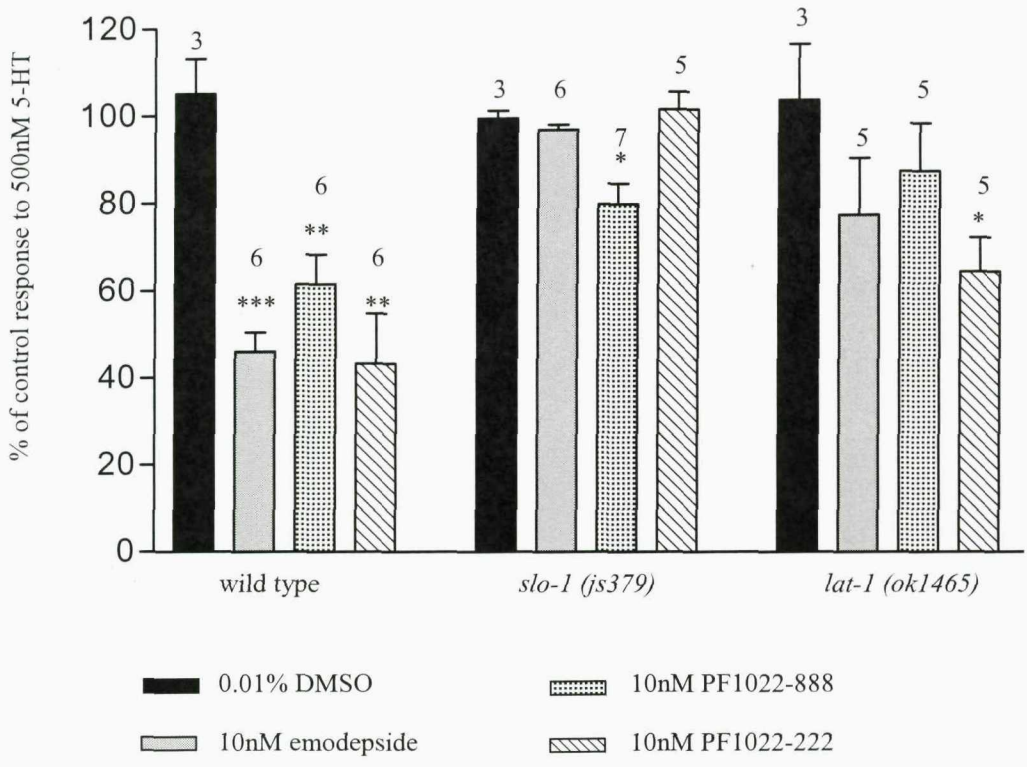

Figure 5.18 The effect of PF1022-222 and PF1022-888 on the response of the *lat-1(ok1465)* and *slo-1 (js379)* pharynx to 500nM 5-HT.
Graph showing the effect of emodepside, PF1022-222, PF1022-888 and 0.01% DMSO (vehicle) on the 5-HT response of the wild type, *slo-1 (js379)* and *lat-1 (ok1465)* pharynx. '% of control response to 5-HT' is the 5-HT response after drug exposure as a % of the response before drug application. Each bar is the mean ± S.E.Mean of (n) pharynx preparations. Significance (Student's t-test) relates to a comparison of the effect of DMSO and either emodepside, PF1022-222 or PF1022-888 on one of the *C. elegans* strains tested, n numbers are given above each bar.

(a) 10nM PF1022-222 on wild type

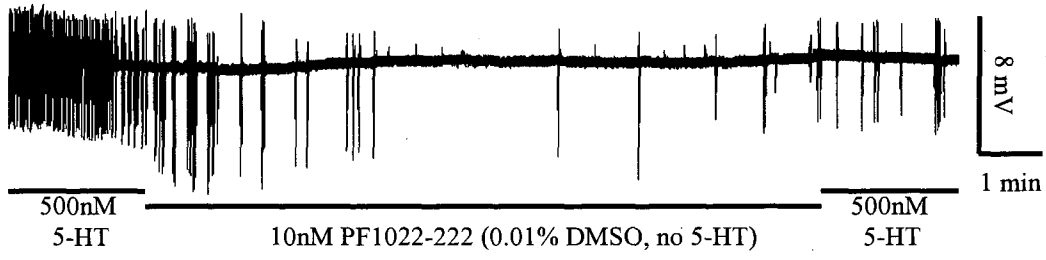

(b) 10nM PF1022-222 on *slo-1 (js379)*

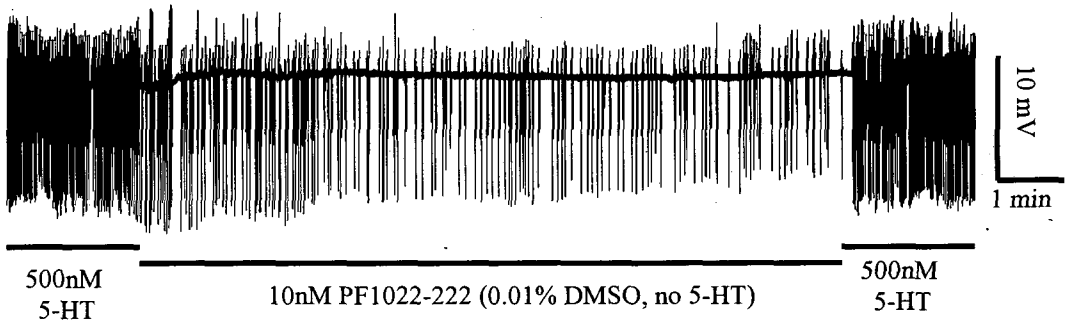

(c) 10nM PF1022-222 on *lat-1 (ok1465)*

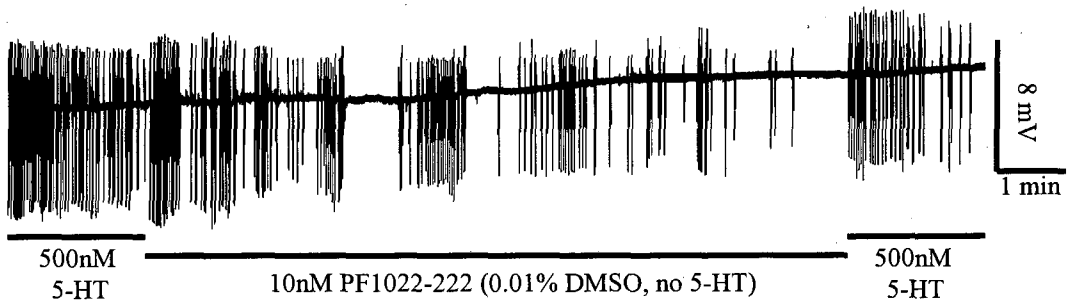

Figure 5.19 The effect of PF1022-222 on the response of the wild type, *lat-1(ok1465)* and *slo-1 (js379)* pharynx to 500nM 5-HT.
Example EPG recordings showing the effect of 10nM PF1022-222 on the 5-HT response of the **(a)** wild type, **(b)** *slo-1 (js379)*, and **(c)** *lat-1 (ok1465)* pharynx. Compare the 5-HT response of each pharynx before and after exposure to PF1022-222, and notice that the anthelmintic inhibits the wild type pharynx with the greatest potency (recording (a)), followed by the *lat-1 (ok1465)* pharynx shown in recording (c). The *slo-1 (js379)* pharynx is not noticeably inhibited in recording (b), indicating the resistance of this strain to the effect of 10nM PF1022-222 on the pharyngeal 5-HT response.

(a) 10nM PF1022-888 on wild type

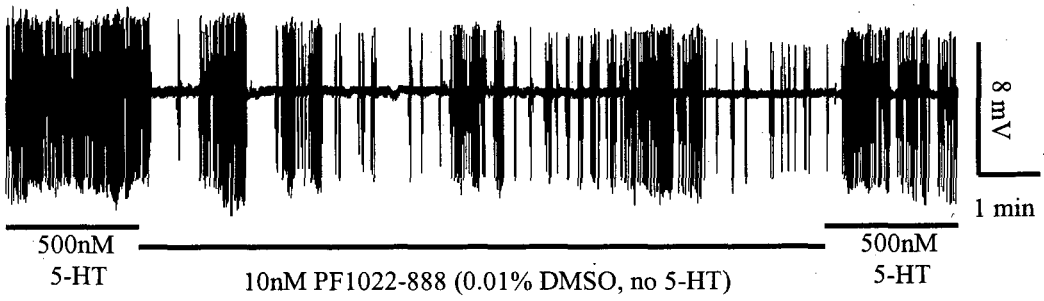

(b) 10nM PF1022-888 on *slo-1 (js379)*

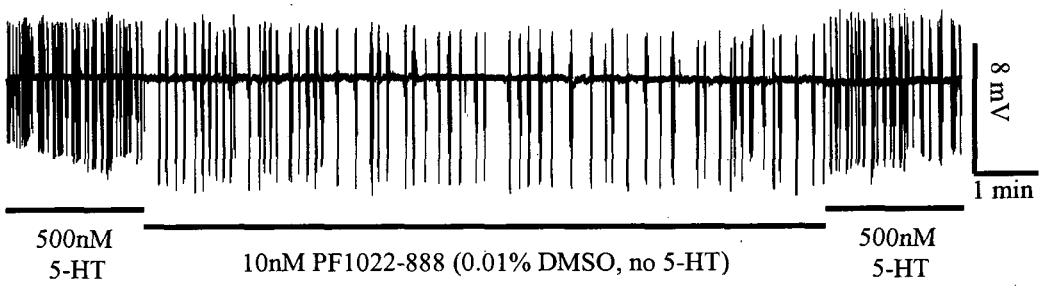

(c) 10nM PF1022-888 on *lat-1 (ok1465)*

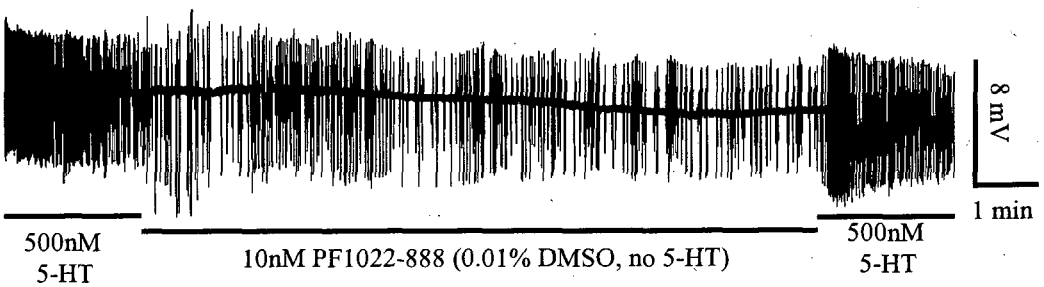

Figure 5.20 The effect of PF1022-888 on the response of the wild type, *lat-1(ok1465)* and *slo-1 (js379)* pharynx to 500nM 5-HT.
Example EPG recordings showing the effect of 10nM PF1022-888 on the 5-HT response of the (a) wild type, (b) *slo-1 (js379)*, and (c) *lat-1 (ok1465)* pharynx. Compare the 5-HT response of each pharynx before and after exposure to PF1022-888, and notice that the anthelmintic inhibits the wild type pharynx with the greatest potency (recording (a)), followed by the *slo-1 (js379)* pharynx (recording (b)), whereas inhibition of the *lat-1 (ok1465)* pharynx is only just discernable at this scale, and is not statistically significant (recording (c)).

5.9 Discussion

In this chapter, the thrashing assay and electropharyngeogram (EPG) techniques were used to identify components of the mechanism of action for emodepside and other anthelmintically active compounds at the neuromuscular junction (NMJ) of the pharyngeal and body wall muscles.

The *C. elegans* latrophilins (LAT-1 and LAT-2) were the initial focus point for studying the mechanism of action for emodepside because they have been previously shown by RNA interference (RNAi) to have a significant role in the activity of the drug in the pharynx and body wall muscles of *C. elegans* (Willson et al., 2004). In agreement with these earlier results, RNAi directed against *lat-1* did significantly reduce the emodepside sensitivity of *rrf-3 (pk1426) C. elegans*. However, examination of the *lat-1 (ok1465)* putative null mutant did not reveal any effect of the mutation on emodepside sensitivity in comparison with wild type *C. elegans*. The apparent disparity in these results could be due to insufficient specificity in the targeting of *lat-1* by RNAi, resulting in other genes being affected. Importantly, Guest et al. (2007) demonstrated that the emodepside sensitivity of thrashing by the *C. elegans lat-2 (tm463)* loss-of-function mutant and the *lat-1 (ok1465); lat-2 (tm463)* double mutant is not significantly different to wild type. This suggests that both LAT-1 and LAT-2 are not involved in emodepside-stimulated paralysis of the body wall muscles, and that sequence similarity between the two latrophilin genes cannot account for any reduction in specificity in the RNAi technique directed against *lat-1*.

In the pharynx, LAT-1, but not LAT-2, appears to have a role in the mechanism of action for emodepside, with *lat-1 (ok1465)* mutants demonstrating significant resistance to emodepside concentrations of 10-100nM. These results, which indicate a role for LAT-1 in the action of emodepside at the NMJ of the pharynx but not body wall muscle, suggests that the mechanism by which emodepside inhibits locomotion and pharyngeal pumping is subtly different, and therefore it was decided that in this project the pharynx would be the focus site for further investigation into emodepside activity.

From the results of pharyngeal assays on the SLO-1 and G protein mutants, it appears that SLO-1 is the major component in the mechanism by which emodepside paralyses pharyngeal pumping in *C. elegans*, with $G\alpha_q$ and $G\alpha_o$, as well as LAT-1 in more minor contributory roles. The $G\alpha_q$ reduction-in-function *egl-30 (ad806)* mutant demonstrated weak hypersensitivity to emodepside, whereas the *egl-30 (tg26)* gain-of-function mutant appeared less sensitive to the anthelmintic, suggesting that emodepside functions to inhibit $G\alpha_q$ activity. It should be noted that an *egl-30* reduction-in-function mutant and not loss-of-function was used due to the larval lethality of the latter (Brundage et al., 1996). Therefore, the weak suppression of $G\alpha_q$ function in the *egl-30 (ad806)* mutant may not have been sufficient to affect emodepside activity more convincingly. Re-examination of the $G\alpha_q$ contribution to the mechanism of action for emodepside could utilize alternative *egl-30* reduction-in-function alleles to obtain a more significant result. Of course, it is entirely possible that $G\alpha_q$ does have only a small contributory role in emodepside-stimulated pharyngeal paralysis, and in agreement with this, the $G\alpha_o$ loss-of-function mutant demonstrated only a small reduction in emodepside sensitivity. This suggests that emodepside may weakly activate the $G\alpha_o$ pathway, which inhibits neurotransmitter release by negatively regulating the $G\alpha_q$ pathway via hydrolysis of PIP2 by PCLβ (Miller et al., 1999; Nurrish et al., 1999). Interestingly, the *dgk-1 (nu62)* mutant did not exhibit any alteration in emodepside sensitivity, suggesting that emodepside targets $G\alpha_o$ but not DGK-1 to inhibit neurotransmitter release. As DGK-1 and $G\alpha_o$ have been suggested to operate in parallel pathways that control $G\alpha_q$ signaling, it certainly is possible that emodepside may target only one of these pathways (Nurrish et al., 1999). Significantly, latrophilin isolated from rat brain has been shown to co-purify with the $G\alpha_o$ protein (Lelianova et al., 1997), suggesting that the binding of emodepside to LAT-1 may stimulate the $G\alpha_o$ pathway, resulting in the inhibition of neurotransmitter release, and flaccid muscle paralysis.

If emodepside is acting to inhibit neurotransmitter release, then this would be facilitated by the activation of the SLO-1 channel if the channel functions as a molecular 'brake' on neurotransmitter release, as has been reported (Wang et al., 2001). Emodepside enhancement of SLO-1 activity directly or indirectly would certainly explain the resistance of the *slo-1 (js379)* null to the anthelmintic, as well as the hypersensitivity of the *slo-1 (ky389)* gain-of-function mutant. The difference in the emodepside response of the two *slo-1* gain-of-function mutants may provide an interesting clue as to the

mechanism by which the anthelmintic alters SLO-1 functioning. The mutations in these two *slo-1* gain-of-function strains are predicted to affect two vital facets of *slo-1* channel regulation: voltage-sensitivity and calcium-sensitivity, and it may be this difference that is responsible for the variation in emodepside sensitivity observed in the two strains. Evidence now strongly suggests that Ca^{2+} and voltage can independently act to regulate BK channel opening (Horrigan & Aldrich, 2002; Lingle, 2002). Three processes are predicted to contribute to BK channel gating: channel opening, Ca^{2+} binding, and voltage-sensor movement (Horrigan & Aldrich, 2002). Each of these processes is in internal equilibrium, for example, Ca^{2+} binds and unbinds with the channel in an equilibrium that shifts according to external factors. The coupling between any two of the three gating processes can be described by observing how alteration to the equilibrium of one process affects the equilibrium of the coupled process.

To determine whether BK channel activation by Ca^{2+} results from its direct effects on the channel opening equilibrium or on the voltage-sensor equilibrium or both, the relationship between channel opening current and voltage was investigated in the presence of 70μM Ca^{2+} and zero Ca^{2+}, with the former Ca^{2+} concentration anticipated to saturate all higher affinity Ca^{2+} binding sites (Horrigan & Aldrich, 2002). Voltage-sensor movement is much faster than channel opening, and therefore the gating current has two components: Q_{fast} occurs within 100μs of a voltage-step and is produced by voltage-sensor movement; Q_{slow} has kinetics identifying it as a product of channel opening. Therefore, the specific effects of Ca^{2+} on voltage-sensor movement (Q_{fast}) can be distinguished from effects on channel opening (Q_{slow}). Horrigan & Aldrich (2002) showed that an increase in Ca^{2+} from zero to 70μM, shifted the voltage at which Q_{fast} occurred by only -33 mV, suggesting that voltage-sensor movement is minimally affected by Ca^{2+}, and therefore, voltage activation of the channel is only slightly altered by Ca^{2+}. However, the increase in Ca^{2+} concentration was found to shift the voltage at which Q_{slow} was observed by -166mV, suggesting that Ca^{2+} can open the BK channel independently of any depolarizing shift in voltage. Therefore, it was concluded that Ca^{2+} and voltage independently act to regulate channel opening, with Ca^{2+} primarily acting to directly modulate channel opening, with only a minor interaction between Ca^{2+} binding and voltage-sensor movement (Horrigan & Aldrich, 2002; Lingle, 2002).

Based on the results of the EPG assay using the *slo-1* gain-of-function mutants, it is possible that emodepside is augmenting Ca^{2+} activation of the SLO-1 channel either directly or indirectly, resulting in constitutive channel activation, the inhibition of neurotransmitter release and muscle paralysis. In support of this, a very recent *C. elegans* mutagenesis screen for resistance to locomotory paralysis by emodepside has identified four *slo-1* mutants containing mutations in the channel RCK domains shown to be important in channel activation by Ca^{2+} (Guest et al., 2007; Xia et al., 2002; see chapter 1, section 1.7.7, page 51).

In MIN6 β cells, latrotoxin has been shown to induce insulin exocytosis by inhibiting iberiotoxin-sensitive outward K^+ currents via binding to the latrophilin receptor (Lajus et al., 2006). These results suggest that emodepside may inhibit neurotransmitter release by the activation of iberiotoxin-sensitive SLO-1 channels, either directly or indirectly, with LAT-1 contributing to an indirect pathway. The hypersensitivity of the *slo-1 (ky389)* mutant suggests that SLO-1 Ca^{2+} sensitivity has a key role in the mechanism of action for emodepside. It is possible that emodepside initially stimulates a rise in intracellular Ca^{2+} in order to activate SLO-1. In MIN6 β cells, latrotoxin binding to latrophilin has been shown to activate protein kinase C (PKC), presumably via stimulation of $G\alpha_q$ and DAG production. This results in the closure of inwardly-rectifying K^+ channels, leading to depolarization, a consequent opening of voltage-dependent Ca^{2+} channels and a rise in intracellular Ca^{2+}. It is possible that emodepside stimulates such a pathway to activate SLO-1, and this would certainly be supported by the findings of Willson et al. (2004), which demonstrated a reduction in emodepside sensitivity in the *egl-30 (ad810)* pharynx and an increase in pharyngeal sensitivity in *egl-30 (tg26)* worms, suggesting that emodepside stimulates the $G\alpha_q$ pathway. Further supporting these findings, Willson et al., (2004) examined other proteins in the $G\alpha_q$ pathway and found a reduction in pharyngeal emodepside sensitivity in loss-of-function mutants for PLCβ and *unc-13*, as well as a synptobrevin reduction-in function mutant. Emodepside sensitivity was found to be increased in the *goa-1 (n1134)* loss-of-function mutant (Willson et al., 2004). These results suggest that emodepside stimulates the $G\alpha_q$ pathway upstream of SNARE complex formation and inhibits the $G\alpha_o$ pathway, and is in contrast to the results for the G protein mutants shown in this chapter. This discrepancy may be partly explained by the severe phenotypes observed in most of the mutants used, which make them highly delicate to dissect and maintain for EPG recording. The *egl-30 (ad806)*, *egl-30 (tg26)* and

goa-1 (n1134) pharyngeal preparations were extremely fragile and susceptible to dying in the absence of any treatment. This could have been mistaken for emodepside hypersensitivity, and therefore, for the work presented in this chapter, each preparation was left for 15 minutes before recording commenced to try and eliminate those that would have died before a full recording had been made. However, this in itself may have positively selected for less severe mutants and may have resulted in a minimization of the emodepside hypersensitivity seen in the *egl-30 (ad806)* pharynx and the resistance of the *egl-30 (tg26)* and *goa-1 (n1134) C. elegans*.

It is possible that emodepside disrupts neurotransmitter release via a number of pathways and uses more than one receptor. Indeed, the low level of resistance observed in the *lat-1 (ok1465)* mutant suggests that emodepside binds other proteins to exert its effects. The strong resistance of the *slo-1 (js379)* mutant, coupled with the results of the most recent mutagenesis screen, which isolated nine emodepside resistant strains all containing mutations in *slo-1* (Guest et al., 2007), supports the hypothesis that emodepside binds to SLO-1 directly with other indirect pathways contributing in a minor fashion.

Latrotoxin, like emodepside, appears to function by a mechanism involving latrophilin, and the possibility of the anthelmintic also sharing the latrotoxin receptor PTPσ (Krasnoperov et al., 2002b, 1997; Lajus et al., 2006) was investigated in the pharynx. The *C. elegans* ortholog of the PTPσ receptor, PTP-3, did not appear to be involved in emodepside-stimulated pharyngeal paralysis. However, the *ptp-3 (op147)* allele contains a mutation predicted to disrupt the catalytic activity of the protein (Harrington et al., 2002), and it is possible that emodepside may not utilize the catalytic capability of PTP-3, but may instead use the protein as a membrane anchor or to form a complex with other proteins which are responsible for facilitating emodepside action. Of course, it is possible that in the *C. elegans* pharynx PTP-3 does not function as a receptor for latrotoxin at all. In retrospect, a comparison of latrotoxin activity in the wild type and *ptp-3 (op147)* pharynx would have provided an initial answer regarding the possibility of PTP-3 acting as a latrotoxin receptor. Interestingly, latrotoxin binding to PTPσ has been shown to reduce repolarizing currents produced by BK potassium channels via the activation of phospholipase in MIN6 β-cells (Lajus et al., 2006). In view of results strongly supporting a role for SLO-1 in pharyngeal paralysis by emodepside, the argument for PTP-3 involvement is strengthened. By examining latrotoxin activity in *ptp-3 (op147) C.*

elegans as well as other *ptp-3* strains mutated at alternative sites in the gene, a role for PTP-3 can be identified if it exists.

The IP3 signaling pathway involving the IP3 receptor ITR-1 is required for the stimulation of pharyngeal pumping in response to food (Walker et al., 2002). The results shown in chapter 3 and 4 suggest that emodepside can inhibit the stimulation of pharyngeal pumping in response to exogenous 5-HT application, suggesting that the anthelmintic could target the IP3/ITR-1 pathway. Such a prediction is especially appealing in view of the proposal that emodepside initially produces a rise in intracellular Ca^{2+} via activation of $G\alpha_q$ in order to activate SLO-1. This is because the $G\alpha_q$ pathway generates IP3, which can bind IP3 receptors to release Ca^{2+} from intracellular stores, and would therefore contribute to such a pathway. However, the *itr-1 (sa73)* mutant did not demonstrate pharyngeal emodepside sensitivity different to that of wild type worms. It is possible that emodepside does not function via the ITR-1 receptor, or that the *sa73* mutation, which is described as a weak loss-of-function (Walker et al., 2002), is not sufficient to affect emodepside activity significantly enough to be visualised with the assay used. Significantly, Walker et al. (2002) did not find that the *sa73* allele altered the stimulation of pharyngeal pumping in response to exogenous 5-HT application, although the stimulation of pumping in response to food was reduced in these mutants. 5-HT can increase pump rate via stimulation of the MC neuron and direct action on the pharyngeal muscle (Avery & Thomas, 1997), and it was suggested that the *itr-1 (sa73)* mutation affects only the neuronal pathway (Walker et al., 2002). Therefore, in the assay used to investigate emodepside sensitivity, the use of 5-HT have masked any alteration to pumping rate due to inhibition of neuronal ITR-1 receptors by emodepside. Repeating the assay using a stronger loss-of-function *itr-1* allele that demonstrates significant alteration in pumping response to 5-HT would aid a more concrete conclusion concerning the role of ITR-1 in the activity of emodepside on the pharynx.

It is clear from the results shown in this chapter, and from previous research by Willson et al. (2004), that the mechanism of action for emodepside in *C. elegans* is intricate and involves many components of the NMJ. It is also clear that SLO-1 has a key role in mediating the activity of emodepside at the pharyngeal NMJ, with the $G\alpha_q$ and $G\alpha_o$ pathways contributing minor roles which may antagonise or complement the effect of the anthelmintic via SLO-1. The relatively minor alteration in the emodepside sensitivity of

the G protein mutants when compared with the resistance of the *slo-1* null, suggests that multiple mechanisms may operate to affect SLO-1 function, and that direct binding of emodepside to the channel may be the major contributor. It is possible that emodepside directly binds to SLO-1 and disrupts regulation of the channel by associated regulatory proteins. BK channels are known to be modulated by associated regulatory proteins, including protein kinases and phosphatases (Chung et al., 1991; Lee et al., 1995; Tian et al., 1998; White et al., 1993). For example, protein kinase A can directly bind the *Drosophila* Slo channel, resulting in down-regulation of channel activity (Wang et al., 1999; Zhou et al., 2002). Therefore, emodepside may modify SLO-1 activity by affecting the ability of channel-regulators to modify channel behaviour.

The results of the assay using the *slo-2 (nf101)* mutant suggest no involvement of SLO-2 in the mechanism of action of emodepside in the pharynx. This is perhaps not surprising as SLO-1 and SLO-2 share only 18% identity in their protein sequences, and it is differences in the structure of SLO-1 and SLO-2 that are believed to produce the differences in the activity of these two channels (Yuan et al., 2000). Significantly, these two channels differ in their Ca^{2+} sensitivity, as SLO-2 requires the presence of both chloride (Cl^-) and Ca^{2+} to activate the channel (Yuan et al., 2000). Negatively charged residues located in the SLO-1 Ca^{2+} bowl are highly conserved amongst SLO-1 channels of invertebrates and vertebrates, and are believed to be important for Ca^{2+} sensing (Schreiber & Salkoff, 1997). However, most of these negative residues are absent in the corresponding region of SLO-2, with some replaced with positive charges which have been shown to mediate the Cl^- sensitivity of the channel (Yuan et al., 2000). Therefore, if emodepside acts to modify the Ca^{2+} sensitivity of SLO-1, then the difference in Ca^{2+} activation exhibited by SLO-1 and SLO-2 may explain why the latter channel is unaffected by emodepside. It is possible that emodepside binds to the extracellular portion of the channel and produces conformational changes in the Ca^{2+} sensing regions that result in an increased affinity of these regions for Ca^{2+}. The BK channel has been shown to possess two high affinity and one low affinity Ca^{2+} binding sites (see chapter 1, section 1.7.7, page 51) and the low affinity site is located in the RCK domain, which has been shown to be mutated in emodepside resistant mutants obtained from a mutagenesis screen (Guest et al., 2007). Therefore, it is possible that emodepside produces conformational changes in the low affinity Ca^{2+} binding site present in the RCK domain,

resulting in this region becoming a high affinity Ca^{2+} binding site, and facilitating the activation of SLO-1.

Interestingly, verticilide, PF1022-888 and PF1022-222, like emodepside, appear to function via the SLO-1 channel and, to a lesser extent, LAT-1. This suggests that the structural similarity between these compounds extends to the mechanism by which they operate to paralyse pharyngeal response to 5-HT. However, PF1022-888 activity did appear to have a reduced dependence on functional *slo-1* expression when compared to the other anthelmintics. By studying the structural differences between PF1022-888 and emodepside, it is possible that additional information could be gained regarding how emodepside utilizes SLO-1 in its mechanism of action.

CHAPTER 6
FURTHER INVESTIGATING THE ROLE OF *slo-1* IN THE MECHANISM OF ACTION OF EMODEPSIDE IN THE *C. elegans* PHARYNX

6.1 Introduction

Based on the results shown in chapter 5 as well as previous research (Willson et al., 2004), it appears that the SLO-1 channel is a key component of the mechanism by which emodepside paralyses pharyngeal pumping in wild type *C. elegans*. How emodepside affects the functioning of SLO-1 to achieve paralysis is not clear from these initial investigations, but it is possible that the anthelmintic activates SLO-1 by binding the channel directly to increase its Ca^{2+} sensitivity and may also act to increase intracellular Ca^{2+} concentration by multiple signaling pathways. In a recent mutagenesis screen for *C. elegans* resistant to the effect of emodepside on locomotion, all the strains obtained fell into a single complementation group mapping closely to the *slo-1* locus on chromosome V (Guest et al., 2007). Also, complementation between the emodepside-resistant strains and the *slo-1(js379)* null reference allele attributed the emodepside resistance in these strains to mutation of *slo-1* (Guest et al., 2007). The finding of only *slo-1* mutations in the mutagenesis screen suggests that emodepside functions primarily by binding directly to SLO-1 and affecting channel activity. To further understand how SLO-1 function is altered in emodepside-stimulated pharyngeal paralysis, it is important to understand the role of the channel and how it operates at the pharyngeal neuromuscular junction (NMJ) in the absence of emodepside.

BK channels, such as SLO-1, are believed to be functionally important for key physiological processes, including neuronal excitability, neurotransmitter release and muscle tone (Marty, 1981; McManus & Magleby, 1991; Pallota et al., 1981). A large body of evidence now suggests that BK channels can operate both presynaptically, postsynaptically or at both locations depending on the species concerned and the location of the synapse within the organism. In the mammalian central nervous system (CNS) mSlo1 channels are localized to the dendrites, cell soma and presynaptic terminals (Knaus et al., 1996). Post-synaptically mSlo1 contributes to the negative-feedback mechanism controlling the timing of Ca^{2+}action potential bursts in the dendrites of cerebellar Purkinje cells (Swensen & Bean, 2003). Pre-synaptically, BK channels such as mSlo1 and SLO-1 have been proposed to provide a homeostatic mechanism for regulating neurotransmitter release, either acting to increase or decrease release depending on the synapse under investigation (Hu et al., 2001; Raffaelli et al., 2004; Sun et al., 2004; Wang et al., 2001; Warbington et al., 1996; Xu & Slaughter, 2005).

In *C. elegans*, presynaptic SLO-1 is believed to contribute to the regulation of neurotransmitter release by exhibiting delayed opening in response to the rise in presynaptic cytosolic Ca^{2+} responsible for depolarization and neurotransmitter release. Opening of SLO-1 channels thereby facilitates membrane repolarization and termination of neurotransmitter release. This is supported by the observed increase in the duration and amplitude of excitatory post-synaptic currents (EPSCs) at the neuromuscular junction (NMJ) of *C. elegans* lacking the SLO-1 channel; suggesting a loss of functional SLO-1 increases neurotransmitter release at the NMJ (Wang et al., 2001). Postsynaptically, SLO-1 has been identified in the *C. elegans* body wall muscle, where it has a critical role in muscle tone, with a loss of channel function resulting in muscle degeneration (Carre-Pierrat et al., 2006).

In the *C. elegans* pharynx, *slo-1* is expressed presynaptically, with examination of extracellular pharyngeal recordings (EPGs) from *slo-1* mutants suggesting that the channel has an integral role in controlling the neurotransmitter release and coordination of isthmus peristalsis and terminal bulb pumping to produce effective pharyngeal functioning (Chiang et al., 2006; Wang et al., 2001). The EPGs of *slo-1* mutants were found to possess larger E1 and IP spikes, indicating an increase in neurotransmitter release from the MC and M3 neurons, respectively, and suggesting a role for SLO-1-mediated termination of neurotransmitter release in these neurons (Chiang et al., 2006; Wang et al., 2001). The reduced efficiency of synaptic transmission in the pharynx of the *unc-64* mutant manifests as a reduction in IPs (inhibitory potentials), but a *slo-1* loss-of-function mutation in the *unc-64* background appeared to compensate for the reduced IP generation of the *unc-64* single mutant, suggesting enhanced M3 neurotransmission in the absence of SLO-1. This further supports a role for SLO-1 in the M3 motor neuron, where the channel acts as a negative controller of glutamate release and thereby contributes to the regulation of pharyngeal muscle repolarization and the timing of pumping (Wang et al., 2001). In agreement with this, *slo-1* loss-of-function mutants in the presence of the 5-HT were found to possess a reduced pharyngeal pump duration when compared to wild type in the same 5-HT concentration, suggesting enhanced M3 glutamate release in the absence of SLO-1 (Wang et al., 2001). However, evidence has also suggested that SLO-1 functions in pharyngeal neurons other than MC and M3. Removal of MC and M3 by laser ablation in the wild type background produces worms with altered EPG recordings,

including the removal of the E1 spike consistent with a loss of MC-stimulated depolarization. However, *slo-1* loss-of-function mutants in which MC and M3 had been ablated still exhibited the E1 spikes, suggesting SLO-1 functions in at least one other neuron than MC and M3 (Chiang et al., 2006). Ablation of the M4 neuron in worms defective for MC and M3 signaling and possessing a *slo-1* loss-of-function mutation was found to inhibit the E1 spike, suggesting that the E1 spikes in the MC/M3-ablated *slo-1* mutants were a result of M4 activity in the absence of SLO-1 (Chiang et al., 2006). During normal pharyngeal pumping, posterior isthmus peristalsis is stimulated by M4, whereas anterior isthmus and terminal bulb contraction is stimulated by gap junction coupling to the corpus. The M4 neuron innervates the terminal bulb, yet stimulation of M4 has no effect on terminal bulb pumping, suggesting that this specific NMJ type is effectively 'silenced' in the wild type worm. However, a *slo-1* loss-of-function mutation in the *eat-5* background (in which gap junctions are mutated to uncouple the terminal bulb and corpus), produces a pharynx in which stimulation of M4 increases terminal bulb pumping, supporting a role for *slo-1* in 'silencing' the M4/terminal bulb NMJ in wild type animals (Chiang et al., 2006).

From the previous research described, SLO-1 appears to function presynaptically in the *C. elegans* pharynx by providing a negative feedback mechanism to terminate neurotransmitter release. A postsynaptic role for the channel has not been demonstrated in the pharynx, and expression of *slo-1* in the pharyngeal muscle is not clear or consistent using a GFP reporter system (Wang et al., 2001). It would be surprising if *slo-1* expression is restricted to only the pharyngeal neurons and not the muscle, as both body wall and vulval muscle have been shown to express *slo-1*, where the channel appears to be functionally important (Wang et al., 2001). For example, the *slo-1 (js118)* null mutant was found to be resistant to the intoxicating effects of ethanol on egg laying and locomotion, and a rescue of both presynaptic and postsynaptic *slo-1* expression in the null background was required to reintroduce the ethanol sensitivity of egg laying behaviour (Davies et al., 2003). However, ethanol inhibition of locomotion appeared to be reliant on only presynaptic expression of the channel, suggesting that evidence of *slo-1* expression postsynaptically may not necessarily indicate a functional role for the channel in certain worm behaviours, and highlighting the need to examine through behavioural analysis whether presynaptic and/or postsynaptic SLO-1 channels facilitate the control of pharyngeal pumping. By identifying specific features of the wild type pharyngeal pump

(recorded by the EPG technique) that were altered in the *slo-1 (js379)* null mutant, these features could then be examined in *slo-1 (js379)* mutants in which *slo-1* expression had been rescued in either the neurons or muscle. This could identify whether SLO-1 has a pre- or postsynaptic role in the control of pharyngeal pumping, and the results of these experiments are shown in this chapter. Expression of *slo-1* in the nervous system was achieved by injecting into the *slo-1 (js379)* gonad of an expression construct containing the *slo-1* gene behind the synaptobrevin (*snb-1*) promoter (kindly provided by M. Guest). Stable lines expressing the transgene were propagated from the injected worms. Expression of *slo-1* in the pharyngeal muscles of the *slo-1 (js379)* was achieved by the same technique, except that the expression construct contained the myosin class II heavy chain (*myo-2*) promoter (see chapter 2, section 2.6.2, page 63). Importantly, the effect of emodepside on these transgenic worms was examined to identify whether the anthelmintic acts via presynaptic and/or postsynaptic SLO-1 to paralyse pumping behaviour, and thereby providing further insight into the mechanism of action used by emodepside.

As explained previously, ethanol can inhibit *C. elegans* locomotion and egg laying behaviour (Davies et al., 2003). Ethanol intoxication has been shown to change the behaviour of a large number of invertebrate and mammal species, but the molecular mechanisms responsible remain unclear. The synapse is believed to be a major site of ethanol activity (Pocock & Richards, 1991; Franks & Lieb, 1994), with specific synaptic proteins identified as ethanol targets *in vitro*, including glutamate receptors, Ca^{2+} channels and neurotransmitter transporters (Diamond & Gordon, 1997; Harris, 1999). In *C. elegans*, a screen of mutagenised *C. elegans* capable of normal locomotion or egg laying behaviour in the presence of 400mM ethanol revealed a central role for the SLO-1 channel in the intoxication of *C. elegans* (Davies et al., 2003). Therefore, it is possible the apparently significant role for *slo-1* in the response of *C. elegans* locomotion and egg laying to ethanol (Davies et al., 2003) may also extend to pharyngeal pumping, which was shown to be affected by emodepside in chapter 3 and 4. Therefore, by determining the effect of ethanol on pharyngeal pumping and the role of SLO-1 in any effect, this would not only reveal a physiological behaviour in addition to locomotion and egg laying that is affected by ethanol via SLO-1, but would also reveal a further parallel between the activity of ethanol and emodepside.

Although EPGs can provide detailed information on the role of *slo-1* in the behavioural consequences of emodepside at the pharynx; yielding information on both the activity of the pharyngeal muscles and neurons, EPGs can not reveal whether emodepside is affecting SLO-1 channel activity itself. Such information is crucial to improving understanding of the mechanism of action of emodepside, as well as the functional role of *slo-1* at the pharyngeal NMJ. Activation of the SLO-1 current by ethanol was observed in excised patches of wild type *C. elegans* VA motor neurons, which directly control worm locomotion (Davies et al., 2003). Additionally, neuronal recordings from the *slo-1* gain-of-function mutant, which phenocopies ethanol intoxicated wild type locomotion and egg laying, have revealed that the SLO-1 channel has an increased frequency of opening. These results have strongly suggested that ethanol affects *C. elegans* locomotory behaviour, at least partially, by alteration of SLO-1 channel activity (Davies et al., 2003). Therefore, it is possible that emodepside can also alter SLO-1 channel activity, and to investigate this, patch clamp recordings from the terminal bulb muscle cells of wild type and *slo-1 (js379)* null *C. elegans* exposed to emodepside were compared. As postsynaptic expression of *slo-1* in the pharynx is not evident (Wang et al., 2001), it is possible that the wild type muscle cells will not exhibit a SLO-1 current, therefore, the transgenic *slo-1 (js379)* null *C. elegans* expressing *slo-1* in the pharyngeal muscle was also examined in the presence of emodepside. In effect, this experiment will not only provide further detail regarding the action of emodepside on SLO-1 channel conductance, but will also confirm whether a SLO-1 current is present in the muscle cells of the terminal bulb in wild type *C. elegans*. The results of these experiments are shown in this chapter.

6.2 The role of *slo-1* in the pumping activity of the *C. elegans* pharynx

Initial comparison of pharyngeal pumping by the wild type and *slo-1 (js379)* pharynx in Dent's saline (4ml min^{-1} perfusion) using the EPG demonstrated no significant difference in mean pumping rate; the wild type pharynx produced 13 pumps/minute, and the *slo-1(js379)* pharynx produced 16 pumps/minute (see figure 6.1(a)). However, measurement of pump duration revealed the *slo-1 (js379)* pumps to be significantly longer than for wild type ($P<0.05$, see figure 6.1(b)). The wild type pharynx produced pumps 187 ms long (mean ± 8), whereas the *slo-1 (js379)* pharynx produced pumps 245 ms long (mean ± 15). Examination of pump shape also revealed another subtle difference between the two strains, as *slo-1 (js379)* pumps were found to contain significantly less inhibitory potentials (IPs) than wild type pumps ($P<0.001$, see figure 6.1(c)). Wild type *C. elegans* pumps contained a mean of four IPs, whereas the *slo-1 (js379)* pumps contained a mean of one IP.

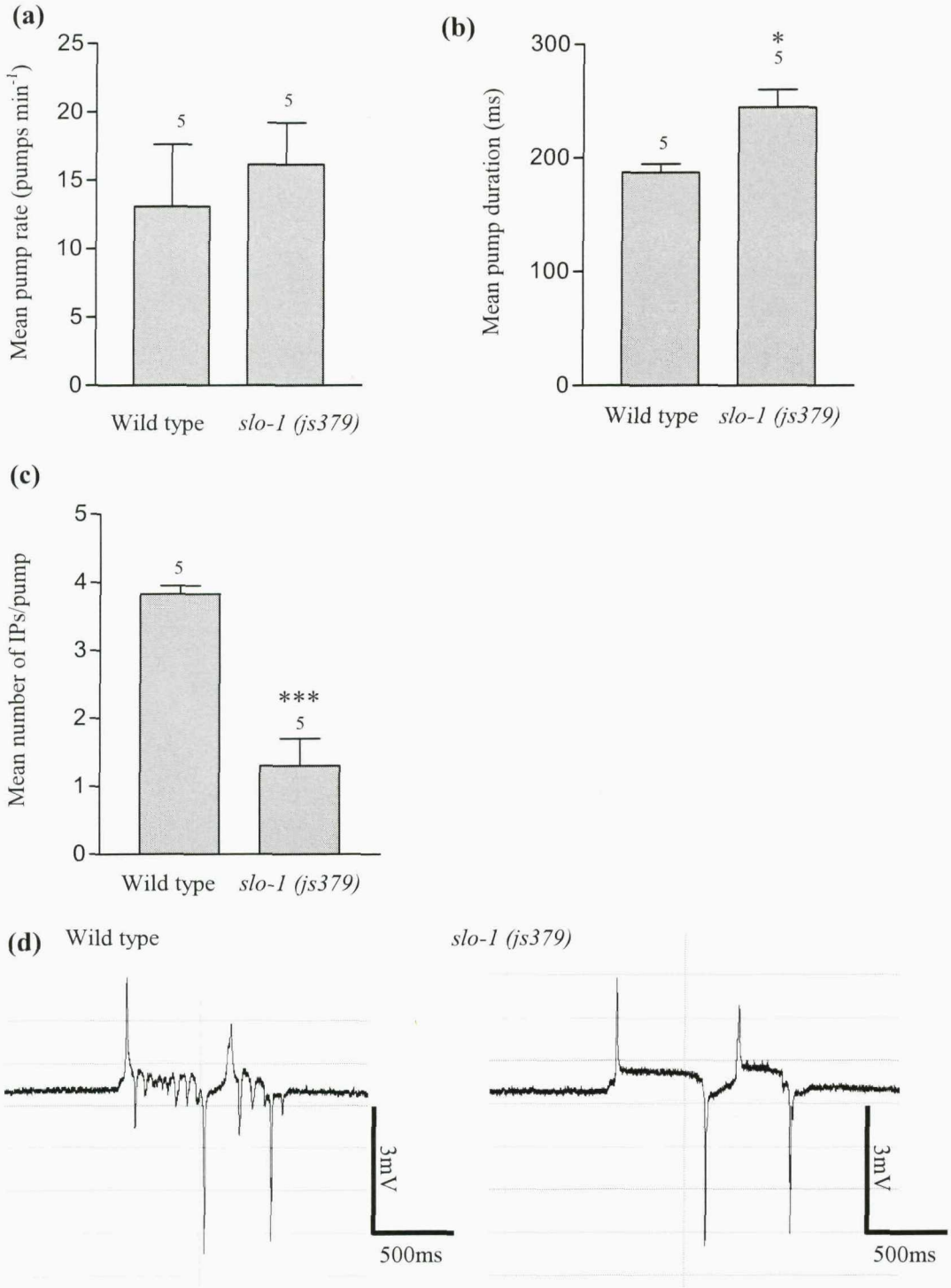

Figure 6.1 Analysis of the *slo-1 (js379)* pharyngeal pumping phenotype using the EPG.
(a) Graph comparing wild type and *slo-1 (js379)* pump rate. Recordings were for 5 minutes in Dent's saline perfusing at 4ml min^{-1}. Each bar is the mean ± S.E.Mean of 5 worms. (b) Graph comparing wild type and *slo-1 (js379)* pump duration. Each bar is the mean ± S.E.Mean of 5 worms, at least 10 pumps per worm analysed. Significance (Student's t test) relates to comparison of wild type and *slo-1 (js379)* mean pump duration, *P<0.05, n = 5 worms. (c) Graph comparing the number of inhibitory potentials (IPs) per pump from wild type and *slo-1 (js379)*. Each bar is the mean ± S.E.Mean of 5 worms. Significance (Student's t-test) relates to comparison of wild type and *slo-1 (js379)* mean IP number, ***P<0.001, n = 5. (d) Example EPGs for wild type (left) and *slo-1 (js379)* (right). Notice that the wild type pumps contain 5 IPs (left pump) and 3 IPs (right pump), whereas the *slo-1 (js379)* pumps contain zero IPs (left pump) and 1 IP (right pump). All pharyngeal preparations were recorded for 5 minutes in Dent's saline (perfusion 4ml min^{-1}).

Another subtle phenotypic difference between the activity of the wild type and *slo-1 (js379)* pharynx is the pattern of pumping. In Dent's saline (4ml min^{-1} perfusion), pumps produced by the wild type pharynx occur mostly as single events or cluster together in groups of two or three. However, *slo-1(js379)* pharynx preparations demonstrated a different pattern of pumping in identical conditions, with pumps occurring in groups containing a much larger number of pumps, and single pumps were very uncommon. To analyse these observations more accurately, all the pumps occurring in five minute EPG recordings of wild type and *slo-1(js379)* pharynx preparations in Dent's saline (4ml min^{-1} perfusion) were measured to calculate the time between them. Pumps were said to be 'grouped' if the R2 spike (or R1 spike if R2 is not evident) of the initial pump occurs 200ms or less before the E1 spike (or E2 spike if E1 is not evident) of the following pump (see figure 6.2).

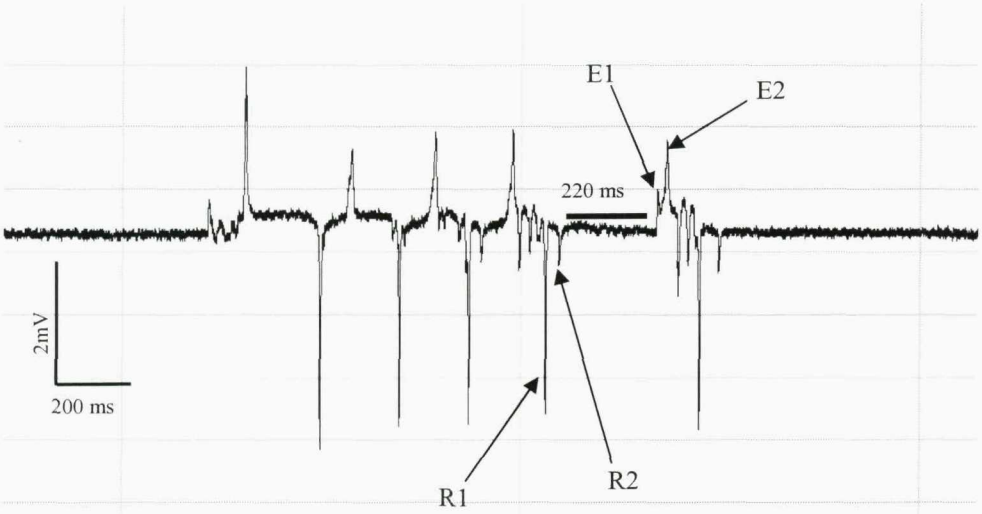

Figure 6.2 Measuring the pattern of pharyngeal pumping by wild type *C. elegans* in Dent's saline. This recording was made using a wild type *C. elegans* preparation. The first four pumps clearly form a group as they are approximately 60 ms or less apart. However, the fifth pump is slightly separated from the initial four, therefore, is this pump part of the same group, or is it a single event? Measuring from the finish of the R2 spike of the fourth pump and the start of the E1 spike of the fifth pump reveals that these two pumps are 220 ms apart. Therefore, the fifth pump is described as a single event using the definition system adopted.

This analysis revealed that 48% of pumps produced by wild type *C. elegans* were single events, compared to just 0.2% of pumps by *slo-1 (js379)*. A large proportion of pumps produced by *slo-1 (js379)* were in groups containing ten or more events (45%), whereas such large groups were not observed at all in the wild type recordings. In fact, 96% of all pumps by the wild type pharynx occurred in groups of three events or less, contrasting

starkly with *slo-1 (js379)* where 91% of pumps occurred as groups of four events or more (see figure 6.3).

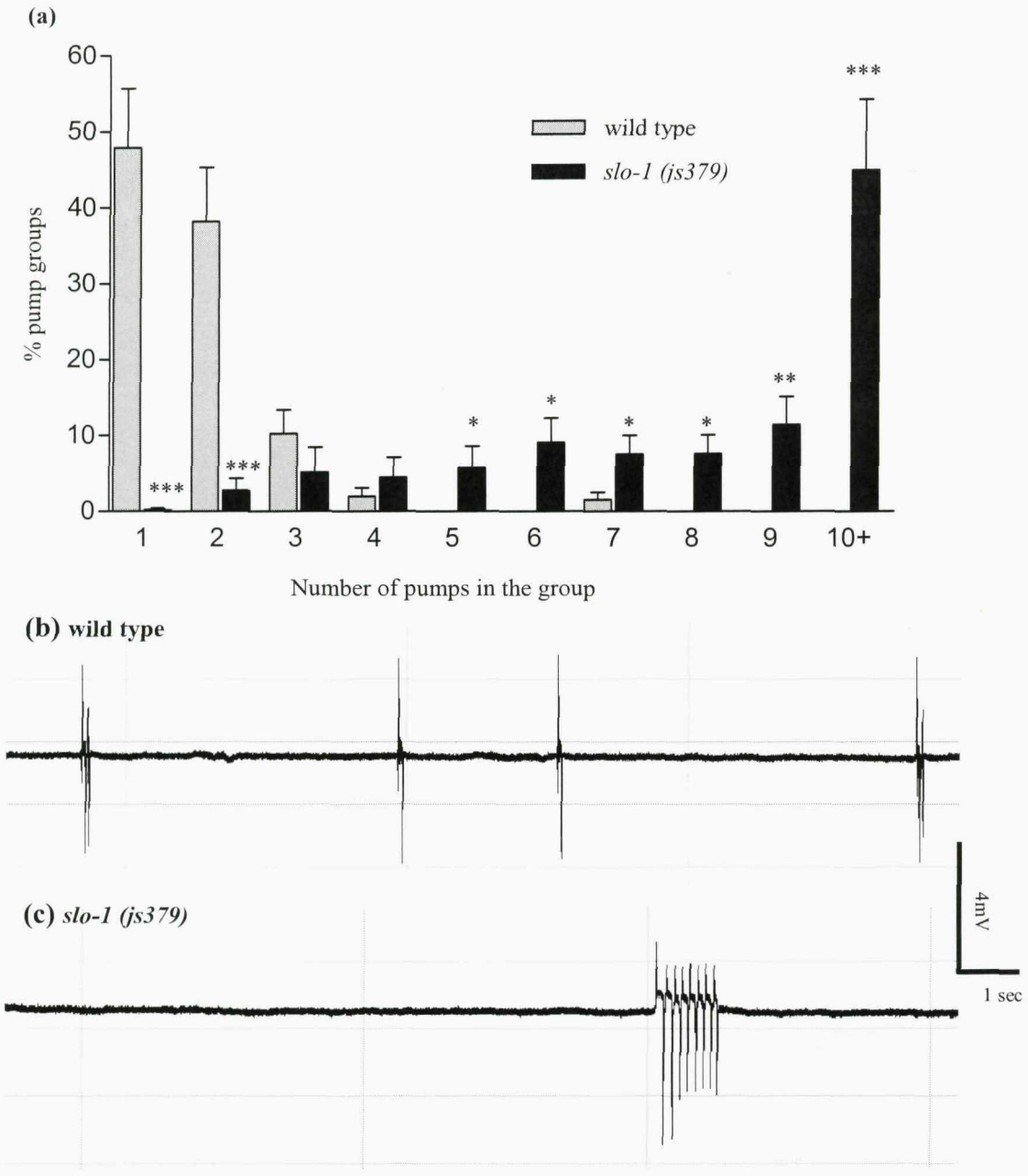

Figure 6.3 Wild type and *slo-1 (js379)* pharyngeal pumping pattern in Dent's saline.
(a) Graph comparing wild type and *slo-1 (js379)* pharyngeal pump grouping. Each bar is the mean ± S.E.Mean of 16 worms. Statistical significance (Student's t-test) relates to a comparison of the % of pump groups produced by the wild type and *slo-1(js379)* pharynx that have a specific number of pumps in the group, *P<0.05; **P<0.01; ***P<0.001, n = 16 worms. Each pharynx was recorded for 5 minutes in Dent's saline (perfusion 4ml min^{-1}). (b) An example of a section from a recording of a wild type pharynx, showing 6 pumps. Notice that 2 pumps are single events, and there are 2 groups of 2 pumps. (c) An example of a section from a recording of a *slo-1 (js379)* pharynx, showing a group of 8 pumps. All pharyngeal preparations were recorded for 5 minutes in Dent's saline (perfusion 4ml min^{-1}).

To examine whether *slo-1* has a postsynaptic and/or presynaptic role in the pharynx, *slo-1* expression in the *slo-1 (js379)* null was rescued in either the nervous system (including pharyngeal nervous system) or the pharyngeal muscles, and the effect of this on pharyngeal pump duration, the number of inhibitory potentials (IPs) per pump and the pattern of pumping, all previously shown to be affected by *slo-1* expression, was examined. Stable lines of *slo-1 (js379) C. elegans* in which presynaptic *slo-1* expression is rescued by the injection of a plasmid containing the *slo-1a* sequence behind the *snb-1* (synaptobrevin) promoter were available to examine the presynaptic activity of SLO-1 (Guest et al., 2007). However, a transgenic line of *slo-1 (js379) C. elegans* in which *slo-1* expression is rescued in the pharyngeal muscles had to be created to enable investigation of the postsynaptic role of SLO-1 in the pharynx.

6.3 Generation of transgenic *C. elegans* in which *slo-1* is expressed in pharyngeal muscle

A construct to drive expression of *slo-1* in the pharyngeal muscles was made by placing the *slo-1a* sequence (*slo-1* splice variant a) from the pBK3.1 plasmid (Wang et al., 2001; kindly provided by L. Salkoff) behind the *myo-2* promoter of the pPD30-69 plasmid (kindly provided by A. Fire). The *myo-2* gene encodes myosin class II heavy-chain and is expressed in pharyngeal muscle (Ardizzi & Epstein, 1987).

Initially, the *slo-1a* sequence was digested from the pBK3.1 plasmid using a triple restriction digest with the restriction enzymes Xba1, Apa1 and Nhe1. Following the digest the plasmid fragment containing the *slo-1* sequence was isolated by agarose gel electrophoresis (see figure 6.4, for method details see chapter 2, section 2.6.2, page 63).

(a) pBK3.1 digestion

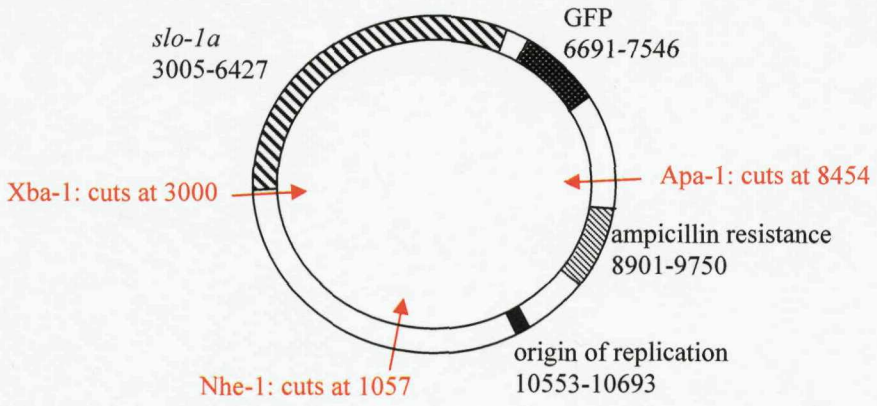

(b) Predicted three fragments

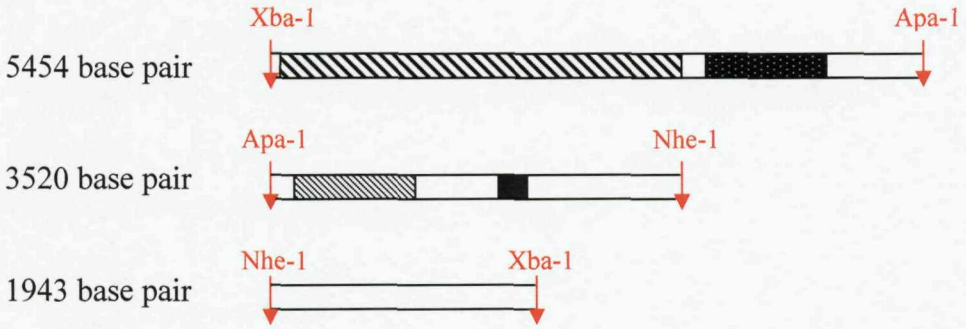

(c) Digestion results

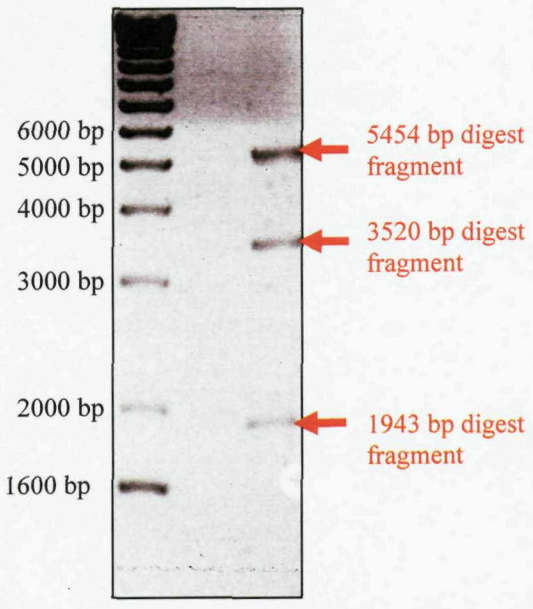

(d) Purification results

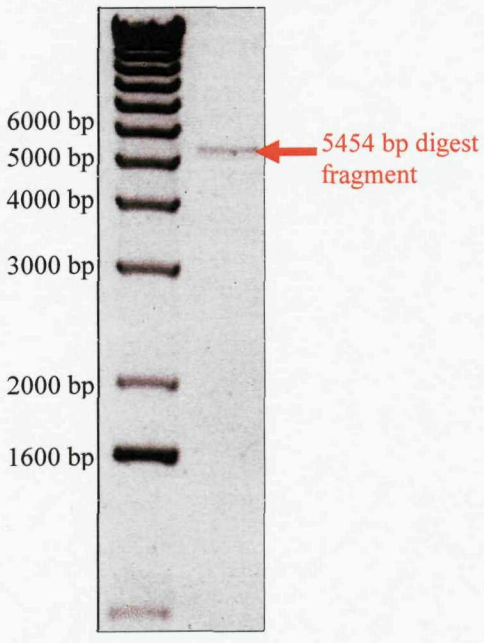

Figure 6.4 Isolation of the *slo-1a* sequence from the pBK3.1 plasmid.
(a) Schematic of pBK3.1 showing the positions at which the three restriction enzymes cut the plasmid in relation to the *slo-1a* sequence. Sites of enzyme cleavage and gene start/finish sites are given in base pairs from origin of replication. **(b)** Schematic of the three fragments predicted from the triple digestion of pBK3.1. **(c)** The three fragments were isolated by agarose gel electrophoresis. **(d)** The 5454 base pair fragment was cut from the gel in (c) and purified. A portion of the purified product was subjected to agarose gel electrophoresis to confirm it as the 5454 base pair fragment.

The pPD30-69 plasmid contains the *myo-2* promoter sequence and transcription start sequence that can drive specific expression in the pharyngeal muscles (Okkema et al., 1993). To prepare pPD30-69 for ligation with the pBK3.1 fragment possessing the *slo-1a* sequence, pPD30-69 was digested to remove the *unc-54* 3' UTR (untranslated) sequence. Removal of the unc-54 3' UTR would allow the *slo-1a* sequence to be ligated into pPD30-69 behind the *myo-2* promoter and transcription start site. To achieve this, a double restriction enzyme digest using the enzymes Apa-1 and Nhe-1 was performed and the plasmid fragment containing the *myo-2* promoter and transcription start site was isolated by agarose gel electrophoresis (see figure 6.5, for method details see chapter 2, 2.6.2, page 63).

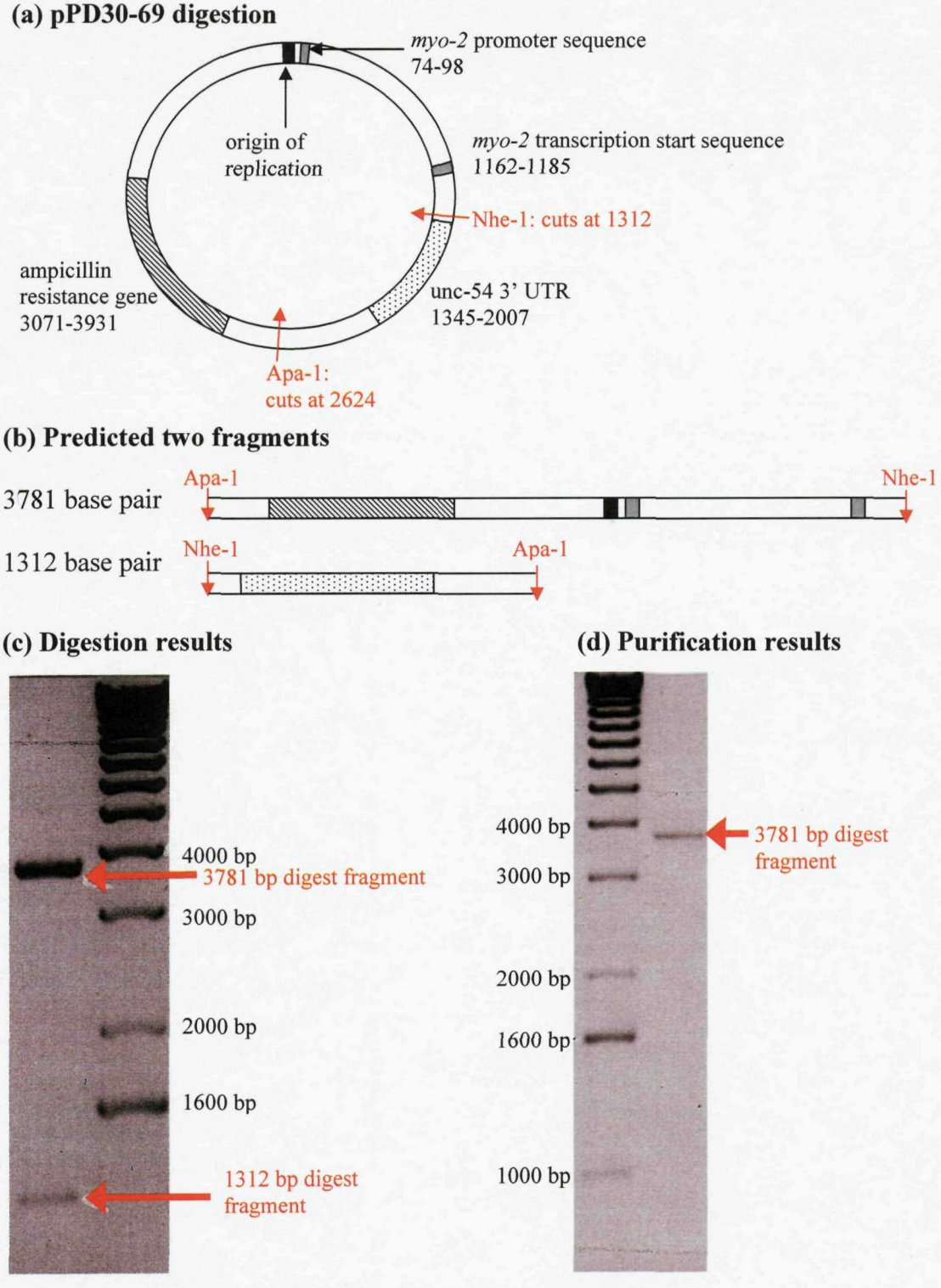

Figure 6.5 Isolation of the *myo-2* sequences from the pPD30-69 plasmid.
(a) Schematic of pPD30-69 showing the positions at which the two restriction enzymes cut the plasmid in relation to the *myo-2* sequences. Sites of enzyme cleavage and gene start/finish sites are given in base pairs from origin of replication. **(b)** Schematic of the two fragments predicted from the double digestion of pBK3.1. **(c)** The two fragments were isolated by agarose gel electrophoresis. **(d)** The 3781 base pair fragment was cut from the gel in (c) and purified. A portion of the purified product was subjected to agarose gel electrophoresis to confirm it as the 3781 base pair fragment.

The *slo-1a* fragment of pBK3.1 and the *myo-2* fragment of pPD30-69 were ligated to produce the new plasmid (see figure 6.6 (a), for method details see chapter 2, section 2.6.2, page 63). Although Apa-1 and Xba-1, rather than Apa-1 and Nhe-1 were used to generate the *slo-1a* pBK3.1 fragment, this would be capable of ligating into the *myo-2* promoter fragment of pPD30-69 because Xba-1 and Nhe-1 cleave to give complementary DNA ends (see figure 6.6 (b)).

(a) The new plasmid

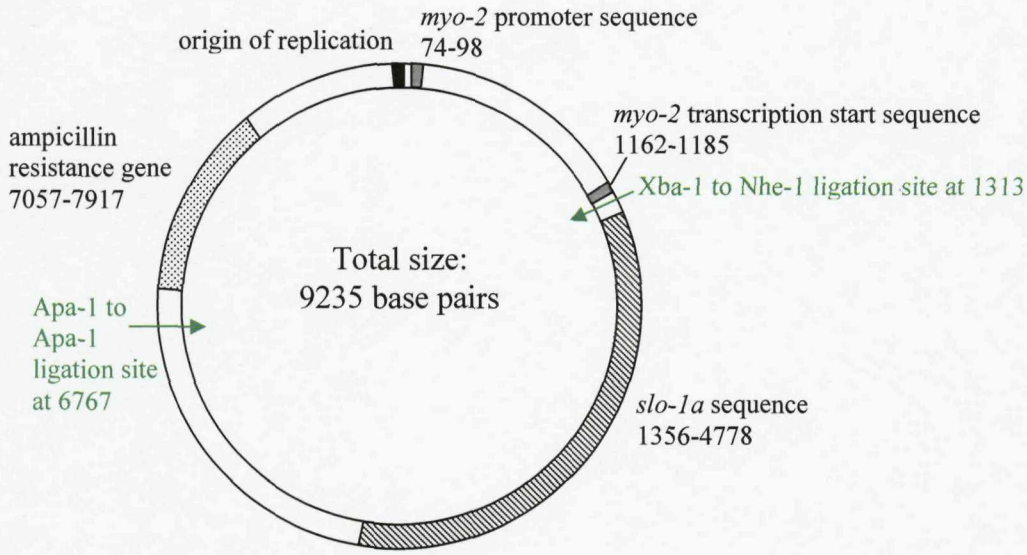

(b) Xba-1 and Nhe-1 cleave to give complementary DNA ends

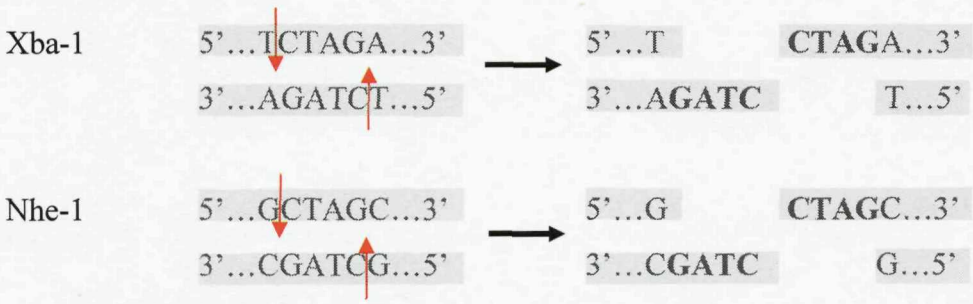

Figure 6.6 Ligation of the *slo-1a* pBK3.1 fragment and *myo-2* promoter fragment of pPD30-69
(a) The new plasmid created by the ligation showing the positions of the two ligation sites (green arrows and text). Gene start/finish sites and the ligation sites are given in base pairs from origin of replication. **(b)** Although Xba-1 and Nhe-1 recognise different cleavage sites, they cut to give 3' DNA 'sticky ends' that are complimentary (in bold), thereby allowing ligation. The red arrows represent cleavage sites.

To increase the quantity of plasmid generated by the ligation, DH5α bacterial cells were transformed with the newly constructed plasmid and allowed to proliferate (for method details see chapter 2, section 2.6.2, page 63). Ten colonies were produced, and a restriction digest using the enzyme HindIII was performed on a small sample of the DNA prepared from each of the colonies to confirm that they contain the new construct, (see figure 6.7, for method details see chapter 2, section 2.6.2, page 63). HindIII is predicted to cut the new construct in two positions to generate two fragments of different sizes (see figure 6.7).

(a) HindIII digest of the new plasmid

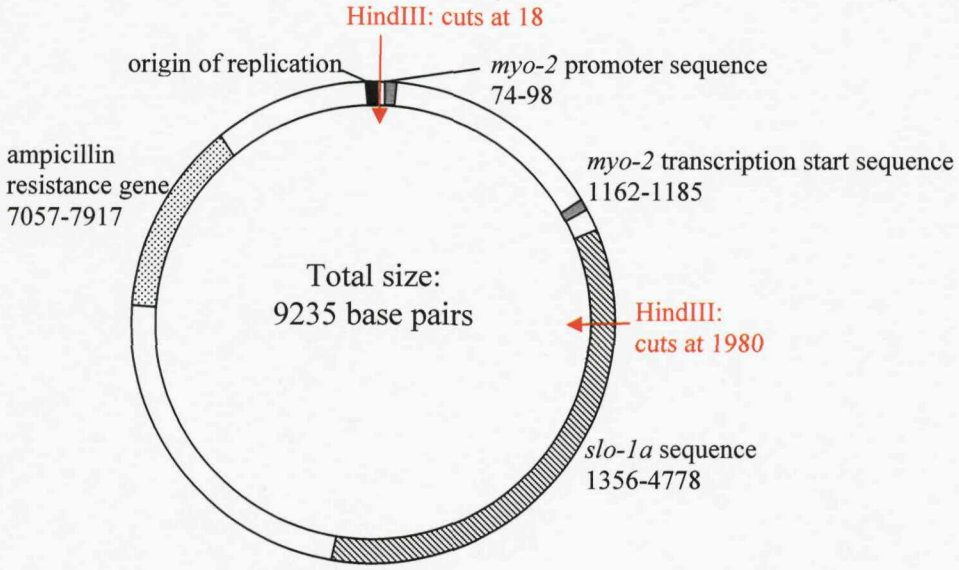

(b) Predicted two fragments

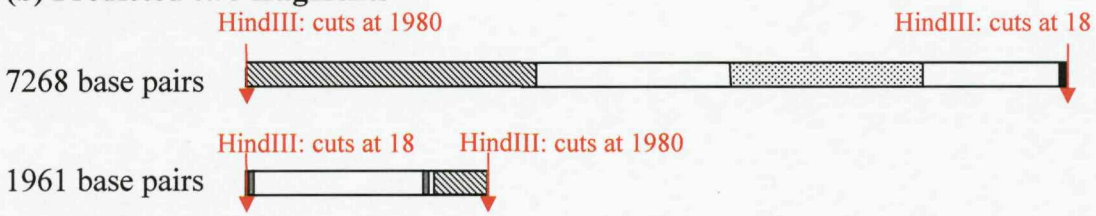

(c) Digest of DNA extracted from the ten DH5α bacteria colonies

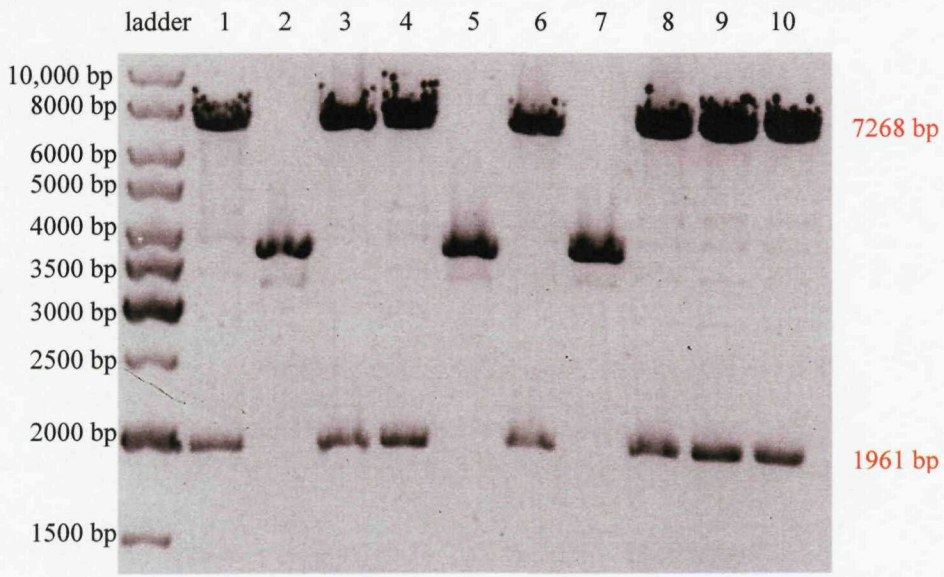

Figure 6.7 Restriction enzyme digest of DNA from transformed DH5α bacteria colonies to confirm the presence of the new plasmid. (a) Schematic of the new plasmid showing the positions at which HindIII cuts. Sites of enzyme cleavage and gene start/finish sites are given in base pairs from origin of replication. **(b)** Schematic of the two fragments predicted from the digestion of the new plasmid. **(c)** Left lane shows 1Kb DNA ladder. Seven of the DH5α colonies (colony 1, 3, 4, 6, 8, 9, and 10) contain the new plasmid.

C. elegans were injected with two constructs: the new plasmid containing the *slo-1a* sequence under the control of the *myo-2* promoter (*myo-2::slo-1*), as well as a reporter construct possessing the *gfp* sequence behind the myo-2 promoter. Therefore, transfected worms could be identified from their green fluorescent pharyngeal muscles, and these worms were likely to possess the *myo-2::slo-1* plasmid as well (see chapter 2, section 2.6.2, page 63 for details on the injection method). Of the 50 worms injected, one produced progeny demonstrating GFP fluorescence. These progeny were transferred to a new plate for further culturing. The incidence of plasmid inheritance was approximately 20% of the progeny produced. When the food had been depleted on an agar plate, fluorescent worms were identified and transferred individually to a new plate to prevent loss of the strain.

6.4 The role of *slo-1* in the pumping activity of the *C. elegans* pharynx when expressed in the pharyngeal neurons or muscles

Expression of *slo-1* in the pharyngeal nervous system of *slo-1 (js379)* null *C. elegans* (described as *slo-1 (js379); snb-1::slo-1*) fully rescued the mean pump duration to resemble the wild type phenotype (see figure 6.8(a) and (b)). However, *slo-1* expression in the pharyngeal muscles of *slo-1 (js379)* worms (described as *slo-1 (js379); myo-2::slo-1*) did not restore pump duration to that of wild type, with the mean duration for wild type and *slo-1 (js379); myo-2::slo-1* remaining significantly different ($P<0.05$, see figure 6.8(a) and (b)).

Interestingly, both the *slo-1 (js379); snb-1::slo-1* mutant and the *slo-1 (js379); myo-2::slo-1* mutant have a mean of one IP per pharyngeal pump, the same as the *slo-1 (js379)* null. Therefore, the mean number of IPs per pump for all three of the *slo-1 (js379)* mutant strain variations are significantly different to wild type ($P<0.001$), but not significantly different to each other (see figure 6.8(c)).

(a)

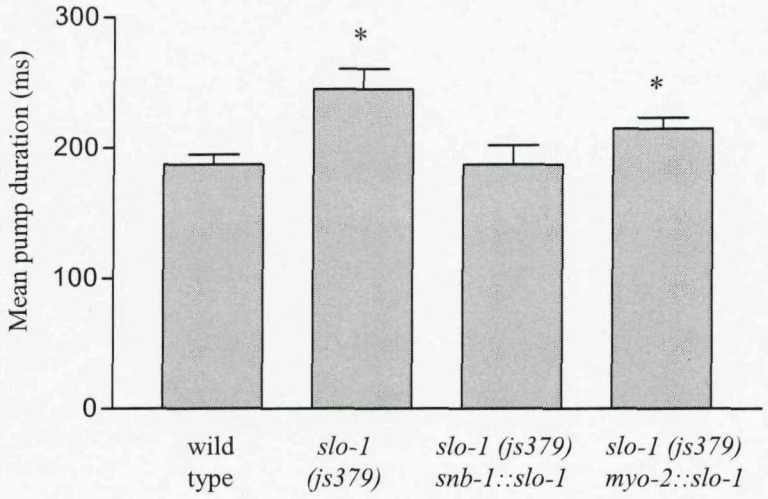

(b)

	mean pump duration (mS)
wild type	187
slo-1 (js379)	245
slo-1 (js379); snb-1::slo-1	187
slo-1 (js379); myo-2::slo-1	215

(c)

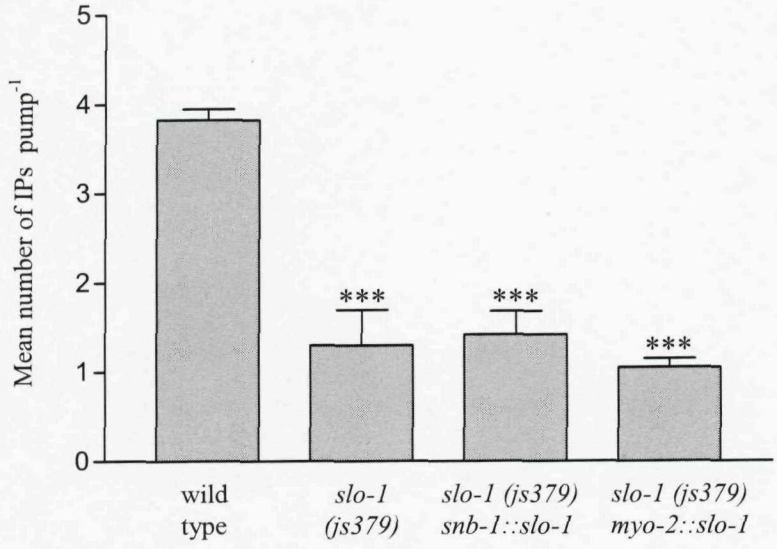

Figure 6.8 The effect of *slo-1* expression in either neurons or pharyngeal muscle on pump duration and IP number.

(a) Graph showing the effect of *slo-1* expression site on pharyngeal pump duration. Each bar is the mean ± S.E.Mean of 5 worms, at least 10 pumps measured per worm. Significance (Student's t-test) relates to comparison of mean pump duration of the *slo-1* mutant strains with wild type; *P<0.05, n = 5 worms per strain. **(b)** The mean pump durations for all four worm strains are given. Notice that the wild type and the *slo-1 (js379); snb-1::slo-1* pharynx have identical mean pump durations. **(c)** Graph showing the effect of *slo-1* expression site on the number of IPs per pump. Each bar is the mean ± S.E.Mean of 5 worms, at least 10 pumps per worm analysed. Significance (Student's t-test) relates to a comparison of mean IP number for the *slo-1* mutant strains and wild type; ***P<0.001, n = 5 worms per strain. All pharyngeal preparations were recorded for 5 minutes in Dent's saline (perfusion 4ml min^{-1}).

The effect of SLO-1 synaptic location on the pattern of pumping (the clustering of pumps in groups) was also examined using the *slo-1 (js379)* transgenic strains *slo-1 (js379); snb-1::slo-1* and *slo-1 (js379); myo-2::slo-1* (see figure 6.9). Expression of *slo-1* in the neurons results in a significant decrease in the number of large groups of pumps (ten or more pumps per group) that are found in the *slo-1 (js379)* null ($P<0.001$). There is also a significant increase in the number of single pumps ($P<0.001$) and groups of two pumps ($P<0.01$) in the *slo-1 (js379); snb-1::slo-1* mutant compared to the *slo-1 (js379)* null. This suggests neuronal expression of *slo-1* enables a partial recovery of the wild type pumping phenotype. Expression of *slo-1* in the pharyngeal muscle results in a significant increase in the number of single pumps ($P<0.001$) and groups of two pumps ($P<0.01$) compared to the *slo-1 (js379)* null. However, the *slo-1 (js379); myo-2::slo-1* mutant produces large groups of ten or more pumps to a statistically similar extent as both the wild type and *slo-1 (js379)* null phenotype, suggesting that pharyngeal muscle expression of *slo-1* does not achieve the level of wild type phenotype recovery achieved by neuronal *slo-1* expression.

In summary, the *slo-1 (js379)* pharynx demonstrates a significantly longer mean pump duration than the wild type pharynx. Neuronal expression of *slo-1* in the *slo-1 (js379)* null background restores the wild type pump duration. EPG recordings from the *slo-1 (js379)* pharynx also demonstrate significantly less IPs than the wild type, a phenotype that persists despite expression of *slo-1* in the neurons or the pharyngeal muscles. The *slo-1 (js379)* null mutant also produces a pattern of pumping distinct from that of the wild type, with pumps in the mutant pharynx occurring more frequently as part of clusters, rather than as single events. A wild type pattern of pumping is partially restored by neuronal expression of *slo-1* in the *slo-1 (js379)* mutant, and to a lesser extent by muscle expression of *slo-1* in the null mutant.

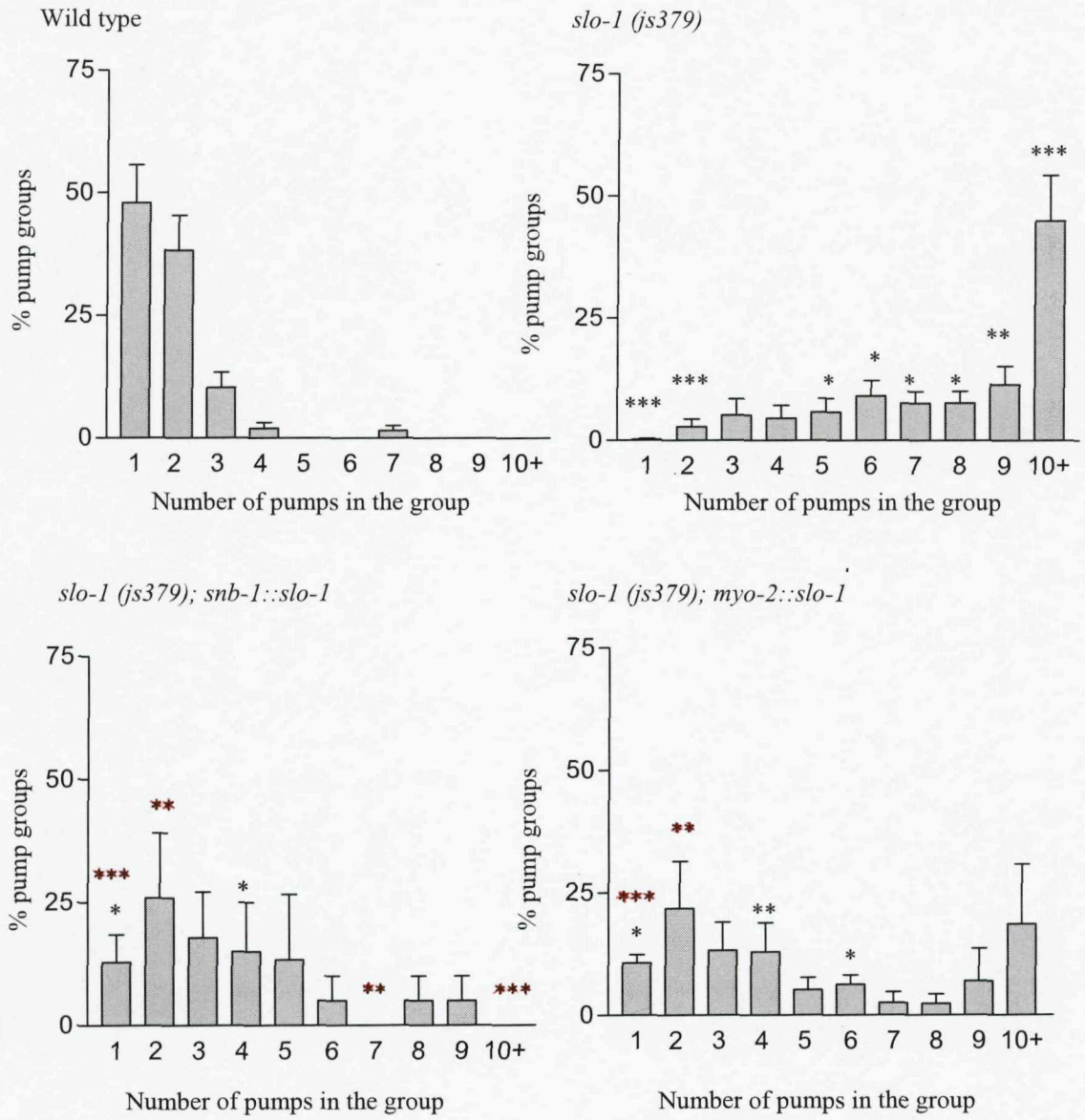

Figure 6.9 The effect of synaptic *slo-1* expression site in the pharynx on the grouping of pumps. Each pharynx preparation was recorded in Dent's saline (4ml min^{-1} perfusion) for 5 minutes. Pump grouping was measured as previously described. Student's t test was used to compare the three *slo-1* mutants with the wild type (black stars) and to compare the two transgenic strains with the *slo-1 (js379)* null (red stars). ***P<0.001; **P<0.01; *P<0.05; n = 16 worms (wild type), 16 worms (*slo-1 (js379)* null), 5 worms (*slo-1 (js379); snb-1::slo-1*), 5 worms (*slo-1 (js379); myo-2::slo-1*).

6.5 Investigating the role of *slo-1* in the ethanol sensitivity of the *C. elegans* pharynx using the electropharyngeogram

Initially it was important to identify any effect of ethanol on pharyngeal pumping in wild type *C. elegans*, before investigating a role for the SLO-1 channel in mediating ethanol activity. Using the EPG technique, a protocol was devised in which the pharyngeal preparation was immersed in a perfusing solution of Dent's saline for five minutes, followed by perfusion of an ethanol solution (10mM to 300mM) for ten minutes, and then a final perfusion of Dent's saline for five minutes (perfusion rate was constant throughout at 4ml min^{-1}). Perfusion was used to stimulate a pumping rate that would enable accurate analysis of any effect of ethanol on the pumping phenotype. A perfusion system was also employed because the highly volatile nature of ethanol meant that there was a strong concern that during a ten minute application of an ethanol solution a significant proportion would evaporate, rendering the results obtained inaccurate. To test the actual evaporation of ethanol from the 1ml recording chamber over a period of ten minutes, five solutions of a known ethanol concentration (100-500mM) were allowed to stand at room temperature for ten minutes and then measured for their ethanol content. The results of this assay demonstrated that up to 29% of the ethanol content evaporated from the recording chamber during a ten minute application of a static 1ml ethanol solution (assay results and ethanol calibration graph are shown in chapter 2, section 2.9, page 76). Due to the high level of ethanol evaporation from the recording chamber, a perfusion system was assembled to enable a constant flow of solution during EPG recording. The benefit of such a system was to minimise ethanol evaporation by ensuring a constant flow of fresh ethanol solution from a sealed container.

The wild type *C. elegans* pharynx demonstrated a concentration-dependent change in the amplitude of the E2 phase of each pump during ethanol exposure (see figure 6.10). The E2 phase is associated with the depolarization of the pharyngeal muscle cell basal membranes and the commencement of pharyngeal muscle contraction (Franks et al., 2006). E2 phase measurements were taken from the base line of the recording to the top-most point of the E2 phase spike.

The lowest ethanol concentration at which a significant change in E phase amplitude was observed was 20mM ($P < 0.05$), which is a physiologically relevant concentration in terms of human intoxication because the legal driving limit is 21.7mM blood ethanol (0.1% blood alcohol). Control experiments were performed using an identical protocol except that only Dent's saline was applied during the ten minute period instead of an ethanol solution.

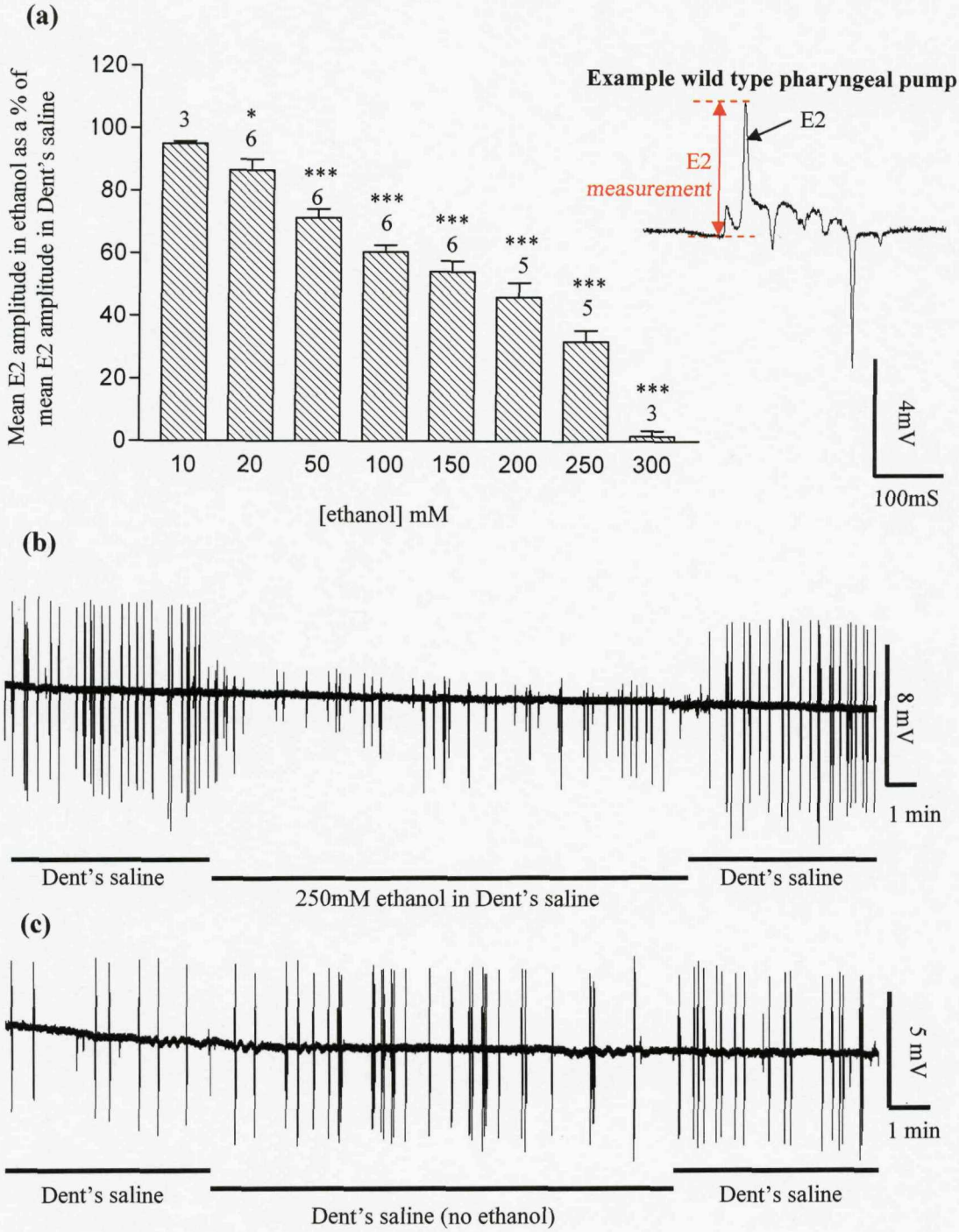

Figure 6.10 The effect of ethanol on pharyngeal pump E2 amplitude in wild type *C. elegans*.
(a) Graph showing the effect of ethanol on E2 amplitude. Each bar is the mean ± S.E.Mean of (n) determinations. Significance (Student's t-test) relates to a comparison of recordings in which ethanol was applied to control experiments (no ethanol applied), *** $P<0.001$, * $P<0.05$, n numbers given above each bar. Inset: a typical wild type pharyngeal pump is shown with the E2 phase indicated. (b) Typical EPG recording from a wild type pharynx exposed to 250mM ethanol. Notice the reduction in E2 amplitude during ethanol application. (c) Typical control EPG recording (wild type). Notice that there is no change in E2 during the recording.

Importantly, the reduction in E2 amplitude during ethanol exposure appeared to be reversible, as can be seen in the example recording in figure 6.10 (b), and in figure 6.11.

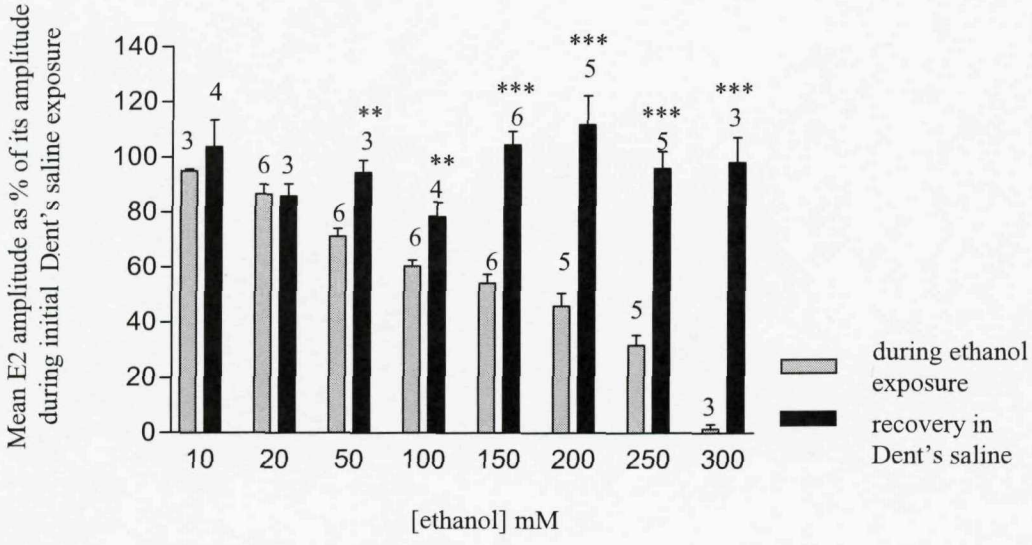

Figure 6.11 The reversibility of the effect of ethanol on E2 amplitude in wild type *C. elegans*. Graph showing that the inhibition of E2 amplitude during ethanol exposure is reversed within 5 minutes of ethanol removal. Each bar is the mean ± S.E.Mean of (n) determinations. Significance (Student's t-test) relates to comparison of mean E2 amplitude during ethanol exposure and during recovery, *** P<0.001, **P<0.01, * P<0.05, n numbers given above each bar.

To investigate whether the SLO-1 channel has a role in the ethanol-stimulated reduction in pharyngeal pump E2 amplitude, the *slo-1 (js379)* null mutant was tested using an identical protocol. The *slo-1 (js379) C. elegans* pharynx preparations demonstrated a concentration-dependent reduction in E2 amplitude during ethanol exposure (figure 6.12 (a)). The lowest ethanol concentration at which a significant change in amplitude was observed was 50mM (P<0.05). Comparison of the wild type response to ethanol shown in figure 6.10(a) and the *slo-1 (js379)* response shown in figure 6.12 (a), appears to suggest that the effect of ethanol on E2 amplitude was not significantly different between the two strains

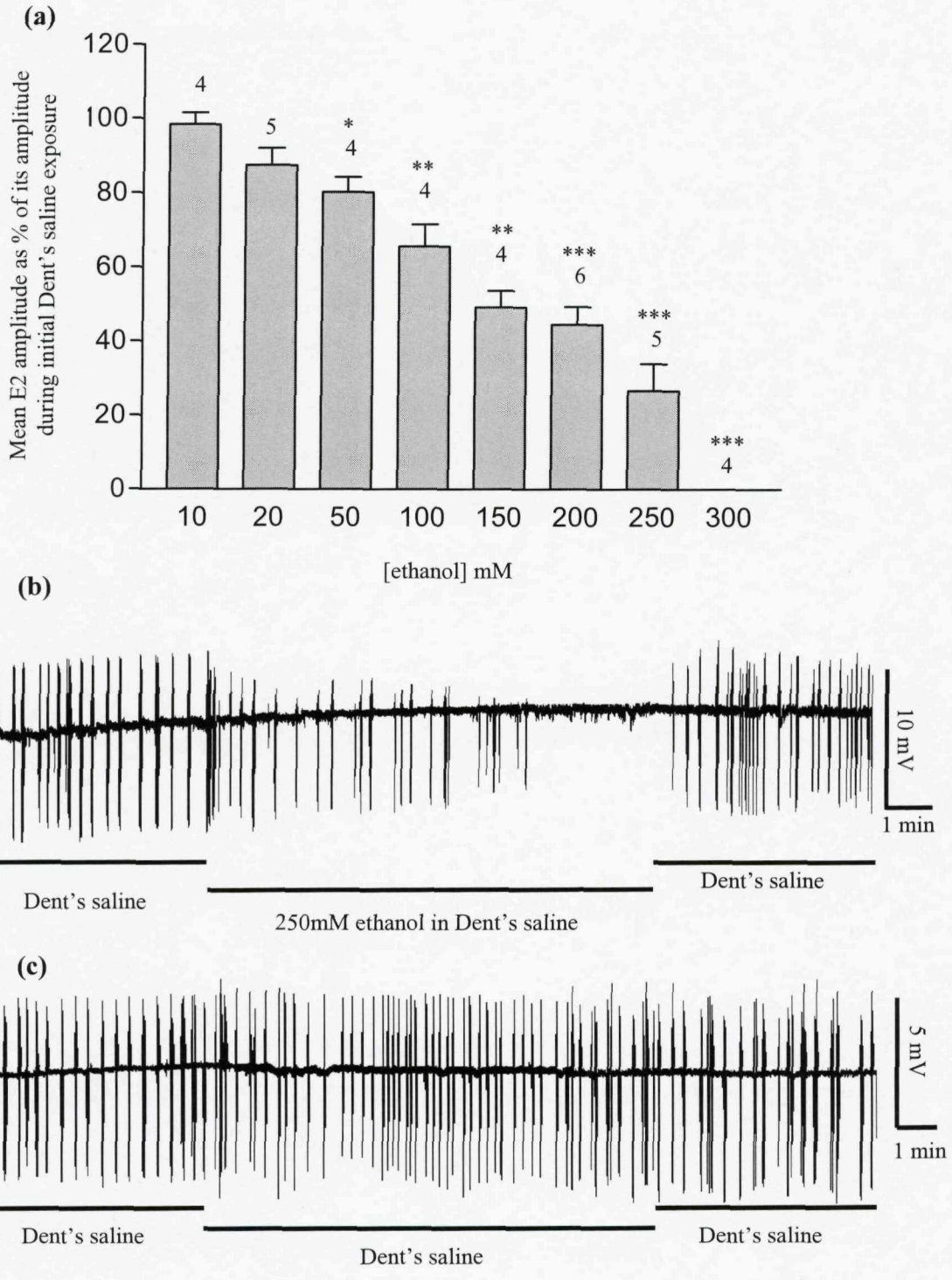

Figure 6.12 The effect of ethanol on pharyngeal pump E2 amplitude in *slo-1 (js379) C. elegans.* (a) Graph showing the effect of ethanol on E2 amplitude. Each bar is the mean ± S.E.Mean of (n) determinations. Significance (Student's t-test) relates to comparison of recordings in which ethanol was applied to control experiments (no ethanol applied), *** P<0.001, **P<0.01, * P<0.05, n numbers given above each bar. (b) Typical EPG recording from a *slo-1 (js379)* pharynx exposed to 250mM ethanol. Notice the reduction in E2 amplitude during ethanol application. (c) Typical control EPG recording (*slo-1 (js379)* pharynx). Notice that there is no change in E2 during the recording.

As with the wild type pharynx, the reduction in *slo-1 (js379)* mutant E2 amplitude during ethanol application is reversible upon removal of the ethanol (see figure 6.13).

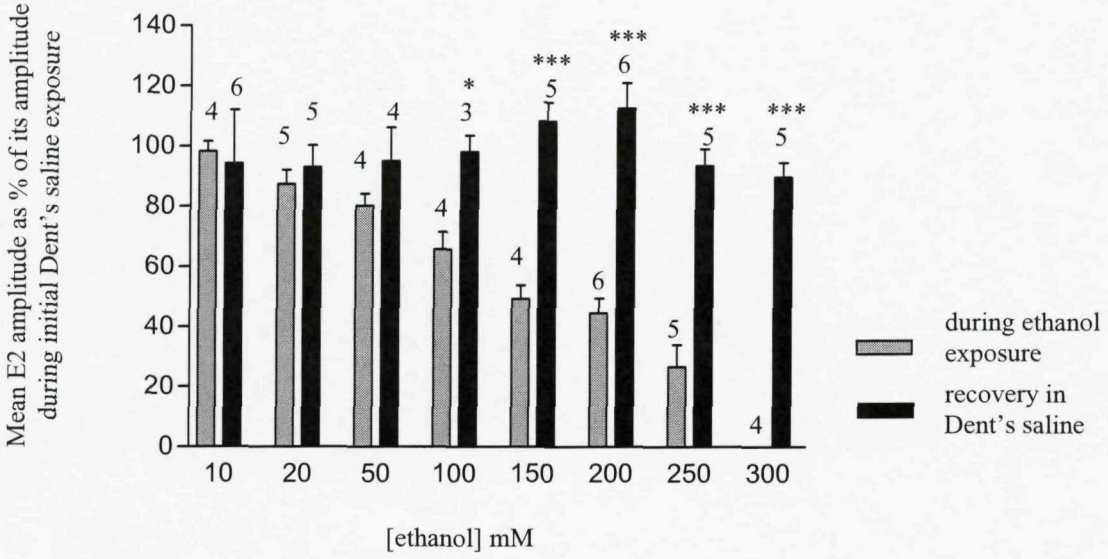

Figure 6.13 The reversibility of the effect of ethanol on E2 amplitude in *slo-1 (js379) C. elegans.* Graph showing that the inhibition of E2 amplitude during ethanol exposure is reversed within 5 minutes of alcohol removal. Each bar is the mean ± S.E.Mean of (n) determinations. Significance (Student's t-test) relates to comparison of mean E2 amplitude during ethanol exposure and during recovery, *** P<0.001, * P<0.05, n numbers given above each bar.

Ethanol was also found to affect pumping rate in both the wild type and *slo-1 (js379)* pharynx (see figure 6.14 (a)). Exactly the same protocol was used as described previously (five minutes Dent's saline, ten minutes ethanol in Dent's saline, five minutes Dent's saline), and perfusion was maintained at 4ml min^{-1}. Control experiments, as before, applied a solution of Dent's saline with no ethanol for the central ten minute period in the protocol.

As shown in figure 6.14, ethanol was found to stimulate wild type pharyngeal pumping when applied at 10-150mM, with 10, 20 and 50mM all stimulating the pharynx to pump at a rate twice that in Dent's saline. However, *slo-1 (js379)* pharyngeal pumping was not stimulated when 10-100mM was applied, and at 150mM pumping rate was actually depressed by 53%. Both wild type and *slo-1 (js379)* pharyngeal pumping rate was inhibited by 250-300mM ethanol, although the mutant pharynx appeared significantly more inhibited than wild type in the presence of 250mM ethanol and only the mutant demonstrated an inhibition of pumping in 200mM ethanol.

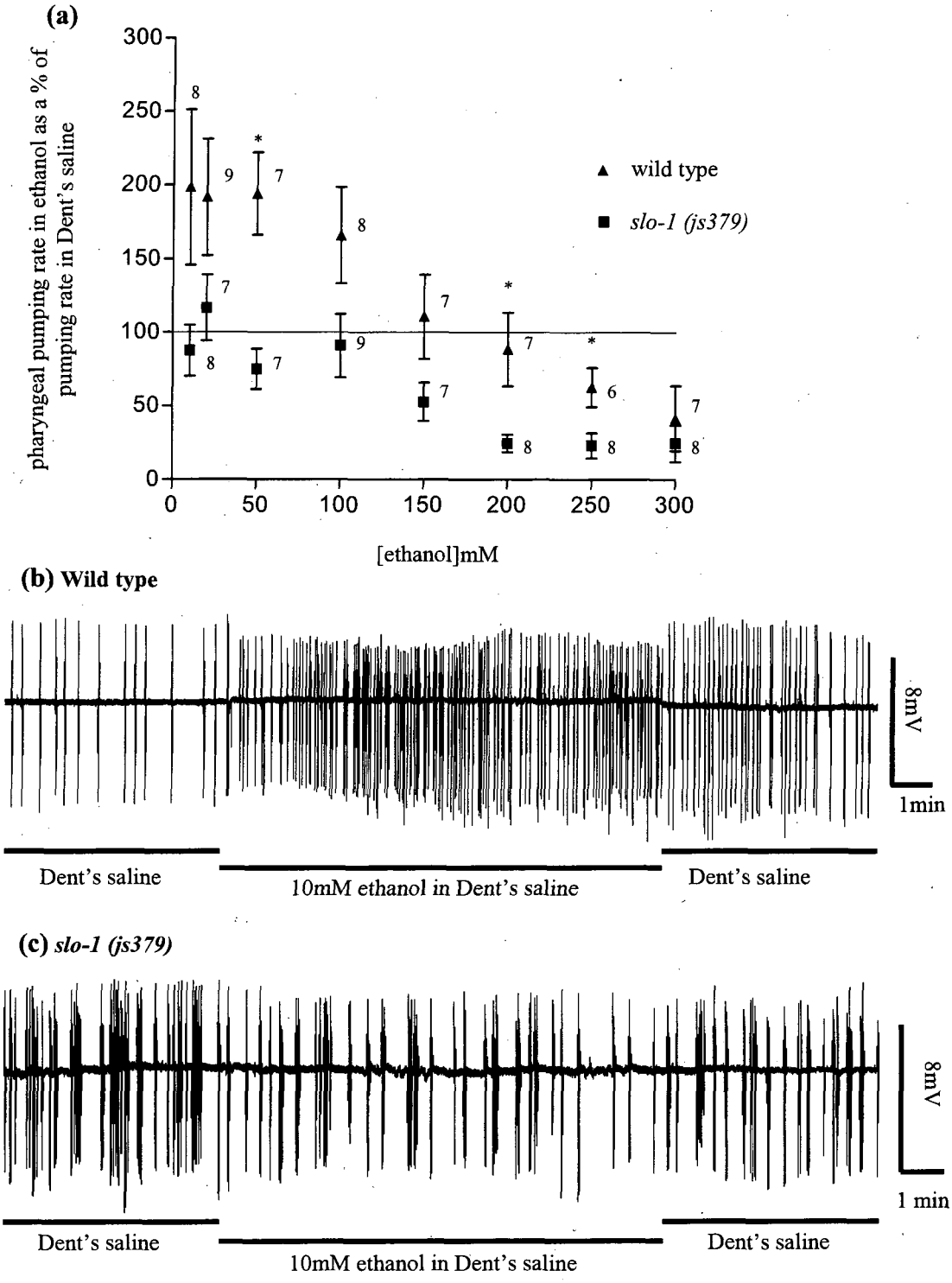

Figure 6.14 A comparison of the effect of ethanol on pharyngeal pumping rate in wild type and *slo-1 (js379)* C. elegans.

(a) Graph showing the mean pump rate for the wild type and *slo-1 (js379)* pharynx during the 10 minute ethanol application expressed as a percentage of the mean pump rate during the initial 5 minutes of Dent's saline. Each datum point is the mean ± S.E.Mean of (n) determinations. Significance (Student's t-test) relates to the comparison of wild type and *slo-1 (js379)* mean pump rate at one ethanol concentration, *P<0.05, n numbers are given beside each datum point. **(b)** A typical EPG recording from a wild type pharynx, demonstrating the increase in pumping during application of 10mM ethanol. **(c)** A typical EPG recording from a *slo-1 (js379)* pharynx, demonstrating the reduction in pump rate during application of 10mM ethanol.

The inhibition of wild type pharyngeal pumping rate by 250-300mM ethanol (shown in figure 6.14 (a)) was reversible by removing ethanol and perfusing the pharynx in Dent's saline for five minutes (within this time pump rate returned to the levels prior to ethanol exposure, see figure 6.15). The *slo-1 (js379)* pharyngeal pumping rate also recovered from inhibition by 150-300mM ethanol in the five minute recovery period (see figure 6.15).

The stimulation of wild type pumping rate by 10-100nM ethanol (shown in figure 6.14 (a)) did not reverse during the five minutes of Dent's saline exposure following ethanol application (an example can be seen in figure 6.14(b)). This could indicate that a longer recovery period than five minutes is required to enable wild type pumping to resume basal rate following stimulation by 10-100mM ethanol, compared to the time required to recover from inhibition by the higher ethanol concentrations.

In summary, ethanol reversibly inhibits the amplitude of the E2 spike in EPG recordings from the wild type and *slo-1 (js379)* null pharynx, with no difference in this effect between the two worm strains. Ethanol also reversibly inhibits pharyngeal pumping rate in the wild type and *slo-1 (js379)* pharynx when applied at concentrations of 250-300mM. However, wild type pharyngeal pumping rate was stimulated by 10-100mM ethanol, which was not observed in the *slo-1 (js379)* mutant. This stimulation was not reversible in the five minutes following ethanol exposure.

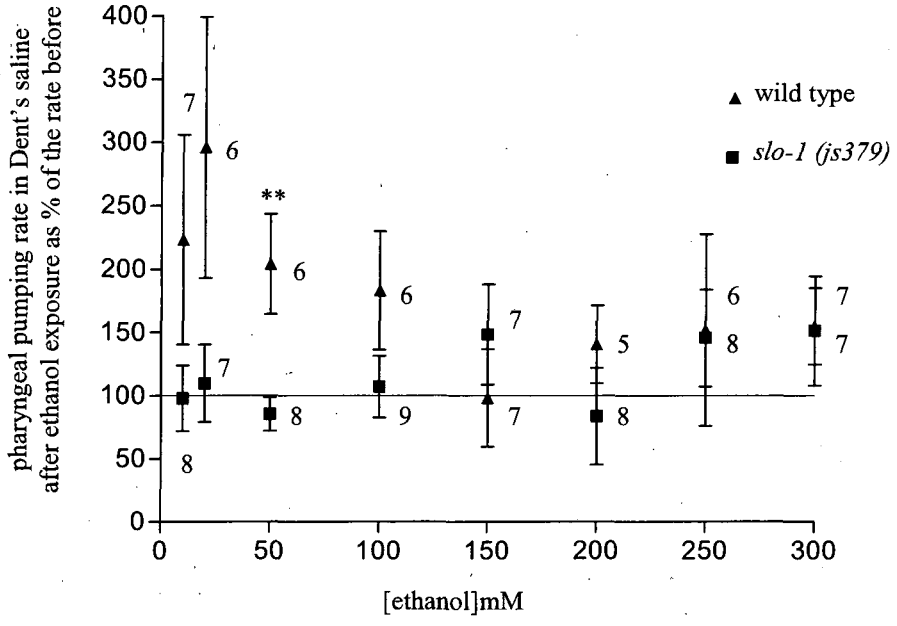

Figure 6.15 Graph comparing the recovery of pharyngeal pumping from inhibition by ethanol in the wild type and *slo-1 (js379)* pharynx.

The mean pump rate during the 5 minute recovery period in Dent's saline is expressed as a percentage of the mean pump rate during the initial 5 minutes in Dent's saline before ethanol exposure. Each datum point is the mean ± S.E.Mean of (n) determinations. Significance (Student's t test) relates to comparison of wild type and *slo-1 (js379)* % pumping rate, *P<0.05, n numbers given beside each datum point. To clarify, n numbers at 250mM ethanol: 6 (wild type), 8 (*slo-1*).

6.6 The effect of SLO-1 on the pharyngeal response to exogenous 5-HT application

As shown in sections 6.2, 6.4 and 6.5, the expression of *slo-1* appears to affect pharyngeal pumping in Dent's saline and the response of the pharynx to ethanol. Previous research has shown how the pharyngeal expression of synaptic proteins that are intimately involved in the regulation of neurotransmission at the neuromuscular junction can affect the response of the pharynx to signaling molecules such as 5-HT. For example, expression of the inositol triphosphate receptor IP3, which is involved in neurotransmission, affects pharyngeal response to 5-HT (Walker et al., 2002). Therefore, as current research has suggested that the SLO-1 channel is important in the regulation of neurotransmission at the synapse, it is possible that *slo-1* expression may also affect the pharyngeal pumping response of the pharynx to exogenous application of 5-HT. To investigate this, the electropharyngeogram was used to record the response of the wild type and *slo-1(js379) C. elegans* pharynx to a range of 5-HT concentrations, thereby enabling comparison of the EC_{50} value for both worm strains.

The addition of exogenous 5-HT to the pharynx preparation of wild type *C. elegans* produced a concentration-dependent increase in pharyngeal pumping, with an EC_{50} of 52nM (95% confidence limits 11 to 234nM). The *slo-1(js379)* mutant also demonstrated a concentration-dependent increase in pharyngeal pumping in response to 5-HT application with an EC_{50} value of 23nM (95% confidence limits 9 to 57nM). Student's t-test analysis showed that the response of wild type *C. elegans* and *slo-1 (js379)* mutants to 5-HT was significantly different only when 1μM 5-HT was applied ($P<0.05$). These results are shown in figure 6.16.

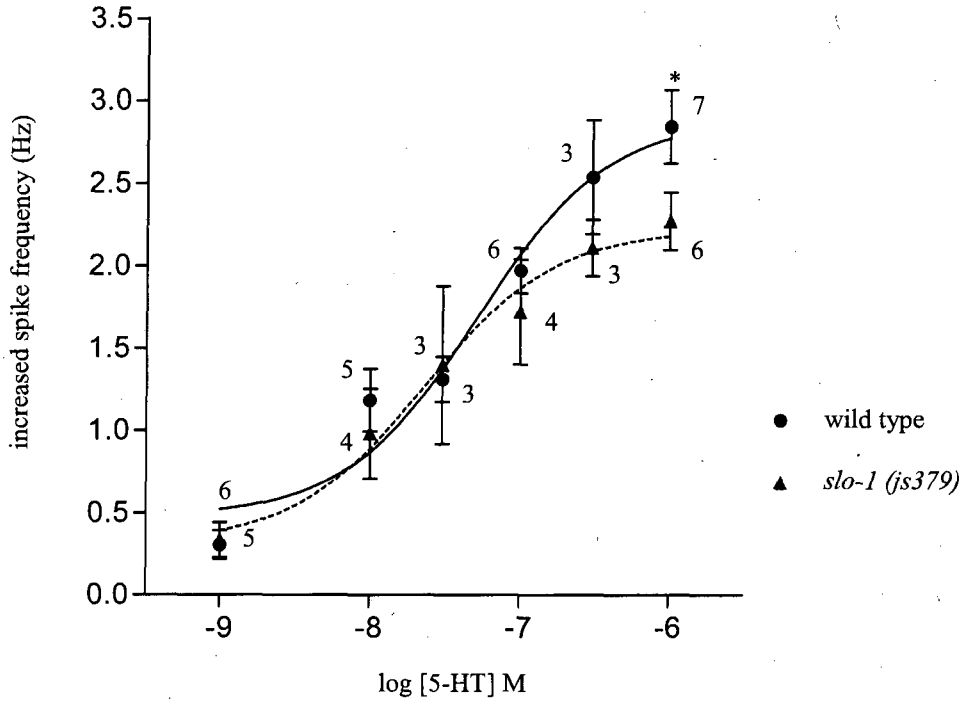

Figure 6.16 Concentration response curve for the effect of 5-HT on pharyngeal pumping in wild type and *slo-1 (js379) C. elegans*.
'Increased spike frequency' is calculated from the pumping frequency prior to the application of 5-HT and the pumping frequency during maximal response to the drug. Each datum point is the mean ± S.E.Mean of (n) determinations. n numbers are given beside each datum point. To clarify, n numbers at 1nM 5-HT: 6 (wild type), 5 (*slo-1*). Note: the *slo-1 (js379)* and wild type datum points superimpose at 1nM 5-HT. Dotted line: nonlinear regression for *slo-1 (js379)*. Statistical significance (Student's t-test) relates to a comparison of wild type and *slo-1 (js379) C. elegans* pharyngeal response (increased spike frequency) at each 5-HT concentration, *P<0.005, (n) determinations. Curves were fitted using the nonlinear regression four-parameter logistic equation described in chapter 2, section 2.10, except that the Bottom and Top Y values were not set as constants of 0 and 100, respectively. All other parameters were as described in section 2.10.

6.7 The effect of either neuronal or muscle expression of *slo-1* on emodepside sensitivity of the pharynx

To investigate whether only neuronal expression of *slo-1* is sufficient to rescue emodepside sensitivity in *slo-1 (js379)* null *C. elegans*, the *slo-1(js379); snb-1::slo-1* mutant was assayed for emodepside sensitivity using the EPG technique. 5-HT was applied before and after emodepside exposure to stimulate pumping so that any effect of emodepside on pump rate could be seen. Prior to the assay 'recording' protocol, each pharynx preparation was 'primed' with 500nM 5-HT (see chapter 2, section 2.7.3, page 73) by repeated application of 5-HT for two minutes interspersed with two minutes recovery in Dent's saline until a 5-HT application produced a pump rate within 2% of the previous rate in 5-HT. Following priming, each pharynx preparation was allowed to recover for three minutes in Dent's saline before commencing the recording protocol (in order of application): two minutes 500nM 5-HT, wash (Dent's saline), ten minutes emodepside (at 100pM-1μM, 0.01% DMSO vehicle, no 5-HT), wash (Dent's saline), two minutes 500nM 5-HT. The pumping rate in 5-HT following emodepside exposure was expressed as a percentage of the rate in 5-HT prior to emodepside application. The wild type and *slo-1 (js379)* null *C. elegans* were also assayed as controls.

The *slo-1 (js379); snb-1::slo-1* mutant pharynx demonstrated an almost identical concentration-dependent inhibition of pharyngeal pumping as the wild type, with an IC_{50} of 7.8nM (95% confidence limits 6.5 to 9.3nM) for *slo-1 (js379); snb-1::slo-1* compared to a wild type IC_{50} of 7.6nM (95% confidence limits 6.0 to 9.6nM) (see figure 6.17). Worms from two stably transformed lines of *slo-1 (js379); snb-1::slo-1 C. elegans* were assayed to ensure that the results observed are due to *slo-1* expression and not spontaneous phenotypes resulting from the transgenic process.

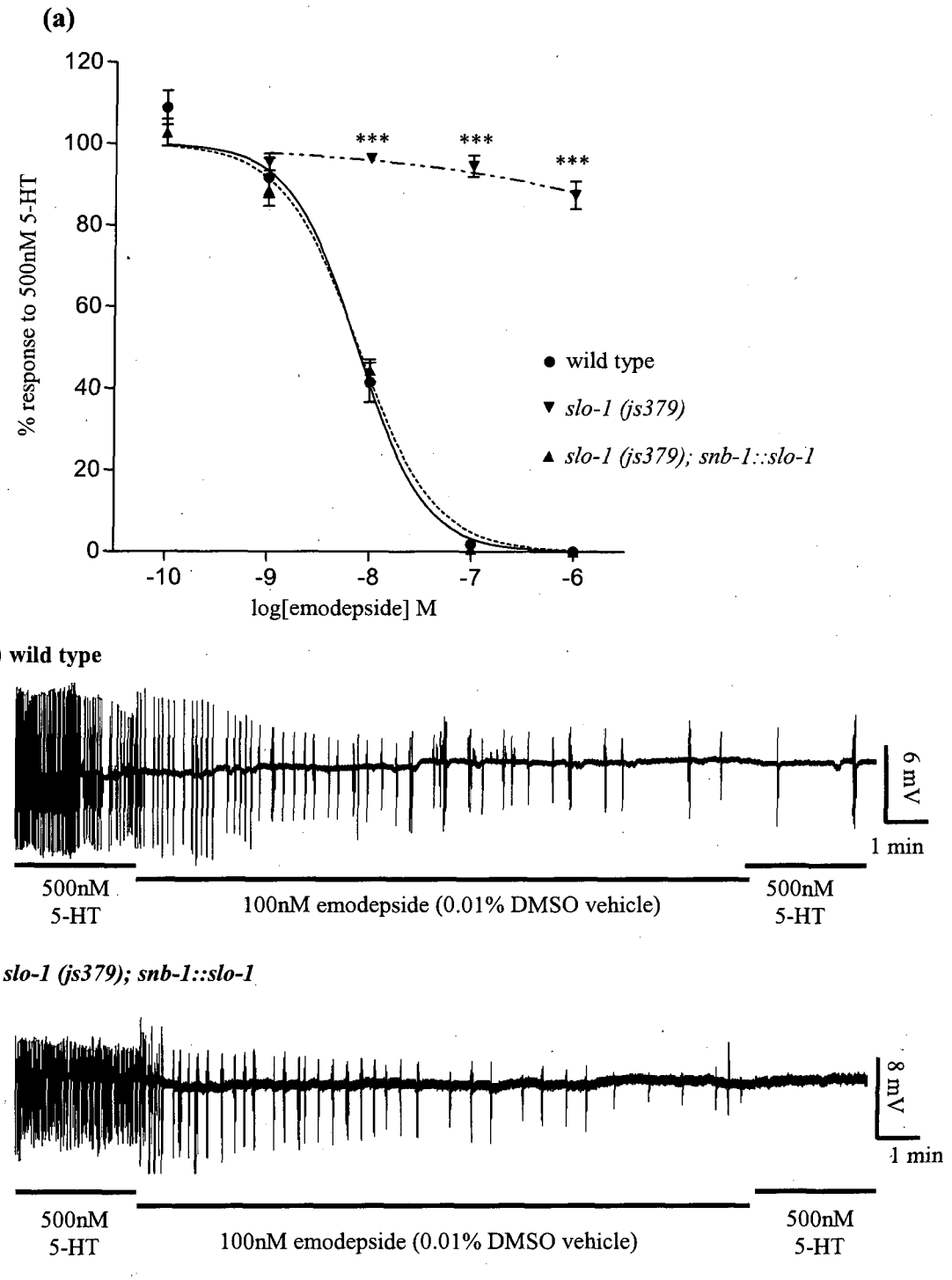

Figure 6.17 The effect of *slo-1* expression in the pharyngeal neurons of the *slo-1 (js379)* null mutant on emodepside sensitivity.

(a) Concentration response curve comparing the emodepside sensitivity of the wild type, *slo-1 (js379)* and *slo-1 (js379); snb-1::slo-1* pharynx. Each datum point is the mean ± S.E.Mean of (n) determinations. Student's t-test was used to compare the results from the *slo-1* mutants with the wild type control; ***P<0.001, n numbers for wild type: 6 (100pM), 7 (1nM), 7 (10nM), 7 (100nM), 7 (1μM), n numbers for *slo-1 (js379); myo-2::slo-1*: 5 (100pm), 6 (1nM), 6 (10nM), 6 (100nM), 5 (1μM), n numbers for *slo-1 (js379)*: 4 (1nM), 5 (10nM), 4(100nM), 5 (1μM). Curves were fitted using the nonlinear regression four-parameter logistic equation described in chapter 2, section 2.10. Solid curve: wild type. **(b)** A typical EPG recording from a wild type pharynx. **(c)** A typical EPG recording from a *slo-1 (js379); snb-1::slo-1* pharynx. Notice the similarity in the response of both pharynx preparations to emodepside.

To investigate whether expression of *slo-1* in the pharyngeal muscle but not the neurons is sufficient to rescue emodepside sensitivity in *slo-1 (js379)* null *C. elegans*, the *slo-1(js379); myo-2::slo-1* mutant was assayed for emodepside sensitivity using the EPG technique. The recording protocol, 5-HT 'priming' method and data analysis were the same as described in the previous assay (page 229).

The *slo-1 (js379); myo-2::slo-1* mutant pharynx demonstrated a concentration-dependent inhibition of pharyngeal pumping with an IC_{50} in excess of 1μM, compared to a wild type IC_{50} of 8nM (95% confidence limits 6 to 10nM) (see figure 6.18(a)). Inhibition of the *slo-1 (js379); myo-2::slo-1* pharyngeal response 5-HT by emodepside was not significantly different to that of the *slo-1 (js379)* null at any of the anthelmintic concentrations tested. However, the *slo-1 (js379); myo-2::slo-1* emodepside response was significantly different to that of the wild type when 10nM ($P<0.01$), 100nM and 1μM ($P<0.001$) of the anthelmintic was applied.

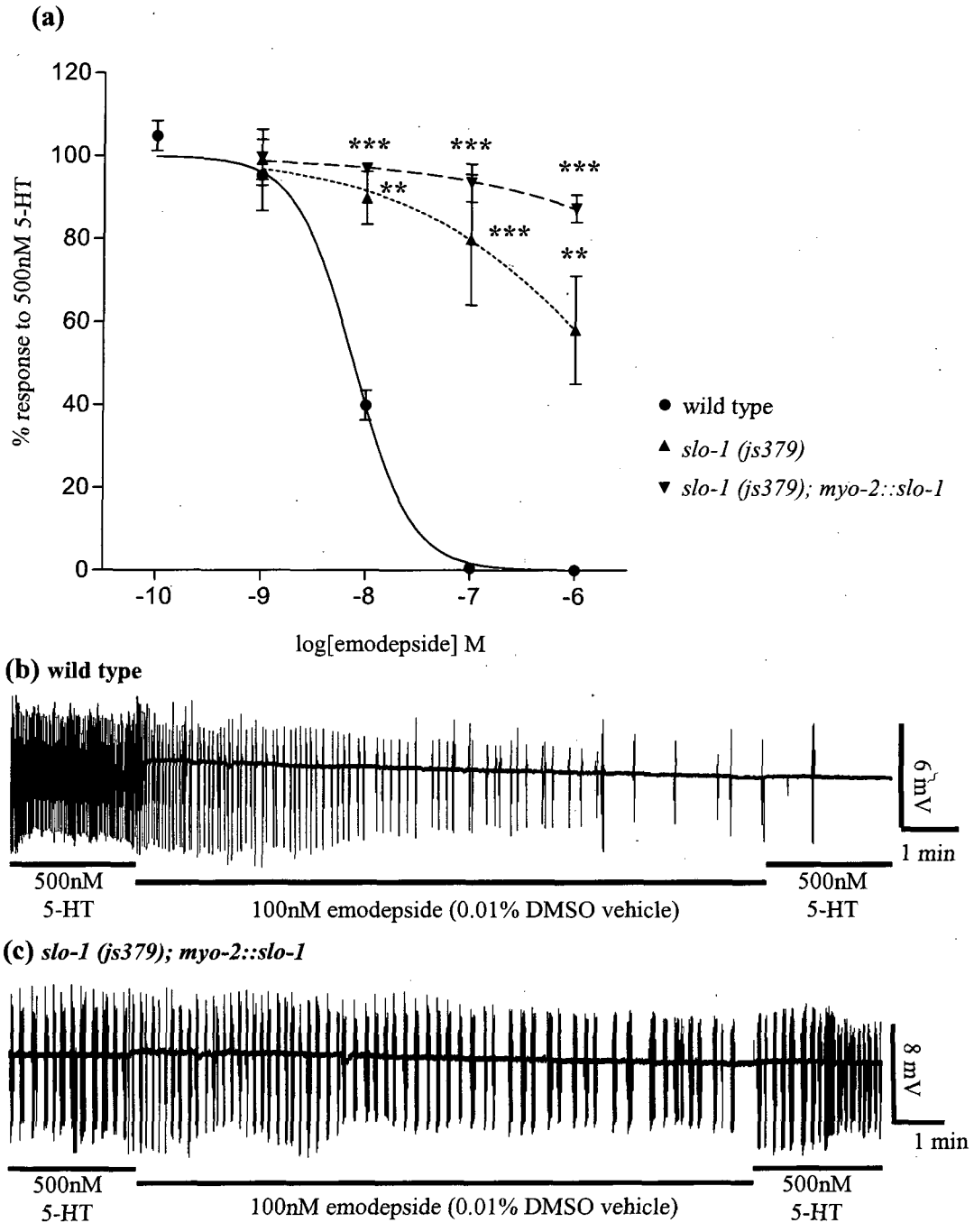

Figure 6.18 The effect of *slo-1* expression in the pharyngeal muscles of the *slo-1 (js379)* null pharynx on emodepside sensitivity.

(a) Concentration response curve comparing the emodepside sensitivity of the wild type, *slo-1 (js379)* and *slo-1 (js379); myo-2::slo-1* pharynx. Each datum point is the mean ± S.E.Mean of (n) determinations. Student's t-test was used to compare the results from the *slo-1* mutants with the wild type control; **P<0.01, ***P<0.001, n numbers for wild type: 6 (100pM), 8 (1nM), 6 (10nM), 6 (100nM), 6 (1μM), n numbers for *slo-1 (js379); myo-2::slo-1*: 6 (1nM), 6 (10nM), 9 (100nM), 6 (1μM), n numbers for *slo-1 (js379)*: 6 (1nM), 6 (10nM), 5 (100nM), 5 (1μM). Curves were fitted using the nonlinear regression four-parameter logistic equation described in chapter 2, section 2.10. **(b)** A typical EPG recording from a wild type pharynx. **(c)** A typical EPG recording from a *slo-1 (js379); myo-2::slo-1* pharynx. Notice that the *slo-1* mutant continues to pump throughout emodepside exposure and during the second 5-HT application. However, wild type pumping rate gradually decreases throughout emodepside exposure and the pharynx only pumps once during the second application of 5-HT.

6.8 The effect of emodepside on the SLO-1 current in pharyngeal muscle cells

In sections 6.5 and 6.7, both ethanol and emodepside are shown to affect pharyngeal pumping and that *slo-1* has a role in these effects. Ethanol has been shown to increase the SLO-1 current and SLO-1 channel opening frequency in patch clamp recordings from *C. elegans* neurons that innervate the body wall muscles (Davies et al., 2003). Therefore, it is possible that emodepside shares the ability of ethanol to alter SLO-1 channel activity. Patch clamp electrophysiological recordings can be used to examine channel currents in a whole cell membrane. Such recordings can be achieved from the terminal bulb muscle cells of the pharynx. As described previously, evidence does not conclusively show that *slo-1* is functionally expressed in the pharyngeal muscles (Chiang et al., 2006; Wang et al., 2001). The results shown in section 6.7 strongly suggest that presynaptic (neuronal) *slo-1* expression is the major component of the mechanism of action of emodepside in the pharynx. It is possible that *slo-1* is not expressed sufficiently (or at all) postsynaptically in the pharynx, and therefore, no *slo-1* currents would be seen in patch clamp recordings from the terminal bulb. Therefore, the *slo-1 (js379); myo-2::slo-1* mutant, expressing *slo-1* in the pharyngeal muscles, was assayed as well as the wild type and *slo-1 (js379)* null mutant.

Initially, it was important to clearly identify the *slo-1* potassium (K^+) current, if it is present, from the terminal bulb muscle cells. By comparing patch clamp recordings from *slo-1 (js379)* null *C. elegans* with the wild type and *slo-1 (js379); myo-2::slo-1* mutant, a difference in outward currents with the appropriate reversal potential for K^+ ions was identified. To further confirm that observed candidate currents are specific to the activity of high-conductance calcium-activated K^+ channels (BK channels), the single chain peptide iberiotoxin (IBTX) was used. IBTX, a component of the venom from the scorpion *Buthus tamulus*, is a highly selective and reversible inhibitor of BK channels, and does not affect other voltage-dependent channel types, including other K^+ channels (Galvez et al., 1990). IBTX acts exclusively at the external face of the channel to reduce the probability of channel opening and mean open time, and functions with an IC_{50} of approximately 259pM (Galvez et al., 1990). Application of 2nM IBTX for five minutes to cultured bovine aortic smooth muscle cells significantly blocks candidate SLO-1 channel activity, with washout of the toxin resulting in a return of channel activity to

almost control levels after 25 minutes (Galvez et al., 1990). Therefore, to ensure maximal IBTX activity when applied to patch clamp recordings from the *C. elegans* terminal bulb, the toxin was applied at 100nM for ten minutes, and recordings were made 30 seconds prior to application, and then 30 seconds, five minutes and ten minutes after application.

Successful identification of SLO-1 currents then enabled the testing of emodepside for the effect of the compound on these currents.

6.8.1 Identification of a SLO-1 current in pharyngeal muscle cells using whole cell patch clamp recording

Whole cell patch clamp recordings from the terminal bulb muscle of wild type, *slo-1 (js379)* null and *slo-1 (js379); myo-2::slo-1 C. elegans* revealed an outward rectifying current with a reversal potential of approximately -80mV for all three worm strains (see figure 6.19 (a)). This reversal potential is close to the expected K^+ equilibrium potential of -86mV (at 25°C, 5mM external K^+, 140mM internal K^+), suggesting that the current identified in all three worm strains is a K^+ current. The overlapping data for the wild type and *slo-1 (js379)* pharyngeal preparations suggest that the two currents are indistinguishable with respect to voltage dependence of activation (compare figure 6.19 (b) and (c)). However, the *slo-1 (js379); myo-2::slo-1* mutant demonstrates a K^+ current larger than wild type and *slo-1 (js379)* when the voltage was stepped between -20mV and 100mV (compare figure 6.19 (b) and (d), note the scale difference). The data shown in figure 6.19 are from recordings made five minutes after whole cell patch clamp was achieved. The K^+ currents of all three *C. elegans* strains were stable for up to 25-30 minutes, whereupon clamp stability declined most likely due to cell deterioration. A period of five minutes was left between initially achieving whole cell access and beginning recording to allow the contents of the patch pipette to equilibrate with the cytoplasm of the muscle cell.

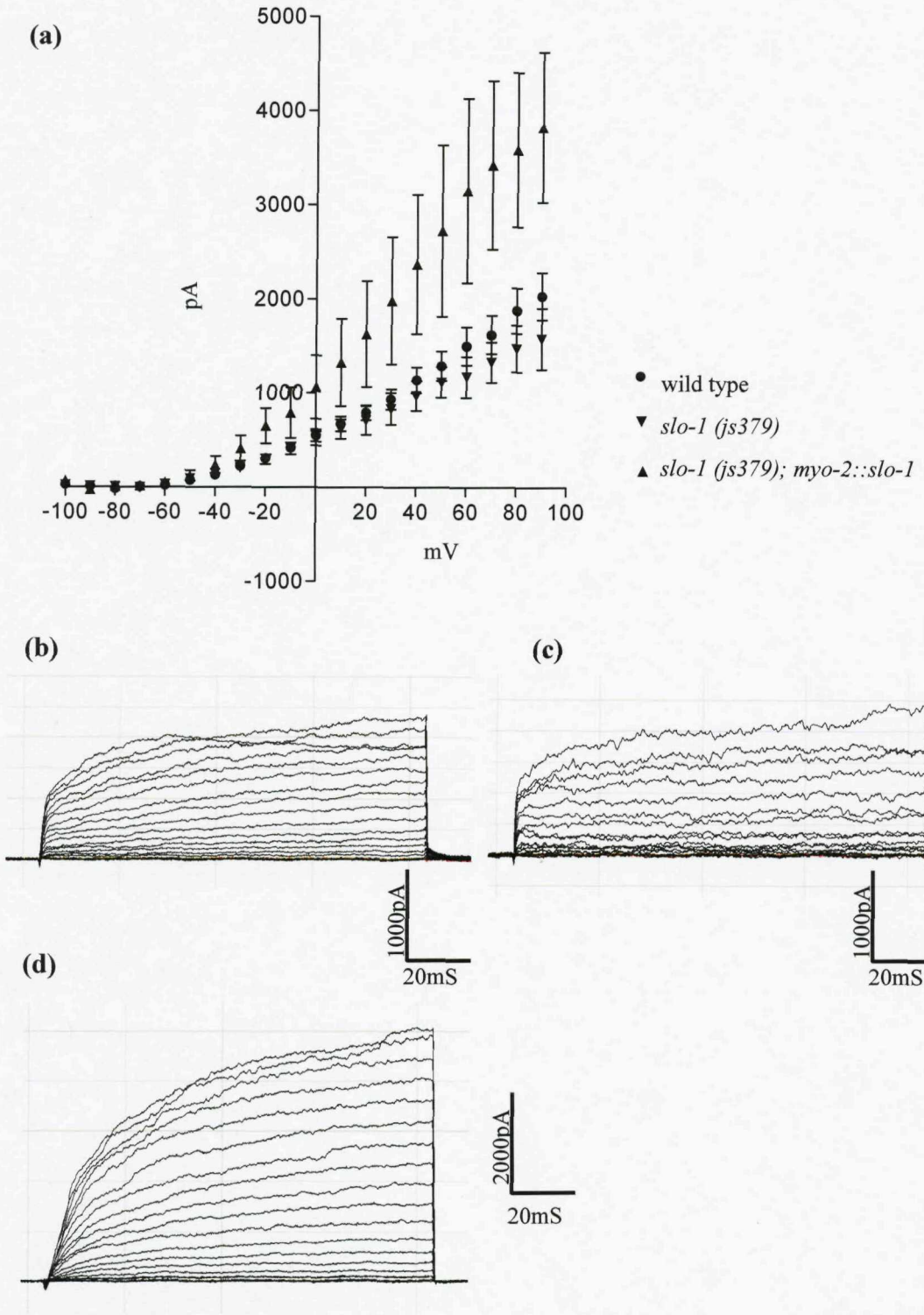

Figure 6.19 Whole cell patch clamp recording from the terminal bulb muscle cells of the wild type, *slo-1 (js379)* null and *slo-1 (js379); myo-2::slo-1* mutant *C. elegans.*

(a) Graph showing the outward currents recorded by whole cell patch clamp from wild type, *slo-1 (js379)* and *slo-1 (js379); myo-2::slo-1* terminal bulb muscle cells. Each datum point is the mean ± S.E.Mean of: 4 wild type worms, 3 *slo-1 (js379)* worms, and 4 *slo-1 (js379); myo-2::slo-1* worms. Currents were elicited from a -80mV holding potential, in 10mV steps from -100 to +90mV. **(b-d)** Example whole cell patch clamp recordings from terminal bulb muscle cells of the: (b) wild type, (c) *slo-1 (js379)*, and (d) *slo-1 (js379); myo-2::slo-1 C. elegans*. Note the difference in the scale used in (d).

Further evidence to suggest that the outward current being recorded is a K^+ current was achieved by increasing the K^+ concentration in the external solution from 5mM KCl to 20mM KCl. Such an increase in external K^+ ions would be predicted to alter the reversal potential of the ion to -50mV (as predicted by the Nernst equation). In support of this, figure 6.20 shows that increasing external KCl concentration when recording from wild type terminal bulb muscle cells reduced current size and shifted the equilibrium potential of the current to a more positive voltage of approximately -50mV. Subsequent reduction of external K^+ to the original concentration (5mM KCl) resulted in an increase in current size (see figure 6.20(c)) and a shift of reversal potential towards the negative.

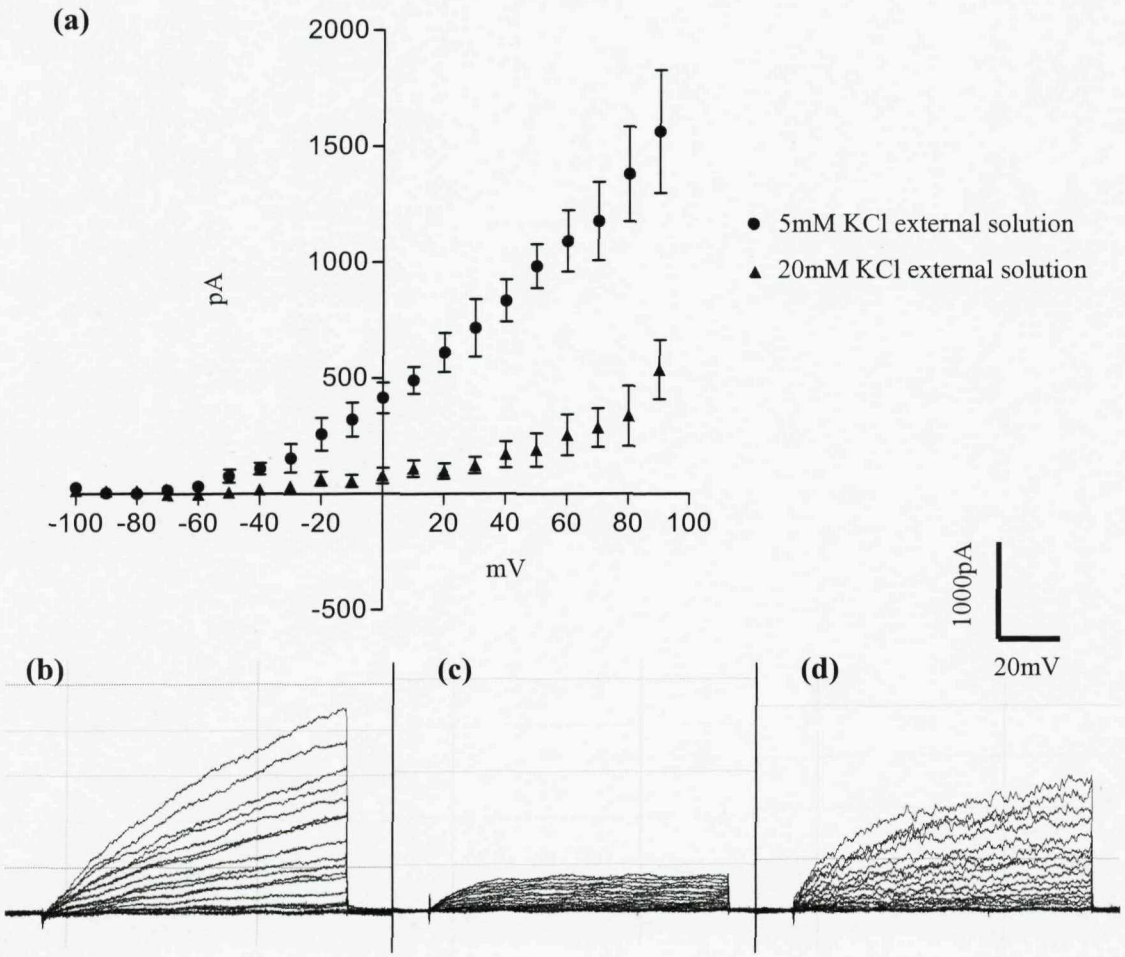

Figure 6.20 The effect of increasing external K^+ concentration on currents recorded from wild type terminal bulb muscle cells.
(a) Graph showing the outward currents recorded by whole cell patch clamp from wild type terminal bulb muscle cells. Each datum point is the mean ± S.E.Mean of: 4 worms. Currents were elicited from a -80mV holding potential, in 10mV steps from -100 to +90mV. Each recording was made 5 minutes after a change to the external solution was made. **(b-d)** Example whole cell patch clamp recordings from a single wild type terminal bulb muscle cell in: (b) 5mM KCl external solution, (c) 20mM KCl external solution, (d) 5mM KCl external solution. The scale bar applies to all 3 recordings.

To identify whether the large K^+ current present only in the *slo-1 (js379); myo-2::slo-1* terminal bulb muscle is a result of SLO-1 channel activity, IBTX, the specific BK channel blocker, was applied to all three strains at 100nM for ten minutes.

IBTX had no effect on the outward K^+ currents recorded from wild type and *slo-1 (js379)* terminal bulb muscle (see figure 6.21 (a) and (b)). However, IBTX did reduce the size of the K^+ currents in the *slo-1 (js379); myo-2::slo-1* preparations to a size overlapping that of wild type and *slo-1 (js379)* (see figure 6.21(c)). A typical whole cell patch clamp recording from a *slo-1 (js379); myo-2::slo-1* cell before and after application of 100nM IBTX are shown in figure 6.21 (d) and (e) respectively. Control experiments were also performed on the *slo-1 (js379); myo-2::slo-1* pharynx preparations using an identical protocol but without IBTX. These control recordings demonstrated that there was no deterioration in the large K^+ current during the duration of the protocol, strongly supporting that the reduction in K^+ current size is due to IBTX application. Taken together these results suggest that the large K^+ current is due to voltage-activation of SLO-1 channels.

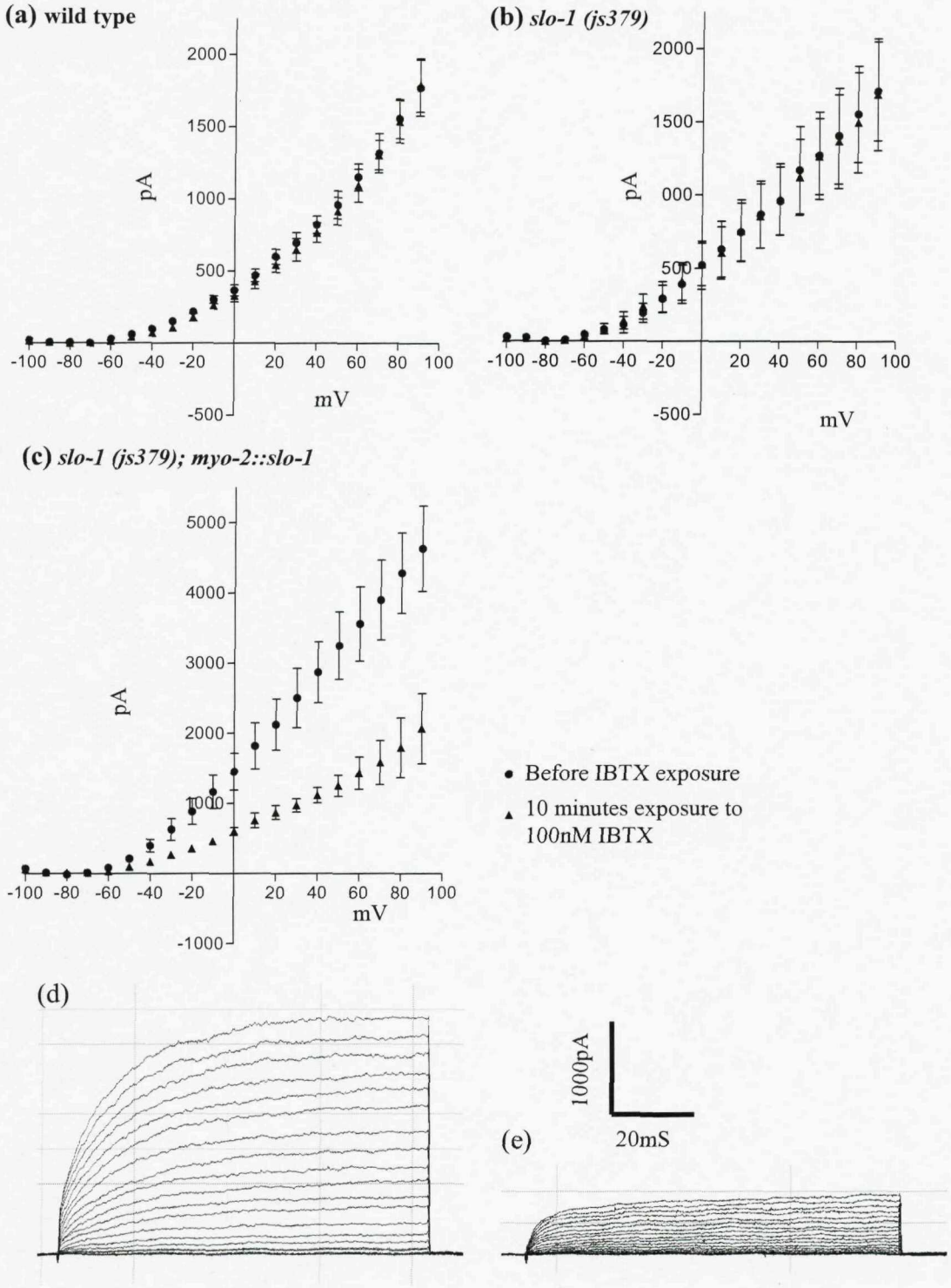

Figure 6.21 The large K^+ current in *slo-1 (js379); myo-2::slo-1* terminal bulb muscle cells is inhibited by IBTX. Graphs showing whole cell patch clamp results for the effect of 10 minutes application of 100nM IBTX on terminal bulb K^+ currents in: **(a)** wild type, **(b)** *slo-1 (js379)*, and **(c)** *slo-1 (js379); myo-2::slo-1* worms. Each datum point is the mean ± S.E.Mean of: (a) 5 wild type worms, (b) 3 *slo-1 (js379)* worms, and (c) 4 *slo-1 (js379); myo-2::slo-1* worms. Currents were elicited from a -80mV holding potential, in 10mV steps from -100 to +90mV. **(d)** A typical whole cell patch clamp recording from a *slo-1 (js379); myo-2::slo-1* cell 30 seconds before IBTX was applied. **(e)** A patch clamp recording from the same cell shown in (d) 10 minutes after IBTX exposure commenced. Notice the dramatic reduction in K^+ current size in (e).

6.8.2 The effect of emodepside on the SLO-1 current in pharyngeal muscle cells

Identification of the SLO-1 channel currents in the terminal bulb muscles of the *slo-1 (js379); myo-2::slo-1* strain enabled examination of the effect of emodepside on these currents. The novel anthelmintic was applied at 1μM for ten minutes, and recordings were made 30 seconds before emodepside application, and then 30 seconds, five minutes and ten minutes after emodepside exposure commenced. Control experiments were performed using an identical protocol but substituting emodepside for the vehicle (0.01% DMSO). Additional control experiments were also performed in which emodepside was applied to the wild type and *slo-1 (js379)* pharyngeal preparations to identify any effect of the compound on the smaller K^+ currents shown by these two worm strains.

Emodepside was found to reduce that size of the K^+ currents observed in the *slo-1 (js379); myo-2::slo-1* muscle cell at depolarizing steps of -40 to 100mV (see figure 6.22 (a), (b) and (c)). Both wild type and *slo-1 (js379)* muscle cell preparations exhibited no effect of emodepside exposure on the K^+ currents (see figure 6.22 (d) and (e)). Control experiments in which only the DMSO vehicle was applied, did not result in any change in the K^+ currents of *slo-1 (js379); myo-2::slo-1*.

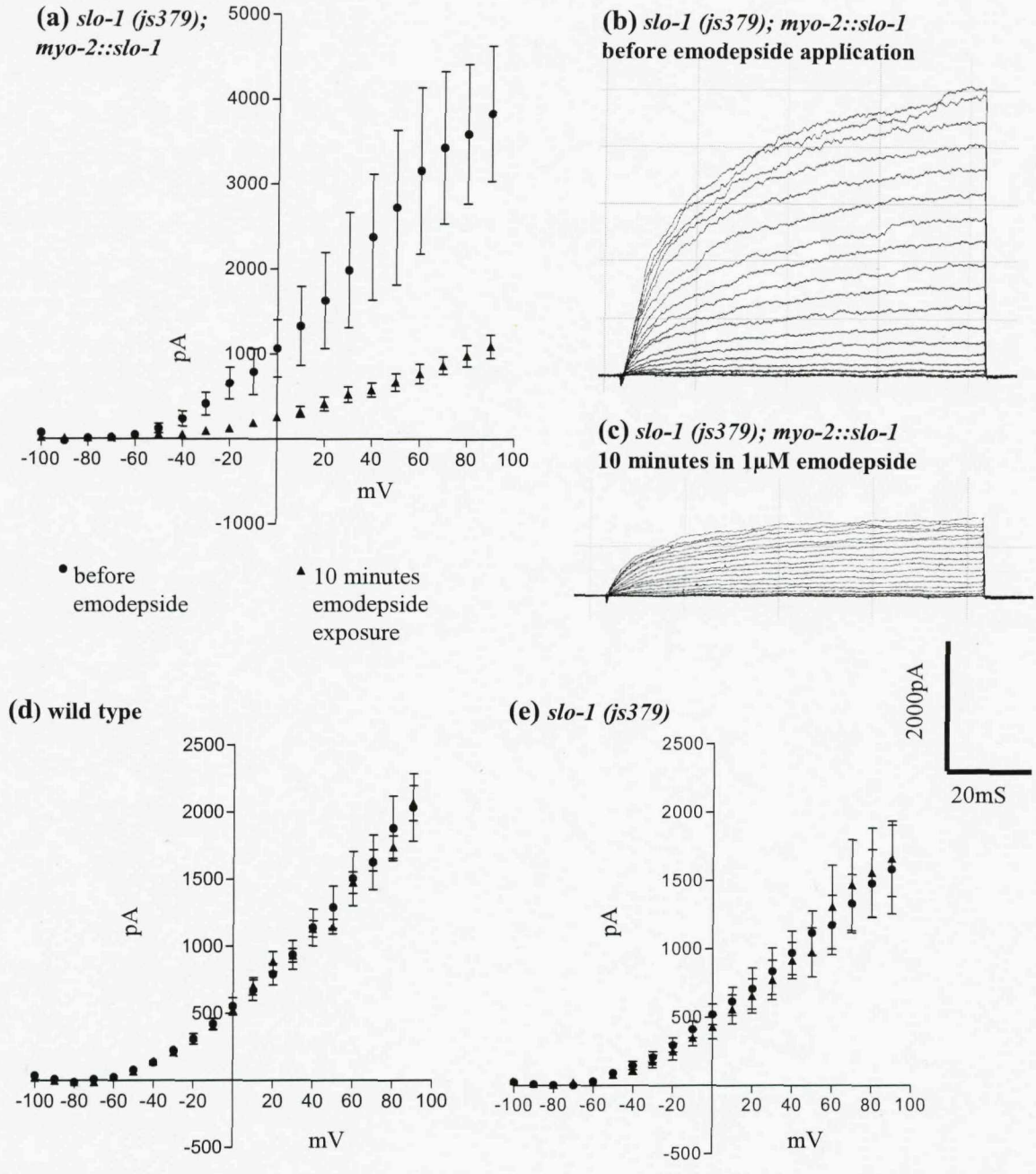

Figure 6.22 The large K^+ current in *slo-1 (js379); myo-2::slo-1* terminal bulb muscle cells is inhibited by 1µM emodepside. Graphs showing whole cell patch clamp results for the effect of 10 minutes application of 100nM emodepside on terminal bulb K^+ currents in: **(a)** *slo-1 (js379); myo-2::slo-1*, **(d)** wild type, and **(e)** *slo-1 (js379)*worms. Each datum point is the mean ± S.E.Mean of: (a) 4 *slo-1 (js379); myo-2::slo-1* worms, (d) 4 wild type worms, and (e) 3 *slo-1 (js379)* worms. Currents were elicited from a holding potential of -80mV, in 10mV steps from -100 to +90mV. **(b)** A typical whole cell patch clamp recording from a *slo-1 (js379); myo-2::slo-1* cell 30 seconds before emodepside was applied. **(c)** A patch clamp recording from the same cell shown in (b) 10 minutes after emodepside exposure commenced. Notice the dramatic reduction in K^+ current size in (c).

6.9 Discussion

The *slo-1 (js379)* null pharynx produced pumps with a significantly longer duration than the wild type, a phenotype rescued by neuronal expression of *slo-1*. Therefore, SLO-1 appears to function in the pharyngeal nervous system to regulate pump duration. Previous research has shown that loss-of-function in *slo-1* confers a shorter pump duration in the presence of 5-HT when compared to the wild type pharynx in the same 5-HT concentration (Chiang et al., 2006). It is possible that the use of 5-HT in the work of Chiang et al. (2006) is responsible for the apparently opposite effect of a loss of SLO-1 on pump duration compared to the results shown in this chapter. In wild type *C. elegans*, 5-HT potently and reversibly increases the frequency of pharyngeal action potentials via a combination of presynaptic signaling at the neuromuscular junction and direct action on the pharyngeal muscles themselves (Rogers et al., 2001). Presynaptically, 5-HT is believed to stimulate the MC and M3 neurons, resulting in the release of acetylcholine (ACh) from the former and glutamate from the latter (Avery & Horvitz, 1989; Niacaris & Avery, 2003; Raizen & Avery, 1994). The release of ACh from MC induces pharyngeal muscle contraction and thereby increases pumping rate, whilst glutamate is released from M3 to produce muscle relaxation and thereby reduce pump duration. If the *slo-1* loss-of-function confers an even shorter pump duration in 5-HT, this suggests that the SLO-1 channels previously identified in M3 act during 5-HT exposure to curtail excessive glutamate release and maintain an appropriate pump duration. The increase in pump duration demonstrated by the *slo-1 (js379)* null in the presence of Dent's saline (and not 5-HT) is a phenotype previously observed in wild type *C. elegans* in which M3 has been ablated (Avery, 1993), suggesting that *slo-1* expression in M3 contributes to the control of pump duration in Dent's saline as well as during 5-HT exposure.

The EPGs of *slo-1 (js379)* null mutants exhibit significantly less inhibitory potentials (IPs) than wild type recordings, which is also a phenotype previously identified in M3-ablated wild type *C. elegans* (Avery, 1993), again suggesting a role for SLO-1 in the M3 neuron in controlling pharyngeal muscle relaxation (Raizen & Avery, 1994). The *unc-64; snb-1* double mutant, which possesses a reduction-in-function mutation for syntaxin and synaptobrevin, has also been shown to produce EPGs with reduced IP numbers (Saifee et al., 1998). Syntaxin and synaptobrevin are crucial elements of the SNARE complex

required for vesicle fusion with the presynaptic membrane and neurotransmitter release (e.g. Rizo & Sudhof, 2002; Soller et al., 1993; Sutton et al., 1998). Therefore, the reduction in IPs in the *slo-1 (js379)* null suggests that SLO-1 functions in M3 to control glutamate release. However, rescue of *slo-1* expression in the pharyngeal neurons or muscles did not restore the IP number to that of wild type. It is possible that extrachromosomal expression of *slo-1* in the transgenic *C. elegans* did not achieve a sufficient level to confer a wild type IP phenotype. It was also found that expression of *slo-1* in the neurons or muscles only partially rescued the wild type pattern of pumping, and this could also indicate that extrachromosomal *slo-1* expression levels were insufficient to fully restore the wild type phenotype. It is also possible that expressing *slo-1* indiscriminately in all pharyngeal neurons does not achieve a possibly more subtle *slo-1* expression pattern found in the wild type pharynx. Such an expression pattern may be responsible for maintaining a balance between the signaling by each neuron to achieve the appropriate pumping pattern. Rescue of *slo-1* expression in all neurons of the pharynx may have induced a functional level of *slo-1* expression in neurons where the channel is not normally prominent or is not normally expressed at all. Of course, it is also possible that both neuronal and muscle expression of *slo-1* is required for the restoration of the wild type IP phenotype and pumping pattern. However, the unsubstantial evidence regarding *slo-1* expression in the pharyngeal muscle (Wang et al., 2001), and absence of a SLO-1 current in patch clamp recordings from the wild type terminal bulb (section 6.8.1) strongly argues against a functional role for the channel in the muscle. Therefore, although *slo-1* expression in the muscles does partially rescue the wild type pumping pattern, the channel may not normally be found in this location, and these particular results may not be relevant in terms of the natural wild type situation. What can be concluded is that neuronal SLO-1 does contribute to the maintenance of a wild type pattern of pumping. Previous research has identified functional *slo-1* expression in MC where it acts in a negative feedback mechanism controlling ACh release (Chiang et al., 2006; Wang et al., 2001). This suggests that a loss of SLO-1 results in excessive ACh release from MC and the triggering of a very rapid rate of pumping, which can presumably be maintained only until the 'ready releasable pool' of neurotransmitter vesicles is depleted, after which, a period of time is required to allow vesicle recycling to 'catch up' and replenish the vesicle supply (Jorgensen et al., 1995).

In summary, SLO-1 channels appear to function in the pharyngeal nervous system to regulate pump duration, possibly by contributing to the control of glutamate release from the M3 neuron and muscle relaxation. Neuronal SLO-1 also appears to contribute to the maintenance of a wild type pattern of pumping, possibly by contributing to the control of ACh release from the MC neuron. These results concur with the findings of Chiang et al. (2006), who also identified a functional role for SLO-1 in MC and M3.

The results shown in section 6.5 suggest that ethanol affects *C. elegans* pharyngeal pumping. As Davies et al. (2003) have also shown that ethanol affects *C. elegans* locomotion and egg laying behaviour this suggests that ethanol targets several physiological behaviours in the worm to produce intoxication. In the pharynx, ethanol appears to inhibit the E2 phase associated with depolarization of the pharyngeal muscle membrane and muscle contraction, as well as stimulating pharyngeal pumping at concentrations of 10-100mM and inhibiting pumping rate at concentrations of 250mM or more.

Extensive research over the last three decades has revealed that ethanol intoxication is achieved via the targeting of a large number of synaptic proteins, both pre- and postsynaptic, including ACh receptors (e.g. Borghese et al., 2003), presynaptic glutamate release (e.g. Roberto et al., 2004), and voltage-sensitive Ca^{2+} channels (Wang et al., 1994). This suggests that, in the pharynx, ethanol could target glutamate release from M3 and glutamate receptors on the pharyngeal muscle, as well as affecting receptors for ACh (released from the MC neuron). ACh and glutamate release by MC and M3 are responsible for regulating pharyngeal pumping rate and pump duration, respectively (Avery & Horvitz, 1989; Niacaris & Avery, 2003; Raizen & Avery, 1994), suggesting that the rapid pumping observed when ethanol was applied at 5-100mM may involve up-regulation of M3 glutamate release and modulation of glutamate receptors and ACh receptors on the muscle cell membranes. The reduction in E2 phase amplitude by ethanol (at 20mM or more) is likely to be associated with a reduction in depolarization of the pharyngeal muscle membrane in response to ACh release by the MC neuron. This suggests that the pharyngeal muscles are stimulated by 20-100mM ethanol to produce more frequent but weaker contractions. Possibly ethanol modulates ACh receptors and voltage-gated Ca^{2+} channels on the muscle cell membrane to reduce the extent of muscle depolarization. The *eat-2(ad465)* loss-of-function mutant possesses a loss-of-function

mutation in the β-subunit of the nicotinic ACh receptor (nAChR) expressed on the pharyngeal muscle and localized to the synapse between the muscle and MC neuron, and thereby abolishes neurotransmission from MC to pharyngeal muscle (McKay et al., 2004). It would be very interesting to investigate whether the *eat-2(ad465)* mutant demonstrates a resistance to the reduction in pharyngeal pump E2 phase amplitude upon exposure to ethanol.

At concentrations of 250mM or more, ethanol inhibited pharyngeal pump rate, suggesting that ethanol has a biphasic effect on pumping. This biphasic response to ethanol which produces excitation or depression depending on the concentration applied has been identified previously upon application of ethanol to several cell types, including neurons, from many species. For example, electrophysiological recordings from rat brain monoaminergic neurons demonstrate an increase in basal firing rate upon application of 0.5-3mM ethanol, and an inhibition of basal firing at higher ethanol concentrations of 10-100mM (Backman & Granholm, 1992; Verbanck et al., 1990). Ethanol has also been shown to have a concentration-dependent biphasic effect on the membrane resistance and firing threshold of the crayfish stretch receptor neuron, with lower concentrations producing a stimulation of neuron activity and higher concentrations an inhibition (MacIver & Roth, 1987).

Anaesthetics, such as ethanol, are known to affect most biological cells in a non-specific fashion via their effect on the physical properties of lipid membranes, but various anaesthetic agents, including ethanol, have been shown to affect specific cell proteins directly to produce an effect that is often clinically relevant in terms of the ethanol concentration used (e.g. Harris & Hitzemann, 1981; Roth, 1980). For example, ethanol has been shown to affect the sodium-potassium ATPase located on rat brain synaptic membranes mainly indirectly by disruption of the lipid membrane but also by directly affecting the enzyme (Marques & Guerri, 1988). The *slo-1 (js379)* null mutant did not demonstrate the excitation of pharyngeal pumping observed in the wild type pharynx upon application of 10-100mM ethanol. However, both the *slo-1 (js379)* and wild type pharyngeal preparations were inhibited by 250mM ethanol or more and demonstrated a reduction in E2 phase amplitude in the presence of 50mM ethanol or more. Additionally, ethanol inhibition of E2 phase amplitude and pharyngeal pumping rate was reversible at all the ethanol concentrations tested within five minutes of ethanol removal, however, the

stimulation of pumping rate by ethanol did not appear to reverse within five minutes of ethanol removal. These results suggest the possibility that ethanol produces the excitation of pharyngeal pumping via a mechanism of action distinct from that used to inhibit E2 phase amplitude and pharyngeal pumping rate. This excitatory mechanism of action appears to involve SLO-1 and occurs when ethanol is applied at a clinically relevant concentration of 10mM. It is possible that the inhibitory effects of ethanol on pump rate and E2 amplitude are due to the effect of ethanol on the lipid membrane or by a direct mechanism of action distinct from that used to stimulate pharyngeal pumping. At present, such conclusions are highly tentative, and further investigation is required to characterize in more detail the biphasic effect of ethanol on pharyngeal pumping rate. Such investigation might include the use of a greater range of ethanol concentrations (particularly at the lower concentrations) and more n numbers, as well as investigating how long the apparent stimulation of pharyngeal pumping by 10-100mM ethanol takes to reverse upon removal of ethanol. It would be interesting to observe whether the sensitivity of the *slo-1 (js379)* null pharynx to stimulation by ethanol can be rescued by expression of *slo-1* in the pharyngeal neurons or muscle. If rescue of ethanol sensitivity does occur, this would strengthen the evidence supporting a role for *slo-1* in the mechanism of action of ethanol in the pharynx. Such an experiment may also indicate whether neuronal or muscle-expressed *slo-1* is functioning in ethanol-mediated pharyngeal stimulation. Further investigation could also record intracellularly from the pharyngeal muscle cells to observe the effect of ethanol on action potential rate, size and duration.

The possible involvement of SLO-1 in the excitation of pharyngeal pumping by 10-100mM ethanol concluded from the results shown in this chapter is supported by previous research suggesting that ethanol targets SLO-1 to affect *C. elegans* locomotion and egg laying behaviour (Davies et al., 2003). Additionally, ethanol has been shown to enhance the conductance of the *slo-1* homolog in rats (mSlo) via direct interaction of ethanol with the channel α-subunit (Dopico et al., 1998, 1996). Combining these previously published results, Crowder (2004) has proposed a model in which ethanol binds to SLO-1 to activate the channel and enhance the repolarization of the presynaptic terminal by the channel, thereby inhibiting neurotransmitter release. In view of the conclusions made in chapter 5, where emodepside was proposed to function via activation of SLO-1 to inhibit pharyngeal pumping, this suggests a possible parallel

between the proposed mechanism of the two compounds via SLO-1 modulation. Significantly, emodepside sensitivity was completely rescued in *slo-1 (js379)* mutants engineered to express *slo-1* neuronally; with the mutant response to emodepside exposure almost identical to the response of wild type control worms. This suggests that presynaptic SLO-1 is operating as a key component of the mechanism of action for emodepside in the pharynx.

Expression of *slo-1* in the pharyngeal muscles of the *slo-1 (js379)* null mutant did not rescue wild type sensitivity to emodepside, suggesting that the channel in this location does not contribute to the effect of emodepside. Comparison of the patch clamp results from the wild type and *slo-1 (js379); myo-2::slo-1* terminal bulb muscles strongly suggests that *slo-1* is either not expressed in the wild type terminal bulb muscles or is present but not functioning in the experimental conditions provided. Importantly, although the expression of *slo-1* in the muscles does not confer emodepside sensitivity, the K^+ currents of muscle-expressed SLO-1 appear to be potently inhibited by emodepside. This suggests that emodepside is capable of affecting SLO-1 in a muscle location, but this effect either does not contribute to, or is not sufficient to induce, the paralysis of pharyngeal pumping by the anthelmintic. This is perhaps significant bearing in mind the conclusions made in chapter 5, in which it was proposed that emodepside activates SLO-1 to inhibit neurotransmitter release and paralyse the muscles, whereas the patch clamp results suggest that emodepside inhibits the channel. It is possible that the effect of the anthelmintic on SLO-1 is dependent on the location of the channel, as BK channels have been shown to be highly modified by post-translational mechanisms that are dependent on the cell in which the channel is expressed. A substantial body of evidence has demonstrated that mammalian and invertebrate BK channels are substrates for modulation by protein kinases, including PKA (cyclicAMP-dependent protein kinase A; Lee et al., 1995; Tian et al., 2001; Zhou et al., 2001), PKC (diacylglycerol/Ca^{2+}-dependent protein kinase C; Barman et al., 2004), and CaM kinase II (Ca^{2+}/calmodulin-dependent protein kinase II; Liu et al., 2006), as well as modulation by fatty acids (Clarke et al., 2003). This modulation may be via direct interaction of the modulator with the channel. For example, fatty acids have been shown to increase BK channel activity in arterial smooth muscle cells by direct interaction with the channel protein (Clarke et al., 2003), and PKA can directly bind and thereby down-regulate the *Drosophila* Slo channel (Wang et al., 1999; Zhou et al., 2002). Indirect regulation of BK channel activity can also

occur by modulation of the activity of regulatory proteins, which changes how these regulatory proteins modulate the channel. For example, PKC has been shown to activate BK channels in rat pulmonary arterial smooth muscle cells by modulation of PKG (cyclicGMP-dependent protein kinase) which then activates the BK channel (Barman et al., 2004).

Significantly, not only can BK channel modulation simply activate or inactivate the channel, but it has also been shown to affect how the channel responds to modulators, for example, CaM kinase II phosphorylation of a specific threonine residue in the bovine BK channel (bSlo) has been shown to not only increase channel activity per se, but also switch the channel response to ethanol from robust activation to inhibition (visualized by patch clamp on *Xenopus* oocytes expressing bSlo; Liu et al., 2006). These results suggest that in this molecular system CaM kinase II phosphorylation works as a 'molecular switch' to modulate alcohol response via the BK channel; a form of neuronal plasticity. Therefore, is it possible that *slo-1* expression in the *C. elegans* pharyngeal neurons produces a channel activated by emodepside (as suggested in the conclusions to chapter 5), but *slo-1* expression in the pharyngeal muscles places the channel in an environment where it is subjected to modulation which modifies the emodepside response of the channel from activation to inhibition. Alternatively, the neuron, but not the muscle, may provide an environment where SLO-1 can be modified to produce channel activation upon emodepside exposure.

The *C. elegans slo-1* gain-of-function mutant strain *slo-1 (ky389)*, which possesses a point mutation in *slo-1* at threonine 1001 (in a putative Ca^{2+} sensing region), was shown to be hypersensitive to emodepside, suggesting that this threonine may be a site for channel modulation by emodepside (see chapter 5, section 5.7, page 173). As the *slo-1 (ky389)* mutants have been previously shown to exhibit phenotypes suggestive of increased SLO-1 activity (Davies et al., 2003), this suggests that emodepside may modify this region of the channel to induce (or contribute to the induction of) SLO-1 channel activation. It is possible that emodepside may bind a extracellular site on SLO-1 to produce conformational changes in the channel that facilitates Ca^{2+} binding to the channel, possibly at the low affinity site located in the RCK domain (Shi & Cui., 2001; Zhang et al., 2001; see chapter 1, section 1.7.7, page 51). Significantly, four of the nine strains isolated from the *C. elegans* mutagenesis screen for resistance to paralysis of

locomotion by emodepside were found to be mutations in the RCK domains of SLO-1 (Guest et al., 2007), suggesting that emodepside may affect Ca^{2+} binding to sites within these domains.

CHAPTER 7
DISCUSSION

Parasite resistance to currently available anthelmintic drugs requires the development of new compounds that operate via novel biological pathways. Therefore, this project aimed to initially investigate the potential of seven novel anthelmintic compounds using the model organism *C. elegans*. Of these seven compounds, those that were members of the cyclooctadepsipeptide group demonstrated the greatest potential. The cyclooctadepsipeptides are derived from the metabolic product of the fungus *M. sterilia* named PF1022A, shown to be a powerful broad-spectrum anthelmintic with low toxicity to host organisms and, importantly, activity against parasite strains resistant to currently available anthelmintics (Jeschke et al., 2005; Samson-Himmelstjerna et al., 2000). In an effort to improve on the anthelmintic potency of PF1022A, modification to the molecular structure of the compound has produced a group of derivatives with potential equal to or surpassing that of PF1022A (Jeschke et al., 2005). One such derivative is emodepside, shown to possess efficacy against a broad range of parasitic nematodes in a number of different host species (Conder et al., 1995; Harder et al., 2003; Samson-Himmelstjerna et al., 2000; Sasaki et al., 1992; Zahner et al., 2001a). Emodepside was also found to be one of the most potent of the anthelmintic compounds tested in this project, and therefore, this compound was selected for further investigation in *C. elegans* to define its physiological effects and the molecular mechanism by which these effects are achieved.

In adult and larval stage 4 (L4) *C. elegans*, emodepside was found to paralyse pharyngeal pumping, inhibiting both the basal pumping rate and pharyngeal response to 5-HT, as well as inhibiting *C. elegans* locomotion in liquid and on solid media. However, *C. elegans* L4 demonstrated reduced sensitivity to the anthelmintic, which, for the pharyngeal effect of the compound, appeared to be linked to a difference in cuticle structure between L4 and adult worms. The nematode cuticle is a major route of entry for a large number of anthelmintic compounds, and therefore, the ability to cross this barrier often defines the potency of drug in a specific nematode species (Alvarez et al., 2007). Significantly, emodepside has been shown to have variable efficacy against the larval and adult forms of several parasitic nematode species *in vivo*. Against adult *Heligmosomoides polygyrus* emodepside is highly active *in vivo*, however, the larval stages of this parasite, found in the intestinal mucosa of the host mouse, were shown to be only partially affected by the drug. This was suggested to be due to the encysted larvae being relatively impermeable to emodepside (Harder & von Samson-Himmelstjerna, 2001).

Other anthelmintics have also been shown to have differing efficacy against larval and adult parasite stages, which has been attributed to their ability to cross the nematode cuticle or tegument. For example, the anthelmintic albendazole, a member of the benzimidazole group, is used extensively in veterinary medicine and is highly effective against mature stages of the liver fluke, *Fasciola hepatica*, but not against the immature form. The major route of entry for albendazole is the fluke tegument, suggesting that the resistance of the immature worm may be partially, or wholly, due to developmental differences in tegument composition or structure (Mottier et al., 2006). The anthelmintic ivermectin, which, like emodepside, inhibits *C. elegans* locomotion, pharyngeal pumping and egg laying behaviour, has also been shown to exert its effects in adult worms in the absence of oral uptake, suggesting that the main route for the entry of ivermectin is through the cuticle (Bernt et al., 1998). Significantly, young juvenile *C. elegans* (L1 to L2), were found to be less sensitive to the effect of ivermectin on locomotion, an effect attributed to structural changes in the cuticle leading to differential penetrance in larvae and adults (Bernt et al., 1998). Drug absorption across the nematode cuticle is mainly dependent on lipophilicity, and in the case of acidic or basic drugs, the proportion of the drug that is non-ionized and therefore lipid-permeable (Alvarez et al., 2007). Therefore, the reduced sensitivity of L4 *C. elegans* to the effect of emodepside on pharyngeal pumping, and possibly locomotion as well, is likely to be due to structural differences between the cuticle of L4 and adult worms which affects drug diffusion across the cuticle.

Emodepside was found to inhibit egg laying behaviour but not egg generation in gravid adult *C. elegans*, resulting in emodepside-exposed gravid adults becoming bloated with eggs that eventually hatched within the parent worm (see chapter 4). Significantly, the emodepside precursor PF1022A also demonstrates an ability to retard *C. elegans* egg laying behaviour, resulting in the accumulation of eggs within the parent worm (Bernt et al., 1998). When embryo development in the presence of PF1022A was examined in detail by Bernt et al. (1998), no abnormalities were identified, and embryos continued to develop normally and hatch when removed from the parent worm and grown in the presence of the drug. Therefore, it was concluded that PF1022A does not affect embryo development or hatching but does inhibit egg laying behaviour, identical to the effects of emodepside observed in this project. Like emodepside and PF1022A, the anthelmintic ivermectin has been shown to impair *C. elegans* egg laying behaviour. However, unlike

the two cyclooctadepsipeptides, ivermectin also inhibits oocyte fertilization by paralysing contractions of the gonad required for oocyte transport towards the spermatheca (Bernt et al., 1998). Although exposure of gravid adult *C. elegans* to ivermectin inhibits oocyte fertilization, Bernt et al. (1998) have demonstrated that oocytes fertilized prior to ivermectin-exposure develop normally in the presence of ivermectin, an ability that could not be attributed to protection by the eggshell or the cuticle of the parent worm. Therefore, ivermectin, like emodepside and PF1022A, does not appear to affect embryo development itself, and gravid worms exposed to all three anthelmintics demonstrate the hatching of larvae inside them (chapter 4; Bernt et al., 1998). Ivermectin is one of the most widely and successfully used members of the avermectin class of anthelmintics, but such wide-spread use has led to the emergence of resistance which is a rapidly growing problem ((Meinke, 2001; Sangster & Gill, 1999). Therefore, because emodepside utilizes a novel mechanism of action previously shown not to involve the glutamate-gated chloride channel utilized by ivermectin (Willson et al., 2004), emodepside demonstrates great promise as a commercial anthelmintic with the potential to break the resistance problem.

The ability of adult worms to lay eggs despite exposure to emodepside during their development from L1 to early L4 stage, suggests that the drug cannot persist in the worm from early L4 to gravid adulthood to exert an inhibitory effect on egg laying. It would be interesting to establish whether *C. elegans* exposed to emodepside only during the L1 to L3 stages demonstrate impaired pharyngeal pumping and locomotion when they reach adulthood. This would reveal whether the effect of emodepside on locomotion and pharyngeal pumping persists in the absence of continual emodepside application. Such information would be very useful in determining a strategy for the application of emodepside as a commercial anthelmintic to the host organism. If emodepside exposure during *C. elegans* L1 to L3 stages is not sufficient to render the worms unviable at that age, and the anthelmintic cannot persist to paralyse the worms when they become adults, this suggests that the anthelmintic would need to be regularly applied to the parasite host to combat infection.

In the *C. elegans* pharynx, the neuronally located SLO-1 channel appears to be the major component in the mechanism by which emodepside paralyses pumping, with $G\alpha_q$, $G\alpha_o$, and LAT-1 in minor contributory roles. The resistance of the *slo-1 (js379)* null to

emodepside suggests that the compound facilitates the activation of SLO-1, which, based on previous research describing the function of the channel, would result in the inhibition of neurotransmitter release (Wang et al., 2001). However, the whole cell patch clamp recordings from the terminal bulb muscle (chapter 6) appear to show that emodepside inhibits the K^+ currents of SLO-1. Initially these results appear to contradict the conclusions made from the EPG data, but it should be noted that the transgenic *slo-1 (js379)* null *C. elegans* with *slo-1* expression in the pharyngeal muscle remained resistant to the effect of emodepside on the pharynx, suggesting that despite the ability of emodepside to inhibit SLO-1 currents in the muscles of these worms, this action does not induce paralysis of pharyngeal pumping. It is possible that in the pharyngeal neurons, but not the muscle, SLO-1 is post-translationally modified to produce a channel that is activated by emodepside either by direct interaction of the anthelmintic with SLO-1, or by the modification of the activity of proteins that in turn regulate SLO-1 activity.

Significantly, the EXP-2 K^+ channel, located in the pharyngeal muscle and believed to be the major facilitator of muscle repolarization and relaxation, has been shown to possess very different conductance characteristics depending on its location (Davis et al., 1999; Shtonda & Avery, 2005; Steger et al., 2005). In the pharyngeal muscle, during the plateau phase of the action potential, the inactivation of EGL-19 Ca^{2+} channels produces a gradual hyperpolarization that reactivates EXP-2 once a specific positive potential is reached. The reactivated EXP-2 channels conduct a large outward K^+ current that drives muscle repolarization (Shtonda & Avery, 2005). However, when expressed in *Xenopus* oocytes, EXP-2 was found to produce only inward currents, and the channel conducted very little current at membrane potentials more positive than -120mV (Fleischhauer et al., 2000; Shtonda & Avery, 2005). In the oocytes, it was concluded that because EXP-2 demonstrates faster deactivation than activation during depolarization, this prevents current conductance until repolarization reaches -120mV when the channels reactivate and produce inward currents (Fleischhauer et al., 2000). The apparent difference in EXP-2 behaviour in the two cellular environments was suggested by Fleischhauer et al. (2000) to be a result of EXP-2 forming homotetrameric channels in *Xenopus* oocytes, whereas in pharyngeal muscle the EXP-2 channels could be hetrotetrameric, with the different subunits modifying channel activity. In *C. elegans*, the *slo-1* gene encodes at least three splice variants (Wei et al., 1996), and it is possible that native SLO-1 in the pharyngeal neurons is a heterotetrameric channel composed of a combination of the three subunits.

However, only the *slo-1a* sequence was included in the construct for expression of *slo-1* in the muscle and the neurons, and the homotetrameric channels produced from this subunit may therefore possess different characteristics to the native channel. This may explain why, in the patch clamp recordings from the terminal bulb muscle cells, the SLO-1 current was inhibited by emodepside. Indeed, this may also explain why in the EPG analysis of the *slo-1* null pharyngeal phenotype, transgenic expression of *slo-1* in the neurons (also producing homotetrameric channels composed of only SLO-1a) did not restore the wild type IP number and only partially restored the wild type pumping pattern. It is possible that the SLO-1b and/or SLO-1c subunits (and possibly other, as yet unidentified, SLO-1 subunits) are required to fully restore a wild type phenotype. For example, it has been shown that when the mammalian Slowpoke (BK) channel β1 subunit is coexpressed with the α subunit, it modulates Slowpoke channel activity and, importantly, influences channel modulation by protein kinases as well as altering toxin binding to the channel (McManus et al., 1995; Dworetzky et al., 1996; Tseng-Crank et al., 1996). Therefore, in the pharyngeal neurons, it is possible that native SLO-1 may be a hetrotetrameric channel, which, due to the presence of the subunits other than SLO-1a, is modified (possibly by protein kinases) to produce a channel that can be stimulated by emodepside action.

The *slo-1 (ky389)* gain-of-function mutant, which contains a point mutation in a region of the SLO-1 channel associated with Ca^{2+} sensitivity, is hypersensitive to emodepside. These results suggest that emodepside modifies (directly or indirectly) SLO-1 sensitivity to Ca^{2+} in order to activate the channel and terminate neurotransmitter release. Supporting these findings, Guest et al. (2007) have demonstrated that *C. elegans* mutants isolated from a mutagenesis screen for emodepside resistance are mutated in the RCK domains of SLO-1. The RCK domains are also regions associated with Ca^{2+} sensitivity, and Xia et al. (2002) have shown that mutation of a specific conserved residue (aspartic acid 367) within the RCK domain produces a SLO-1 channel with reduced Ca^{2+}-dependent regulation of activation. Therefore, to further support the apparent link between emodepside action and SLO-1 Ca^{2+} sensitivity, future experiments could examine the emodepside sensitivity of pharyngeal pumping in the RCK mutants isolated as resistant to emodepside-induced paralysis of locomotion by Guest et al. (2007).

Previous research has demonstrated that emodepside stimulates neurotransmitter release at the pharyngeal neuromuscular junction (Willson et al., 2004). Therefore, it is possible that emodepside stimulates SLO-1 by increasing not only channel Ca^{2+} sensitivity but also intracellular Ca^{2+} concentration. Latrotoxin, which also stimulates neurotransmitter release to paralyse muscle function, has been shown in MIN6 β cells to activate protein kinase C (PKC) via latrophilin binding and $G\alpha_q$ pathway activation, resulting in the closure of inwardly-rectifying K^+ channels and membrane depolarization, which then triggers the opening of voltage-dependent Ca^{2+} channels and produces a rise in intracellular Ca^{2+}. It is possible that emodepside stimulates such a pathway to activate SLO-1. However, by stimulating a rise in intracellular Ca^{2+}, emodepside would inevitably be expected to cause neurotransmitter release before the delayed opening of SLO-1 repolarizes the presynaptic membrane and stops further neurotransmitter release. This might explain why Willson et al. (2004) observed a loss of fluorescence in active pharyngeal synapses labelled with FM4-64 (rhodamine fluorescent marker) upon application of emodepside: the anthelmintic had initially stimulated neurotransmitter release, before inhibiting any further release. It is possible that emodepside increases SLO-1 sensitivity to Ca^{2+} (as well as increasing intracellular Ca^{2+}) so that the SLO-1 channels are activated when Ca^{2+} levels have just begun to rise, resulting in SLO-1 currents terminating neurotransmitter release earlier than in the absence of emodepside, thereby minimizing neurotransmitter release.

The SLO-1 channel appears to function in the pharyngeal nervous system to regulate the pattern of pumping, as well as regulating individual pump duration by contributing to the control of neurotransmitter release from the M3 and MC neurons (chapter 6). Therefore, emodepside may activate SLO-1 channels to inhibit acetylcholine (ACh) release from MC, and thereby prevent pharyngeal muscle contraction. However, previous research has shown that the effect of emodepside on pharyngeal pumping in *eat-2 (da465) C. elegans*, deficient in a non-alpha nicotinic ACh receptor, is not significantly different to wild type, suggesting that ACh is not solely involved in emodepside action (Willson, 2003). It is therefore possible that emodepside affects the release of a number of neurotransmitters and neuropeptides to exert its anthelmintic effects. Significantly, previous research has demonstrated that the *unc-31 C. elegans* strain, defective for neuronal exocytosis of large dense core vesicles, has reduced sensitivity to emodepside in the pharynx (Willson, 2003). As dense core vesicles are considered the site for the storage of neuropeptides

within neurons (Burgoyne & Morgan, 2003; Salio et al., 2006), the reduced emodepside sensitivity of the *unc-31* mutants suggests that neuropeptide release may contribute to the mode of action for the anthelmintic. Supporting these findings, Willson (2003) also demonstrated in *C. elegans* that RNAi directed against the *flp-1* and *flp-13* genes, which encode peptides capable of inhibiting pharyngeal pumping (Rogers et al., 2001), reduces pharyngeal sensitivity to emodepside. Therefore, the initial stimulation of presynaptic vesicle release upon application of emodepside to the pharynx may include the release of inhibitory neuropeptides in addition to neurotransmitters such as ACh. It is possible that the activity of the mixture of neurotransmitters and neuropeptides released by emodepside is dominated by the inhibitory neuropeptide component, producing an overall result of pharyngeal inhibition, which is maintained by the delayed opening of SLO-1 and suppression of all further neurotransmitter and neuropeptide release.

A key feature of the mechanism of action for emodepside in the pharynx proposed from the results shown in this project is the activation of SLO-1 by the anthelmintic, and therefore, future investigation should focus on demonstrating if emodepside does facilitate SLO-1 activity in pharyngeal neurons. Due to the small size of the *C. elegans* pharyngeal neurons and the difficulty of accessing them within the intact pharynx without imposing damage, electrophysiological recordings are more likely to be achieved using cultured pharyngeal neurons. Recently, techniques have been described which enable *C. elegans* embryonic cells to be robustly cultured on a large scale. These cultured cells have been shown to differentiate into various cell types including neurons, from which whole cell recordings have been made and have been shown to be similar to those measured *in vivo* (Christensen et al., 2002; Strange et al., 2007). Therefore, culturing embryonic cells from the *slo-1 (js379); snb-1::slo-1 C. elegans* that also express a pharyngeal neuron specific GFP-reporter gene, will allow the generation of a primary culture of identifiable pharyngeal neurons expressing *slo-1*. A possible reporter gene could place the *gfp* sequence behind the promoter for *ceh-28*, which is a NK-2 homeobox gene previously shown to be expressed as a *ceh-28*::GFP transcriptional fusion in only the M4 neuron of the pharynx (Harfe & Fire, 1998). Whole cell patch clamp recording from the cultured cells exhibiting GFP fluorescence would then enable the effect of emodepside on neuronal SLO-1 K^+ currents to be examined, and inside-out patch recordings would allow channel opening in the presence of the anthelmintic to be investigated as well. A further advantage of using cultured pharyngeal neurons is that,

unlike the pharyngeal muscle cells, the neurons are not coupled by gap junctions, and therefore the current density can be normalized to the cell capacitance to allow accurate voltage-current relationship results to be obtained. When performing patch clamp recordings on pharyngeal muscle cells, the electrical connectivity between the cells means that membrane capacitance cannot be accurately measured, although valuable results can be still obtained as shown by Shtonda & Avery (2005).

In summary, the results of this project have provided a hypothesis for emodepside induced pharyngeal paralysis in which emodepside increases intracellular Ca^{2+} (partially by stimulation of the presynaptic $G\alpha_q$ pathway as well as by, as yet, unidentified pathways) to activate the SLO-1 which would inhibit further neurotransmitter release and paralyse the muscles. To combat the neurotransmitter release inevitably stimulated by the increase in intracellular Ca^{2+}, emodepside may also modulate SLO-1 Ca^{2+}sensitivity, possibly by directly binding the channel, resulting in a channel that activates at a lower Ca^{2+} concentration and thereby terminates neurotransmitter release more rapidly (see figure 7.1).

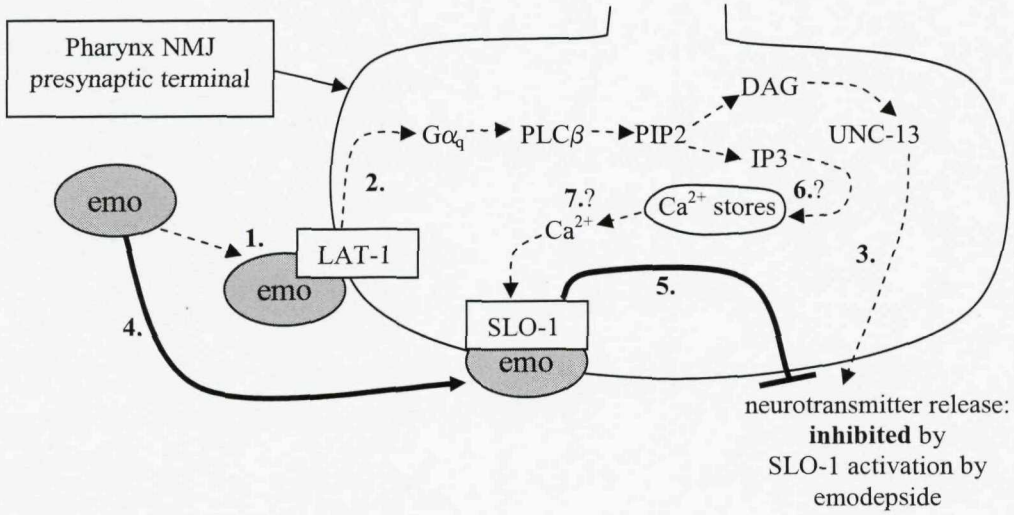

Figure 7.1 A model for the mechanism of action of emodepside at the presynaptic terminal of the wild type *C. elegans* pharyngeal neuromuscular junction (NMJ). Emodepside binding to LAT-1 (**1.**) results in stimulation of the $G\alpha_q$ pathway (**2.**), leading to the release of neurotransmitters, possibly including inhibitory neuropeptides (**3.**). Emodepside also binds to SLO-1 (**4.**), enhancing channel Ca^{2+} sensitivity and resulting in SLO-1 activation at lower intracellular Ca^{2+} concentrations, and premature termination of neurotransmitter release (**5.**). It is possible that stimulation of the $G\alpha_q$ pathway by emodepside also results in the release of Ca^{2+} from intracellular stores (**6.**), contributing to the activation of SLO-1 channels (**7.**) and resulting in the inhibition of neurotransmitter release.

Interestingly, ethanol has been shown to modulate the Ca^{2+} sensitivity of mouse Slo channels (mSlo) expressed in *Xenopus* oocytes, resulting in channel activation at intracellular Ca^{2+} concentrations lower than those normally required to activate the channel (Dopico et al., 1998). Human BK channels expressed in human embryonic kidney (HEK) cells have also been shown to be activated by ethanol, but this effect required coexpression of the channel β subunit known to be important in modulating mammalian BK channel Ca^{2+}sensitivity (Feinberg-Zadek & Treistman, 2007; Qian & Magleby, 2003). These results suggest that the activation of human BK channels by ethanol also involves the modulation of channel sensitivity to Ca^{2+} (Feinberg-Zadek & Treistman, 2007). In *C. elegans*, SLO-1 has previously been identified as a component in the mechanism by which ethanol affects worm locomotion and egg laying (Davies et al., 2003). In this project, SLO-1 also appears to have a role in the stimulation of pharyngeal pumping by ethanol at concentrations of 10-100mM. However, when viewed objectively, the pharyngeal resistance of the *slo-1* null mutant to ethanol was by no means as obvious as the resistance of the *slo-1* null to the effects of ethanol on locomotion and egg laying demonstrated by Davies et al. (2003). It is possible that the EPG assay utilized to examine the role of SLO-1 in *C. elegans* pharyngeal sensitivity to ethanol was not sensitive enough to reveal the extent of SLO-1 involvement in mediating ethanol stimulation of pharyngeal pumping. However, it is more likely that ethanol affects a variety of pre- and postsynaptic proteins in the pharynx to exert its effects, and SLO-1 contributes only a minor role in the mechanism that leads to pharyngeal intoxication. How ethanol is affecting the SLO-1 channel at a molecular level cannot be resolved from the investigations presented in this project. The patch clamp recordings shown in chapter 6 suggest that pharyngeal SLO-1 is only present in the neurons. Therefore, if ethanol is activating the channel, as has been shown in patch clamp recordings from wild type *C. elegans* CEP neurons (Davies et al., 2003), it could stimulate pharyngeal pumping rate if SLO-1 activation significantly inhibits glutamate release from M3 and inhibitory neuropeptide release from other pharyngeal neurons. Alternatively, ethanol may inhibit SLO-1 in the pharynx, resulting in excessive acetylcholine release from the MC neuron and the observed increase in pharyngeal pumping. To resolve the effect of ethanol on SLO-1 activity, patch clamp recordings from cultured pharyngeal neurons, previously described in this discussion, could be used to observe the effect of ethanol on the SLO-1 K^+ currents. Of course, such an investigation would also resolve how significant the effect of ethanol on SLO-1 activity actually is.

Further investigation to extend the results presented in this project could also focus on establishing whether emodepside binds to SLO-1 directly. To achieve this, a radioligand binding study using radiolabelled (^{3}H) emodepside could be used to investigate whether emodepside binds cultured pharyngeal neurons from *slo-1 (js379) C. elegans* with less affinity than cultured pharyngeal neurons from the wild type strain.

BK channels have been shown to be the molecular target for a vast array of endogenous and exogenous compounds, including terpenes, phenols, flavonoids, hormones, tamoxifen, cannabinoids, synthetic benzimidazolone derivatives, alkaloids, peptides and toxins (e.g. Coiret et al., 2007; Davies et al., 2003; Nardi et al., 2003; Sade et al., 2006). Significantly, some of these compounds have been shown to activate BK channels by increasing intracellular Ca^{2+}; a similar mechanism to that proposed for emodepside in this project. For example, when the activity of the human BK channel was examined by patch clamp in coronary myoctyes, the channel was found to activated by diazepam, GABA and progesterone via a stimulated increase in intracellular Ca^{2+} (Jacob & White, 2000). Other BK channel modulators have been shown to target the channel itself to alter the Ca^{2+} sensitivity, which is another mechanism suggested in this project to be used by emodepside to activate SLO-1. For example, Evans blue (EB) has been shown to activate human BK channels expressed in endothelial cells of human umbilical veins. This effect was attributed to a direct effect of EB on the Ca^{2+} sensitivity of the BK channel (Wu et al., 1999). The high level of emodepside resistance exhibited by the *slo-1 (js379)* null pharynx, combined with the identification of only *slo-1* mutations from the mutagenesis screen for emodepside resistance (Guest et al., 2007), strongly favours a direct interaction of emodepside with SLO-1.

Despite continued research adding ever more compounds to the list of identified BK channel modulators, emodepside appears to be the first anthelmintic to be included, highlighting the novelty of the mechanism of action for this compound. Given the vital role that BK channels such as *C. elegans* SLO-1 play in regulating fundamental cellular processes, including neurotransmitter release and neuronal and muscle excitability, it is perhaps not surprising that emodepside, by targeting SLO-1, is an extremely effective compound. It is particularly exciting that the cyclooctadepsipeptides PF1022-222, PF1022-888 and verticilide also examined in this project appear to share with

emodepside a mechanism of action in *C. elegans* that involves the SLO-1 channel. Therefore, the cyclooctadepsipeptide group appear to possess a mode of action unique among existing anthelmintics, and thereby have the potential to be successful anthelmintic compounds capable of breaking resistance.

CHAPTER 8.
REFERENCES

Ackley, B. D., Harington, R. J., Hudson, M. L., Williams, L., Kenyon, C. J., Chisholm, A. D., Jin, Y. (2005) The two isoforms of the *Caenorhabditis elegans* leukocyte-common antigen related receptor tyrosine phosphatase PTP-3 function independently in axon guidance and synapse formation. *The Journal of Neuroscience*, **25**, 7517-7528.

Ahmed, S., Maruyama, I. N., Kozma, R., Lee, J., Brenner, S. & Lim, L. (1992) The *Caenorhabditis elegans unc-13* gene product is a phospholipid-dependent high affinity phorbol ester receptor. *The Biochemical Journal*, **287**, 995-999.

Albertson, D. G. & Thomson, J. N. (1976) The pharynx of *Caenorhabditis elegans*. *Philosophical Transactions of the Royal Society of London. Series B. Biological Sciences,* **275**, 299-325.

Alfonso, A. K., Grundahl, K., McManus, J. R., Rand, J. B. (1994) Cloning and characterization of the choline acetyltransferase structural gene (*cha-1*) from *C. elegans*. *Journal of Neuroscience*, **14**, 2290-2300.

Alvarez, L. I., Lourdes Mottier, M., Lanusse, C. E. (2007) Drug transfer into target helminth parasites. *Trends in Parasitology*, **23**, 97-104

Ambros, V. (1989) A hierarchy of regulatory genes controls a larva-to-adult developmental switch in *C. elegans*. *Cell*, **57**, 49-57.

Amliwala, K. Molecular and genetic determinants of the inhibitory action of emodepside on *C. elegans* muscle. Ph.D. Thesis (1995) University of Southampton, School of Biological Sciences, Southampton, U.K.

Arena, J. P., Liu, K. K., Paress, P. S., Frazier, E. G., Cully, D. F., Mrozik, H., Schaeffer, J. M. (1995) The mechanism of action of avermectins in *Caenorhabditis elegans* – correlation between activation of glutamate-sensitive chloride current, membrane-binding and biological activity. *Journal of Parasitology*, **81**, 286-294.

Arena, J. P., Liu, K. K., Paress, P. S., Cully, D. F. (1992) Expression of a glutamate-activated chloride current in *Xenopus* oocytes injected with *Caenorhabditis elegans* RNA: evidence for modulation by avermectin. *Molecular Brain Research*, **15**, 339-348.

Arena, J. P., Liu, K. K., Paress, P. S., Cully, D. F. (1991) Avermectin-sensitive chloride currents induced by *Caenorhabditis elegans* RNA in *Xenopus* oocytes. *Molecular Pharmacology*, **40**, 368-374.

Atkinson, N. S, Robertson, G. A., Ganetzky, B. (1991) A component of calcium-activated potassium channels encoded by the *Drosophila slo* locus. *Science*, **253**, 551-555.

Augustin, I., Rosenmund, C., Südhof, T. C., Brose, N. (1999) Munc-13 is essential for fusion competence of glutamatergic synaptic vesicles. *Nature*, **400**, 457-461.

Avery, L. & Thomas, J. H. (1997) Feeding and defecation. In: *C. elegans* II (Riddle, D. L., Blumenthal, T., Meyer, B. J. and Preiss, J. R.), pp. 679-719. Cold Spring Harbor Laboratory Press, Cold Spring Harbor Press, New York.

Avery, L. (1993) Motor neuron M3 controls pharyngeal muscle relaxation timing in *Caenorhabditis elegans*. *Journal of Experimental Biology*, **175**, 283-297.

Avery, L. & Horvitz, H. R. (1990) Effects of starvation and neuroactive drugs on feeding in *Caenorhabditis elegans*. *Journal of Experimental Zoology*, **253**, 263-270.

Avery, L. & Horvitz, H. R. (1989) Pharyngeal pumping continues after laser killing of the pharyngeal nervous system of *C. elegans*. *Neuron*, **3**, 473-485.

Backman, C. & Granholm, A. C. (1992) Effects of ethanol on development of dorsal raphe transplants in oculo: a morphological and electrophysiological study. *Journal of Comparative Neurology*, **320**, 136-144.

Baird, S.E. & Chamberlin, H.M. (2006) *Caenorhabditis briggsae* methods. In: *The C. elegans Research Community*, WormBook. Worm-Book, doi/10.1895/wormbook. 1.128.1, <http://www.wormbook.org>.

Ballivet, M., Alliod, C., Bertrand, S., Bertrand, D. (1996) Nicotinic acetylcholine receptors in the nematode *Caenorhabditis elegans*. *Journal of Molecular Biology*, **258**, 261-269.

Bany, I. A., Dong, M-Q. & Koelle, M. R. (2003) Genetic and Cellular Basis for Acetylcholine Inhibition of *Caenorhabditis elegans* Egg-Laying Behaviour. *The Journal of Neuroscience*, **23**, 8060-8069.

Bao, L., Raoin, A. M., Holmstrand, E. C., Cox, D. H. (2002) Elimination of the BKCa channel's high-affinity Ca^{2+} sensitivity. *Journal of General Physiology*, **120**, 173-189.

Barman, S. A., Zhu, S., White, R. E. (2004) Protein kinase C inhibits BK_{Ca} channel activity in pulmonary arterial smooth muscle. *American Journal of Physiology. Lung Cellular and Molecular Physiology,* **286**, L149–L155.

Barnes, R. S. K., Calow, P., Olive, P. J. W. (1993) Chapter 4: The Worms. In: *The Invertebrates: A New Synthesis*, Second Edition, pp. 83-121. Blackwell Science, U.K.

Barnett, D. W., Liu, J., Misler, S. (1996) Single-cell measurements of quantal secretion induced by α-latrotoxin from rat adrenal chromaffin cells: dependence on extracellular Ca^{2+}. *Pflugers Archives*, **432**, 1039-1046.

Bastiani, C. A., Gharib, S., Simon, M. I., Sternberg, P. W. (2003) *Caenorhabditis elegans* Galphaq regulates egg-laying behavior via a PLCbeta-independent and serotonin-dependent signaling pathway and likely functions both in the nervous system and in muscle. *Genetics*, **165**, 1805-1822.

Baylis, H. A., Furuichi, T., Yoshikawa, F., Mikoshiba, K., Sattelle, D. B. (1999) Inositol 1, 4, 5-trisphosphate receptors are strongly expressed in the nervous system, pharynx, intestine, gonad and excretory cell of *Caenorhabditis elegans* and are encoded by a single gene (*itr-1*). *Journal of Molecular Biology*, **294**, 467-476.

Behm, C. A., Bendig, M. M., McCarter, J. P., Sluder, A.E. (2005) RNAi-based discovery and validation of new drug targets in filarial nematodes. *Trends in Parasitology*, **21**, 97-100.

Berman, D. M. & Gilman, A. G. (1998) Mammalian RGS proteins: barbarians at the gate. *The Journal of Biological Chemistry*, **273**, 1269-1272.

Bernstein, E., Caudy, A. A., Hammond, S. M., Hannon, G. J. (2001) Role for a bidentate ribonuclease in the initiation step of RNA interference. *Nature*, **409**, 363-366.

Bernt, U., Junkersdorf, B., Londershausen, M., Harder, A., Schierenberg, E. (1998) Effects of Anthelmintics with Different Modes of Action on the Behavior and Development of *Caenorhabditis elegans*. *Fundamental and Applied Nematology*, **21**, 251-263.

Berridge, M. J. (1993) Inositol trisphosphate and calcium signaling. *Nature*, **361**, 315-325.

Bezprozvanny, I., Watras, J., Ehrlich, B. E. (1991) Bell-shaped calcium-response curves of Ins (1, 4 ,5) P3- and calcium-gated channels from endoplasmic reticulum of cerebellum. *Nature*, **351**, 751-754.

Bittner, M.A. (2000) α-Latrotoxin and its receptors CIRL (latrophilin) and neurexins 1α mediate effects on secretion through multiple mechanisms. *Biochimie*, **82**, 447-452.

Blackburn, C. C. & Selkirk, M. E. (1992) Inactivation of platelet-activating factor by a putative acetylhydrolase from the gastrointestinal nematode parasite *Nippostrongylus brasiliensis*. *Immunology*, **75**, 41-46.

Blaxter, M. (1998) *Caenorhabditis elegans* is a Nematode. *Science*, **282**, 2041-2046.

Blaxter, M. L., Page, A. P., Rudin, W., Maizels, R. M. (1992) Nematode surface coats: Actively evading immunity. *Parasitology Today*, **8**, 243-247.

Borghese, C. M., Henderson, L. A., Bleck, V., Trudell, J. R., Harris, R. A. (2003) Sites of excitatory and inhibitory actions of alcohols on neuronal alpha2beta4 nicotinic acetylcholine receptors. *Journal of Pharmacology and Experimental Therapeutics*, **307**, 42-52.

Brenner, S. (1974) The genetics of *Caenorhabditis elegans*. *Genetics*, **77**, 71-94.

Britton, C. & Murray, L. (2006) Using *Caenorhabditis elegans* for functional analysis of genes of parasitic nematodes. *International Journal for Parasitology*, **36**, 651–659.

Britton, C. & Murray, L. (2004) Cathepsin L protease (CPL-1) is essential for yolk processing during embryogenesis in *Caenorhabditis elegans*. *Journal of Cell Science*, **117**, 5133–5143.

Britton, C. & Murray, L. (2002) A cathepsin L protease essential for *Caenorhabditis elegans* embryogenesis is functionally conserved in parasitic nematodes. *Molecular and Biochemical Parasitology*, **122**, 21–33.

Brockie, P. J., Mellem, J. E., Hills, T., Madsen, D. M., Maricq, A. V. (2001) The *C. elegans* Glutamate Receptor Subunit NMR-1 Is Required for Slow NMDA-Activated Currents that Regulate Reversal Frequency during Locomotion. *Neuron*, **31**, 617-630.

Brownlee, D., Holden-Dye, L., Walker, R. (2000) The Range and Biological Activity of FMRFamide-related Peptides and Classical Neurotransmitters in Nematodes. *Advances in Parasitology*, **45**, 109-180.

Brownlee, D. J., Holden-Dye, L., Walker, R. J. (1997) Action of the anthelmintic ivermectin on the pharyngeal muscle of the parasitic nematode, *Acsaris suum*. *Parasitology*, **115**, 553-561.

Brownlee, D. J., Fairweather, I., Johnston, C. F., Smart, D., Shaw, C., Halton, D. W. (1993) Immunocytochemical demonstration of neuropeptides in the central nervous system of the roundworm, *Ascaris suum* (Nematoda: Ascaridia). *Parasitology*, **106**, 305-316.

Brose, N., Rosenmund, C., Rettig, J. (2000) Regulation of transmitter release by *Unc-13* and its homologues. *Current Opinion in Neurobiology*, **10**, 303-311.

Brundage, L., Avery, L., Katz, A., Kim, U. J., Mendel, J. E., Sternberg, P. W. & Simon, M. I. (1996) Mutations in a *C. elegans* Gqalpha gene disrupt movement, egg laying, and viability. *Neuron*, **16**, 999-1009.

Bundy, D. A. & De Silva, N. R. (1998) Can we deworm this wormy world? *British Medical Bulletin*, **54**, 421-432.

Burglin, T. R., Lobos, E., Blaxter, M. L. (1998) *Caenorhabditis elegans* as a model for parasitic nematodes. *International Journal for Parasitology*, **28**, 395-411.

Burgoyne, R. D. & Morgan, A. (2003) Secretory granule exocytosis. *Physiological Reviews*, **83**, 581-632.

Bush, A. O., Fernandez, J. C., Esch, G. W., Seed, J. R. (2001) Nematoda: the Roundworms. In: *Parasitism, the Diversity and Ecology of Animal Parasites*, pp. 160-196. Cambridge University Press, Cambridge, U.K.

Campbell, W. C., Fisher, M. H., Stapley, E. O., Albers-Schonberg, G. & Jacob, T. A. (1983). Ivermectin: a potent new antiparasitic agent. *Science*, **221**, 823–828.

Capogna, M., Gahwiler, B. H., Thompson, S. M. (1996) Calcium-independent actions of α-latrotoxin on spontaneous and evoked synaptic transmission in the hippocampus. *Journal of Neurophysiology*, **76**, 3149-3158.

Carre-Pierrat, M., Grisoni, K., Gieseler, K., Mariol, M., Martin, E., Jospin, M., Allar, B., Segalat, L. (2006) The SLO-1 BK channel of *Caenorhabditis elegans* is critical for muscle function and is involved in dystrophin-dependent muscle dystrophy. *Journal of Molecular Biology*, **358**, 387-395.

Ceccarelli, B., Grohovaz, F., Hurlbut, W. P. (1979) Freeze-fracture studies of frog neuromuscular junctions during intense release of neurotransmitter. I. Effects of black widow spider venom and Ca^{2+}-free solutions on the structure of the active zone. *The Journal of Cell Biology*, **81**, 163-177.

Chalfie, M. & White, J. (1988) The Nervous System. In: *The Nematode Caernorhabditis elegans* (Wood, W. B., ed), chapter 11, pp. 358-363.

Chalfie, M. & Sulston, J. (1981) Developmental genetics of the mechanosensory neurons of *Caenorhabditis elegans*. *Developmental Biology*, **82**, 358-370.

Changeux, J. P. & Edelstein, S. J. (1998) Allosteric receptors after 30 years. *Neuron*, **21**, 959-980.

Chiang, J. A., Steciuk, M., Shtonda, B., Avery, L. (2006) Evolution of pharyngeal behaviours and neuronal functions in free-living soil nematodes. *The Journal of Experimental Biology*, **209**, 1859-1873.

Christensen, M., Estevez, A., Yin, X., Fox, R., Morrison, R., McDonnell, M., Gleason, C., Miller, D. M., Strange, K. (2002) A Primary Culture System for Functional Analysis of *C. elegans* Neurons and Muscle Cells. *Neuron*, **33**, 503–514.

Chung, S. K., Reinhart, P. H., Martin, B. L., Brautigan, D., Levitan, I. B. (1991) Protein kinase activity closely associated with a reconstituted calcium-activated potassium channel. *Science*, **253**, 560-562.

Clarke, A. L., Petrou, S., Walsh, J. V., Singer, J. J. (2003) Site of action of fatty acids and other charged lipids on BK_{Ca} channels from arterial smooth muscle cells *American Journal of Physiology. Cell Physiology,* **284**, C607–C619.

Coiret, G., Borowiec, A. S., Mariot, P., Ouadid-Ahidouch, H., Matifat, F. (2007) The antiestrogen tamoxifen activates BK channels and stimulates proliferation of MCF-7 breast cancer cells. *Molecular Pharmacology*, **71**, 843-51.

Conder, G.A., Johnson, S.S., Nowakowski, D.S. (1995) Anthelmintic profile of the cyclodepsipeptide PF 1022A in *in vitro* and *in vivo* models. *Journal of Antibiotics*, **48,** 820-823.

Cowden, C., Sithigorngul, P., Brackley, P., Guastella, J., Stretton, A. O. (1993) Localization and differential expression of FMRFamide-like immunoreactivity in the nematode *Ascaris suum*. *Journal of Comparative Neurology*, **333**. 455-468.

Cox, D H., Cui, J., Aldrich, R. W. (1997) Allosteric gating of a large conductance Ca-activated K^+ channel. *Journal of General Physiology*, **110**, 257-281.

Crowder, M. C. (2004) Ethanol targets: a BK channel cocktail in *C. elegans*. *Trends in Neurosciences*, **27**, 579-581.

Cui, J. & Aldrich, R. W. (2000) Allosteric linkage between voltage and $Ca^{(2+)}$-dependent activation of BK-type mslo1 $K^{(+)}$ channels. *Biochemistry*, **39**, 15612-15619.

Culetto, E., Baylis, H. A., Richmond, J. E., Jones, A. K., Fleming, J. T., Squire, M. D., Lewis, J. A., Sattelle, D. B. (2004) The *Caenorhabditis elegans unc-63* gene encodes a levamisole sensitive nicotinic acetylcholine receptor α subunit. *The Journal of Biological Chemistry*, **279**, 42476–42483.

Cully, D. F., Wilkinson, H., Vassilatis, D. K., Etter, A., Arena, J. P. (1996) Molecular biology and electrophysiology of glutamate-gated chloride channels of invertebrates. *Parasitology*, **113**, Suppl: S191-200.

Cully, D. F., Vassilatis, D. K., Liu, K. K., Paress, P. S., Vander Ploeg, L. H. T., Schaeffer, J. M., Arena, J. P. (1994) Cloning of an avermectin-sensitive glutamate-gated chloride channel from *Caenorhabditis elegans*. *Nature*, **371**, 707-711.

Dal Santo, P., Logan, M. A., Chisholm, A. D., Jorgensen, E. M. (1999) The inositol trisphosphate receptor regulates a 50-second behavioral rhythm in *C. elegans*. *Cell*, **98**, 757-767.

Davies, A. G., Pierce-Shimomura, J. T., Kim, H., VanHoven, M. K., Thiele, T. R., Bonci, A., Bargmann, C. I., McIntire, S. L. (2003) A Central Role of the BK Potassium Channel in Behavioral Responses to Ethanol in *C. elegans*. *Cell*, **115**, 655-666.

Davis, M. W., Somerville, D., Lee, R. Y., Lockery, S., Avery, L., Famborough, D. M. (1995) Mutation in the *Caenorhabditis elegans* Na,K-ATPase alpha-subunit gene, *eat-6*, disrupts excitable cell function. *Journal of Neuroscience*, **15**, 8408-8418.

Davletov, B. A., Krasnoperov, V., Hata, Y., Petrenko, A. G., Sudhof, T. C. (1995) High affinity binding of alpha-latrotoxin to recombinant neurexin 1 alpha. *Journal of Biological Chemistry*, **270**, 23903-23905.

De la Cruz, I. P., Levin, J. Z., Cummins, C., Anderson, P., Horvitz, H. R. (2003) *sup-9*, *sup-10*, and *unc-93* may encode components of a Two-Pore K^+ Channel that coordinates muscle contraction in *Caenorhabditis elegans*. *The Journal of Neuroscience*, **23**, 9133-9145.

Del Castillo, J., Morales, T. & Sanchez, V. (1963) Action of piperazine on the neuromuscular system of *Ascaris lumbricoides*. *Nature*, **200**, 706-707.

Den Hertog, J. (1999) Protein-tyrosine phosphatases in development. *Mechanisms of Development*, **85**, 3-14.

Dent, J. A., Smith, M.M., Vassilatis, D. K., Avery, L. (2000) The genetics of avermectin resistance in *Caenorhabditis elegans*. *Proceedings of the National Academy of Sciences, U.S.A*, **97**, 2674–2679.

Dent, J. A., Davis, M. W., Avery, L. (1997) *avr-15* encodes a chloride channel subunit that mediates inhibitory glutamatergic neurotransmission and ivermectin sensitivity in *Caenorhabditis elegans*. *The EMBO Journal*, **16**, 5867-5879.

De Potter, W. P., Partoens, P., Schoups, A., Llona, I., Coen, E. P. (1997) Noradrenergic neurons release both noradrenaline and neuropeptides Y from a single pool: the large dense cored vesicles. *Synapse*, **25**, 44-55.

Desai, C., Garriga, G., McIntire, S., Horvitz, H. R. (1988) A genetic pathway for the development of the *Caenorhabditis elegans* HSN motor neurons. *Nature*, **336**, 638-646.

Diamond, I. & Gordon, A. S. (1997) Cellular and molecular neuroscience of alcoholism. *Physiological Review*, **77**, 1-20.

Diaz, L., Meera, P., Amigo, J., Stefani, E., Álvarez, O., Toro, L., Latorre, R. (1998) Role of the S4 segment in a voltage-dependent calcium-sensitive potassium (hSlo) channel. *Journal of Biological Chemistry*, **273**, 32430-32436.

Doi, M. & Iwasaki, K. (2002) Regulation of retrograde signaling at neuromuscular junctions by the novel C2 domain protein AEX-1. *Neuron*, **33**, 249-259.

Doncaster, C. C. (1962) Nematode feeding mechanisms. I. Observations on *Rhabditis* and *Pelodera*. *Nematologica*, **8**, 313-320.

Dong, M-Q., Chase, D., Patickoglou, G. A., Koelle, M. R. (2000) Multiple RGS proteins alter neural G protein signaling to allow *C. elegans* to rapidly change behavior when fed. *Genes and Development*, **14**, 2003-2014.

Dopico, A. M., Anantharam, V., Treistman, S. N. (1998) Ethanol increases the activity of Ca^{2+}-dependent K^+ (mslo) channels: functional interaction with cytosolic Ca^{2+}. *Journal of Pharmacology and Experimental Therapeutics*, **284**, 258-268.

Dopico, A. M., Lemos, J. R., Treistman, S. N. (1996) Ethanol increases the activity of large conductance Ca(2+)-activated K^+ channels in isolated neurohypopysial terminals. *Molecular Pharmacology*, **49**, 40-48.

Driscoll, M., Dean, E., Reilly, E., Bergholz, E., Chalfie, M. (1989) Genetic and molecular analysis of a *Caenorhabditis elegans* β-tubulin that conveys benzimidazole sensitivity. *Journal of Cell Biology*, **109**, 2993-3003.

Du, W., Bautista, J. F., Yang, H., Diez-Sampedro, A., You, S. A., Wang, L., Kotagal, P., Luders, H. O., Shi, J., Cui, J., Richerson, G. B., Wang, Q. K. (2005) Calcium-sensitive potassium channelopathy in human epilepsy and paroxysmal movement disorder. *Nature Genetics*, **37**, 733-738.

Dworetzky, S. I., Boissard, C. G., Lum-Ragan, J. T., McKay, M. C., Post-Munson, D. J., Trojnacki, J. T., Chang, C. P., Gribkoff, V. K. (1996) Phenotypic alteration of a human BK (hSlo) channel by hSlobeta subunit coexpression: changes in blocker sensitivity, activation/relaxation and inactivation kinetics, and protein kinase A modulation. *Journal of Neuroscience*, **16**, 4543–4550.

Edgley, M. L. & Riddle, D. L. (2001) LG II balancer chromosomes in *Caenorhabditis elegans*: mT1 (II; III) and the mIn1 set of dominantly and recessively marked inversions. *Molecular Genetics and Genomics*, **266**, 385-395.

Elbashir, S. M., Lendeckel, W., Tuschl, T. (2001) RNA interference is mediated by 21- and 22-nucleotide RNAs. *Genes and Development*, **15**, 188-200.

Elkins, T., Ganetzky, B., Wu, C. R. (1986) *Drosophila* mutation that eliminates a calcium-dependent potassium current. *Proceedings of the National Academy of Sciences, U.S.A*, **83**, 8415-8419.

Ensslen-Craig, S. E. & Brady-Kalnay, S. M. (2004) Receptor protein tyrosine phosphatases regulate neuronal development and axon guidance. *Developmental Biology*, **275**, 12-22.

Feinberg, E.H. & Hunter, C.P. (2003) Transport of dsRNA into cells by the transmembrane protein SID-1. *Science*, **301**, 1545–1547.

Feinberg-Zadek, P. L. & Treistman, S. N. (2007) Beta-subunits are important modulators of the acute response to alcohol in human BK channels. *Alcohol Clinical and Experimental Research*, **31**, 737-44.

Fire, A. (1999) RNA-triggered gene silencing. *Trends in Genetics*, **15**, 358-363.

Fire, A., Xu, S. Q., Montogomery, M. K., Kostas, S. A., Driver, S. E., Mello, C. C. (1998) Potent and specific genetic interference by double-stranded RNA in *Caenorhabditis elegans*. *Nature*, **391**, 806-811.

Fleischhauer, R., Davis, M. W., Dzhura, I., Neely, A., Avery, L. & Joho, R. H. (2000) Ultrafast Inactivation Causes Inward Rectification in a Voltage-Gated K^+ Channel from *Caenorhabditis elegans*. *The Journal of Neuroscience*, **20**, 511-520.

Fleming, J. T., Squire, M. D., Barnes, T. M., Tornoe, C., Matsuda, K., Ahnn, J., Fire, A., Sulston, J. E., Barnard, E. A., Sattelle, D. B., Lewis, J. A. (1997) *Caenorhabditis elegans* levamisole resistance genes *lev-1*, *unc-29*, and *unc-38* encode functional nicotinic acetylcholine receptor subunits. *The Journal of Neuroscience*, **17**, 5843-5857.

Francis, M. M., Evans, S. P., Jensen, M., Madsen, D. M., Mancuso, J., Norman, K. R., Maricq, A. V. (2005) The Ror receptor tyrosine kinase CAM-1 is required for ACR-16-mediated synaptic transmission at the *C. elegans* neuromuscular junction. *Neuron*, **46**, 581-594.

Franks, C. J., Holden-Dye, L., Bull, K., Luedtke, S., Walker, R. J. (2006) Anatomy, physiology and pharmacology of *Caenorhabditis elegans* pharynx: a model to define gene function in a simple neural system. *Invertebrate Neuroscience*, **6**, 105-122.

Franks, C. J., Pemberton, D., Vinogradova, I., Cook, A., Walker, R. J., Holden-Dye, L. (2002) Ionic Basis of the Resting Membrane Potential and Action Potential in the Pharyngeal Muscle of *Caenorhabditis elegans*. *Journal of Neurophysiology*, **87**, 954-961.

Franks, N. P. & Lieb, W. R. (1994) Molecular and cellular mechanisms of general anaesthesia. *Nature*, **367**, 607-614.

Fraser, A. G., Kamath, R. S., Zipperlen, P., Martinez-Campos, M., Sohrmann, M., Ahringer, J. (2000) Functional genomic analysis of *C. elegans* chromosome 1 by systematic RNA interference. *Nature*, **408**, 325-330.

Galvez, A., Gimenez-Gallego, G., Reuben, J. P., Roy-Contancin, L., Feigenbaum, P., Kaczorowski, G. J., Garcia, M. L. (1990) Purification and characterization of a unique, potent, peptidyl probe for the high conductance calcium-activated potassium channel from venom of the scorpion *Buthus tamulus*. *The Journal of Biological Chemistry*, **265**, 11083-90.

Geary, T. G. & Thompson, D. P. (2003) Development of antiparasitic drugs in the 21st century. *Veterinary Parasitology*, **115**, 167-184.

Geary, T.G., Sangster, N.C., Thompson, D.P. (1999a) Frontiers in anthelmintic pharmacology. *Veterinary Parasitology*, **84,** 275-295.

Geary, T. G., Thompson, D. P., Klein, R. D. (1999b) Mechanism-based screening: discovery of the next generation of anthelmintics depends upon more basic research. *International Journal for Parasitology*, **29**, 105-112.

Geary, T. G., Sims, S. M., Thomas, E. M., Vanover, L., Davis, J. P., Winterrowd, C. A., Klein, R. D., Ho, N. F., Thompson, D. P. (1993) *Haemonchus contortus*: ivermectin-induced paralysis of the pharynx. *Experimental Parasitology*, **77**, 88-96.

Geldhof, P., Murray, L., Couthier, A., Gilleard, J.S., McLauchlan, G., Knox, D.P., Britton, C. (2006) Testing the efficacy of RNA interference in *Haemonchus contortus*. *International Journal of Parasitology*, **36**, 801–810.

Geppert, M., Khvotchev, M., Krasnoperov, V., Goda, Y., Missler, M., Hammer, R. E., Ichtchenko, K., Petrenko, A. G., Südhof, T. C. (1998) Neurexin Iα is a major α-latrotoxin receptor that cooperates in α-latrotoxin action. *Journal of Biological Chemistry*, **273**, 1705-1710.

Gibbons, L. M. (2002) General Organisation of Nematodes. In: *Biology of Nematodes* (Lee, D. L. ed.), pp.31. Taylor & Francis, London.

Goodman, M. B., Hall, D. H., Avery, L., Lockery, S. R. (1998) Active Currents Regulate Sensitivity and Dynamic Range in *C. elegans* Neurons. *Neuron*, **20**, 763-772.

Grasso, A., Alema, S., Rufini, S., Senni, M. I. (1980) Black widow spider toxin-induced calcium fluxes and transmitter release in a neurosecretory cell line. *Nature*, **283**, 774-776.

Greenwald, I. (1997) Development of the vulva. In: *C. elegans* II (Riddle, D. L., Blumenthal, T., Meyer, B. J., Priess, J. R., ed.), pp. 519-541. Cold Spring Harbour Laboratory Press.

Grieve, R. B. (1990) Immunologic relevance of the cuticle and epicuticle of larval *Dirofilaria immitis* and *Toxocara canis*. *Acta Tropica*, **47**, 399.

Guest, M., Bull, K., Walker, R.J., Amliwala, K., O'Connor, V., Harder, A., Holden-Dye, L., Hopper, N.A. (2007) The calcium-activated potassium channel, SLO-1, is required for the action of the novel cylco-octadepsipeptide anthelmintic, emodepside, in *Caenorhabditis elegans*. *International Journal for Parasitology*, **37**, 1577-1588.

Hamdan, F. F., Ungrin, M. D., Abramovitz, M., Ribiero, P. (1999) Characterization of a novel serotonin receptor from *Caenorhabditis elegans*: cloning and expression of two splice variants. *Journal of Neurochemistry*, **72**, 1372-1383.

Hammond, S. M., Boettcher, S., Caudy, A. A., Kobayashi, R., Hannon, G. J. (2001) Argonaute 2, a link between genetic and biochemical analysis of RNAi. *Science*, **293**, 1146-1150.

Hammond, S. M., Bernstein, E., Beach, D., Hannon, G. J. (2000) An RNA-directed nuclease mediates post-transcriptional gene silencing in *Drosophila* cells. *Nature*, **404**, 293-296.

Harder, A., Schmitt-Wrede, H., Krücken, J., Marinovski, P., Wunderlich, F., Willson, J., Amliwala, K., Holden-Dye, L., Walker, R. J. (2003) Cyclooctadepsipeptides – an anthelmintically active class of compounds exhibiting a novel mode of action. *International Journal of Antimicrobial Agents*, **22**, 318-331.

Harder, A., & von Samson-Himmelstjerna, G. (2001) Activity of the cyclic depsipeptide BAY 44-4400 against larval and adult stages of nematodes in rodents and the influence on worm survival. *Parasitology Research*, **87**, 924–928.

Hare, E. E. & Loer, C. M. (2004) Function and evolution of the serotonin-synthetic *bas-1* gene and other aromatic amino acid decarboxylase genes in *Caenorhabditis*. *BMC Evolutionary Biology*, **2**, 24.

Harfe, B. D. & Fire, A. (1998) Characterization of NK-2 Class Homeobox Genes in *C. elegans*. *East Coast Worm Meeting*, available at www.wormbase.org. ID number: WBPaper00011243

Harrington, R. J., Gutch, M. J., Hengartner, M. O., Tonks, N. K., Chisholm, A. D. (2002) The *C. elegans* LAR-like receptor tyrosine phosphatase PTP-3 and the VAB-1 Eph receptor tyrosine kinase have partly redundant functions in morphogenesis. *Development*, **129**, 2141-2153.

Harris, R. A. (1999) Ethanol actions on multiple ion channels: Which are important? *Alcoholism, Clinical and Experimental Research*, **23**, 1563-1570.

Harris, R. A. & Hitzemann, R. J. (1981) Membrane fluidity and alcohol actions. *Currents in Alcoholism*, **8**, 379-404.

Harris, J. E. & Crofton, H. D. (1957) Structure and function in the nematodes. Internal pressure and cuticular structure in *Ascaris*. *Journal of Experimental Biology*, **34**, 116-130.

Harrow, I. D. & Gration, K. A. F. (1985) Mode of action of the anthelmintics morantel, pyrantel and levamisole on the muscle cell membrane of the nematode *Ascaris suum*. *Pesticide Science* (now *Pest Management Science*), **16**, 672.

Hart, A. C., Kass, J., Shapiro, J. E., Kaplan, J. M. (1999) Distinct signaling pathways mediate touch and osmosensory responses in a polymodal sensory neuron. *Journal of Neuroscience*, **19**, 1952-1958.

Hart, A. C., Sims, S., Kaplan, J. M. (1995) Synaptic code for sensory modalities revealed by *C. elegans* GLR-1 glutamate receptor. *Nature*, **378**, 82-85.

Hashmi, S., Britton, C., Liu, J., Guiliano, D.B., Oksov, Y., Lustigman, S. (2002) Cathepsin L is essential for embryogenesis and development of *Caenorhabditis elegans*. Journal of Biological Chemistry, **277**, 3477–3486.

Hashmi, S., Tawe, W., Lustigman, S. (2001) *Caenorhabditis elegans* and the study of gene function in parasites. *Trends in Parasitology*, **17**, 387-393.

Heer, E. J. (1995) Heterotrimeric G Proteins: Organizers of Transmembrane Signals. *Cell*, **80**, 249-257.

Henkel, A.W. & Sankaranarayanan, S. (1999) Mechanisms of α-latrotoxin action. *Cell and Tissue Research*, **296**, 229-233.

Hobson, R. J., Hapiak, V. M., Xiao, H., Buehrer, K. L., Komuniecki, P. R., Komuniecki, R. W. (2006) SER-7 a *Caenorhabditis elegans* 5HT7-like receptor is essential for the 5-HT stimulation of pharyngeal pumping and egg-laying. *Genetics*, **172**, 159-169.

Hobson, R. J., Geng, J., Gray, A. D., Komuniecki, R. W. (2003) SER-7b, a constitutively active $G\alpha_s$ coupled 5-HT_7-like receptor expressed in the *Caenorhabditis elegans* M4 pharyngeal motorneuron. *Journal of Neurochemistry*, **87**, 22-29.

Holden-Dye, L. & Walker, R. J. (1990) Avermectin and avermectin derivatives are antagonists at the 4-aminobutyric acid (GABA) receptor on the somatic muscle cells of *Ascaris* – Is this the site of anthelmintic action? *Parasitology*, **101**, 265-271.

Holden-Dye, L., Krogsgaard-Larsen, P., Nielsen, L., Walker, R. J. (1989) GABA receptors on the somatic muscle cells of the parasitic nematodes, *Ascaris suum*: stereoselectivity indicates similarity to a GABAA-type agonist recognition site. *British Journal of Pharmacology*, **98**, 841-850.

Holden-Dye, L., Hewitt, G. M., Wann, K. T., Krogsgaardlarsen, P., Walker, R. J. (1988) Studies involving avermectin and the 4-aminobutyric acid (GABA) receptor of *Ascaris suum* muscle. *Pesticide Science*, **24**, 231-245.

Horoszok, L., Raymond, V., Sattelle, D. B., Wolstenholme, A. J. (2001) GLC-3: a novel fipronil and BIDN-sensitive, but picrotoxinin-insensitive, L-glutamate-gated chloride channel subunit from *Caenorhabditis elegans*. *British Journal of Pharmacology*, **132**, 1247–1254.

Horrigan, F. T. & Aldrich, R. W. (2002) Coupling between voltage sensor activation, Ca^{2+} binding and channel opening in large conductance (BK) potassium channels. *Journal of General Physiology*, **120**, 267-305.

Horrigan, F. T., Cui, J., Aldrich, R. W. (1999) Allosteric voltage gating of potassium channels I. Mslo ionic currents in the absence of $Ca^{(2+)}$. *Journal of General Physiology*, **114**, 277-304.

Horvitz, H. R., Chalfie, M., Trent, C., Sulston, J. E., Evans, P. D. (1982) Serotonin and octopamine in the nematode *Caenorhabditis elegans*. *Science*, **216**, 1012-1014.

Hu, H., Shao, L. R., Chavoshy, S., Gu, N., Trieb, M., Behrens, R., Laake, P., Pongs, O., Knaus, H. G., Ottersen, O. P., Storm, J. F. (2001) Presynaptic Ca^{2+}-activated K^+ channels in glutamatergic hippocampal terminals and their role in spike repolarization and regulation of transmitter release. *The Journal of Neuroscience*, **21**, 9585-97.

Islam, M.K., Miyoshi, T., Yamada, M., Tsuji, N. (2005) Pyrophosphatase of the roundworm *Ascaris suum* plays an essential role in the worm's molting and development. *Infection and Immunity*, **73**, 1995–2004.

Issa, Z., Grant, W.N., Stasiuk, S., Shoemaker, C.B. (2005) Development of methods for RNA interference in the sheep gastrointestinal parasite, *Trichostrongylus colubriformis*. *International Journal of Parasitology*, **35**, 935–940.

Jackson, F. & Coop, R. L. (2000) The development of anthelmintic resistance in sheep nematodes. *Parasitology*, **120**, S95-S107.

Jacob, M. K. & White, R. E. (2000) Diazepam, g-aminobutyric acid, and progesterone open Kq channels in myocytes from coronary arteries. *European Journal of Pharmacology*, **403**, 209–219.

Jerng, H. H., Shahidullah, M., Covarrubias, M. (1999) Inactivation gating of Kv4 potassium channels: molecular interactions involving the inner vestibule of the pore. *Journal of General Physiology*, **113**, 641-660.

Jeschke, P., Linuma, K., Harder, A., Schindler, M., Murakami, T. (2005) Influence of the cyclooctadepsipeptides PF1022A and PF1022E as natural products on the design of *semi*-synthetic anthelmintics such as emodepside. *Parasitology Research*, **97**, S11-S16.

Jiang, Y., Pico, A., Cadene, M., Chait, B. T., Mackinnon, R. (2001) Structure of the RCK domain from the *E. coli* K^+ channel and demonstration of its presence in the human BK channel. *Neuron*, **29**, 593-601

Johnson, C. D. & Stretton, A. O. (1985) Localization of choline acetyltransferase within identified motoneurons of the nematode *Ascaris*. *The Journal of Neuroscience*, **5**, 1984-1992.

Johnstone, C. (1998) *Parasites and Parasitic Diseases of Domestic Animals* (Online Book of Text and Images). University of Pennsylvania. http://cal.vet.upenn.edu/merial/index.html.

Jones, A. K. & Satelle, D. B. (2004) Functional genomics of the nicotinic acetylcholine receptor gene family of the nematode, *Caenorhabditis elegans*. *BioEssays*, **26**, 39-49.

Jorgensen, E. M., Hartwieg, E., Schuske, K., Nonet, M. L., Jin, Y., Horvitz, H. R. (1995) Defective recycling of synaptic vesicles in synaptotagmin mutants of *Caenorhabditis elegans*. *Nature*, **378**, 196-199.

Jose, A. & Koelle, M. (2005) Domains, amino acid residues, and new isoforms of *Caenorhabditis elegans* diacylglycerol kinase 1 (DGK-1) important for terminating diacylglycerol signaling *in vivo*. *The Journal of Biological Chemistry*, **280**, 2730-2736.

Kachi, S., Ishih, A., Terada, M. (1995) Effects of PF1022A on adult *Angiostrongylus cantonensis* in the pulmonary arteries and larvae migration into the central nervous system of rats. *Parasitology Research*, **81,** 631-637.

Kachi, S., Ishih, A., Terada, M. (1994) Effects of PF1022A on *Angiostrongylus cantonensis* staying in the central nervous system of rats and mice. *Japanese Journal of Parasitology,* **43,** 438-488.

Kamath, R. S. & Ahringer, J. (2003) Genome-wide RNAi screening in *Caenorhabditis elegans*. *Methods*, **30**, 313-321.

Kaplan, J. M. & Horvitz, H. R. (1993) A dual mechanosensory and chemosensory neuron in *Caenorhabditis elegans*. *Proceedings of the National Academy of Sciences, U.S.A*, **90**, 2227-2231.

Karlin, A. (2002) Emerging structure of the nicotinic acetylcholine receptors. *Nature Reviews Neuroscience*, **3**, 102–114.

Kass, I. S., Stretton, A. O., Wang, C. C. (1984) The effects of avermectin and drugs related to acetylcholine and 4-aminobutyric acid on neurotransmission in *Ascaris suum*. *Molecular and Biochemical Parsitiology*, **13**, 213-225.

Kazanietz, M. G., Lewin, N. E., Bruns, J. D., Blumberg, P. M. (1995) Characterization of the cysteine-rich region of the *Caenorhabditis elegans* protein UNC-13 as a high affinity phorbol ester receptor. Analysis of ligand-binding interactions, lipid cofactor requirements, and inhibitor sensitivity. *Journal of Biological Chemistry*, **270**, 10777-83.

Kennedy, S., Wang, D., Ruvkun, G. (2004) A conserved siRNA-degrading RNase negatively regulates RNA interference in *C. elegans*. *Nature*, **427**, 645-649.

Khvotchev, M., & Südhof, T.C. (2000) α-latrotoxin triggers transmitter release via direct insertion into the presynaptic plasma membrane. *The EMBO Journal*, **19**, 3250-3262.

Kim, K. & Li, C. (2004) Expression and regulation of an FMRFamide-related neuropeptide gene family in *Caenorhabditis elegans*. *The Journal of Comparative Neurology*, **475**, 540-550.

Knaus, H. G., Schwarzer, C., Koch, R. O., Eberhart, A., Kaczorowski, G. J., Glossman, H., Wunder, F., Pongs, O., Garcia, M. L., Sperk, G. (1996) Distribution of high-conductance Ca(2+)-activated K+ channels in rat brain: targeting to axons and nerve terminals. *The Journal of Neuroscience*, **16**, 955-63.

Knox, D. P., Geldhof, P., Visser, A., Britton, C. (2007) RNA interference in parasitic nematodes of animals: a reality check? *Trends in Parasitology*, **23**, 105-107.

Korswagen, H. C., Park, J. H., Ohshima, Y., Plasterk, R. H. (1997) An activating mutation in a *Caenorhabditis elegans* Gs protein induces neural degeneration. *Genes and Development*, **11**, 1493-1503.

Kramer, J.M. (1997) Extracellular matrix. In: *C. elegans II.* (Riddle, D.L., Blumenthal, T., Meyer, B.J., Priess, J.R. ed.), pp. 471–500, Cold Spring Harbor Laboratory Press, United States of America.

Krasnoperov, V., Bittner, M. A., Mo, W., Buryanovsky, L., Neubert, T. A., Holz, R. W., Ichtchenko, K., Petrenko, A. G. (2002a) Protein-tyrosine phosphatase-σ is a novel member of the functional family of α-latrotoxin receptors. *The Journal of Biological Chemistry*, **277**, 35887-35895.

Krasnoperov, V., Lu, Y., Buryanovsky, Y., Neubert, T. A., Ichtchenko, K., Petrenko, A. G. (2002b) Post-translational proteolytic processing of the calcium-independent receptor of alpha-latrotoxin (CIRL), a natural chimera of the cell adhesion protein and the G protein-coupled receptor. Role of the G protein-coupled receptor proteolysis site (GPS) motif. *The Journal of Biological Chemistry*, **277**, 46518-46526.

Krasnoperov, V.G., Bittner, M.A., Beavis, R., Kuang, Y., Salnikow, K.V., Chepurny, O.G., Little, A.R., Plotnikov, A.N., Wu, D., Holz, R.W., Petrenko, A.G. (1997) α-Latrotoxin Stimulates Exocytosis by the Interaction with a Neuronal G Protein-Coupled Receptor. *Neuron*, **18**, 925-937.

Kwa, M. S., Veenstra, J. G., Van Dijk, M., Roos, M. H. (1995) Beta-tubulin genes from the parasitic nematode *Haemonchus contortus* modulate drug resistance in *Caenorhabditis elegans*. *Journal of Molecular Biology*, **246**, 500-510.

Kwa, M. S. G., Veenstra, J. G., Roos, M. H. (1994) Benzimidazole resistance in *Haemonchus contortus* is correlated with a conserved mutation at amino acid 200 in β-tubulin isotype 1. *Molecular and Biochemical Parasitology*, **63**, 299-303.

Kwa, M. S. G., Kooyman, F. N. J., Boersema, J. H., Roos, M. H. (1993) Effect of selection for benzimidazole resistance in *Haemonchus contortus* on β-tubulin isotype 1 and isotype 2 genes. *Biochemical and Biophysical Research Communications*, **191**, 413-419.

Lajus, S., Vacher, P., Huber, D., Dubois, M., Benassy, M. N., Ushkaryov, Y., Lang, J. (2006) Alpha-latrotoxin induces exocytosis by inhibition of voltage-dependent K+ channels and by stimulation of L-type Ca^{2+} channels via latrophilin in beta-cells. *The Journal of Biological Chemistry*, **281**, 5522-5531.

Lambright, D. G., Sondek, J., Bohm, A., Skiba, N. P., Hamm, H. E., Sigler, P. B. (1996) The 2.0 A crystal structure of a heterotrimeric G protein. *Nature*, **379**, 311-319.

Lang, J., Ushkaryov, Y. A., Grasso, A., Wollheim, C. B. (1998) Ca^{2+} independent insulin exocytosis induced by α-latrotoxin requires latrophilin, a G protein-coupled receptor. *The EMBO Journal*, **17**, 648-657.

Latorre, R., Vergara, C., Hidalgo, C. (1982) Reconstitution in planar lipid bilayers of a Ca^{2+}-dependent K^+ channel from transverse tubule membranes isolated from rabbit skeletal muscle. *Proceedings of the National Academy of Sciences, U.S.A*, **79**, 805-809.

Laughton, D. L., Lunt, G. G., Wolstenholme, A. J. (1997) Alternative splicing of a *Caenorhabditis elegans* gene produces two novel inhibitory amino acid receptor subunits with identical ligand-binding domains but different ion channels. *Gene*, **201**, 119–125.

Lee, R. Y., Lobel, L., Hengartner, M., Horvitz, H. R., Avery, L. (1997) Mutations in the α1 subunit of an L-type voltage-activated Ca^{2+} channel cause myotonia in *Caenorhabditis elegans*. *The EMBO Journal*, **16**, 6066-6076.

Lee, D. L. (1996) Why do some nematode parasites of the alimentary tract secrete acetylcholinesterase? *International Journal for Parasitology*, **26**, 499-505.

Lee, K., Rowe, I. C. M., Ashford, M. L. J. (1995) Characterization of an ATP-modulated large conductance Ca^{2+}-activated K^+ channel present in rat cortical neurones. *The Journal of Physiology*, **488**, 319-337

Lee, C. H., Park, D., Wu, D., Rhee, S. G., Simon, M. I. (1992) Members of the Gq alpha subunit gene family activate phospholipase C beta isozymes. *Journal of Biological Chemistry*, **267**, 16044-16047.

Lees-Miller, J. P., Duan, Y., Teng, G. Q., Duff, H. J. (2000) Molecular determinant of high-affinity dofetillide binding to HERG1 expressed in *Xenopus oocytes*: Involvement of S6 sites. *Molecular Pharmacology*, **57**, 367-374.

Lelianova, V. G., Davletov, B. A., Sterling, A., Rahman, M. A., Grishin, E. V., Totty, N. F., Ushkaryov, Y. A. (1997) α-latrotoxin receptor, latrophilin, is a novel member of the secretin family of G protein-coupled receptors. *The Journal of Biological Chemistry*, **272**, 21504-21508.

Lewis, J. A. & Fleming, J. T. (1995) Basic culture methods. *Methods in Cell Biology*, **48**, 3-29.

Lewis, J. A. & Berberich, S. (1992) A detergent-solubilized nicotinic acetylcholine receptor of *Caenorhabditis elegans*. *Brain Research Bulletin*, **29**, 667-674.

Lewis, J. A., Wu, C. H., Berg, H., Levine, J. H. (1980) The genetics of levamisole resistance in the nematode *Caenorhabditis elegans*. *Genetics*, **95**, 905-28.

Li, C. (2005) The ever-expanding neuropeptide gene families in the nematode *Caenorhabditis elegans*. *Parasitology*, **131**, S109-S127.

Li, C., Kim, K., Nelson, L. S. (1999) FMRFamide-related neuropeptide gene family in *Caenorhabditis elegans*. *Brain Research*, **848**, 26-34.

Li, H., Avery, L., Denk, W., Hess, G. P. (1997) Identification of chemical synapses in the pharynx of *Caenorhabditis elegans*. *Proceedings of the National Academy of Sciences USA*, **94**, 5912-5916.

Lingle, C. J. (2002) Setting the stage for molecular dissection of the regulatory components of BK channels. *Journal of General Physiology*, **120**, 261-265.

Liu, J., Asuncion-Chin, M., Liu, P., Dopico, A. M. (2006) CaM kinase II phosphorylation of slo Thr107 regulates activity and ethanol responses of BK channels. *Nature Neuroscience*, **9**, 41-49.

Longenecker, H. E., Hurlbut, W. P, Mauro, A., Clark, A. W. (1970) Effects of black widow spider venom on the frog neuromuscular junction. Effects on end-plate potential, miniature end-plate potential and nerve terminal spike. *Nature*, **225**, 701-703.

Loveridge, B., McArthur, M., McKenna, P., Mariadass, B. (2003) Probable multigeneric resistance to macrocyclic lactone anthelmintics in cattle in New Zealand. *New Zealand Veterinary Journal*, **51**, 139-141.

Lubega, G. W. & Prichard, R. K. (1990) Specific interaction of benzimidazole anthelmintics with tubulin: high-affinity binding and benzimidazole resistance in *Haemonchus contortus*. *Molecular and Biochemical Parasitology*, **38**, 221-232.

Lustigman, S., Zhang, J., Liu, J., Oksov, Y., Hashmi, S. (2004) RNA interference targeting cathepsin L and Z-like cysteine proteases of *Onchocerca volvulus* confirmed their essential function during L3 molting. *Molecular and Biochemical Parasitology*, **138**, 165–170.

MacIver, M. B. & Roth, S. H. (1987) Anesthetics produce differential actions on membrane responses of the crayfish stretch receptor neuron. *European Journal of Pharmacology*, **141**, 67-77.

Magleby, K. L. (2003) Gating mechanism of BK (Slo1) channels: so near, yet so far. *Journal of General Physiology*, **121**, 81-96.

Maricq, A. V., Peckol, E., Driscoll, M., Bargmann, C. I. (1995) Mechanosensory signaling in *C. elegans* mediated by the GLR-1 glutamate receptor. *Nature*, **378**, 78-91.

Marques, A. & Guerri, C. (1988) Effects of ethanol on rat brain (Na + K) ATPase from native and delipidized synaptic membranes. *Biochemical Pharmacology*, **37**, 601-606.

Marrion, N. V. & Tavalin, S. J. (1998) Selective activation of Ca^{2+}-activated K^+ channels by co-localized Ca^{2+} channels in hippocampal neurons. *Nature*, **395**, 900-905.

Martin, R. J., Bai, G., Clark, C. L., Robertson, A. P. (2003) Methyridine (2-[2-methoxyethyl]-pyridine]) and levamisole activate different ACh receptor subtypes in nematode parasites: a new lead for levamisole-resistance. *British Journal of Pharmacology*, **140**, 1068-1076.

Martin, R. J. (1997) Modes of action of anthelmintic drugs. *Veterinary Journal*, **154**, 11-34.

Martin, R.J., Harder, A., Londershausen, M., Jeschke, P. (1996) Anthelmintic actions of the cyclic depsipeptides PF 1022A and its electrophysiological affects on muscle cells of *Ascaris summ. Pesticide Science*, **48**, 343-349.

Martin, R. J. & Pennington, A. J. (1989) A patch-clamp study of effects of dihydroavermectin on *Ascaris* muscle. *British Journal of Pharmacology*, **98**, 747-756.

Marty, A. (1981). Ca^{2+}-dependent K^+ channels with large unitary conductance in chromaffin cell membranes. *Nature*, 291, 497–500.

Matteoli, M., Haimann, C., Torri-Tarelli, F., Polak, J. M., Ceccarelli, B., De Camilli, P. (1988) Differential effect of α-latrotoxin on exocytosis from small synaptic vesicles and from large dense-core vesicles containing calcitonin gene-related peptide at the frog neuromuscular junction. *Proceedings of the National Academy of Sciences, U.S.A*, **85**, 7366-7370.

Maule, A. G., Bowman, J. W., Thompson, D. P., Marks, N. J., Friedman, A. R., Geary, T. G. (1996) FMRFamide-related peptides (FaRPs) in nematodes: occurrence and neuromuscular physiology. *Parasitology*, **113**, S119-S135.

McCavera, S., Walsh, T. K., Wolstenholme, A. J. (2007) Nematode ligand-gated chloride channels: an appraisal of their involvement in macrocyclic lactone resistance and prospects for developing molecular markers. *Parasitology*, **134**, 1111-1121.

McIntire, S. L., Jorgensen, E., Kaplan, J., Horvitz, H. R. (1993) The GABAergic nervous system of *Caenorhabditis elegans*. *Nature*, **364**, 337-341.

McKay, J. P., Raizen, D. M., Gottschalk, A., Schafer, W. R., Avery, L. (2004) *eat-2* and *eat-18* are required for nicotinic neurotransmission in the *Caenorhabditis elegans* pharynx. *Genetics*, **166**, 161-169.

McManus, O.B., Helms, L.M., Pallanck, L., Ganetzky, B., Swanson, R., Leonard. R.J. (1995) Functional role of the beta subunit of high conductance calcium-activated potassium channels. *Neuron*, 14, 645–650.

McManus, O. B. & Magleby, K. L. (1991) Accounting for the Ca(2+)-dependent kinetics of single large-conductance Ca(2+)-activated K+ channels in rat skeletal muscle. *Journal of Physiology*, **443**, 739-77.

Meldolesi, J., Huttner, W. B., Tsien, R. Y., Pozzan, T. (1984) Free cytoplasmic Ca^{2+} and neurotransmitter release: studies on PC12 cells and synaptosomes exposed to alpha-latrotoxin. *Proceedings of the National Academy of Sciences U.S.A*, **81**, 620-624.

Mendel, J. E., Korswagen, H. C., Liu, K. S., Hajdu-Cronin, Y. M., Simon, M. I., Plasterk, R. H., Sternberg, P. W. (1995) Participation of the protein Go in multiple aspects of behavior in *C. elegans*. *Science*, **267**, 1652-1655.

Miller, K. G., Emerson, M. D., Rand, J. B. (1999) Goalpha and diacyglycerol kinase negatively regulate the Gqalpha pathway in *C. elegans*. *Neuron*, **24**, 323-333.

Miller, K. G., Alfonso, A., Nguyen, M., Crowell, J. A., Johnson, C. D., Rand, J. B. (1996) A genetic selection for *Caenorhabditis elegans* synaptic transmission mutants. *Proceedings of the National Academy of Sciences, U.S.A*, **93**, 12593-12598.

Misler, S. & Hurlbut, W. P. (1979) Action of black widow spider venom on quantized release of acetylcholine at the frog neuromuscular junction: dependence upon external Mg2+. *Proceedings of the National Academy of Sciences, U.S.A*, **76**, 991-995.

Misquitta, L. & Paterson, B.M. (1999) Targeted disruption of gene function in *Drosophila* by RNA interference (RNA-i): a role for nautilus in embryonic somatic muscle formation. *Proceedings of the National Academy of Sciences, USA*, **96**, 1451–1456.

Mongan, N. P., Jones, A. K., Smith, G. R., Sansom, M. S., Sattelle, D. B. (2002) Novel alpha7-like nicotinic acetylcholine receptor subunits in the nematode *Caenorhabditis elegans*. *Protein Science*, **11**, 1162-1171.

Moss, B. L. & Magleby, K. L. (2001) Gating and conductance properties of BK channels are modulated by the S9-S10 tail domain of the alpha subunit. A study of mSlo1 and mSlo3 wild-type and chimeric channels. *Journal of General Physiology*, 118, 711-734.

Mottier, L., Alvarez, L., Ceballos, L., C. Lanusse. (2006) Drug transport mechanisms in helminth parasites: Passive diffusion of benzimidazole anthelmintics. *Experimental Parasitology*,**113**, 49–57.

Nardi, A., Calderone, V., Chericoni, S., Morelli, I. (2003) Natural modulators of large-conductance calcium-activated potassium channels. *Planta Medica*, **69**, 885-92.

Nathoo, A. N., Moeller, R. A., Westlund, B. A., Hart, A. C. (2001) Identification of *neuropeptide-like* protein gene families in *Caenorhabditis elegans* and other species. *Proceedings of the National Academy of Sciences, U.S.A*, **98**, 14000-14005.

Natochin, M. & Artemyev, N. O. (2003) A point mutation uncouples transducin-alpha from the photoreceptor RGS and effector proteins. *Journal of Neurochemistry*, **87**, 1262-1271.

Nelson, L. S., Kim, K., Memmott, J. E., Li, C. (1998a) FMRFamide-related gene family in the nematode, *Caenorhabditis elegans*. *Molecular Brain Research*, **58**, 103-111.

Nelson, L. S., Rosoff, M. L., Li, C. (1998b) Disruption of a neuropeptide gene, *flp-1*, causes multiple behavioral defects in *Caenorhabditis elegans*. *Science*, **281**, 1686-1690.

Newman, A. P., White, J. G., Sternberg, P. W. (1996) Morphogenesis of the *C. elegans* hermaphrodite uterus. *Development*, **122**, 3617-3626.

Ngo, H., Tschudi, C., Gull, K., Ullu, E. (1998) Double-stranded RNA induces mRNA degradation in *Trypanosoma brucei*. *Proceedings of the National Academy of Sciences, U.S.A*, **95**, 14687–14692.

Niacaris, T. & Avery, L. (2003) Serotonin regulates repolarization of the *C. elegans* pharyngeal muscle. *The Journal of Experimental Biology*, **206**, 223-231.

Nicholls, D. G., Rugolo, M., Scott, I. G., Meldolesi, J. (1982) α-Latrotoxin of black widow spider venom depolarizes the plasma membrane, induces massive calcium influx, and stimulates transmitter release in guinea pig brain synaptosomes. *Proceedings of the National Academy of Sciences, U.S.A*, **79**, 7924-7928.

Nicolay, F., Harder, A., von Samson-Himmelstjerna, G., Mehlhorn, H. (2000) Synergistic action of a cyclic depsipeptide and piperazine on nematodes. *Parasitology Research*, **86**, 982-992.

Niu, X., Qian, X., Magleby, K. L. (2004) Linker-gating ring complex as passive spring and $Ca^{(2+)}$-dependent machine for a voltage- and $Ca^{(2+)}$-activated potassium channel. *Neuron*, **42**, 745-756.

Nurrish, S., Segalat, L., Kaplan, J. M. (1999) Serotonin inhibition of synaptic transmission: Galpha(o) decreases the abundance of UNC-13 at release sites. *Neuron*, **24**, 231-242.

Nykanen, A., Haley, B., Zamore, P. D. (2001) ATP requirements and small interfering RNA structure in the RNA interference pathway. *Cell*, **107**, 309-321.

Oberhauser, A., Alvarez, O., Latorre, R. (1988) Activation by divalent cations of a Ca^{2+}-activated K^{+} channel from skeletal muscle membrane. *Journal of General Physiology*, **92**, 67-86.

Okkema, P. G., Harrison, S. W., Plunger, V., Aryana, A., Fire, A. (1993) Sequence Requirements for Myosin Gene Expression and Regulation in *Caenorhabditis elegans*. *Genetics*, **135**, 385-404.

Olde, B. & McCombie, W. R. (1997) Molecular cloning and functional expression of a serotonin receptor from *Caenorhabditis elegans*. *Journal of Molecular Neuroscience*, **8**, 53-62.

Omura, S. & Crump, A. (2004) The life and times of ivermectin – a success story. *Nature Reviews Microbiology*, **2**, 984-989.

Orlova, E.V., Atiqur Rahman, M., Gowen, B., Volynski, K.E., Ashton, A.C., Manser, C., van Heel, M., Ushkaryov, Y.A. (2000) Structure of α-latrotoxin oligomers reveals that divalent cation–dependent tetramers form membrane pores. *Nature Structural Biology*, **7**, 48-53.

Pallotta, B. S., Magleby, K. L., Barrett, J. N. (1981) Single channel recordings of Ca^{2+}-activated K^+ currents in rat muscle cell culture. *Nature*, **293**, 471-474.

Papaioannou, S., Marsden, D., Franks, C. J., Walker, R. J., Holden-Dye, L. (2005) Role of a FMRFamide-like family of neuropeptides in the pharyngeal nervous system of *Caenorhabditis elegans*. *Journal of Neurobiology*, **65**, 304-319.

Parkinson, J., Mitreva, M., Whitton, C., Thomson, M., Daub, J., Martin, J., Schmid, R., Hall, N., Barrell, B., Waterston, R.H., McCarter, J.P., Blaxter, M.L. (2004) A transcriptomic analysis of the phylum Nematoda. *Nature Genetics*, **36**, 1259–1267.

Parrish, S. N. & Fire, A. (2001) Distinct roles for RDE-1 and RDE-4 during RNA interference in *C. elegans*. *RNA*, **7**, 1397-1402.

Pemberton, D. J., Franks, C. J., Walker, R. J., Holden-Dye, L. (2001) Characterization of glutamate-gated chloride channels in the pharynx of wild-type and mutant *Caenorhabditis elegans* delineates the role of the subunit GluCl-alpha2 in the function of the native receptor. *Molecular Pharmacology*, **59**, 1037-1043.

Petrenko, A. G., Kovalenko, V. A., Shamotienko, O. G., Surkova, I. N., Tarasyuk, T. A., Ushkaryov, Y. A., Grishin, E. V. (1990) Isolation and properties of the alpha-latrotoxin receptor. *The EMBO Journal*, **9**, 2023-2027.

Pocock, G. & Richards, C. D. (1991) Cellular mechanisms in general anaesthesia. *The British Journal of Anaesthesia*, **66**, 116-128.

Prakriya, M. & Lingle, C. J. (1999) BK channel activation by brief depolarizations requires Ca^{2+} influx through L- and Q-type Ca^{2+} channels in rat chromaffin cells. *Journal of Neurophysiology*, **81**, 2267-2278.

Pritchard, D. I., Lawrence, C. E., Appleby, P., Gibb, I. A., Glover, K. (1994) Immunosuppressive proteins secreted by the gastrointestinal nematode parasite *Heligmosomoides polygyrus*. *International Journal for Parasitology*, **24**, 495-500.

Pulido, R., Serra-Pages, C., Tang, M., Streuli, M. (1995) The LAR/PTP delta/PTP sigma subfamily of transmembrane protein-tyrosine-phosphatases: multiple human LAR, PTP delta, and PTP sigma isoforms are expressed in a tissue-specific manner and associate

with the LAR-interacting protein LIP.1. *Proceedings of the National Academy of Sciences, U.S.A*, **92**, 11686-11690.

Qian, X. & Magleby, K. L. (2003) Beta1 subunits facilitate gating of BK channels by acting through the Ca^{2+}, but not the Mg^{2+}, activating mechanisms. *Proceedings of the National Acadamy of Sciences, U.S.A*, **100**, 10061-6.

Raffaelli, G., Saviane, C., Mohajerani, M. H., Pedarzani, P., Cherubini, E. (2004) BK potassium channels control transmitter release at CA3-CA3 synapses in the rat hippocampus. *The Journal of Physiology*, **557**, 147-157.

Rahman, M. A., Ashton, A. C., Meunier, F. A., Davletov, B. A., Dolly, J. O., Ushkaryov, Y. A. (1999) Norepinephrine exocytosis stimulated by alpha-latrotoxin requires both external and stored Ca^{2+} and is mediated by latrophilin, G proteins and phospholipase C. *Philosophical Transactions of the Royal Society of London. Series B. Biological Sciences*, **354**,379-386.

Raizen, D. M., Lee, R. Y. N., Avery, L. (1995) Interacting Genes Required for Pharyngeal Excitation by Motor Neuron MC in *Caenorhabditis elegans*. *Genetics*, **141**, 1365-1382.

Raizen, D. M. & Avery, L. (1994) Electrical activity and behavior in the pharynx of *Caenorhabditis elegans*. *Neuron*, **12**, 483-495.

Ranganathan, R., Cannon, S. C., Horvitz, H. R. (2000) MOD-1 is a serotonin-gated chloride channel that modulates locomotory behaviour in *C. elegans*. *Nature*, **408**, 470-475.

Raymond, V., Mongan, N.P., Sattelle, D.B. (2000) Anthelmintic actions on homomer-forming nicotinic acetylcholine receptor subunits: chicken alpha7 and ACR-16 from the nematode *Caenorhabditis elegans*. *Neuroscience*, **101**, 785–791.

Richmond, J. E. & Broadie, K. S. (2002) The synaptic vesicle cycle: exocytosis and endocytosis in *Drosophila* and *C. elegans*. *Current Opinion in Neurobiology*, **12**, 499-507.

Richmond, J. E., Weimer, R. M., Jorgensen, E. M. (2001) An open form of syntaxin bypasses the requirement for UNC-13 in vesicle priming. *Nature*, **412**, 338-341.

Richmond, J. E. & Jorgensen, E. M. (1999) One GABA and two acetylcholine receptors function at the *C. elegans* neuromuscular junction. *Nature Neuroscience*, **2**, 791-797.

Rizo, J. & Südhof, T. C. (2002) Snares and Munc18 in synaptic vesicle fusion. *Nature Review Neuroscience*, **3**, 641-653.

Roayaie, K., Crump, J. G., Sagasti, A., Bargmann, C. I. (1998) The G alpha protein ODR-3 mediates olfactory and nociceptive function and controls cilium morphogenesis in *C. elegans* olfactory neurons. *Neuron*, **20**, 55-67.

Roberto, M., Schweitzer, P., Madamba, S. G., Stouffer, D. G., Parsons, L. H., Siggins, G. R. (2004) Acute and chronic ethanol alter glutamatergic transmission in rat central amygdala: an *in vitro* and *in vivo* analysis. *Journal of Neuroscience*, **24**, 1594-1603.

Rogers, C. M., Franks, C. J., Walker, R. J., Burke, J. F., Holden-Dye, L. (2001) Regulation of the pharynx of *Caenorhabditis elegans* by 5-HT, octopamine, and FMRFamide-like neuropeptides. *Journal of Neurobiology*, **49**, 235-244.

Rosenthal, L., Zacchetti, D., Madeddu, L., Meldolesi, J. (1990) Mode of action of alpha-latrotoxin: role of divalent cations in Ca2(+)-dependent and Ca2(+)-independent effects mediated by the toxin. *Molecular Pharmacology*, **38**, 917-923.

Ross, E. M. & Wilkie, T. M. (2000) GTPase-activating proteins for heterotrimeric G proteins: regulators of G protein signaling (RGS) and RGS-like proteins. *Annual Reviews of Biochemistry*, **69**, 795-827.

Roth, S. H. (1980) Membrane and cellular actions of anesthetic agents. *Federation Proceedings*, **39**, 1595-1599.

Rothberg, B. S., Magleby, K. L. (2000) Voltage and Ca^{2+} activation of single large-conductance Ca^{2+}-activated K^+ channels described by a two-tiered allosteric gating mechanism. *Journal of General Physiology*, **116**, 75-99.

Rothberg, B. S. & Magleby, K. L. (1999) Gating kinetics of single large-conductance Ca^{2+}-activated K^+ channels in high Ca^{2+} suggest a two-tiered allosteric gating mechanism. *Journal of General Physiology,* **114**, 93-124.

Sade, H., Muraki, K., Ohya, S., Hatano, N., Imaizumi, Y. (2006) Activation of large-conductance, Ca^{2+}-activated K^+ channels by cannabinoids. *American Journal of Physiology, Cell Physiology*, **290**, C77-86.

Saeger, B., Schmitt-Wrede, H-P., Dehnhardt, M., Benten, W. P. M., Krüchen, J., Harder, A., Samson-Himmelstjerna, G., Wiegand, H., Wunderlich, F. (2001) Latrophilin-like receptor from the parasitic nematode *Haemonchus contortus* as a target for the anthelmintic depsipeptide PF1022A. *The FASEB Journal*, **15**, 1332-1334 (abbreviated version), & express article 10.1096/fj00-0664fje, published online March 28, 2001 (full version).

Saifee, O., Wei, L., Nonet, M. L. (1998) The *Caenorhabditis elegans unc-64* locus encodes a syntaxin that interacts genetically with synaptobrevin. *Molecular Biology of the Cell*, **9**, 1235-1252.

Sakamoto, R., Byrd, D. T., Brown, H. M., Hisamoto, N., Matsumoto, K., Jin, Y. (2005) The *Caenorhaditis elegans* UNC-14 RUN domain protein binds to the kinesin-1 and UNC-16 complex and regulates synaptic vesicle localization. *Molecular Biology of the Cell*, **16**, 483-96.

Salio, C., Lossi, L., Ferrini, F., Merighi, A. (2006) Neuropeptides as synaptic transmitters. *Cell and Tissue Research*, **326**, 583–598.

Salkoff, L., Butler, A., Ferreira, G., Santi, C., Wei, A. (2006) High-conductance potassium channels of the SLO family. *Nature Reviews Neuroscience*, **5**, 921-931.

Samson-Himmelstjerna, G., Harder, A., Schnieder, T., Kalbe, J., Mencke, N. (2000) *In vivo* activities of the new anthelmintic depsipeptide PF 1022A. *Parasitology Research*, **86**, 194-199.

Sangster, N. C. & Dobson, R. J. (2002) Anthelmintic Resistance. In: *The Biology of Nematodes* (Lee, D. L., ed.), Harwood.

Sangster, N.C. & Gill, J. (1999) Pharmacology of Anthelmintic Resistance. *Parasitology Today*, **15**, 141-146.

Sangster, N. C., Riley, F. L., Wiley, L. J. (1998) Binding of [3H]m-aminolevamisole to receptors in levamisole-susceptible and –resistant *Haemonchus contortus*. *International Journal for Parasitology*, **28**, 707-717.

Santi, C. M., Yuan, A., Fawcett, G., Wang, Z. W., Butler, A., Nonet, M. L., Wei, A., Rojos, P., Salkoff, L. (2003) Dissection of K^+ currents in *Caenorhabditis elegans* muscle cells by genetics and RNA interference. *Proceedings of the National Academy of Sciences, U.S.A*, **100**, 14391-14396.

Sasaki, T., Takagi, M., Yaguchi, T., Miyadoh, S., Okada, T., Koyama, M. (1992) A new anthelmintic cyclodepsipeptide, PF 1022A. *Journal of Antibiotics,* **45**, 692-697.

Sausbier, M., Hu, H., Arntz, C., Feil, S., Kamm, S., Adelsberger, H., Sausbier, U., Sailer, C. A., Feil, R., Hofmann, F., Korth, M., Shipston, M. J., Knaus, H. G., Wolfer, D. P., Pedroarena, C. M., Storm, J. F., Ruth, P. (2004) Cerebellar ataxia and Purkinje cell dysfunction caused by Ca^{2+}-activated K^+ channel deficiency. *Proceedings of the National Academy of Sciences, U.S.A*, **101**, 9474-9478.

Schafer, W. R. & Kenyon, C. J. (1995) A calcium-channel homologue required for adaptation to dopamine and serotonin in *Caenorhabditis elegans*. *Nature*, **375**, 73.

Schinkmann, K. & Li, C. (1992) Localization of FMRF amide-like peptides in *Caenorhabditis elegans*. *Journal of Comparative Neurology*, **316**, 251-260.

Schreiber, M., Wei, A., Yuan, A., Gaut, J., Saito, M., Salkoff, L. (1998) Slo3, a novel pH-dependent sensitive K^+ channel from mammalian spermatocytes. *Journal of Biological Chemistry*, **273**, 3509-3516.

Schreiber, M. & Salkoff, L. (1997) A novel calcium-sensing domain in the BK channel. *Biophysical Journal*, **73**, 1355–1363.

Segalat, L., Elkes, D. A., Kaplan, J. M. (1995) Modulation of serotonin-controlled behaviors by Go in *Caenorhabditis elegans*. *Science*, **267**, 1648-1651.

Seymour, M. K., Wright, K. A., Doncaster, C. C. (1983) The action of the anterior feeding apparatus of *Caenorbabditis elegans* (Nematoda: Rhabditida). *The Journal of Zoology (London)*, **201**, 527-539.

Shi, J., Krishnamoorthyet, G., Yang, Y., Hu, L., Chaturvedi, N., Harital, D., Qin, J., Cui, J. (2002) Mechanism of magnesium activation of calcium-activated potassium channels. *Nature*, **418**, 876-880.

Shi, J. & Cui, J. (2001) Intracellular Mg^{2+} enhances the function of BK-type Ca^{2+}-activated K^{+} channels. *Journal of General Physiology*, **118**, 589-606.

Shtonda, B. & Avery, A. (2005) CCA-1, EGL-19 and EXP-2 currents shape action potentials in the *Caenorhabditis elegans* pharynx. *The Journal of Experimental Biology*, **208**, 2177-2190

Sidow, A. (1996) Gen(om)e duplications in the evolution of early vertebrates. *Current Opinion in Genetics & Development*, **6**, 715-722.

Sijen, T., Fleenor, J., Simmer, F., Thijssen, K. L., Parrish, S., Timmons, L., Plasterk, R. H., Fire, A. (2001) On the role of RNA amplification in dsRNA-triggered gene silencing. *Cell*, **107**, 465-476.

Simmer, F., Moorman, C., van der Linden, A. M., Kuijk, E., van den Berghe, P. V. E., Kamath, R. S., Fraser, A. G., Ahringer, J., Plasterk, R. H. A. (2003) Genome-Wide RNAi of *C. elegans* using the Hypersensitive *rrf-3* Strain Reveals Novel Gene Functions. *PLos Biology*, **1**, 077-084.

Simmer, F., Tijsterman, M., Parrish, S., Koushika, S. P., Nonet, M. L., Fire, A., Ahringer, J., Plasterk, R. H. A. (2002) Loss of the Putative RNA-Directed RNA Polymerase RRF-3 makes *C. elegans* Hypersensitive to RNAi. *Current Biology*, **12**, 1317-1319.

Sims, S. M., Ho, N. F., Geary, T. G., Thomas, E. M., Day, J. S., Barsuhn, C. L., Thompson, D. P. (1996) Influence of organic acid excretion on cuticle pH and drug absorption by *Haemonchus contortus*. *International Journal of Parasitology*, **26**, 25.

Soller, T., Bennett, M. K., Whiteheart, S. W., Scheller, R. H., Rothman, J. E. (1993) A protein assembly-disassembly pathway *in vitro* that may correspond to sequential steps of synaptic vesicle docking, activation, and fusion. *Cell*, **75**, 409-418.

Steger, K. A., Shtonda, B. B., Thacker, C., Snutch, T. P., Avery, L. (2005). The *Caenorhabditis elegans* T-type calcium channel CCA-1 boosts neuromuscular transmission. *Journal of Experimental Biology*, **208**, 2191-2203.

Strange, K., Christensen, M., Morrison, R. (2007) Primary culture of *Caenorhabditis elegans* developing embryo cells for electrophysiological, cell biological and molecular studies. *Nature Protocols*, **2**, 1003-12.

Stretton, A. O., Cowden, C., Sithigorngul, P., Davis, R. E. (1991) Neuropeptides in the nematode *Ascaris suum*. *Parasitology*, **102**, S107-116.

Stretton, A. O. W., Davis, R. E., Angstadt, J. D., Donmoyer, J. E., Johnson, C. D. (1985) Neural control of behaviour in *Ascaris*. *Trends in Neurosciences*, **8**, 294-300.

Stretton, A. O., Fishpool, R. M., Southgate, E., Donmoyer, J. E., Walrond, J. P., Moses, J. E., Kass, I. S. (1978) Structure and physiological activity of the motorneurons of the nematode *Ascaris*. *Proceedings of the National Academy of Sciences, U.S.A*, **75**, 3493-3497.

Südhof, T.C. (2001) α-Latrotoxin and Its Receptors: Neurexins and CIRL/Latrophilins. *Annual Review of Neuroscience,* **24**, 933-962.

Südhof, T. C. (1995) The synaptic vesicle cycle: a cascade of protein-protein interactions. *Nature*, **375**, 645-653.

Sugita, S., Khvotchev, M., Südhof, T. C. (1999) Neurexins are functional α-latrotoxin receptors. *Neuron*, **22**, 489-496.

Sugita, S., Ichtchenko, K., Khvotchev, M., Südhof, T.C. (1998) α-Latrotoxin Receptor CIRL/Latrophilin 1 (CL1) Defines an Unusual Family of Ubiquitous G protein-linked Receptors. *The Journal of Biological Chemistry*, **273**, 32715-32724.

Sulston, J., Dew, M. & Brenner, S. (1975) Dopaminergic neurons in the nematode *Caenorhabditis elegans*. *Journal of Comparative Neurology*, **163**, 215-226.

Sun, X. P., Yazejian, B., Grinnell, A. D. (2004) Electrophysiological properties of BK channels in *Xenopus* motor nerve terminals. *The Journal of Physiology*, **557**, 207-228.

Sutton, R. B., Fasshauer, D., Jahn, R., Brunger, A. T. (1998) Crystal structure of a SNARE complex involved in synaptic exocytosis at 2.4 Å resolution. *Nature*, **395**, 347-353.

Swensen, A. M. & Bean, B. P. (2003) Ionic mechanisms of burst firing in dissociated Purkinje neurons. *The Journal of Neuroscience*, **23**, 9650-9663.

Tabara, H., Yigit, E., Soimi, H., Mello, C. C. (2002) The dsRNA binding protein RDE-4 interacts with RDE-1, DCR-1, and a DExH-box helicase to direct RNAi in *C. elegans*. *Cell*, **109**, 861-871.

Taylor, S. J. & Exton, J. H. (1991) Two alpha subunits of the Gq class of G proteins stimulate phosphoinositide phospholipase C-beta 1 activity. *FEBS Letters*, **286**, 214-216.

Terada, M. (1992) Neuropharmacological mechanism of action of PF 1022A, an antinematode anthelmintic with a new structure of cyclic depsipeptides, on *Angiostrongylus cantonensis* and isolated frog rectus. *Japanese Journal of Parasitology*, **41,** 108-117.

Tian, L., Duncan, R. R., Hammond, M. S., Coghill, L. S., Wen, H., Rusinova, R., Clark, A. G., Levitan, I. B., Shipston, M. J. (2001) Alternative splicing switches potassium channel sensitivity to protein phosphorylation. *Journal of Biological Chemistry*, **276**, 7717-7720.

Tian, L., Knaus, H., Shipston, M. J. (1998) Glucocorticoid regulation of calcium-activated potassium channels mediated by serine/threonine protein phosphatase. *Journal of Biological Chemistry*, **273**, 13531-13536.

Tijsterman, M., May, R.C., Simmer, F., Okihara, K.L., Plasterk, R.H.A. (2004) Genes required for systemic RNA interference in *Caenorhabditis elegans*. *Current Biology*, **14**, 111–116.

Timmons, L. (2004) Endogenous inhibitors of RNA interference in *Caenorhabditis elegans*. *Bioessays*, **26**, 715-718.

Timmons, L., Court, D. L., Fire, A. (2001) Ingestion of bacterially expressed dsRNAs can produce specific and potent genetic interference in *Caenorhabditis elegans*. *Gene*, **263**, 103-112.

Timmons, L. & Fire, A. (1998) Specific interference by ingested dsRNA. *Nature*, **395**, 854.

Tobaben, S., Südhof, T. C., Stahl, B. (2002) Genetic analysis of alpha-latrotoxin receptors reveals functional interdependence of CIRL/latrophilin 1 and neurexin 1 alpha. *The Journal of Biological Chemistry*, **277**, 6359-6365.

Touroutine, D., Fox, R.M., Von Stetina, S.E., Burdina, A., Miller, D.M., Richmond, J.E. (2005) *acr-16* encodes an essential subunit of the levamisole-resistant nicotinic receptor at the *Caenorhabditis elegans* neuromuscular junction. *Journal of Biological Chemistry*, **280**, 27013–27021.

Towers, P. R., Edwards, B., Richmond, J. E., Sattelle, D. B. (2005) The *Caenorhabditis elegans lev-8* gene encodes a novel type of nicotinic acetylcholine receptor α subunit. *Journal of Neurochemistry*, **93**, 1–9.

Trent, C., Tsung, N., Horvitz, H. (1983) Egg-laying defective mutants of the nematode *Caenorhabditis elegans*. *Genetics*, **104**, 619-647.

Trim, J. E., Holden-Dye, L., Willson, J., Lockyer, M., Walker, R. J. (2001) Characterization of 5-HT receptors in the parasitic nematode, *Ascaris suum*. *Parasitology*, **122**, 207-217.

Tseng-Crank, J., Godinot, N., Johansen, T. E., Ahring, P. K., Strøbaek, D., Mertz, R., Foster, C. D., Olesen, S.P., Reinhart, P. H. (1996) Cloning, expression, and distribution of a Ca(2+)-activated K+ channel beta-subunit from human brain. *Proceedings of the National Academy of Sciences, U.S.A*, **93**, 9200-5.

Tzeng, M. C. & Siekevitz, P. (1979) Action of alpha-latrotoxin from black widow spider venom on a cerebral cortex preparation: release of neurotransmitters, depletion of synaptic vesicles, and binding to the membrane. *Advances in Cytopharmacology*, **3**, 117-127.

Unwin, N. (1995) Acetylcholine receptor channel imaged in the open state. *Nature*, **373**, 37-43.

Ushkaryov, Y. A., Petrenko, A. G., Geppert, M. & Südhof, T. C. (1992) Neurexins: synaptic cell surface proteins related to the alpha-latrotoxin receptor and laminin. *Science*, **257**, 50-56.

Valtorta, F., Madeddu, L., Meldolesi, J., Ceccarelli, B. (1984) Specific localization of the alpha-latrotoxin receptor in the nerve terminal plasma membrane. *The Journal of Cell Biology*, **99**, 124-132.

Van den Bossche, H., Roshette, F., Horig, C. (1982) Mebendazole and related anthelmintics. *Advances in Pharmacology and Chemotherapy*, **19**, 67-128.

Verbanck, P., Seutin, V., Dresse, A., Scuvee, J., Massotte, L., Giesbers, I., Kornreich, C. (1990) Electrophysiological effects of ethanol on monoaminergic neurons: an *in vivo* and *in vitro* study. *Alcohol Clinical and Experimental Research*, **14**, 728-735.

Viney, M.E., Thompson, F.J. (2008) Two hypotheses to explain why RNA interference does not work in animal parasitic nematodes. *International Journal for Parasitology*, **38**, 43–47.

Visser, A., Geldhof, P., DeMarre, V., Knox, D.P., Vercruysse, J., Claerebout, E. (2006) Efficacy and specificity of RNA interference in larval life-stages of *Ostertagia ostertagi*. *Parasitology*, **133**, 777–783.

Volynski, K. E., Capogna, M., Ashton, A. C., Thomson, D., Orlova, E. V., Manser, C. F., Ribchester, R. R., Ushkaryov, Y. A. (2003) Mutant alpha-latrotoxin (LTXN4C) does not form pores and causes secretion by receptor stimulation: this action does not require neurexins. *The Journal of Biological Chemistry*, **278**, 31058-31066.

Volynski, K. E., Meunier, F. A., Lelianova, V. G., Dudina, E. E., Volkova, T. M., Rahman, M. A., Manser, C., Grishin, E. V., Dolly, J. O., Ashley, R. H., Ushkaryov, Y. A. (2000) Latrophilin, neurexin, and their signaling-deficient mutants facilitate α-latrotoxin insertion into membranes but are not involved in pore formation. *The Journal of Biological Chemistry*, **275**, 41175-41183.

Wacker, I., Kaether, C., Kromer, A., Migala, A., Almers, W., Gerdes, H. H. (1997) Microtubule-dependent transport of secretory vesicles visualized in real time with a GFP-tagged secretory protein. *Journal of Cell Science*, **110**, 1453-1463.

Waggoner, L. E., Hardaker, L. A., Golik, S., Schafer, W. R. (2000) Effect of a neuropeptide gene on behavioral states in *Caenorhabditis elegans* egg-laying. *Genetics*, **154**, 1181-1192.

Walker, G., Houthoofd, K., Vanfleteren, J.R., Gems, D. (2005). Dietary restriction in *C. elegans*: from rate-of-living effects to nutrient sensing pathways. *Mechanisms of Ageing and Development*, **126**, 929–937.

Walker, D. S., Gower, N. J. D., Ly, S., Bradley, G. L., Baylis, H. A. (2002) Regulated disruption of inositol 1, 4, 5-trisphosphate signaling in *Caenorhabditis elegans* reveals

new functions in feeding and embryogenesis. *Molecular Biology of the Cell*, **13**, 1329-1337.

Walker, R. J., Franks, C. J., Pemberton, D., Rogers, C., Holden-Dye, L. (2000) Physiological and pharmacological studies on nematodes. *Acta. Biol. Hung*, **51**, 379-394.

Walker, R. J., Colquhoun, L., Holden-Dye, L. (1992) Pharmacological profiles of the GABA and acetylcholine receptors from the nematode, *Ascaris suum*. *Acta. Biol. Hung*, **43**, 59-68.

Waller, P. J. (1997) Anthelmintic resistance. *Veterinary Parasitology*, **72**, 391-412.

Walrond, J. P., Kass, I. S., Stretton, O. W., Donmoyer, J. E. (1985) Identification of Excitatory and Inhibitory Motoneurons in the Nematode *Ascaris* by Electrophysiological Techniques. *The Journal of Neuroscience*, **5**, 1-8.

Walrond, J. P., Stretton, A. 0. W. (1985) Reciprocal inhibition in the motor nervous system of the nematode *ascaris*: direct control of ventral inhibitory motoneurons by dorsal excitatory motoneurons. *The Journal of Neuroscience*, **5**, 9-15.

Wang, J. & Barr, M.M. (2005) RNA interference in *Caenorhabditis elegans*. *Methods in Enzymology*, **392**, 36–55.

Wang, Z-W., Saifee, O., Nonet, M. L., Salkoff, L. (2001) SLO-1 potassium channels control quantal content of neurotransmitter release at the *C. elegans* neuromuscular junction. *Neuron*, **32**, 867-881.

Wang, J., Zhou, Y., Wen, H., Levitan, I. B. (1999) Simultaneous binding of two protein kinases to a calcium-dependent potassium channel. *The Journal of Neuroscience*, **19**, RC4 (1-7).

Wanke, E., Ferroni, A., Gattanini, P., Meldolesi, J. (1986) Alpha latrotoxin of the black widow spider venom opens a small, non-closing cation channel. *Biochemical and Biophysical Research Communications*, **134**, 320-325.

Warbington, L., Hillman, T., Adams, C., Stern, M. (1996) Reduced transmitter release conferred by mutations in the slowpoke-encoded Ca2(+)-activated K+ channel gene of *Drosophila*. *Invertebrate Neuroscience*, **2**, 51-60.

Ward, S. (1973) Chemotaxis by the nematode *Caenorhabditis elegans*: identification of attractants and analysis of the response by use of mutants. *Proceedings of the National Academy of Sciences*, **70**, 817-821.

Waterston, R. H. (1988) Muscle. In: *The Nematode Caenorhabditis elegans* (Wood, W. B., ed.), chapter 10, pp. 281-335, Cold Spring Harbor Laboratory Press, U.K.

Weckwerth, W., Miyamoto, K., Iinuma, L., Krause, M., Glinski, M., Storm, T., Bonse, G., Kleinkauf, H., Zocher, R. (2000) Biosynthesis of PF1022A and related cyclooctadepsipeptides. *The Journal of Biological Chemistry*, **275**, 17909-17915.

Wei, A., Jegla, T., Salkoff, L. (1996) Eight potassium channel families revealed by the *C. elegans* genome project. *Neuropharmacology*, **35**, 805–829.

White, R. E., Lee, A. B., Shcherbatko, A. D., Lincoln, T. M., Schonbrunn, A., Armstrong, D. L. (1993) Potassium channel stimulation by natriuretic peptides through cGMP-dependent dephosphorylation. *Nature*, **361**, 263-266.

White, J. G., Southgate, E., Thomson, J. N., Brenner, S. (1986) The structure of the nervous system of the nematode *Caenorhabditis elegans*. *Philosophical Transactions of the Royal Society of London, Series B, biological Sciences*, **314**, 1-340.

Whitfield, P.J. (1993) Parasitic Helminths. In: *Modern Parasitology* (Cox, F. E. G., ed.), pp.24-52. Blackwell Science, U.K.

Wianny, F. & Zernicka-Goetz, M. (2000) Specific interference with gene function by double-stranded RNA in early mouse development. *Nature Cell Biology*, **2**, 70–75.

Wicks, S. R. & Rankin, C. H. (1997) Effects of tap withdrawal response habituation on other withdrawal behaviours: the localization of habituation in the nematode *Caenorhabditis elegans*. *Behavioural Neuroscience*, **111**, 342-353.

Wilkie, T. M. (2000) G-protein signaling: Satisfying the basic necessities of life. *Current Biology*, **10**, R853-R856.

Willson, J., Amliwala, K., Davis, A., Cook, A., Cuttle, M. F., Kriek, N., Hopper, N. A., O'Connor, sV., Harder, A., Walker, R. J., Holden-Dye, L. (2004) Latrotoxin Receptor Signaling Engages the UNC-13-Dependent Vesicle-Priming Pathway in *C. elegans*. *Current Biology*, **14**, 1374-1379.

Willson, J., Amliwala, K., Harder, A., Holden-Dye, L., Walker, R. J. (2003) The effects of the anthelmintic emodepside at the neuromuscular junction of the parasitic nematode *Ascaris suum*. *Parasitology*, **126**, 79-86.

Winston, W.M., Sutherlin, M., Wright, A.J., Feinberg, E.H., Hunter, C.P. (2007) *Caenorhabditis elegans* SID-2 is required for environmental RNA interference. *Proceedings of the National Academy of Sciences, USA*, **104**, 10565–10570.

Winston, W.M., Molodowitch, C., Hunter, C.P. (2002) Systemic RNAi in *C. elegans* requires the putative transmembrane protein SID-1. *Science*, **295**, 2456–2459.

Wintle, R. F. & Van Tol, H. H. M. (2001) Dopamine signaling in *Caenorhabditis elegans* – potential for parkinsonism research. *Parkinsonism and Related Disorders*, **7**, 177-183.

Wolstenholme, A. J. & Rogers, A. T. (2005) Glutamate-gated chloride channels and the mode of action of the avermectin/milbemycin anthelmintics. *Parasitology*, **131**, S85-S95.

Wood, W. B. (1988) Introduction to *C. elegans* Biology. In: *The Nematode Caenorhabditis elegans* (Wood, W. B., ed.), chapter 1, pp. 1-16, Cold Spring Harbor Laboratory Press, U.K.

Wu, S. N., Jan, C. R., Li, H. F., Chen, S. A. (1999) Stimulation of large-conductance Ca^{2+}-activated K^+ channels by Evans blue in cultured endothelial cells of human umbilical veins. *Biochemical and Biophysical Research Communications*, **254**, 666-74.

Xia, X., Zeng, X., Lingle, C. J. (2002) Multiple regulatory sites in large-conductance calcium-activated potassium channels. *Nature*, **418**, 880-884.

Xu, J. W. & Slaughter, M. M. (2005) Large-conductance calcium-activated potassium channels facilitate transmitter release in salamander rod synapse. *The Journal of Neuroscience*, **25**, 7660-7668.

Yates, D. M., Portillo, V., Wolstenholme, A. J. (2003) The avermectin receptors of *Haemonchus contortus* and *Caenorhabditis elegans*. *International Journal for Parasitology*, **33**, 1183–1193.

Yuan, A., Dourado, M., Butler, A., Walton, N., Wei, A., Salkoff, L. (2000) SLO-2, a K^+ channel with an unusual Cl^- dependence. *Nature Neuroscience*, **3**, 771-779.

Zahner, H., Taubert, A., Harder, A., Samson-Himmelstjerna, G. (2001a) Filaricidal efficacy of anthelmintically active cyclodepsipeptides. *International Journal for Parasitology*, **31**, 1515-1522.

Zahner, H., Taubert, A., Harder, A., Samson-Himmelstjerna, G. (2001b) Effects of Bay 44-4400, a new cyclodepsipeptide, on developing stages of filariae (*Acanthocheilonema viteae, Brugia malayi, Litomosoides sigmodontis*) in the rodent *Mastomys coucha*. *Acta Tropica*, **80**, 19-28.

Zappe, S., Fish, M., Scott, M.P., Solgaard, O. (2006) Automated MEMSbased *Drosophila* embryo injection system for high-throughput RNAi screens. *Lab Chip*, **6**, 1012–1019.

Zeng, X. H., Xia, X. M., Lingle, C. J. (2005) Divalent cation sensitivity of BK channel activation supports the existence of three distinct binding sites. *Journal of General Physiology*, **125**, 273-286.

Zhang, X., Solaro, C. R., Lingle, C. J. (2001) Allosteric regulation of BK channel gating by Ca(2+) and Mg(2+) through a nonselective, low affinity divalent cation site. *Journal of General Physiology*, **118**, 607-636.

Zheng, Y., Brockie, P. J., Mellem, J. E., Madsen, D. M., Maricq, A. V. (1999) Neuronal control of locomotion in *C. elegans* is modified by a dominant mutation in the GLR-1 ionotropic glutamate receptor. *Neuron*, **24**, 347-61.

Zhou, Y., Wang, J., Wen, H., Kucherovsky, O., Levitan, I. B. (2002) Modulation of *Drosophila* slowpoke calcium-dependent potassium channel activity by bound protein kinase a catalytic subunit. *The Journal of Neuroscience*, **22**, 3855-3863.

Zhou, X., Arntz, C., Kamm, S., Motejlek, K., Sausbier, U., Wang, G., Ruth, P., Korth, M. (2001) A molecular switch for specific stimulation of the BK_{Ca} channel by cGMP and cAMP kinase. *The Journal of Biological Chemistry*, **276**, 43239-43245.

Zwaal, R. R., Mendel, J. E., Sternberg, P. W., Plasterk, R. H. (1997) Two neuronal G proteins are involved in chemosensation of the *Caenorhabditis elegans* Dauer-inducing pheromone. *Genetics*, **145**, 715-27.

Appendix 1

The *C. elegans* strains used in the project

C. elegans STRAINS USED IN THE PROJECT

A detailed description of the mutation in each strain is provided in the chapter where the strain is used. A reference page is provided in this table.

Strain (allele)	Protein(s) mutated	Strain ID	Location Obtained	Mutation. Page reference.
Wild Type Bristol N2	-	Bristol N2	Caenorhabditis Genetics Centre (CGC)	Standard laboratory strain.
lat-1 (ok1465)	LAT-1	XA3750	Generated by M. Guest. (Guest et al., 2007)	Loss-of-function. See page 147.
lat-2 (tm463)	LAT-2	VC158	CGC	Loss-of-function. See page 152.
lat-1 (ok1465); lat-2 (tm463)	LAT-1, LAT-2	XA3749	Generated by M. Guest. (Guest et al., 2007)	Double loss-of-function. See page 157.
ptp-3 (op147)	PTP-3	CZ540	CGC	Loss-of-function. See page 159.
egl-30 (ad806)	$G\alpha_q$	DA1084	CGC	Reduction-in-function. See page 161.
egl-30 (tg26)	$G\alpha_q$	KY26	CGC	Gain-of-function. See page 161.
goa-1 (n1134)	$G\alpha_o$	MT2426	CGC	Loss-of-function. See page 162.
itr-1 (sa73)	ITR-1	JT73	CGC	Reduction-in-function. See page 162.
dgk-1 (nu62)	DGK-1	KP1097	CGC	Loss-of-function. See page 162.
slo-1 (js379)	SLO-1	NM1968	CGC	Null. See page 173.
slo-1 (ky399)	SLO-1	CX3940	CGC	Gain-of-function. See page 173.
slo-1 (ky389)	SLO-1	CX3933	CGC	Gain-of-function. See page 173.
slo-2 (nf101)	SLO-2	LY101	CGC	Loss-of-function. See page 173.
rrf-3 (pk1426)	RdRP	NL2099	CGC	Loss-of-function mutation in a RNA-directed RNA polymerase. See page 13.